IDENTIFICATION OF NOVEL KINASES REGULATING LUNG CANCER METASTASIS

BY

ROMAIN LARA

A thesis submitted for the degree of
Doctor of Philosophy at Imperial College London

Imperial College London, Faculty of Medicine
Division of Surgery Oncology Reproductive Biology & Anaesthetics (SORA)
Department of Oncology

Supervisor: Dr. Olivier Pardo
Co-supervisor: Prof. Michael J. Seckl
Co-supervisor: Prof. Julian Downward

Unless otherwise stated, the present thesis is the result of my own work.

To my family.

Abstract

Lung cancer is the commonest cancer killer worldwide. The appearance of distant metastasis is one of the main reasons for failing to cure patients with this disease. Thus, understanding the mechanisms regulating lung cancer metastasis should highlight novel therapeutic strategies to improve clinical outcome.

We performed an RNA interference screen for cell migration using A549 non-small cell lung cancer (NSCLC) cells. Seventy kinases modulating A549 cell motility were identified, including several members of the ribosomal-S6 kinase (Rsk) family. Indeed, Rsk1 silencing increased, while Rsk2 and Rsk4 downregulation decreased, cell migration. We then assessed the ability of our candidates to regulate A549 cell invasiveness in a 3-D invasion assay. We found that 38 of these similarly regulated cell migration and invasion, including Rsk1 and Rsk4 but not Rsk2. Further work demonstrated that the motility effects of Rsk1, but not Rsk2 or 4, silencing were reproduced in additional NSCLC cell lines. Hence, we focussed on Rsk1 as the principal Rsk isoform regulating NSCLC cell motility. *In silico* analysis and biochemical experimentation revealed that Rsk1 interacted with the actin regulators Vasp and Mena. This correlated with the ability of Rsk1 to phosphorylate Vasp on Thr-278, a site regulating Vasp-mediated actin dynamics. Furthermore, Vasp and Mena downregulation prevented the migratory effects of Rsk1 silencing. To assess the *in vivo* relevance of our findings, we developed a zebrafish metastasis model and showed that Rsk1 silencing enhanced the metastatic potential of A549 cells. Moreover, immunohistochemical staining of human isogenically-matched samples demonstrated that Rsk1 expression decreased, while Rsk2 or 4 expression increased, in metastatic versus primary lung cancer lesions. Also, patients with Rsk1-negative primary tumours

showed an increased number of metastases. Taken together, our findings establish that Rsk1 is a metastasis suppressor in NSCLC and may be a biomarker for the progression of this disease.

Acknowledgements

I wish to thank my supervisors, Dr. Olivier E. Pardo, Prof. Michael J. Seckl and Prof. Julian Downward for their constant attention and interest to this work, as well as for their patience and kindness. My gratitude goes to our collaborators, Dr. Francesco A. Mauri, Dr. Paul Bates, Prof. Etienne Waelkens, Prof. Maggie Dallman who kindly provided me with their help and support throughout this work. I am grateful to Dr. David Hancock, Diane Waltling, Dr. Ana P. Costa-Pereira, Dr Edward Schofield, Dr. Colin Gray, Dr. Alastair Nicols, Dr. Daniel Zicha, Dr. Mark Dodding, Harriet Taylor, Rita Derua, Alice Shia and Dr. Robert J. Shiner for their advice and participation to some parts of this work. I also wish to thank the members from the lung cancer group in Hammersmith and the Signal transduction laboratory in CRUK-LIF for their help and support all along my thesis. Finally, I wish to give credit to the charities Cancer Treatment and Research Trust and Cancer Research UK for their financial support.

CONTENTS

LIST OF FIGURES

LIST OF TABLES

ABBREVIATIONS

4.1B	non-erythroid protein 4.1 brain types
ACAP1	ADP-ribosylation factor directed GTPase-activating protein 1
Af6	Acute lymphoblastic leukaemia‑1 fused gene on chromosome 6
Ago2	Argonaute 2
As160	Akt substrate 160- kDa
Alk	Anaplastic lymphoma kinase
Ampk	AMP-activated protein kinase
Apc	Adenomatous polyposis of the colon
Ape	Akt-phosphorylation enhancer
APS	Ammonium persulphate
Arp2/3	Actin related protein 2 and 3
Atm	Ataxia-telangiectasia mutated gene
Atf4	Activating transcription factor 4
ATP	Adenosine triphosphate
Bad	Bcl2-associated agonist of cell death
BADJ	Bronchioalveolar duct junction
BASC	Bronchioalveolar stem cell
Bcl-2	B-cell leukaemia/lymphoma-2
Bcl-X_L	Bcl2-related protein long isoform
Bcr-Abl	Breakpoint cluster region-Abelson murine leukemia viral
BET	Ethidium bromide
BM	Basement membrane
BSA	Bovine serum albumin
Bub1	Budding uninhibited by benzimidazoles 1
Camk	Calcium/calmodulin dependent protein kinase
Cbl	Casitas B-lineage lymphoma proto-oncogene
CC10	Clara cell-specific 10-kDa protein
Cdc42	Cell division cycle 42
Cdk	Cyclin-dependent kinase
Cdkn2a	Cyclin-dependent kinase inhibitor 2a
C/Ebpβ	CCAAT/Enhancer-binding protein β

c-Fos	Finkel-Biskis-Jinkins (FBJ) osteosarcoma virus
Chrna	nicotinic acetylcholine receptor alpha
Clasp1/2	Cytoplasmic linker associated protein 1/2
Clip170	Cytoplasmic linker protein 170
Co-IP	Co-immunoprecipitation
cm	Centimeters
CMFDA	5’chloromethylfluorescein diacetate
CML	Chronic myelogenous leukemia
Creb	cAmp response element-binding protein
CRUK	Cancer Research UK
Csf	Colony-stimulating factor
C-term	C-terminal
CTKD	C-terminal kinase domain
Cxcr4	Chemokine cxc motif receptor 4
DAB	Diamino-benzidine
DAG	Diacylglycerol
DAPI	4',6-diamidino-2-phenylindole
Dapk1	Death-associated protein kinase 1
Deptor	DEP-domain-containing mTor-interacting protein
DMEM	Dulbecco's modified Eagle's medium
DNA	Deoxyribonucleic acid
dNTP	Deoxyribonucleotide triphosphate
DioC6	3,3′-dihexyloxacarbocyanine iodide
DTT	Dithiothreitol
Dusp	Dual specific phosphatases
Eb1	End binding protein 1
ECL	Enhanced chemo-luminescence
ECM	Extra cellular matrix
EDTA	Ethylenediamine tetracetic acid
eEF2	eukaryotic translation elongation factor 2
Egf	Epidermal growth factor
Egfr	Epidermal growth factor receptor
EGTA	Ethylenebis(oxyethylenetrilo)tetracetic acid
EHS	Engelbreth-Holm-Swarm

elF4B	e74-like factor 4 B
Elk1	ETS-like gene 1
Emi2	Endogenous meiotic inhibitor 2
Eml4	Echinoderm microtubule-associated protein-like 4
EMT	Epithelial to mesenchimal transition
ER	Endoplasmic reticulum
Erα	Estrogen receptor α
Erbb	v-erb-b erythroblastic leukemia viral oncogene homolog
Erk	Extracellularly-regulated kinase
EVH	Ena/Vasp homology domain
FAB	G-Actin binding motif
Fak	Focal adhesion kinase
FCS	Foetal calf serum
Fgf	Fibroblast growth factor
Fgfr	Fibroblast growth factor receptor
FH	Formin homology domain
Flna	Filamin A
Fos	fbj murine osteosarcoma viral oncogene homolog
Fra-1	Fos-like antigen 1
g	Gravity
G_1	Gap 1 phase
G_2/M	Gap 2 / mitosis phase
GAB	G-Actin binding motif
GAP	GTPase-activating proteins
Gapdh	Glyceraldehyde 3-phosphate dehydrogenase
GDP	Guanosine diphosphate
GEF	Guanine nucleotide-exchange factor
GFP	Green fluorescence protein
Grb2	Growth factor receptor-bound 2
Gsk3β	Glycogen synthase kinase 3-β
GTP	Guanosine triphosphate
h	Hours
HEPES	N-2-hydroxyethylpiperazine-N'-2-ethanesulphonic acid
Hgf	Hepatocyte growth factor

Hgfr	Hepatocyte growth factor receptor
HNSCC	Head and neck squamous cell carcinomas
Hrp	Horseradish peroxidase
Hsp27	Heat-shock protein 27-kDa
IEG	Immediate early gene
IgG	Immunoglobulin
IκB	Inhibitor of kappa light polypeptide gene enhancer in b cells
Ip	Immunoprecipitation
Jmy	Junction mediating and regulatory protein, p53 cofactor
kDa	Kilo Dalton
Klf8	kruppel-like factor 8
Ksr	Kinase suppressor of RAS
L1cam	L1 cell adhesion molecule
LB	Lysis buffer
LRI	London Research Institute
M	Molar
Map4k4	Mitogen-activated protein kinase kinase kinase kinase 4
MAPK	Mitogen-activated protein kinases
Mek	Mitogen-acivated Erk kinase
MET	Mesenchimal to epithelial transition
mg	Milligram
Mi	Microphthalmia
min	Minutes
µg	Microgram
µL	Microlitre
µM	Micromolar
mL	Millilitre
Mlc	Myosin light chain
Mlck	Myosin light chain kinase
mLst8	mammalian Lethal with Sec13 protein 8
MNF116	pan-cytokeratin mouse monoclonal antibody
Mrlc	Myosin regulatory light chain
mRNA	Messenger ribonucleic acid
mSin1	mammalian stress-activated protein kinase interacting protein 1

Msk	Mitogen- and stress-activated kinases
MT	Microtubule
MTOC	Microtubule organising center
mTor	Mammalian target of rapamycin
mTorC	mTOR complex
Mad1	Mitotic arrest-deficient 1
Myt1	Myelin transcription factor 1
NA	Numerical aperture
Nf1	type I neurofibromatosis
Nfatc4	Nuclear factor of activated T cells calcineurin-dependent 4
Nfat3	Nuclear factor of activated T cells 3
Nf-κb	Nuclear factor of kappa light polypeptide gene enhancer in B-cells
ng	Nanogram
NH_2	Amino terminal domain
Nhe-1	Na+/H+ exchanger protein 1
nNos	neural Nitric oxide synthase
NP-40	Nonidet-P40
NS	Non-specific
NSCLC	Non-small cell lung cancer
NTKD	N-terminal kinase domain
Nur77	Nuclear hormone receptor 77
PAGE	Polyacrylamide gel electrophoresis
Pak	p21/Cdc42/Rac1 activated kinase
PBS	Phosphate buffered saline
Pdgf	Platelet derived growth factor
Pdgfr	Platelet derived growth factor receptor
Pdk1	Phosphoinositide-dependent kinase-1
PFA	Paraformaldehyde
PH	Pleckstrin-homology
Pi3k	Phosphatidylinositol 3-kinase
Pka	cAMP-dependent protein kinase
Pkb	Protein kinase B
Pkc	Protein kinase C

Pkg	cGMP-dependent protein kinase
PIP_2	Phosphatidyl inositol (4,5) bisphosphate
PIP_3	Phosphatidyl inositol (3,4,5) trisphosphate
Plc	Phospholipase C
Plk1	Polo-kike kinase 1
PNEC	Pulmonary neuroendocrine cells
PM	Post-mortem
PPI	Protein-protein interactome
Pras40	Proline-rich AKT substrate 40 kDa
Pten	Phosphatase and tensin homologue deleted on chromosome 10
RPM	Rotation per minute
Rac	Ras-related c3 botulinum toxin substrate
Raf	raf murine leukaemia viral oncogene homolog
RanBP3	Ran-binding protein 3
Raptor	Regulatory-associated protein of mTOR
Ras	Sarcoma virus-associated oncogene
Rassf	Ras association domain- containing family
Rb	Retinoblastoma
Rheb	Ras homolog enriched in brain
RhoA	Ras homolog gene family member A
Rictor	Rapamycin-insensitive companion of mTOR
Rin1	Ras interaction/interference protein-1
RISC	RNA-induced silencing complex
RNA	Ribonucleic acid
RNAi	RNA Interference
RNAse	Ribonuclease
Rock	Rho-associated coiled-coil-containing protein kinase
RpS6	Ribosomal protein S6
R-Ras	Related Ras viral oncogene homolog
Rsk	Ribosomal S6 Kinase
RTK	Receptor tyrosine kinase
RT-PCR	Reverse transcription polymerase chain reaction
S	Synthesis phase
S6k	p70 S6 kinase

Sc	Scramble
Scar	Suppressor of cyclic AMP receptor mutation
SCC	Squamous cell carcinoma
SCLC	Small cell lung cancer
SDS	Sodium dodecylsulphate
SDS-PAGE	Sodium dodecyl sulphate polyacrylamide gel electrophoresis
Sdf 1	Stromal cell-derived factor 1
SEM	Standard error of the mean
Ser	Serine
SH2	src homology domain 2
SH3	src homology domain 3
siRNA	small interfering RNA
SNP	Single-nucleotide polymorphism
Sos	Son of sevenless
SPC	Surfactant Protein C
Src	v-src sarcoma viral oncogene homolog
Srebp1	Sterol regulatory element-binding protein 1
Srf	Serum response factor
Stat	Signal transducer and activator of transcription
Stk11	Serine/Threonine kinase 11
T_a	Annealing temperature
Tcp-1	T-complex protein-1
TEMED	Tetramethylethylenediamine
Tgf-β	Transforming growth factor-β
Thr	Threonine
Tiam1	T‑cell lymphoma invasion and metastasis-1
Titf1	Thyroid transcription factor 1
Tma	Tissue microarray
Tp53	Tumor protein p53
TRITC	Tetramethylrhodamine B isothiocyanate
Tsc	Tuberous sclerosis complex
Tyr	Tyrosine
Tris	Tris(hydroxymethyl)aminomethane

UK	United Kingdom
USA	United States of America
v	Volume
Vcl	Vinculin
Vegf	Vascular endothelial growth factor
Vegfr	Vascular endothelial growth factor receptor
Vim	Vimentin
w	Weight
Wash	Wasp family homologue
Wasp	Wiskott-Aldrich syndrome protein
Wave	Wasp family verprolin homologue proteins
WB	Western blot
Whamm	Wasp homolog associated with actin, golgi membranes and microtubules
Yb-1	Y box-binding protein 1
Zeb1/2	Zinc finger box-binding homeobox 1/2

CHAPTER 1

Introduction

1.1 Cancer

1.1.1 Cancer is a leading cause of death worldwide

Cancer is a leading cause of death worldwide with 7.6 million deaths in 2008. In 2030, cancer is projected to kill 13.2 million individuals worldwide [1] (Figure 1). Yet, cancer burden shows strong inequalities. These include:

- Inequalities between sexes as men are at significantly greater risk than women for nearly all cancer types common to both genders.
- Inequalities between ethnic groups as genetic background influences the propensity to certain cancer types [2]. However, socioeconomic parameters also influence ethnic groups' predisposition to cancer [3].
- Inequalities between developed and developing countries as the proportion of all deaths due to cancer vary from only 4% in Africa to 23% in Northern America. However, the lack of infrastructure to diagnose and register cancer in a developing country might partly explain this discrepancy. Indeed, the real impact of cancer in developing countries might be far higher than reported [4].

In the United Kingdom, cancer was killing one in four persons (21.8%) in 2005 making it the third biggest killer behind cardiovascular and chronic diseases. 2030 projections for the UK show no improvement in this situation with 22.6% of all deaths likely to be attributed to Cancer [5].

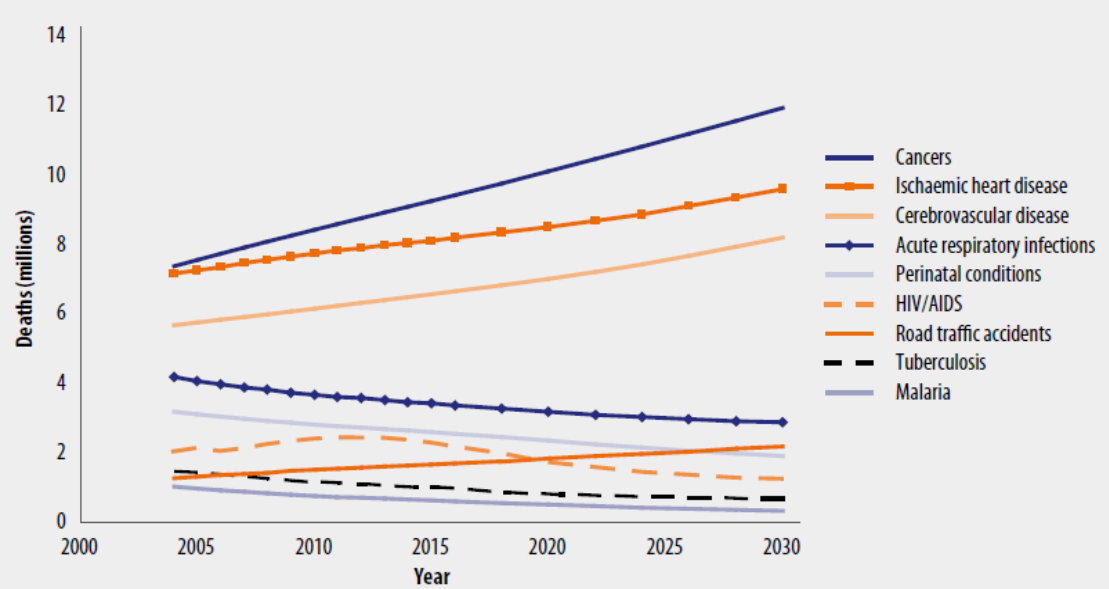

Figure 1: Cancer is a leading cause of death worldwide. (A) Projected global death for selected causes between 2005 and 2030 worldwide. Chart obtain from [6] (http://www.who.int/healthinfo/global_burden_disease/GBD_report_2004update_full.pdf).

The vast majority of cancers (~ 85%) are carcinomas that arise from epithelial cells. To better comprehend this complex disease, it is essential to understand the biology and environment of epithelial cells.

1.1.2 General structure of an epithelium

Epithelial cells constitute the structural unit of epithelia. They show a strong apical–basolateral polarity and the capacity to establish cell-cell contacts with neighbouring epithelial cells as well as with the surrounding extracellular matrix. Epithelia are supported by a semi-permeable basement membrane, a stroma and, depending on the organ, a layer of muscle or bone [7] (Figure 2). Both basement membrane and stroma form the extra cellular matrix (ECM) and are constituted of three types of macromolecules: (1) the fibrous structural proteins, such as the collagens, fibrillin and elastins; (2) the adhesive glycoproteins including fibronectin and laminin; and (3) the gel-forming proteoglycans and hyaluronan. There are important differences in the structure and composition of the basement membrane and stroma (Figure 2).

- **The basement membrane** is a fine layer of 30 to 70 nm made of a network of macromolecules secreted by epithelial and mesenchymal cells. Its main function is to anchor the epithelium to the loose stroma. It consists of a mixture of nonfibrillar amorphous collagen (mostly type IV), laminin, heparan sulphate, proteoglycans, and other glycoproteins [8].
- **The stroma (also called mesenchyme)** takes its name from the Greek word for "bed" or "bed covering". It is a loose connective and supportive framework that hosts the blood and lymphatic vessels allowing the diffusion of nutrient and waste to and from the epithelium, respectively. Various cell types can be found in the stroma such as fibroblasts, immune and inflammatory cells (Figure 2). The composition of the stroma consists of fibrillar (types I, III, V) as well as

nonfibrillar collagens, elastin, fibronectin, proteoglycans, hyaluronan, and other components. Besides its support function for the epithelium, the ECM plays an active role in the epithelium's biology. For example, by sequestering water and minerals, it provides turgor or rigidity to the underlying skeletal tissues. It acts as a reservoir for growth factors influencing directly the proliferation of epithelial cells [9]. During the metastatic process, it constitutes both a mechanical barrier preventing the invasion of the deeper tissue and a substratum allowing malignant cells to adhere and migrate.

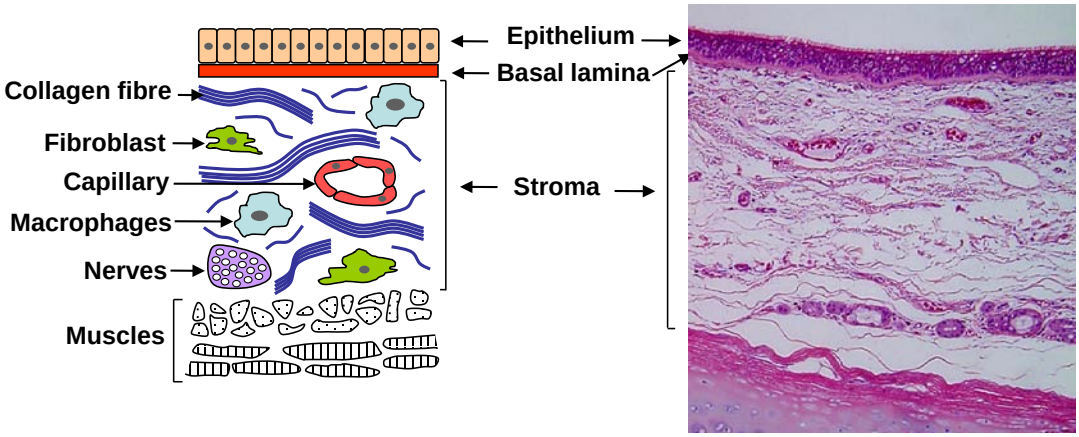

Figure 2: Epithelial cells and their environment. Schematic representation of a prototypical epithelium showing the epithelial and stromal compartments (left panel)**.** Various cell types are highlighted together with structural elements (Modifed from [7]). Right, the corresponding image of an epithelial tissue from the upper respiratory track is stained with haematoxylin and eosin. Haematoxylin reveals the nuclei in blue while the eosin stains the protein rich structures.

1.2 From abnormal growth to metastatic cells

In 1836, Johannes Muller, a German physiologist, showed that tumours were made up of cells [10]. Although the exact mechanisms leading to a cancer are not fully understood and differ between cancer types, several cellular traits are commonly accepted to characterise cancer cells [7, 11]. These include:

(1) Uncontrolled cell proliferation and immortalisation;

(2) Qualitative and/or quantitative changes in the response to growth factor stimulation;

(3) Modifications in cell-cell and ECM-cell contacts that prevent cancer cells from maintaining normal tissue organisation;

(4) Resistance to cell death;

(5) Ability to promote the formation of new vessels (neoangiogenesis) and

(6) Increased tissue invasiveness.

Because of the limited scope of this thesis, we will here elaborate only on the latter process of invasion / metastasis.

1.2.1 The Metastatic process

Metastasis is the spread of a disease from one organ (or part of an organ) to another. Although it was previously believed that the systemic dissemination of tumour cells is associated with advanced disease, recent evidence suggests that appearance of micrometastasis can occur concomitant to the development of early lesions both in mouse and human [12]. In extreme cases, the development at the metastatic site can overtake that of the primary tumour. Hence, in approximately 3% of all cancers the primary tumour is undetectable and the metastatic lesion is classified as a cancer of unknown primary origin (CUP) [13]. One alternative explanation for CUPs may be the spontaneous regression of the primary tumour following the appearance of secondary metastatic sites.

A series of steps are commonly associated with the establishment of metastasis (Figure 3). These include:

(1) Invasion and infiltration of tumour cells into the surrounding tissue and attraction towards nearby blood or lymphatic vessels;

(2) Intravasation into the lumen of the colonised vessel;

(3) Survival in the circulation;

(4) Arrest in the capillary beds of distant organs;

(5) Extravasation and proliferation to form a secondary tumour.

Although breaking the metastatic process into this organised series of steps simplifies its visualisation, the exact process of metastatic invasion remains to be fully demonstrated.

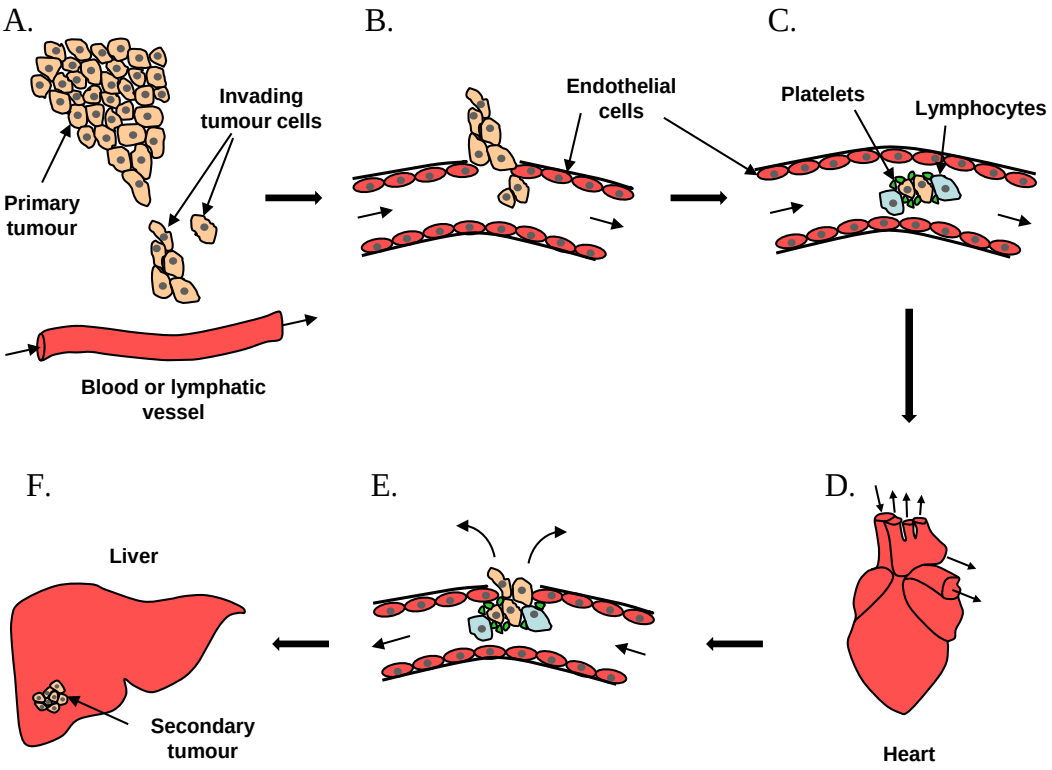

Figure 3: The main steps of the metastastatic process. (A) Invasion and infiltration of tumour cells into the surrounding tissue and attraction towards nearby blood or lymphatic vessels. (B) Intravasation into the lumen of the colonised vessel. (C) Tumour cells interact with circulating host cells including platelets and lymphocytes. (D) Transport of tumour cells throughout the body. Few cells survive this step. (E) Arrest and extravasation in the capillary beds of distant organs. This step may involve circulating host cells that agregate with the tumour cells and form micro emboli. (F) Proliferation to form a secondary tumour (here illustrated in the liver). Figure adapted from [7].

1.2.1.1 Step by step overview of the metastasis process

1.2.1.1.1 Invasion and infiltration of tumour cells into the surrounding tissue

In order to invade the surrounding tissue tumour cells need to acquire increased deformability and/or be capable of breaking-down the basement membrane and the surrounding extra-cellular matrix (ECM). This process has been described for both single cell and multiple cell invasion [14].

1.2.1.1.1.1 Single cell invasion

In the case of single cell invasion, it is proposed that epithelial cells undergo a transition leading to the acquisition of mesenchymal traits. This epithelial to mesenchymal transition (EMT) is characterised by the loss of cell-cell contacts and cell polarity, and acquisition of a mesenchymal appearance with pro-migratory and pro-invasive properties that allow the detachment of the cancer cells from the primary tumour [15]. The EMT and its reverse; the mesenchymal to epithelial transition (MET), are critical processes followed by stem cells during normal development (e.g. gastrulation, neural crest formation and tissue differentiation) [15]. Thus, it has been hypothetised that cancer cell undergoing EMT acquire stem cell-like characteristics [16]. At the molecular level, cells undergoing EMT downregulate the expression of epithelial marker such as E-Cadherin [17] and up-regulate the expression of mesenchymal markers including N-Cadherin, Vimentin and Fibronectin [16]. A number of transcription factors have been identified that orchestrate these changes. These include Snail homologue 1 (Snail) and 2 (Slug), the basic helix-loop-helix Twist and E47, the kruppel-like factor 8 (Klf8) and the zinc finger E-box binding homeobox (Zeb1 and 2) [15, 18-19]. Changes in

expression of these transcription factors correlate with increased malignancy and metastasis in many neoplasms [19] including lung cancer [20]. In keeping with the cancer stem cell hypothesis, it has been proposed that heterogeneous tumours contain a subpopulation of cells (11 to 35%) that show stem cell-like properties and are characterised by high levels of CD44 and low levels of CD24 expression [21]. Further work has proposed that the EMT process generates cells with this molecular signature [16]. However, conflicting evidence presented below suggest that the relevance of this signature might be controversial.

The P-selectin receptor CD24 is an adhesion molecule that facilitates cellular interaction with platelets and endothelial cells [22]. Previous reports showed that high levels of CD24 are associated with poor prognosis in multiple neoplasms including NSCLC [23], breast [24], prostate [25], pancreatic [26] and colorectal cancers [27] and correlates with cancer metastasis. Hence, the reasons why EMT might decrease CD24 protein levels and how this impacts on the metastatic process remain to be clarified.

CD44 is a transmembrane glycoprotein involved in the regulation of cell adhesion, growth, survival, differentiation and motility [28]. Previous studies have highlighted the importance of both CD44 expression and mRNA splicing in cancer. Indeed, the splice variants CD44v4-7 have been linked to metastatic progression [29]. In colorectal cancer, up-regulation as well as specific splicing of CD44 correlates with poor prognosis [30] [31] [32]. However, in neuroblastoma and prostate cancer, the absence of CD44 (including its splice variants) correlates with transformation and poor prognosis [33] [34]. In prostate cancer, over expression of CD44 abrogates metastatic behaviour [35]. Thus, the role of CD44 in metastasis seems to be tissue-specific and depends on both the variants and the total amount of CD44 expressed.

1.2.1.1.1.2 Multiple cell invasion

In the case of multiple cell invasion, invading cells maintain cell-cell contact to form a moving clump. By preserving cell-cell junctions, the cells synchronise their actin cytoskeleton to generate traction and protrusion forces at a multicellular level [14, 36]. This mechanism also called tumour budding has been reported in renal and colorectal cancer [37] [38] [39]. At the molecular level, these cells do not undergo the switch between epithelial and mesenchymal markers characteristic of EMT. Wicki et al. recently highlighted the ability of the small mucin-type transmembrane glycoprotein, podoplanin, to induce collective tumour cell invasion [40]. This correlated with an increase in filopodia formation and the inhibition of small Rho family GTPases [40]. Podoplanin is up-regulated in various neoplasms [40] including lung cancer [41] and correlates with lymph node metastasis [42]. Interestingly, podoplanin is specifically expressed by lymphatic endothelial cells and is widely used as a marker for lymphangiogenesis [43]. Hence, the up-regulation of this protein by malignant tumour cells may reveal a mechanism by which tumour cells mimic the multicellular lymphovascular invasion.

1.2.1.1.1.3 ECM degradation and remodelling

The remodelling of the ECM has been shown to play a critical role in tumour progression and the ability of cancer cells to invade [44-45]. However, there are contradictory reports on the requirement for metastatic cells to use matrix proteases in order to remodel and invade the surrounding tissue [46-47]. At least three parameters will influence the requirement for metastatic cells to harbour proteolytic activity.

(1) **The type of invasion** (e.g. single cell or multicellular) as a single cell will be less affected by the mechanical constraints of the ECM than a clump of cells [44].

(2) **The composition and structure of the ECM surrounding the tumour**. *In vivo* observation of the interstitial tissue has revealed long fibres of collagen together with fibrillar meshwork [48]. The density, spatial alignment and structure of the collagen define the mechanical properties of the ECM and influence the invasion process [49]. Indeed, a low collagen fibre concentration promotes amoeboid type invasion while an increase in collagen fibre density reduces the "pores" size of the matrix forcing the cell and its nucleus to deform. A further increase in collagen fibre density generates a "pore" size below the cell diameter. This may block the invasion process or induce a switch to a proteolytic type of invasion where cells cleave and realign the collagen fibres to form tracks that can then be re-used by following invading cells [45].

(3) **The presence of stromal** cells that can substitute for the need of cancer cells to display proteolytic activity. Stromal cells such as fibroblasts and macrophages have been shown to infiltrate malignant lesions where they participate in the onset of inflammation and provide paracrine factors stimulating cell invasion [50]. Expression of various membrane-bound and secreted proteases confers upon these cells intrinsic invasiveness including ECM remodelling capabilities. By doing so, stromal cells create migration tracks between the tumour and the nearby blood vessels. This remodelling includes the deposition of basement membrane components and changes to the architecture/orientation of collagen fibres [45, 51-52]. Once formed by the stromal cells, these tracks can be followed by tumour cells devoid of intrinsic proteolytic activity thereby promoting tumour cell dissemination [51].

1.2.1.1.1.4 Transcoelomic spread

Malignant cells can escape the primary tumour by invading through the serosal lining of an organ in a process known as transcoelomic spread. Here, malignant cells trigger an inflammatory response resulting in serous exudates that excrete tumour cells into the peritoneal or pleural cavities [53]. From there, tumour cells can colonise other organs contained within the same cavity. This mechanism highlights another way in which tumour cells can use the immune system to promote their metastatic potential. This is a mode of invasion commonly found in ovarian and lung cancer [54]. Indeed, it is noteworthy that a large proportion of lung cancer cell lines have been established from patients' pleural effusions [55].

A. Carcinoma *in situ*

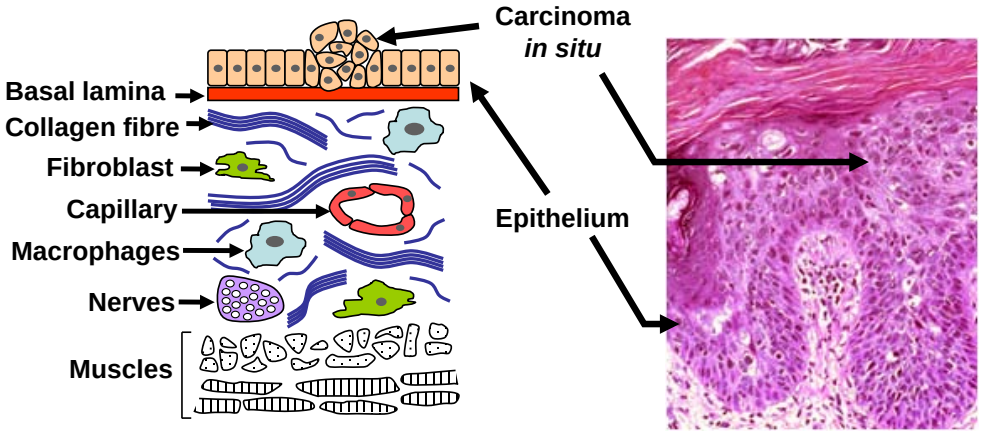

B. Microinvasion

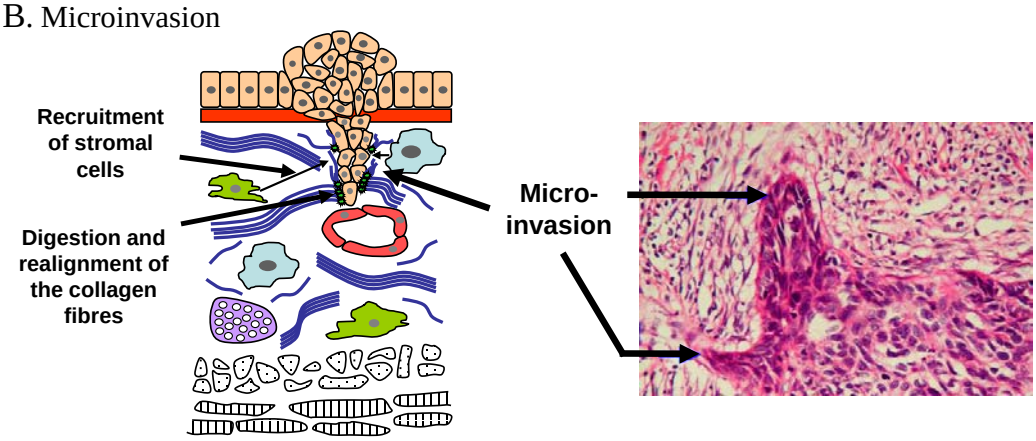

C. Vascular colonisation

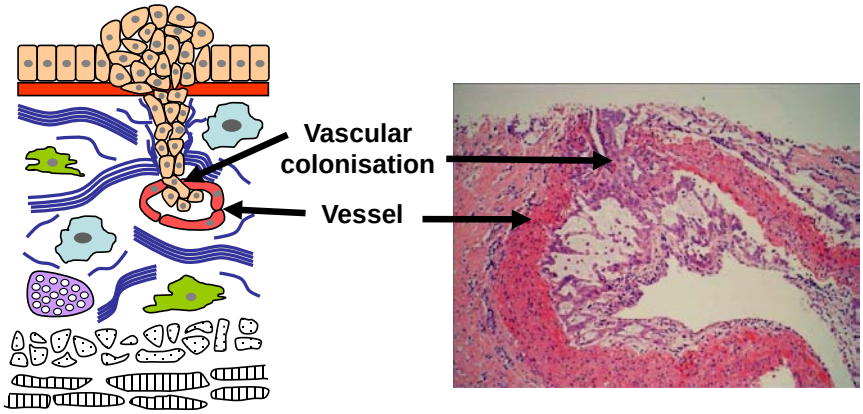

Figure 4: Invasion and infiltration of tumour cells into the surrounding tissue. (A) Carcinoma *in situ* (B) Microinvasion (C) Vascular colonisation. Left panels are schematic representations with various structural components highlighted (For the clarity of the schematic representations, the legend described in (A) is not repeated in (B) and (C). Right panels are representative haematoxylin and eosin staining illustrating these three steps. Haematoxylin reveals the nuclei in blue while the eosin stains the protein rich structures. Magnification of all pictures is not identical. Images were courtesy of Dr Francesco Mauri.

1.2.1.1.2 Intravasation

The increase in the number of new vessels within or adjacent to the tumour correlates with the appearance of metastasis and worsening prognosis [56] [56]. These new vessels usually result from an intense angiogenesis and/or lymphangiogenesis triggered by the tumour. The vessels are characterised by a discontinuous basement membrane, a lack of a surrounding layer of pericytes and poor inter-endothelial junctions. Thus, tumour-associated vessels are disorganised, leaky structures that offer poor resistance to invading tumour cells. Although the increase in hydrostatic pressure commonly observed within the tumour mass goes against the presence of lymphatic vessels within solid tumours, recent studies using specific lymphatic markers have shown the presence of lymphatic vessel around and within tumour masses [57]. This supports clinical observations showing that carcinomas can spread via the lymphatic system to colonise the lymph nodes [58].

Using human tumour cells injected into translucent zebrafish and high-resolution confocal microscopy, Stoletov et al. were able to image the intravasation process [59]. This work has revealed a cross-talk between tumour cells and the vasculature. Indeed, the authors showed that tumour cells develop dynamic actin-based protrusions penetrating the blood vessel wall at sites of vascular remodelling but not at regions of intact vessels. This vascular remodelling requires tumour cells to secrete Vegf and generates portholes for tumour cells to enter the circulation.

Further work using intra-vital imaging in mouse has shown the importance of tumour associated macrophages to promote tumour cell intravasation in the absence of local angiogenesis [52]. In this study, although the macrophages have not been shown to associate directly with tumour cell, they do interact directly with the vasculature and

promote tumour cell intravasation by secreting paracrine factors such as epidermal growth factor (Egf) and colony-stimulating factor 1 (Csf-1).

1.2.1.1.3 Survival in the circulation

Reaching the circulation provides cancer cells with a very efficient way to disseminate. However, circulating tumour cells are exposed to stressful conditions including high pressure, sheer stress, absence of cell-cell or cell-ECM contacts and the presence of immune cells that can potentially detect and eliminate cancer cells. Hence, this step in the metastatic process is very stringent with less than 0.01% of cells successfully initiating a secondary tumour [60], suggesting that the appearance of metastasis is statistically favoured by the high number of circulating tumour cells. This number increases with disease progression and is associated with poor prognosis [61] [62].

1.2.1.1.3.1 Anoikis

Amongst the stress affecting circulating tumour cells is the absence of adhesion to substratum. This usually triggers a cell death programme closely related to apoptosis called anoikis [63] [64]. Indeed, Frisch et al. showed that cells deprived of attachment to the ECM underwent classical apoptosis that could be rescued by overexpression of the pro-survival protein B-cell lymphoma 2 (Bcl2) [63]. Furthermore, they showed that activation of the ECM receptors of the integrin family is critical for cells to resist anoikis. Indeed, the exogenous re-expression of integrins has been shown to protect cells from anoikis by providing survival signals to the cell [65] although different isoforms seem to mediate this effect depending on the cell system considered [65]. Finally, they demonstrated that oncogenic transformation (e.g. overexpression of H-Ras, see section 1.5.1.1) could render epithelial cells resistant to anoikis suggesting that loss of anoikis sensitivity is linked to the malignant process. Three phases can be

distinguished during the apoptotic and anoikic cascade: initiation, effector and degradation [66] [67]. While the initiating insult differs between anoikis and apoptosis, the subsequent effector and degradation phases are common to both processes. Contradictory reports have highlighted the role of various signalling pathways in anoikis, suggesting broad differences amongst cellular systems (reviewed in [68]). Amongst the proteins shown to prevent the initiation phase of anoikis is the neurotrophic tyrosine kinase receptor TrkB [69-70]. TrkB is a membrane located receptor that gets activated upon binding of its ligand, the brain-derived neurotrophic factor (BDNF). Overexpression of TrkB has been shown in several human malignancies, including neuroblastoma, prostate and pancreatic cancer [71]. Ectopic expression of TrkB in epithelial cells has been shown to protect cells from anoikis by promoting growth in suspension of cellular aggregates [69]. This mechanism requires TrkB kinase activity [70].

1.2.1.1.4 Arrest and extravasation into distant organs

The most common places for circulating tumour cells to arrest and form secondary tumours are the lung, liver, brain, and bones. This can be seen as a consequence of a slower local blood flow and the presence of thin capillaries that offer little resistance to invading cancer cells. However, different cancer types will metastasise preferentially to certain organs suggesting that physical constraints are not the only decisive factor in this process. For example, neuroblastoma commonly metastasizes to the liver while osteosarcomas and breast cancer will commonly target the lung. In the case of lung cancer, the main organs affected are in order of preference, brain, bone, liver and adrenal glands. Two hypotheses have been advanced to explain these patterns.

The first hypothesis, called mechanistic theory, was proposed by James Ewing in 1928. It postulated that the anatomy and haemodynamics of the vasculature determine the dissemination pattern of the tumour cells [72]. One supporting evidence for this hypothesis is the case of bowel cancer that frequently spreads to the liver via the portal veins that drain blood flow from the bowel to the liver. However, several facts challenge this hypothesis. Organs such as the kidney and the muscle receive large amounts of blood. Yet they are rarely subject to the development of metastasis. Likewise, breast cancer commonly metastasises to the liver but not to the equally vascularised spleen.

The second hypothesis was proposed by Stephen Paget in 1889 and named the "seed and soil" hypothesis by analogy to plant seeding [73]. Stephen Paget wrote: "When a plant goes to seed, its seeds are carried in all directions but they can only live and grow if they fall on congenial soil." The tumour cells (seeds) will find in some organs a more fertile environment (soil) where to develop a metastasis [73]. This hypothesis was later confirmed by Hart et al. using ectopic transplantation of various organ tissue such as lung and kidney into the muscle mass of a mouse left hind leg. This procedure was followed by intravenous (i.v.) injection into syngeneic mouse of radiolabelled B16-F10 melanoma cells. Using such procedure, Hart et al. were able to show that melanoma cells were equally delivered to the kidney and lung graft but only able to develop metastases in the lung graft [74]. Thus, the blood flow cannot alone explain the organ specificity observed during metastasis.

Further studies have shown that arrest in the capillary beds and extravasation are supported by interaction between tumour cells and host cells such as lymphocytes and platelets forming micro emboli (Figure 3) [75] [76]. However, *in situ* imaging of fluorescently labelled circulating tumour cells in the mouse lung capillary suggests that

neither the interaction with the lymphocytes and platelets nor the extravasation are required for the development of a secondary tumour [77]. Indeed, Al-Mehdi et al. have been able to observe interactions between tumour cells and the capillary endothelium followed by the development of a secondary tumour site within the haematogenous compartment. They suggest that this mechanism is predominant compared to the rare extravasations of tumour cells. Furthermore, they do not observe a passive filtering of tumour cells by the lung capillary but rather an active adhesion of tumour cell to the capillary wall involving actin-based protrusions, called invadopodia, that insert themselves in between endothelial cells. These observations suggest that the reason for organ selectivity during tumour cell metastasis lies at the interface between the tumour cell and the endothelium. Microarray analysis of metastatic lesions in specific organs has highlighted changes in the expression of several genes known to play an active role in the dynamics of the endothelium [78]. These include, the cytokines stromal cell derived factor-1 (Sdf-1) and its receptor the chemokine cxc motif receptor 4 (Cxcr4) shown to be determinant in the homing of prostate cancer to the bone marrow [79]. Similarly, expression of the Platelet-derived growth factor receptor (Pdgfr) at the surface of the endothelial cells is essential for the specific metastasis of hepatocellular carcinomas to the lung as well as that of pancreatic tumour cells to the liver [80] [81]. Hence, while the blood flow might predispose tumour cell dissemination to particular distant organs (as in bowel cancer), molecular determinants seem to dictate the successful colonisation of metastatic sites by circulating cancer cells.

1.3 Cell Motility

Alongside the two types of invasion (e.g. single cell and collective cell invasion), both collective and single cell migration have been described during physiologic processes [14, 82]. During embryonic development, cell migration involving both mechanisms drives gastrulation and organogenesis [14-15]. In the adult, cell migration contributes to tissue regeneration as well as wound healing and immune surveillance. Aberrant acquisition of cell motility has been shown to occur in several pathological processes such as vascular disease, osteoporosis, chronic inflammation, mental retardation and cancer [82]. Identifying the signalling pathways, temporal triggers and/or spatial cues that regulate cell migration during these pathological processes is critical for the development of new therapy.

During metastasis, migration through the tumour microenvironment is mediated by both mesenchymal and amoeboid type migration [83-84]. During amoeboid migration, cells appear rounded and lack mature adhesion foci and stress fibres to create pro-motile traction forces. Instead, the movement is mediated by actin protrusions called blebs that generate propulsive force (Figure 5B) [85]. In contrast, mesenchymal migration is characterised by more elongated cells displaying filopodia protrusions at the leading edge that generate adhesive contact with the surrounding matrix (Figure 5C) [44, 86].

In vivo studies of tumour cell movement have shown increased speed and persistence as compared to their slow random mode of migration *in vitro* [87]. One reason for this difference is thought to lie in the production of a growth factor gradient by the tumour microenvironment that promotes cancer cell migration [87-88]. The presence of ECM components providing an optimal adhesive substratum has also been advanced [48], although, cell migration velocity *in vivo* will heavily depend on the

composition and concentration of these ECM components [45, 89]. Alternatively, cells that migrate away to establish distant metastasis might show inherent genetic differences that distinguish them from other cells within the primary tumour. Isolation of a subpopulation of invasive cells from primary mammary tumours has suggested the existence of a gene expression signature for invasive cells that include a minimum motility machinery [90]. This machinery has been extensively studied using an *in vitro* 2-dimensional migration model [82] leading to the identification of a series of coordinated steps that cells need to perform in order to migrate. These include: (1) cell polarisation, (2) appearance of protrusions at the leading edge, (3) cellular adhesion to the substratum and (4) retraction of the cell trailing edge (Figure 5). Each step involves tightly regulated modifications to the actin and microtubule cytoskeleton and changes in cell adhesion [82].

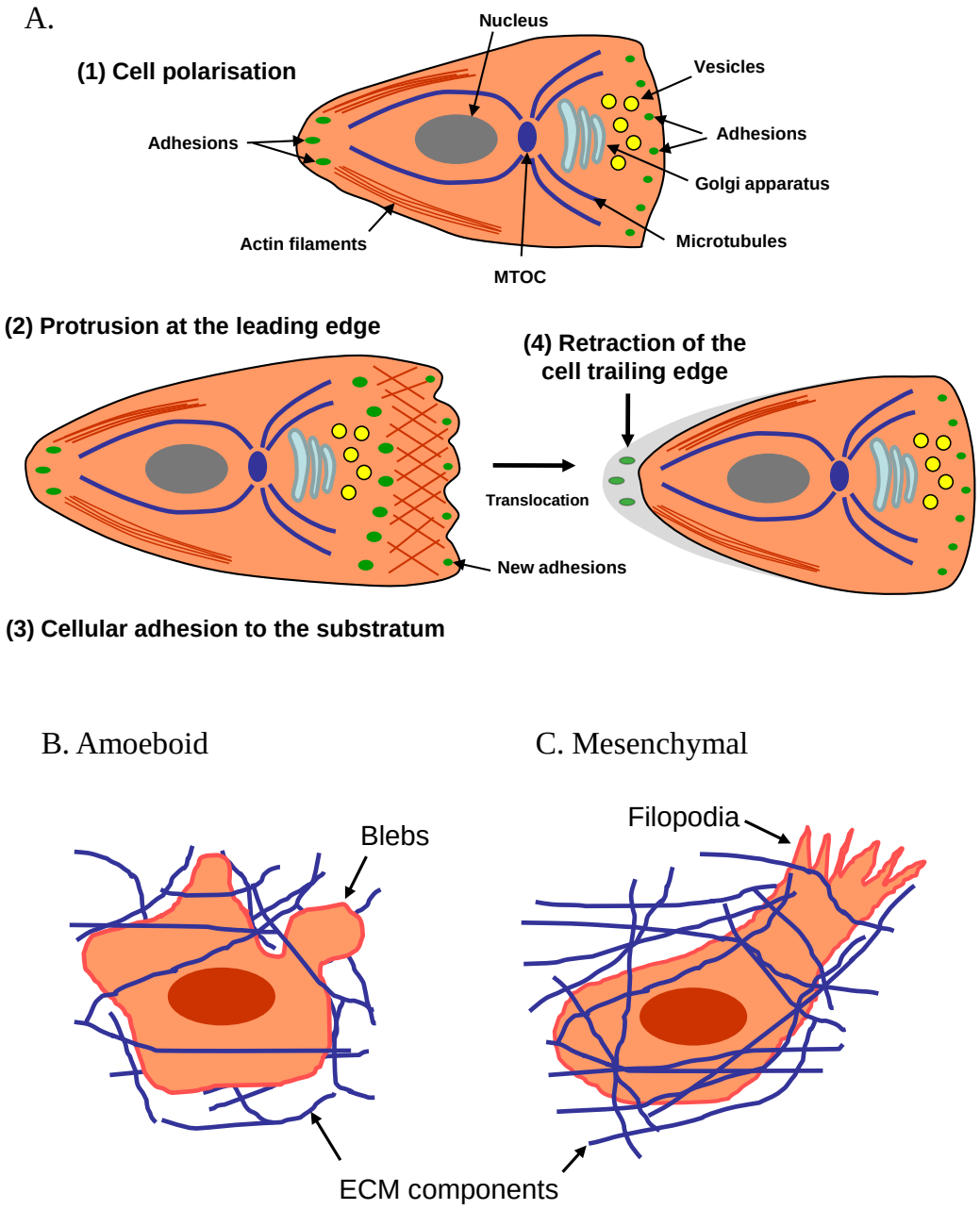

Figure 5: Different types of cellular motility. (A) 2D migration showing a series of four steps. Figure modified from [82]. (B) 3D matrix amoeboid type migration. (C) 3D matrix mesenchymal type migration. (B and C) Extra cellular matrix (ECM) components such as collagen are represented in blue.

1.3.1 Molecular mechanisms driving cell migration

1.3.1.1 Actin Cytoskeleton

Actin is a globular protein that polymerises in a helical fashion to form a polarised actin filament with a fast growing "barbed" end and a slow growing "pointed" end. Actin filaments form a three-dimensional network that provides a mechanical support for cell shape. During cell migration, actin polymerisation enables sheet-like membrane protrusion (lamellipodia), finger-like protrusions (filopodia) and participates to cell junctions [91]. Three main mechanisms drive actin dynamics during cell motility, (1) polymerisation of actin filaments at the leading edge of the migrating cell, (2) depolymerisation of the actin filaments' pointed end and (3) coupling of the actin fibres to myosin II leading to actomyosin contraction [82, 91]. The initiation of new actin filaments is promoted by two main actin nucleators, the actin related protein 2 and 3 (Arp2/3) complex and the Formins [92]. While lamellipodia protrusions are mainly driven by the Arp2/3 complex that generates a dense actin filament network, finger-like filopodia protrusions result from long parallel bundles of actin filament [91-93].

1.3.1.1.1 Arp2/3 mediated actin polymerisation

Arp2/3 complex is an evolutionarily conserved protein complex containing seven polypeptides that include the actin-related proteins Arp2 and Arp3 and five additional subunits, p41 Arp2/3 complex (p41-Arc), p34-Arc, p21-Arc, p20-Arc and p16-Arc [94]. Critical upstream activators of the Arp2/3 complex include members of the Wiskott-Aldrich syndrome protein (Wasp) family. Wasp was initially identified on the basis of its mutations that are responsible for a range of immune system dysfunctions known as the Wiskott-Aldrich syndrome [95]**.** Three groups form the structurally homologous Wasp family in mammals. Wasps (Wasp and N-Wasp); the suppressor of

cyclic AMP receptor mutation and Wasp family, verprolin homologue proteins 1-3 (Scar/Wave1–3); and a newly discovered third group containing the Wasp family homolog (Wash), Wasp homolog associated with actin, golgi membranes and microtubules (Whamm) and the junction mediating and regulatory protein, p53 cofactor (Jmy) [92]. While Wasps are activated by the Rho-GTPase Cdc42 (see section 1.3.1.4) and the membrane lipid phosphatidylinositol 4,5-bisphosphate (PIP2), Scare/Waves appear to be specifically controlled by the Ras-related GTPases Rac proteins. In its inactive state, Wasps are found in a 'closed' auto-inhibited conformation. Upon activation, Wasp switches to an 'open' conformation capable of binding and activating the Arp2/3 complex [92].

Two models have been proposed to explain the mechanism by which actin polymerisation drives membrane protrusion from the Arp2/3 complex (Figure 6).

In the first model (Figure 6A), the activated Arp2/3 complex nucleates to the side of an existing actin filament initiating a new barbed end with a 70° angle from the pre-existing filament [91, 96]. By doing so, Arp2/3 promotes a branched actin filament network driving the formation of sheet-like lamellipodia protrusions [91] (Figure 6A).

In the second model proposed by Urban et al. (Figure 6B), activation of Wasp family proteins at the membrane induce Arp2/3 complex activation in the sub-membrane compartment. The Arp2/3 complex can then initiate a new actin filament from the plasma membrane. This model supports the idea of an un-branched actin filament network as the driving force behind the formation of lamellipodia protrusions [93] (Figure 6B).

1.3.1.1.2 Formin-mediated actin polymerisation

Formins are a large family of proteins containing the two highly conserved Formin homology 1 and 2 (FH1 and 2) domains [97]. These allow Formins to generate a

new filament seed by recruiting actin monomers while remaining continuously associated with the elongating barbed end [98]. This processive association prevents capping proteins from binding to the filament's barbed end to stop actin polymerisation [97]. Furthermore, the association of Formins to the barbed end stimulates the addition of Profilin–actin units (see below) at a 5 to 10 fold faster rate than free-actin monomers [99]. Thus, by promoting the assembly of long actin filaments, Formins cooperate with the Arp2/3 complex to form filopodia and lamellipodia [92].

1.3.1.1.3 Regulation of the actin monomer reservoir by Profilin, Thymosin-β4 and Cofilin

1.3.1.1.3.1 Profilin

Profilin is a small protein (15kDa) that binds actin monomers in a 1:1 ratio. In mammals, four Profilin genes have been identified: Profilin I that is ubiquitously expressed [100], Profilin II [101] predominantly found in the brain and kidney [102] and Profilin III and IV found in the testis [103] [104]. Profilin-actin complexes enable the elongation of the barbed ends of actin filaments at rates similar to free-actin monomers but prevent the binding of actin to the filaments' pointed ends (Figure 6A) [91]. Moreover, Profilin has been shown to bind to the poly-proline rich region of actin nucleators such as the Formins and protein regulating barbed end elongation including N-Wasp and vasodilator stimulated phosphoprotein (VASP) [105] [106]. This binding is critical for Profilin to promote actin filament growth and act as an anti-capping protein [107].

1.3.1.1.3.2 Thymosin-β4

In contrast to Profilin, Thymosin-β4 binding to actin monomer blocks all actin assembly reactions and prevents actin binding to Profilin [91]. Hence, while Thymosin-β4 regulates the actin reservoir, Profilin maintains a pool of actin monomers ready for elongation. This situation is dynamic as both Thymosin-β4 and Profilin exchange actin monomers on a sub-second time scale (Figure 6A) [108] [91].

1.3.1.1.3.3 Cofilin

Cofilin is part of the Cofilin/Actin depolymerising factor (ADF) family that contains several isoforms including Cofilin-1, 2 and ADF. While Cofilin-1 is ubiquitously expressed, Cofilin-2 expression is limited to the muscle [109]. During actin polymerisation, Cofilin activity mediates the severing of actin filament pointed ends. This activity allows the depolymerisation of actin filaments and recycling of actin molecules to the pool of actin monomers [110] [111]. By severing actin filaments, Cofilin also creates new free barbed ends for actin polymerisation at the leading edge [112] [113]. Hence the localisation and regulation of Cofilin activity is critical for directed cell migration [114] [115]. Regulation of Cofilin activity includes its inhibition following binding to PIP2 [116] or Cortactin [109]. Cofilin is also regulated by Lim domain kinase (Limk) phosphorylation that inhibits its binding to actin [117]. These regulation mechanisms are particularly important as the Cofilin pathway has recently been identified as a major determinant of metastasis (Figure 6A) [118].

1.3.1.1.4 Actomyosin contraction

Following the formation of cellular adhesion to the substratum (see section 1.3.1.3), actin filaments establish links between adhesion complexes and interact with myosin II to promote actomyosin-based contraction [119]. This ATP-dependent

phenomenon generates intracellular contractile forces similar to the one observed during muscle contraction. In migrating cells, this mechanism is critical to retract the rear end of the cell [82]. Myosin II activity depends on the state of myosin light chain (Mlc) phosphorylation that is regulated by the opposing action of Mlc Kinase (Mlck) and Mlc Phosphatase. Upstream regulators of this pathway include the Rho Kinase (Rock) which triggers actomyosin-based contraction by both activating Mlck and inhibiting Mlc phosphatase through differential phosphorylation of these two targets [82].

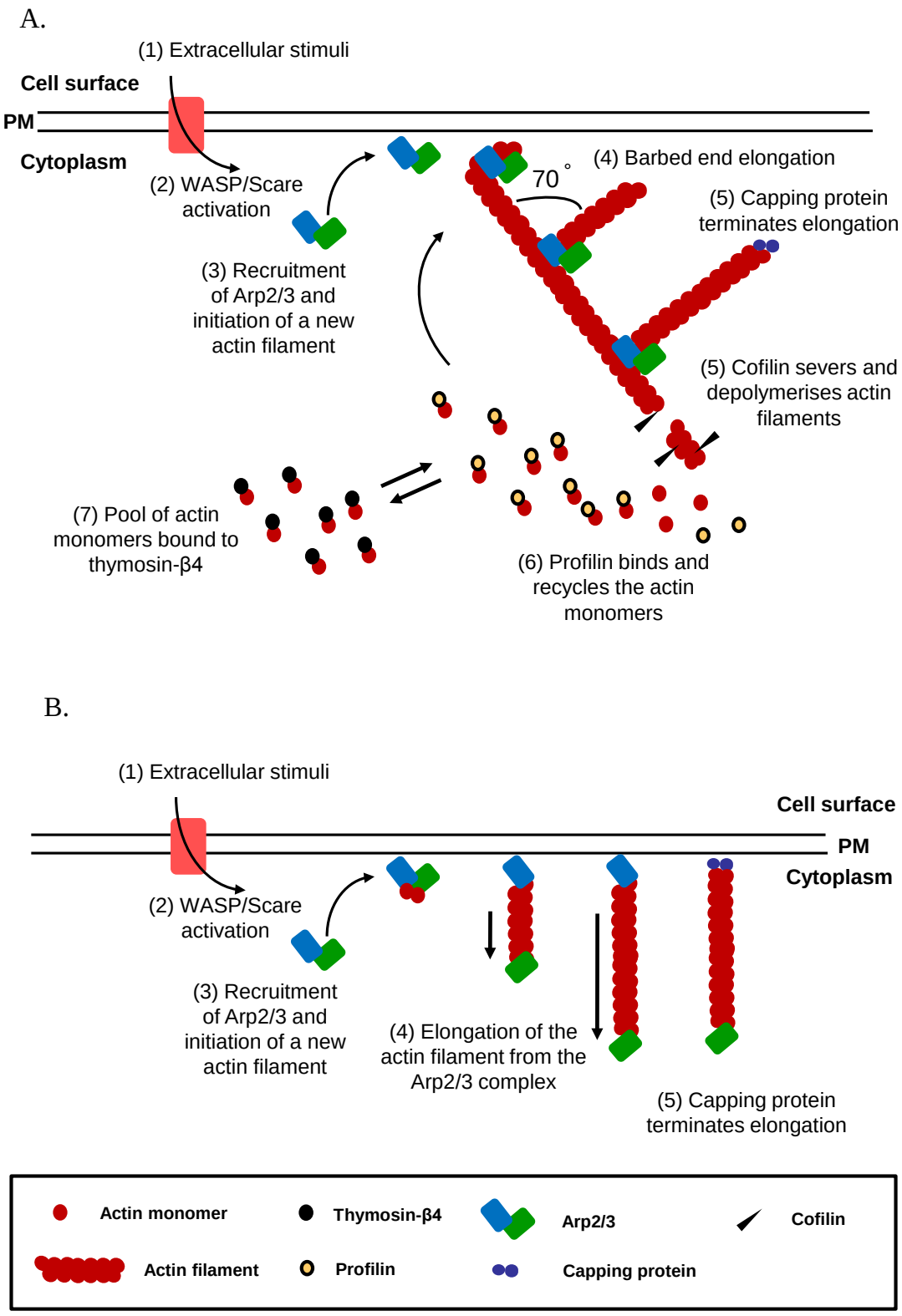

Figure 6: Alternative models of actin polymerisation through the Arp2/3 complex. (A) Dendritic branching view of actin polymerisation [91]. (B) Unbranched view of actin polymerisation [93]. PM: Plasma Membrane. Figure adapted from [91] and [93].

1.3.1.2 Microtubule dynamics

Tubulin is a globular protein that polymerises to form a polarised hollow tube, called microtubule (MT), with a fast-growing "plus" end and a slow-growing "minus" end. MTs form a three-dimensional network in which their minus ends are centralised at the microtubule-organizing center (MTOC) while their plus ends are projected towards the periphery of the cell (Figure 5). During cell migration, the MT cytoskeleton has been shown to play a crucial role in determining cell polarity. Indeed, MTs are required to maintain the polarised distribution of the actin-dependent protrusions at the leading edge allowing for the proper localisation of actin polymerisation- and contraction-based activity [120]. Hence, disruption of MT dynamics leads to the random localisation and reduced amplitude of lamellipodia [121].

MTs also collaborate with the actin-myosin machinery to regulate the localisation of the nucleus, the Golgi apparatus and the Microtubule Organising Center (MTOC) in respect to the leading edge of the migrating cell [120]. The regulation of the MT-driven cell polarity is orchestrated by a complex constituted by the partitioning defective protein 3 and 6 (Par3 and 6) together with the atypical protein kinase Cs (aPkc), Pkcζ and Pkcλ. This complex is activated downstream of the small RhoGTPase cell division cycle 42 (Cdc42) [122]. The "plus end" of MTs is characterised by dynamic instability with successive phases of growth and shrinkage at the periphery of the cell [123]. Recent studies have shown the involvement of MT "plus end" tracking proteins in MT dynamics. The MT "plus end" tracking proteins include the cytoplasmic linker protein 170 (CLIP-170), Adenomatosis polyposis coli (Apc), Cytoplasmic linker associated protein 1 and 2 (Clasp1 and 2) and the End binding protein 1 (Eb1) [124]. They have been shown to promote MT stabilisation at the leading edge, but also MT capture at cortical sites. MT "plus end" tracking proteins also promote relaxation

signals for the focal adhesion complexes in a process that involves dynamin and focal adhesion kinase (Fak) [125]. During the dynamic instability, the targeting frequency of the adhesion foci by the MT is inversely proportional to the focal contact lifetime [120]. Hence, induced depolymerisation of the MT using chemicals such as nocodazole leads to a delay in the normal turnover of the focal adhesion complexes [126] associated with an increased formation of stress fibres [127].

1.3.1.3 Integrin mediated cell adhesion

Integrins are α/β heterodimeric trans-menbrane glycoproteins. Their large ectodomains interact with ECM proteins while their short cytoplasmic tails engage the cytoskeleton [128]. 18 α-subunits and 8 β-subunits of integrins have been shown to assemble into 24 distinct receptors in mammals. These receptors are involved in various adhesion structures including focal adhesion complexes, podosomes, immunological synapses and fibrillar adhesions. The composition and morphology of these structures vary with the cell type, ECM and integrin considered.

Focal adhesion complexes, also known as adhesion foci, are molecular complexes that link the ECM to the actin cytoskeleton via integrins. These assemble and disassemble in response to intra- and extra-cellular cues. During cell migration, a quick turnover at the leading edge is associated to nascent adhesion foci. Pre-existing adhesions can stabilise and grow into larger complexes called focal adhesions [129]. At the opposite end of the cell, the disassembly of focal adhesions triggers the retraction of the trailing edge through actomyosin-based contraction. However, the size and dynamics of the adhesion foci highly depend on the cell type (slower or faster-moving cells) and microenvironment (*in vivo*, 3D ECM or *in vitro* 2D culture dishes) considered [83]. Over 50 different components have already been identified at focal adhesions including Fak, Src, Talin, Vinculin, Paxillin, and p21/Cdc42/Rac1 activated

kinase (Pak) [130] (Figure 7). Some of these molecules enter the adhesion site with the same kinetics suggesting that they exist as part of preformed cytoplasmic complexes. The recruitment of other components such as Talin and Paxillin follow a faster kinetic profile that is consistent with nascent adhesions [131]. Post-translational modifications of some of these components also regulate the dynamics of these foci. Indeed, phosphorylation of Paxillin by the Fak-Src complex correlates with the turnover of existing focal adhesions [129, 132]. The molecular mechanisms regulating the dynamics of adhesion complexes are controlled by feedback signalling from adhesion-related proteins themselves as well as actin, MT associated proteins and small GTPases. Adhesion disassembly is achieved through dissolving of these complexes by phosphatases such as calcineurin, or by proteolysis of some adhesion components including talin by proteases such as Calpain [133]. The activity of both calcineurin and calpain is calcium dependent. Thus, the intracellular calcium concentration is a key modulator of adhesion disassembly.

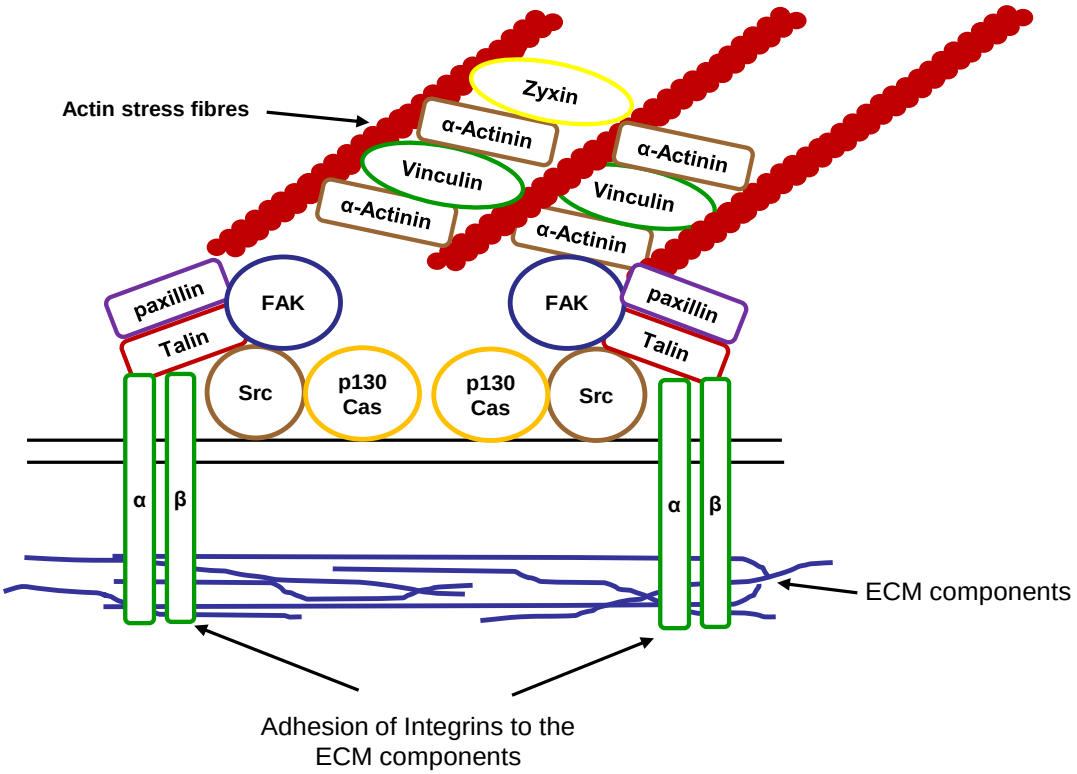

Figure 7: Structure of a Focal Adhesion complex. The α- and β-Integrin subunits (α and β on the scheme) cluster to link the extracellular matrix with the actin cytoskeleton. Following integrin clustering, the recruitment of Paxillin and Talin leads to the binding of Fak, Src, p130Cas and vinculin to the focal contact. α-Actinin, an actin filament-bound protein phosphorylated by Fak, crosslinks the actin stress fibres and connects them to the focal contact by binding Vinculin. Zyxin joins the mature focal contacts by binding both α-Actinin and the stress fibres. Figure modified from [134].

1.3.1.4 Rho-GTPase signalling and the regulation of cell migration

Small Rho-GTPases are molecular switches that control a variety of cellular processes [135]. They cycle between two conformational states; the GTP-bound or activated state and the GDP-bound or inactivated state. Small GTPase activity is promoted by Guanine exchange factor (GEFs) and inhibited by GTPase activating proteins (GAPs). Once activated, the Rho-GTPases can interact with their downstream targets which include protein kinases or lipid modifying enzymes [135-136]. The Rho-GTPase family includes Rac1, Cdc42 and RhoA that have been implicated in each step of cell migration [136].

During cell polarisation, Cdc42 through its interaction with Par6 and atypical Pkcs regulates the repositioning of the MTOC and Golgi apparatus toward the leading edge.

During actin-based membrane protrusion RhoA and Cdc42 respectively regulate the two formins mDia1 and mDia2 while Rac1 activates the Wasp/Scar complex leading to actin polymerisation.

During cell adhesion, Rho-GTPases are critical effectors controlled by signals emanating from adhesion-related signalling molecules such as Fak, Src, Paxillin, and Pak.

During Actomyosin-based contraction Cdc42, Rac and RhoA play antagonistic roles [137]. RhoA activates Rock and Cdc42 activates Mrck (myotonic dystrophy kinase-related Cdc42-binding kinase) to promote contractility [138]. Conversely, Rac activates Pak, which phosphorylates and inactivates Mlc kinase, thus leading to decreased contractility and increased cell spreading. However, Pak can also phosphorylate Mlc directly, resulting in increased contractility.

Interestingly, recent studies have shown that Mena, a member of the actin-binding proteins family Ena/Vasp interacts with and regulates the activity of Rac1 [139]. The Ena/Vasp family has been shown to play a crucial role during cell migration and invasion [107, 140].

1.3.1.5 Vasp, Mena and Evl

The Ena/Vasp family of actin-binding proteins is involved in various processes including cell migration, cell-cell contact, phagocytosis and neurite outgrowth [107, 141-142] by remodelling and promoting actin filament formation [143-144]. Three human family members exist; Mena, Vasp, and Evl. Their overlapping function is modulated by both homo- [145-146] or hetero-tetramerisation [147] [148] and phosphorylation events [149]. In migratory cells, they localise within cellular compartments where actin polymerisation takes place. These include the adhesion foci, the rim of the lamellipodium and the tips of filopodia [144]. Structurally, Ena/Vasp family members share conserved functional domains including a central proline-rich region surrounded by two Ena/Vasp homology domains 1 and 2 (EVH1 and 2) (Figure 8A). While the EVH1 domain is crucial to localise Ena/Vasp to the focal adhesion complexes by interacting with proteins such as Zyxin and Vinculin [150] [151], the EVH2 mediates the binding of this protein to F- and G-actin [145, 152]. The central proline-rich region is required for the binding of profilin [153]. Finally, the C-terminal extremity of the EVH2 domain contains a tetramerisation site mediating the oligomerisation of Ena/Vasp family members [145, 147]. Three main phosphorylation sites have been described to regulate Vasp function (Figure 8). These are the Ser-157 (conserved in Mena and Evl) and Ser-239 (conserved in Mena only) characterised as cAMP/cGMP-dependent protein kinase (Pka/Pkg) substrates [149] [154] and the Thr-278, targeted by the AMP-activated protein kinase (Ampk) (Figure 8A) [155] [149]. While Ser-157 phosphorylation mainly regulates Vasp localisation to the plasma

membrane and adhesion foci, the Ser-239 and Thr-278 influence Vasp-driven actin filament formation [149].

Although, the exact mechanisms of action of the Ena/Vasp family members remain controversial, these protein have been shown to promote F-actin assembly using anti-capping [156] [157], anti-branching [158] [159] and bundling [145] [160] [161] activities and promoting profilin-actin recruitment [162]. Also, Ena/Vasp proteins have recently been involved in directing the E-cadherin/catenin complexes to cell-cell contacts [141, 163] as well as in the integrin-mediated control of cell adhesion and migration [164].

Triple knockout mice for Vasp, Mena and Evl are lethal after embryonic stage E16.5 [165] demonstrating that these proteins are required for normal development. Study of the early embryos revealed a lack of axon fibre tract formation during corticogenesis resulting in exencephaly and cobblestone cortex [165]. This severe neuronal phenotype was supplemented by disruption in endothelial barrier function. Indeed, loss of Vasp, Mena and Evl disrupted stress fibre formation, compromising actinomyosin contraction and resulting in weakened cell-cell junctions [166]. Surprisingly, reintroduction of a single Mena allele was sufficient to recover viability and fertility in these mice (although with reduced frequency). However reintroduction of two Vasp or two Evl alleles was not sufficient to recover viability. Thus Mena appears to be critical for survival [165]. Mouse models with disrupted expression of individual Ena/Vasp family members are viable and present with only minor defects suggesting a partial functional overlap between family members. Vasp knockout mice show reduced, cAMP- and cGMP-mediated inhibition of platelet aggregation [167] as well as a hyperplasia of megakaryocytes in the bone marrow and the spleen [168]. Mena-deficient mice suffer from neuronal malformations due to a defect in axon guidance during neurulation and commisure formation [169]. Finally Evl knockout mice did not

have an obvious phenotype [165]. In cancer, increased expression of Ena/Vasp family members has been shown to enhance tumour cell invasiveness *in vitro* and *in vivo* [140, 170] and correlates with tumour progression in several malignancies [170-172], including lung adenocarcinoma [173].

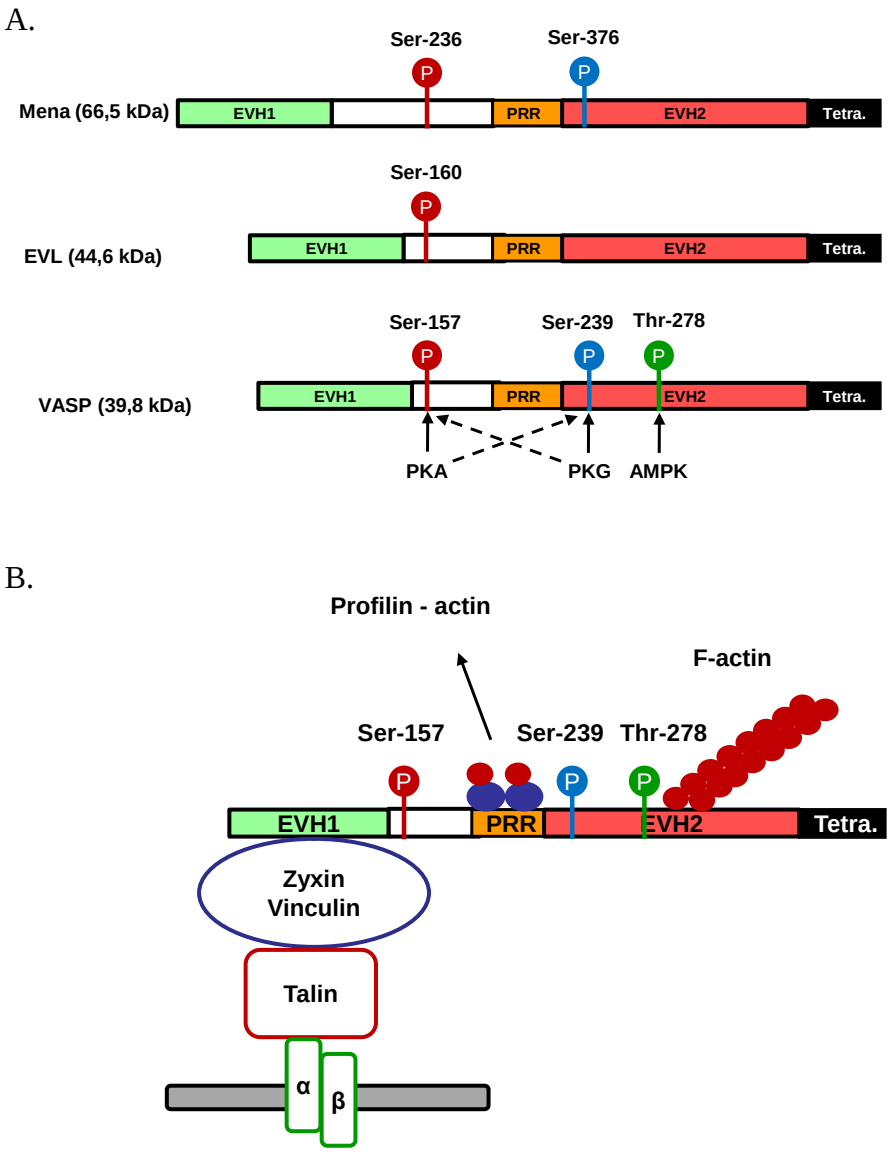

Figure 8: Ena/Vasp family members. (A) Conserved functional domains of the Ena/Vasp family members. (B) Model of regulation of Vasp activity by phosphorylation. Vasp binds to Vinculin, Zyxin and Profilin irrespective of its phosphorylation status and localises to the focal adhesion complexes. Phosphorylation of Ser-157 affects mainly Vasp localisation while phosphorylation of Ser-239 or Thr-278 disrupts its ability to induce F-actin polymerisation. α and β stand for the two integrin subunits [149]. (Figure modified from [154])

1.4 Modulation of the cell migration machinery

1.4.1 Kinases and phosphorylation

Cells have developed various levels of control to modulate the motility machinery. Amongst these, changes in the phosphorylation status of molecular effectors play a central role. Systematic analysis of the human genome for sequence similarity has revealed 518 kinases classified in 134 families [174]. Phospho-proteomic analysis performed in the quiescent cervical cancer HeLa cell line revealed 6,600 phosphorylation sites on 2,244 different proteins with a relative distribution of 1.8% phosphotyrosine, 11.8% phosphothreonine and 86.4% phosphoserine [175]. Stimulation of these cells with the promigratory chemo-attractant, epidermal growth factor (Egf) modulated 14% of these phosphosites by at least 2 fold, highlighting the scale of changes in phosphorylation events in response to this growth factor [175].

The addition of a phosphoryl group modifies the overall charge of a protein leading to changes in its 3-dimensional structure and its affinity to binding partners. In turn, these changes will modulate the activation status or the subcellular localisation of the target proteins [176]. These changes are dynamic as phosphorylations are reversed by another family of proteins, the phosphatases, that catalyses the hydrolysis of the phosphoryl groups.

Abnormal activity of kinases can drive cancer progression as demonstrated by the fusion protein Breakpoint cluster region-Abelson murine leukemia viral (Bcr-Abl) responsible for the chronic myelogenous leukemia (CML) [177] or Egfr mutations in various malignancies [178]. While phosphatases demonstrate a low specificity, kinases harbour a relatively high degree of stringency for their substrates [176]. Hence, kinases are very amenable targets for therapeutic drug discovery [179]. A number of signalling

pathways have been involved in the regulation of the motility machinery [82]. Amongst these are the Ras/Raf/Mek/Erk signalling pathway also called mitogen activated protein kinase (MAPK) pathway and the Pi3k/Pten/Pkb/mTor signalling pathway.

1.5 The main signalling pathways of cancer

1.5.1 The MAPK signalling pathway

MAPK signalling is evolutionarily highly conserved [180]. Figure 9 shows a simplified representation of the pathway. A wide range of stimuli have been shown to initiate its activation leading to various biological outcomes including cell migration, differentiation, proliferation, survival and metabolism (reviewed by [181] and [182]) (Figure 9).

Amongst the many proteins capable of initiating the activation of the MAPK pathway are the membrane-localised receptor tyrosine kinases (RTKs). Activation of these receptors involves ligand binding to their extracellular part and subsequent dimerisation (except for the insulin and hepatocyte growth factor (Hgf) RTKs which pre-exist as dimers). Once activated, the receptors undergo allosteric rearrangement leading to auto- and trans-phosphorylation of tyrosine residues within their cytoplasmic tail [183-185]. These phosphotyrosine residues act as docking sites for the src homology-2 (SH-2) domain-containing proteins [186] including adaptor proteins (Nck, Grb2), scaffolds (slp76, Shc), kinases (Btk, Src, Fps), phosphatases (Shp1/2), phospholipases (PLCγ) and transcription factors (Stats) [187]. Upon recruitment to the receptor, these molecules propagate the signal to downstream effectors. For instance, following binding to the RTK, Grb2 recruits Son of sevenless (Sos) via its SH3 domain [188]. Sos, as a GTP exchange factor (GEF), activates the small rho GTPase p21 Ras (Ras) by exchanging the GDP bound to Ras (GDP-Ras inactive) for a GTP (GTP-Ras

active). The reverse inactivating reaction is catalysed by GTPase activating proteins (GAPs) such as type I neurofibromatosis (NF1) that hydrolyse the GTP to GDP [189] [190]. Upon activation, Ras binds the N-terminal part of p74 Raf (Raf) and promotes its activation [191] [192] [193] [194]. Activated Raf in turn phosphorylates and activates mitogen activated protein kinase kinase also known as the dual-specificity protein kinases 1 and 2 (Mek1/2, the term Mek will thereafter refer to both isoforms, unless specified) [195] [194] [193]. Similarly, Mek activates p42 and p44 mitogen activated protein kinase (p42/44MAPK) also known as extracellular signal regulated kinases 1 and 2 (Erk1/2, the term Erk will thereafter refer to both isoforms, unless specified). Once activated Erk1/2 can phosphorylate a variety of substrates in all cellular compartments. These include various plasma membrane proteins (CD120a, Syk, and Calnexin), cytosolic proteins (eg. Rsk1/2/3/4, Msk1/2, the term Rsk and Msk will refer to both isoforms, unless specified), cytoskeletal proteins (e.g. Neurofilaments protein, Paxillin) as well as nuclear substrates such as transcription factors (e.g. Paired box gene 6 (Pax6), Nuclear Factor of Activated T Cell (Nfat), Elk-1, Mad box transcription enhancer factor 2 (Mef2), c-Fos, c-Myc and Signal Transducer and Activator of Transcription 3 (Stat3)) [196-197]. The ability of Erk to interact with such a diverse range of substrates is explained by the wide representation of the two Erk docking sites, D-domain and DEF domain within the proteome [197-198] (Figure 9).

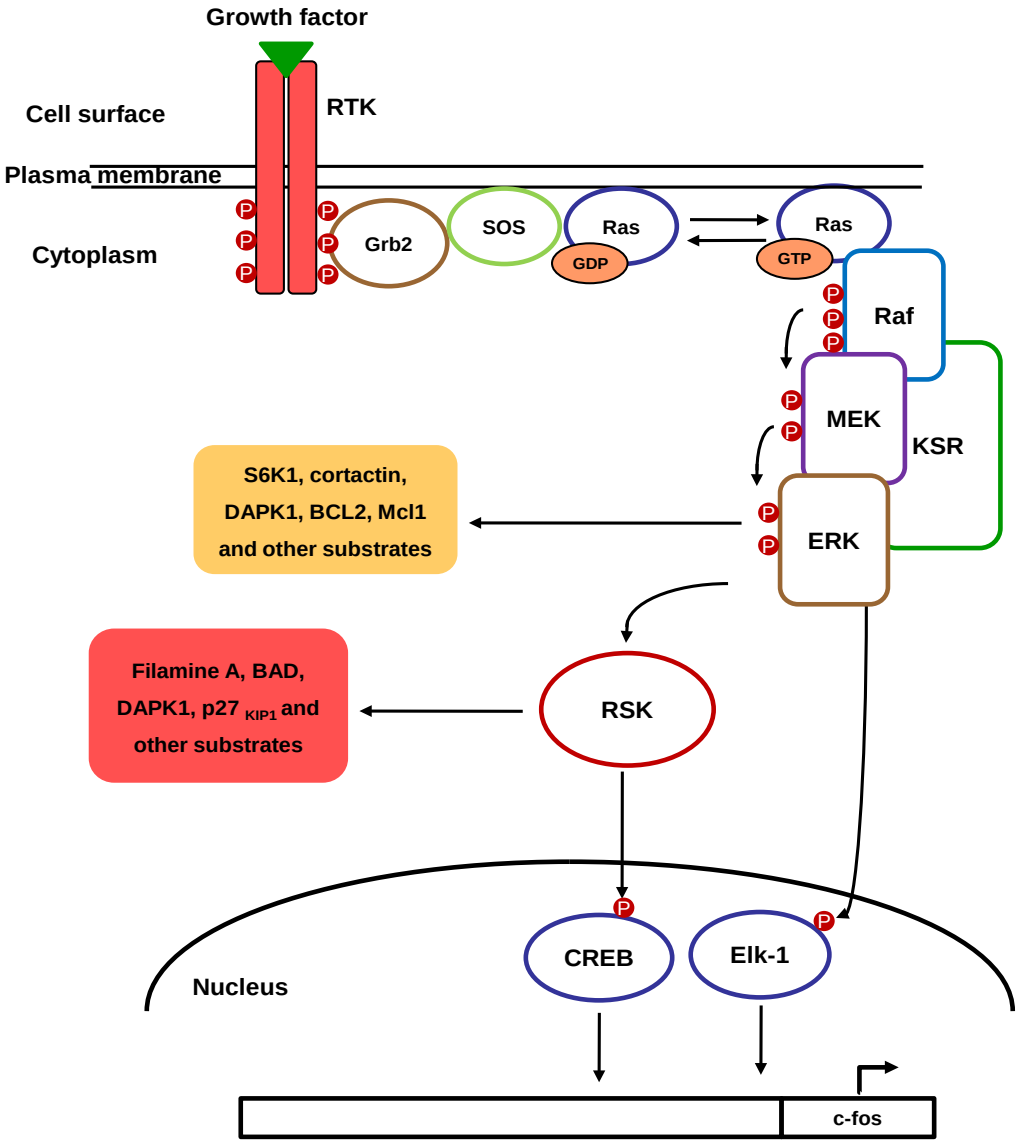

Figure 9: Schematic representation of the MAP Kinase pathway activated by a receptor tyrosine kinase (Rtk). Grb2; Growth factor receptor-bound 2, Sos; Son of Sevenless, Raf; Raf murine leukaemia viral oncogene homolog, Mek; Mitogen-acivated Erk kinase, Erk; extracellular signal regulated kinase, S6k1; p70 S6 kinase, Dapk1; Death-associated protein kinase 1, Bcl2; B-cell leukaemia/lymphoma-2, Mcl1; Myeloid cell leukemia sequence 1, Bad; Bcl2-associated agonist of cell death, Creb; cAmp response element-binding protein, Elk-1; ETS-like gene 1, c-fos; cellular-fbj murine osteosarcoma viral oncogene homolog. Figure modified from [182].

.

The apparent simplicity of this linear canonical MAPK signalling representation hides complexity at each levels of this pathway.

Several mammalian isoforms exist for each signalling intermediate. This applies to both the RTKs of which more than 50 have been cloned [184, 199] and downstream signalling mediators (H/K/N-Ras, A/B/c-Raf, Mek1/2, Erk 1/2/3/5). Although these isoforms are closely related, they can have very selective functions. For example, Erk2, but not Erk1, has been shown to specifically mediate a pro-invasive programme [200].

The spatial localisation of the proteins taking part in the pathway. Post-translational modifications such as farnesylation allow the recruitment of Ras in close proximity with the RTK adaptors and are required for Ras activity [190]. In the cytosol, co-localisation of these signalling intermediates is mediated by scaffolding proteins such as Kinase suppressor of Ras (Ksr) that simultaneously bind Raf, Mek and Erk [182]. On the other hand, the focal adhesion protein Paxillin harbours scaffolding properties similar to Ksr by binding Raf, Mek and Erk. Once activated, Erk can phosphorylate Paxillin to promote the binding of focal adhesion kinase (Fak). Hence paxillin can specifically localise MAP Kinase activity to focal adhesions in order to regulate their turnover.

The duration and amplitude of the signal mediated by the MAP Kinase pathway affects its biological function. Transient stimulation of the pathway (e.g. by the epidermal growth factor receptor (Egfr) and Insulin receptor) in the neuronal cell line PC12, stimulates cell proliferation while sustained and robust MAPK stimulation (e.g., by nerve growth factor receptor (Ngfr), fibroblast growth factor receptor (Fgfr)) promotes neuronal differentiation in the same cell system. Thus, the biological outcome of activating this pathway can be determined by signal strength and duration [180, 184,

201]. One explanation for this is the ability of Erk proteins to become bistable. According to Markevich et al. : “A system is termed bistable if it can switch between two distinct stable steady states but cannot rest in intermediate states”. The transition from one state to the other is mediated by a stimulus that must exceed a predetermined threshold [202]. The passage of this threshold switches the protein to an activated steady state at which it remains in absence of stimulus [202]. This process is tightly regulated by feed-back loops initiated by phosphatases such as the dual-specificity protein phosphatases (Dusp1 and 6) [202] [203]. Other feed-back loops affecting specific growth factor-mediated pathways have also been identified. These include the Sprouty and Spred protein families identified as transcriptionally-induced inhibitors of Fgf signalling. This effect is mediated by the binding of these proteins to and inactivation of B-Raf in an Fgf dependent manner [204].

Mutations within the Ras-Mek-Erk pathway have been reported in greater than 30% of human cancers [205]. These are typically gain of function mutations in components located upstream of Erk1/2, such as RTKs, Ras and Raf [190] [206]. Although all these mutations will lead to increased Erk activation, the effective outcome will depend on the nature of the upstream mutation. For example, cells harbouring a mutation of the valine 600 to a glutamic acid (V600E) in B-Raf will display a specific transcriptional response that differs from that elicited by Ras or RTKs mutations [204].

1.5.1.1 Ras

The Sarcoma virus-associated oncogene Ras is part of a family of small GTPases made of 39 proteins [207]. Similarly to small Rho-GTPases, Ras behaves as a molecular switch with an active (GTP-bound) and inactive (GDP-bound) state (see section 1.3.1.4). Once activated, Ras has been shown to interact and activate various downstream target such as the phosphatidylinositol 3-kinase catalytic subunit

(Pi3KCA) [208], c-Raf [209], phospholipase Cε [210] the Rac-specific GEF T-cell lymphoma invasion and metastasis-1 (Tiam1) [211] (reviewed by [207]) (Figure 10). The variety of these downstream targets explains the involvement of Ras in multiple cellular processes ranging from cell growth, differentiation, survival, endocytosis, cytoskeleton remodelling and motility. Amongst the Ras family, three main members, Harvey- (H-), Kirsten (K-) and Neuroblastoma (N-) Ras share a high degree of homology (85% Amino acid sequence identity) and are widely expressed [190].

1.5.1.1.1 Oncogenic Ras mutations

H-, K- and N-Ras have been found to have activating mutations in 20% of human cancers. Amongst these mutations, 85% are found in K-Ras, 15% in N-Ras and less than 1% in H-Ras (reviewed by [207], [190] and [212]). These mutations inhibit Ras GTPase activity and prevent GAP induced hydrolysis of Ras-bound GTP resulting in the accumulation of active Ras. Ras activating mutations have been shown to drive several fundamental oncogenic traits including uncontrolled cell proliferation, resistance to programmed cell death, and increased invasiveness [190]. The accumulation of these oncogenic traits is commonly named cellular transformation. Increased Ras activation can also be mediated by mutation in Ras associated GAP protein such as Nf1 [213]. Indeed Nf1 mutations are frequent in human cancer including NSCLC [206, 214].

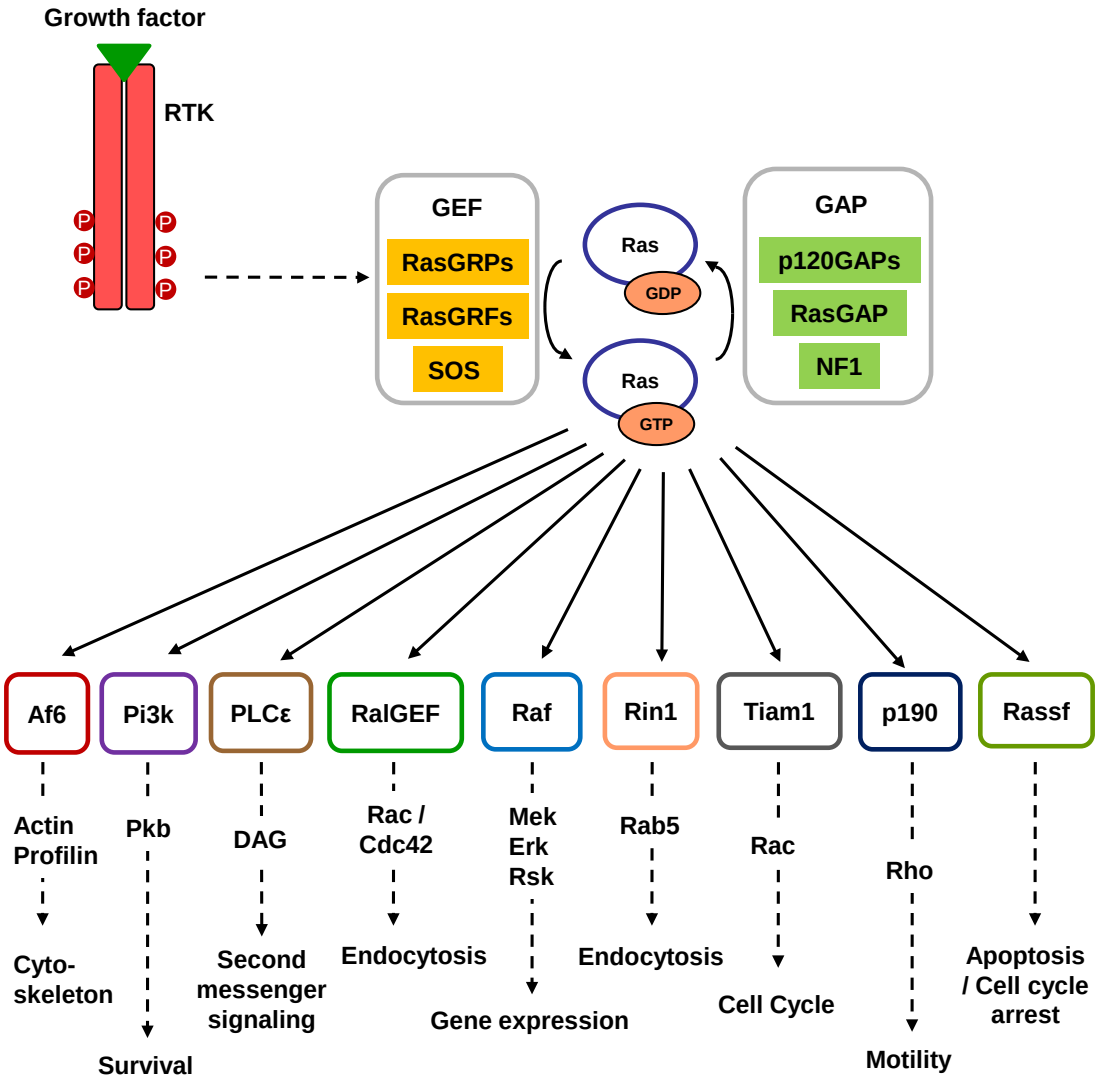

Figure 10: Ras signalling pathway. Schematic representation of Ras signalling pathway downstream of activation by a receptor tyrosine kinase (RTK). Activation of Ras is mediated by the ejection of the GDP to facilitate the loading of the GTP. This is catalysed by guanine-nucleotide exchange factors (GEFs) such as son of sevenless (Sos) or GTP-releasing proteins/factors (RasGRPs or RasGRFs). Conversely, Ras inactivation is mediated by its intrinsic GTPase activity that cleaves off the loaded GTP into GDP. This activity is promoted by GTPase-activating proteins (GAPs) such as p120GAP, RasGAP or type I neurofibromatosis NF1. Upon activation, Ras interacts with multiple downstream effectors. Representative Ras effectors are indicated together with downstream effectors and the main function being regulated. Af6, acute lymphoblastic leukaemia-1 fused gene on chromosome 6; Cdc42, cell division cycle-42; DAG, Diacylglycerol; Erk, extracellular signal regulated kinase; Mek, mitogen-activated protein kinase/Erk kinase; Pi3k, phosphoinositide 3-kinase; Pkb, protein kinase B; Plcε, phospholipase Cε; Rassf, Ras association domain- containing family; Rin1, Ras interaction/interference protein-1; Tiam1, T-cell lymphoma invasion and metastasis-1. (Figure adapted from [207])

1.5.1.1.2 Other Ras family members

Other family members include the related Ras viral oncogene homolog (R-Ras) subfamily that share over 50% of homology with H- K- and N-Ras [215]. Similarly to H-, K- and N-Ras, R-Ras proteins can promote cell growth, transformation and impair cellular differentiation [216] via common downstream effectors such as phosphatidylinositol 3-kinase [217]. However, in contrast to other Ras family members, activated R-Ras binds but does not activate Raf and thus does not induce Erk activation [218] [217]. Furthermore, R-Ras activation is independent of the ubiquitous Ras GEF Sos [219]. Instead, R-Ras gets activated by the Ras protein-specific guanine nucleotide-releasing factor 1 and 2 (RasGFR1 and 2) [216]. Another R-Ras specificity is the capacity to promote integrin-mediated cell adhesion in contrast to H-Ras that suppresses integrin signalling via c-Raf [220] [221]. Moreover, R-Ras has been shown to regulate Rac1 and modulate cell motility, invasiveness and metastasis [222] [223].

1.5.1.1.3 Ras localisation

Once synthesised in the cytoplasm, Ras family members undergo multiple post-translational modifications. First, a farnesyl isoprenyl lipid is added to Ras C-terminal CAAX sequence by a farnesyltransferase that address Ras to the endoplasmic reticulum (ER) where the AAX amino acids are removed and the new C-terminal cysteine residue is methylated. While this modification is enough to address K-Ras to the inner part of the plasma membrane, H-Ras and N-Ras travel to the Golgi where one or two palmitate chains are added to them before shuttling to the plasma membrane [224]. Upon localisation to the membranous compartment Ras family members can interact with their activators, receptor-associated adaptator proteins (e.g. Sos) and downstream targets (e.g. Raf and Pi3k) [190] [207]. In the case of K-Ras, further phosphorylation by

protein kinase C (Pkc) within its polybasic region relocalises K-Ras to the intracellular compartments including the endoplasmic reticulum (ER) and the outer membrane of the mitochondria. The later localisation allows K-Ras to interact with Bcl2-related protein, long isoform (Bcl-X_L) and induce apoptosis [225]. K-Ras recycling from the plasma membrane can also be promoted by the calcium dependent Calmodulin that sequesters the polybasic domain of K-Ras [226]. On the other hand, H- and N-Ras can be re-localised to the Golgi apparatus following depalmitoylation at the membrane [224]. This re-localisation does not abrogate their activity. Instead, endogenous (e.g. Golgi apparatus and ER) activated H- and N-Ras promote a delayed activation of the MAPK pathway [227]. In the case of R-Ras proteins, addition of a geranyl isoprenyl lipid by the geranylgeranyltransferase is responsible for its membrane targeting and is required for R-Ras to regulate integrin activation [216, 228]. Hence, the sub-cellular distribution of Ras family members is critical for the regulation of their activation and functions.

1.5.2 Pi3k/Pten/Pkb/mTor signalling pathway

The Pi3k/Pten/Pkb/mTor signalling pathway has been extensively studied for its involvement in cell growth, proliferation, survival, metabolism, inflammation and is commonly activated in human cancers [229]. There are three classes of Pi3k (class I to III), divided according to their structural characteristics and substrate specificity [230]. Pi3k consists of a p85 regulatory subunit together with a p110 catalytic subunit (also named Pi3kCA). Binding of p85 to p110 is necessary for Pi3k to be active. Following growth factor or hormone stimulation, many RTKs can activate Pi3k. This activation is mediated either by the recruitment of Pi3k to the RTK or via activation of Ras which in turn binds and activates Pi3k [231]. Upon activation, Pi3kCA catalyses the phosphorylation of plasma membrane-located phosphatidylinositol lipids converting phosphatidylinositol-4,5- bisphosphate (PIP_2) into phosphatidylinositol-3,4,5-

trisphosphate (PIP_3) [232]. The reverse reaction from PIP_3 to PIP_2 is catalysed by the tumour suppressor, the phosphatase and tensin homolog (Pten) [233]. PIP_3 acts as a docking site recruiting to the plasma membrane pleckstrin-homology (PH) domain-containing proteins such as protein kinase B (Pkb also named Akt) and phosphatidylinositol dependent kinase 1 (Pdk1) [230, 234]. Thus, the tight regulation of the PIP2 / PIP3 balance by Pi3k and Pten is critical to control signalling downstream of this pathway. Indeed, loss of Pten protein or function is associated with uncontrolled Pi3k signalling and cancer [235] [236]. Pdk1 is a constitutively active kinase in the cytoplasm. Upon its recruitment to the plasma membrane, Pdk1 can phosphorylate Pkb on Thr-308 [237]. In addition, Pdk1 directly phosphorylates and promotes the activation of ribosomal S6 kinase 1 (S6k1) [238] and p90 ribosomal S6 kinase isoforms (Rsk) [239]. Activated Pkb then phosphorylates the mammalian target of rapamycin (mTor) to promote its activation.

mTor is found as part of two multi-protein complexes named mTorC1 and mTorC2 (reviewed by [240]). mTorC1 is both rapamycin- and nutrient-sensitive and contains the regulatory associated protein of mTor (Raptor), mammalian lethal with Sec13 protein 8 (mLst8, also known as GβL); proline-rich Akt substrate 40 kDa (Pras40); and DEP-domain-containing mTor-interacting protein (Deptor) [240]. In contrast mTorC2 is formed by the association of mTor with the rapamycin-insensitive companion of mTor (Rictor) [240], mammalian stress-activated protein kinase interacting protein (mSin1); protein observed with Rictor-1 (Protor-1); mLst8; and Deptor [241] [240]. Upon activation, Pkb de-represses mTorC1 by inhibiting phosphorylation of Pras40, a component of mTorC1 that suppresses the function of this complex [242] [243]. Pkb also activates mTorC1 by inhibiting tuberous sclerosis complex 2 (Tsc2) phosphorylation, relieving the inhibitory effect of this protein on mTorC1 via the Ras homolog enriched

in brain (Rheb) [244]. There are many substrates of mTorC1 including S6k1 [245] that regulate protein translation; the transcription factor sterol regulatory element-binding protein 1 (Srebp1) involved in the regulation of metabolism and the cytoplasmic linker protein 170 (Clip170) that regulates microtubule plus end dynamics [241, 246]. On the other hand, reported substrates of mTorC2 include Pkb and serum- and glucocorticoid-induced protein kinase 1 (Sgk1) [241]. mTorC2 mediated phosphorylation of Pkb on Ser-473 and Sgk1 on Ser-422 leads to full activation of both kinases and is critical for mTorC2 dependant regulation of cellular metabolism [247] [248]. Other substrates of Pkb include the actin binding protein Girdin also named Akt-phosphorylation enhancer (APE). Phosphorylation of Girdin by Pkb promotes its recruitment to the leading edge of migrating cells where it interacts with the actin cytoskeleton to regulate the formation of lamellipodia and stress fibres [249]. Pkb has also been reported to phosphorylate the ADP-ribosylation factor directed GTPase-activating protein 1 (ACAP1). Upon phosphorylation by Pkb, ACAP1 participates in the recycling of integrin β1 from the membrane and promotes cell migration [250].

1.5.3 p90Rsk

The 90 kDa ribosomal S6 kinase (Rsk) family is composed of four isoforms (Rsk 1, 2, 3 and 4) and two related homologues, mitogen- and stress-activated kinase (Msk1 and 2) in human [251]. While Rsks are activated by Erk, Msks integrate both mitogen and stress signals from Erk and mitogen activated protein kinase 14 (also known as p38), respectively [197]. Increased expression of Rsks has been shown in breast [252] and prostate cancer [253] while Rsk2 activity has been linked to cell transformation [254-255] and metastatic progression in head and neck squamous cell carcinomas (HNSCC) [256]. Originally identified on the basis of their ability to phosphorylate the 40S ribosomal subunit protein S6 (RpS6) [257-258], the four Rsk

isoforms display a high degree of homology (75 to 80% amino-acid sequence identity) (Figure 11B). They are characterised by the presence of two distinct kinase domains that do not originate from a gene duplication [259] (Figure 11). The N-terminal kinase domain (NTKD) is homologous to the kinase domain found in the AGC kinase family (Pka, Pkg and Pkc). In contrast, the C-terminal kinase domain (CTKD) is similar to that found in calcium/calmodulin dependent protein kinases (Camks). Both kinase domains are separated by a conserved linker region (also called turn motif) and flanked by N- and C-terminal tails. The latter contains a sequence termed the D-domain sequence that allows the docking of Erk [260] ; an event required for further Rsk activation [261] (Figure 11 and Figure 12).

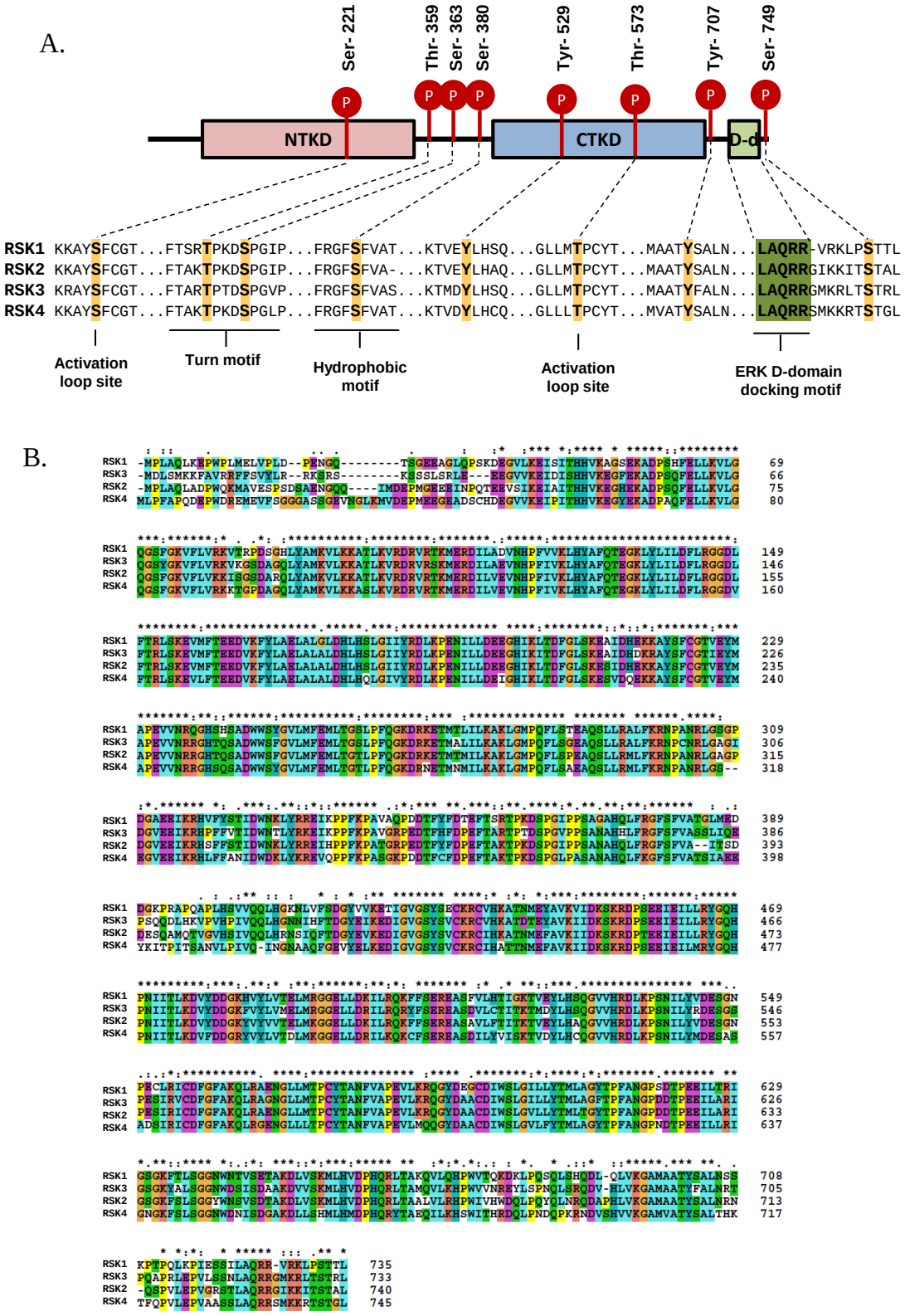

Figure 11: Rsk domain organisation. (A) Rsk exhibit two kinase domains (N-terminal kinase domain (NTKD) and the C-terminal kinase domain (CTKD)) separated by a conserved linker region also named turn motif and flanked by N- and C-terminal tails. The latter contains a sequence termed the D-domain sequence (D-d) that allows the docking of Erk. Phosphorylation sites required for Rsk activation are conserved in all four isoforms. The Amino-acid numbering refers to human RSK1 sequence. (Figure modified from [251]). (B) Multiple alignement of Rsk 1, 2, 3 and 4 amino-acid sequence showing the high degree of homology between isoforms. Alignement performed using ClustaX2 [262]. '*'; identical residue. ':'; conserved substitutions. '.'; semi-conserved substitution.

1.5.3.1 Mechanism of activation of Rsks

Activated Erk phosphorylates Rsk on Thr-573 located in the activation loop of the CTKD. This activates, the CTKD that autophosphorylates Rsk on Ser-380 located in the central linker region. This motif might also be a substrate of additional kinases (Figure 12). Further phosphorylation of Thr-359 and Ser-363, probably by Erk itself, leads to the recruitment of Pdk1 to the phosphorylated hydrophobic motif in the linker region [263]. Pdk1 in turn phosphorylates Ser-221 located in the activation loop of the NTKD leading to a fully active Rsk. The NTKD is responsible for phosphorylation of Rsk substrates. Finally, autophosphorylation of Ser-749 near the Erk docking site (D-domain) by the NTKD may result in the dissociation of Erk from Rsk thereby mediating a negative feedback loop on Rsk activation [260]. Recent reports revealed the phosphorylation of Rsk isoforms directly by RTKs including Fgfr1, Fgfr3 and Kgfr as well as by Src and Fyn downstream of Egfr [255] [264] [265] [266] [267]. These reports have highlighted the importance of phosphorylation on tyrosine residues during the initial steps of Rsk activation. Phosphorylation of Rsk2, but not Rsk1, on Tyr-529 by Fgfr3 and/or Src and Fyn downstream of Egfr promotes the binding of inactive Erk to Rsk2 and is required for further activation of Rsk2 by Erk [255]. Furthermore, phosphorylation of Tyr-707 by Fgfr3 contributes to Rsk2 CTKD activation by disrupting the autoinhibitory αL-helix in the C-terminus of Rsk2 [267]. Although, it does not appear to be phosphorylated by Fgfr3, Rsk1 has been shown to interact with active Kgfr to mediate some of its biological functions [266]. Furthermore, Fgfr1 has been shown to bind to the N-terminus part of Rsk1 in the nucleus and to a lesser extent in the cytoplasm [265]. Thus both Rsk1 and 2 interact with RTKs to regulate their activation and/or subcellular localisation.

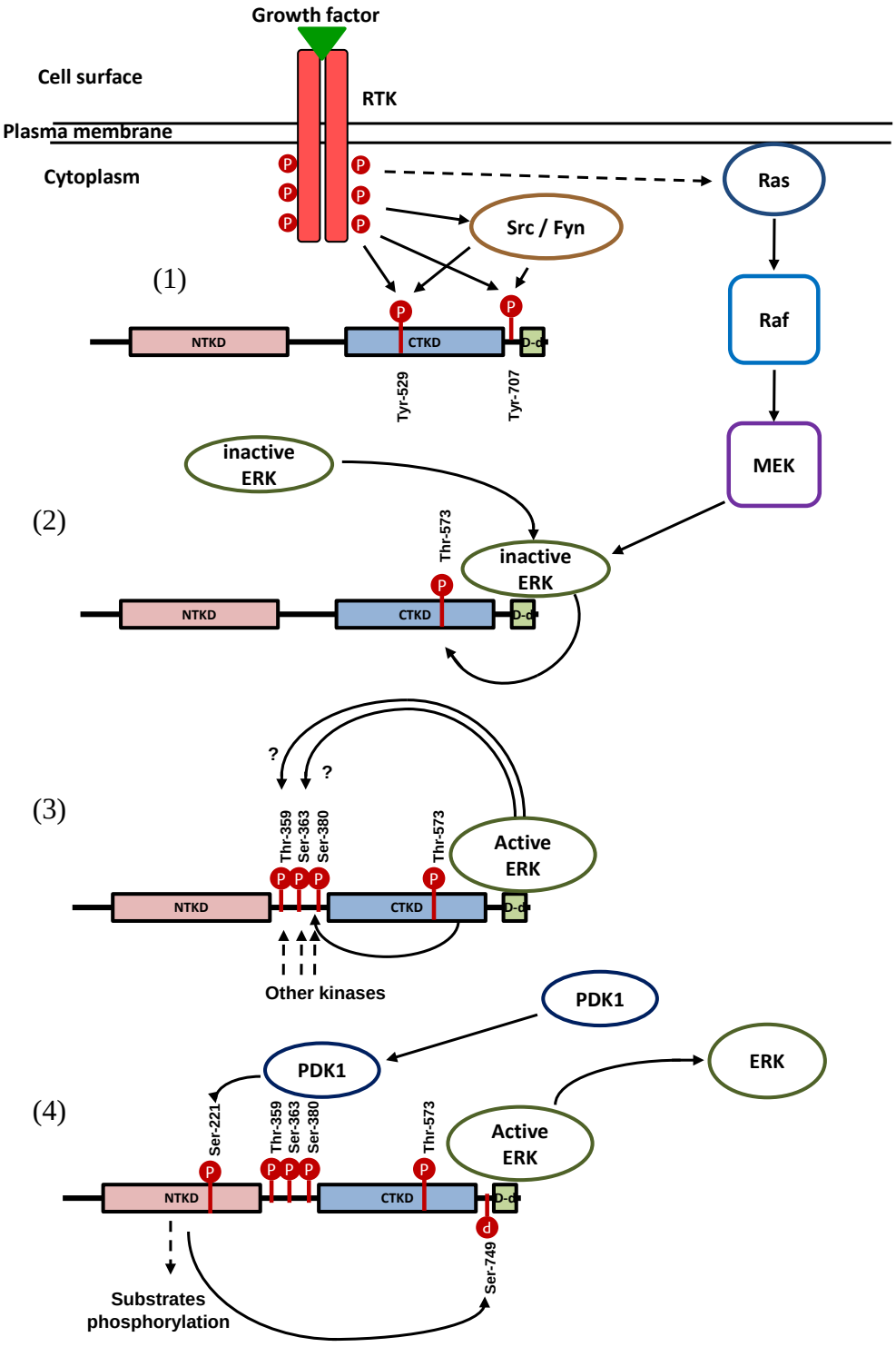

Figure 12: Mechanisms of activation of Rsk isoforms. NTKD: N-Term Kinase Domain, CTKD: C-Term Kinase Domain, D-d: D-domain (Erk docking site). (1) Phosphorylation of Rsk on Tyr-529 and Tyr-707 by RTKs and Src/Fyn induces the (2) recruitment of inactive Erk to the D-domain of Rsk. Parallel signalling through the Ras/Raf/Mek pathway leads to the activation of Erk which in turn phosphorylates Thr-573 within the activation loop of the CTKD. (3) Once activated, the CTKD autophosphorylates Rsk on Ser-380 within the hydrophobic motif. This site might also be targeted by other kinases. Erk may also phosphorylate Thr-359 and Ser-363. (4) Phosphorylation of the hydrophobic motif leads to the recruitment of Pdk1 which in turn phosphorylates Ser-221 within the activation loop of the NTKD. The NTKD is then responsible for the phosphorylation of downstream substrates. Finally, autophosphorylation of Ser-749 by the NTKD releases Erk from Rsk.

1.5.3.2 Cellular Processes regulated by Rsks

More than 30 proteins have been identified to be substrates of Rsks. These are in all three cellular compartments (plasma membrane, cytoplasm and nucleus). A list of these targets is provided in Table 1. The variety of these substrates explains the involvement of Rsk isoforms in multiple cellular processes ranging from transcription and translation regulation to cell cycle progression, cell survival and cell motility (Reviewed by [251]).

1.5.3.2.1 Regulation of transcription by Rsk

The regulation of transcription by Rsk is mainly mediated by the phosphorylation of transcription factors including the cAMP response element binding (Creb), Fos related antigen 1 (Fra1), serum response factor (Srf), the Ets transcription factor (Er81), oestrogen receptor-α (ER-α), nuclear factor-κB (Nf-κb) and the transcription initiation factor 1A (Tif1A) (Table 1) [251]. Once activated, these transcription factors induce the expression of immediate early genes (IEG) such as Fos and Myc. On the other hand, Rsk can also directly phosphorylate IEG including c-Fos, Jun, and Nur77 [268] [269] [270]. In the case of c-Fos, the phosphorylation of this protein by Rsk results in its stabilisation and promotes c-Fos mediated cell growth [271] [272].

Protein name	Biological process	Phosphorylation site (organism)	Function proposed for phosphorylation	Refs
Creb	Transcription	Ser-133 (m, h)	Promotes cell survival	[273][274][275]
Nfatc4	Transcription	Ser-676 (h, m)	Potentiates DNA binding	[276]
Nfat3	Transcription	Multiple Ser sites (m, h)	Promotes myotube differentiation	[277]
Atf4	Transcription	Ser-245 (h), Ser-251 (m)	Promotes osteoblast differentiation	[278]
Tif-1A	Transcription	Ser-649 (h)	Promotes cellular rRNA synthesis	[279]
Er81	Transcription	Ser-191 (h), Ser-216 (m)	Promotes DNA binding	[280]
Nur77, Nor1	Transcription	Ser-354 (h), Ser-377 (h)	Function unknown	[270]
IκBα	Transcription	Ser-32 (r)	Activation of Nfκb	[281][282]
p65	Transcription	Ser-536 (r, m)	Activation of Nfκb	[284]
IκBβ	Transcription	Ser-19, Ser23 (r)	Activation of Nfκb	[285]
Srf	Transcription	Ser-103 (h)	Activation of c-fos transcription	[286]
Tsc2	Translation	Ser-1798 (h)	Promotes mTor signalling and translation	[287]
elF4B	Translation	Ser-422 (h)	Enhances the interaction between elF4B and elF3	[288]
eEF2 kinase	Translation	Ser-366 (h)	Inhibits the activity of eEF2 kinase and promotes translation elongation	[289]
RpS6	Translation	Ser-235, 236 (h)	Promotes cap-dependant translation	[290]
Er-α	Proliferation	Ser-167 (h, r)	Regulates the transcriptional activity of estrogen receptor	[291]
Gsk3β	Proliferation	Ser-9 (r)	Inhibits Gsk3β activity	[292]
Nhe-1	Proliferation	Ser-703 (h)	Stimulates serum-mediated Na^+/H^+ exchange	[293]
Mi	Proliferation	Ser-409 (h)	Activation followed by proteolytic degradation of Mi	[294]
Lkb1	Proliferation	Ser-431 (m)	Inhibits cell growth	[295]
Sos	Proliferation		Downregulates Ras-MAPK activity	[296]
c-Fos	Proliferation	Ser-362 (r)	Stabilizes c-Fos and promotes cell growth	[269][297]
$p27^{kip1}$	Proliferation, Motility	Thr-198 (h)	Promotes 14-3-3 binding and cytoplasmic localization	[298]
Bub1	Cell cycle progress	Xenopus	Inhibition of Apc and metaphase arrest	[299]
Myt1	Cell cycle progress	Xenopus	Downregulates its inhibitory activity	[300]
Emi2/Erp1	Cell cycle progress	Ser-335, Thr-336, Ser-342, Ser-344 (x)	Promotes interaction of Emi2 with Pp2a	[301][302]
Bad	Cell survival	Ser-112 (h, r)	Supression of Bad-mediated apoptosis	[273][303]
C/Ebpβ	Cell survival	Ser-105, Thr-217 (m)	Promotes hepatic stellate cell survival	[304]
Dapk	Cell survival	Ser-289 (h)	Suppresses its pro-apoptotic activity	[305]
Flna	Motility	Ser-2152 (h, r)	Regulates actin-cytoskeleton	[306]
L1cam	Motility	Ser-1152 (r)	Regulates neurite outgrowth	[307]
RanBP3	Nuclear transport	Ser-58 (h)	Regulates nuclear transport	[308]
nNos	Brain function	Ser-847 (h)	Inhibits nNos enzyme activity	[309]
Mad1	Proliferation	Ser-145 (h)	Promotes cell proliferation and Myc-mediated transcription	[310]
As160	Glut4 translocation	Ser-318, Ser-588, Thr-642, Ser-341, Ser-751, Thr-568	Inactivation of the GAP activity of As160	[311]
Raptor	mTOR activation	Ser-719, Ser-721, 722	Regulates mTorC1 activity independent of PI3K-AKT pathway	[312]
Yb-1	Proliferation, Motility	Ser-102 (h)	Promotes Egfr and Pik3CA transcription	[313]
Hsp27	Motility, Invasion	Ser-78, Ser-82 (h)	Regulates Actin cytoskeleton	[256]
Tcp-1	Cell proliferation	Ser-260 (h)	Mediates MAPK induced proliferation	[314]
Histone H3	Tumorogenesis	Ser-10 (h)	Promotes transformation	[254]
Mrlc	Migration	Ser-19 (h)	Promotes acto-myosin contraction	[315]

Table 1: List of Rsk substrates. The table shows the protein names, biological processes in which the substrates are mainly involved, the phosphorylation sites affected if known, the functions associated to the phosphosites and the corresponding bibliographic references. (h): human, (m):mouse, (r): rat, (x): xenopus. The full protein names corresponding to the abbreviations used in this table are given in the Abbreviation section. This table has been modified from [251].

1.5.3.2.2 Regulation of translation by Rsk

The translation machinery can be fine-tuned to regulate protein synthesis in response to environmental cues. The mammalian target of rapamycin (mTor) pathway plays a central role in this phenomenon [316]. Rsk has been shown to modulate protein translation both in an mTor-dependent and independent manner. By phosphorylating and inhibiting the tumour suppressor tuberous sclerosis complex-2 (Tsc2), Rsk promotes mTorC1 mediated translation. mTorC1 activates p70 ribosomal S6 kinase 1 and 2 (S6k1 and 2) which in turn phosphorylate the eukaryotic translation initiation factor 4E-binding protein 1 (4Ebp1) and the eukaryotic translation initiation factor 4B (eIF4B). Thus, there is a degree of overlap in the regulation of translation by Rsk and the closely related proteins S6k1 and 2 [288] [316]. However, Rsk can also directly phosphorylate elF4B independently of mTor. eIF4B phosphorylation promotes its interaction with eIF3 and correlates with an increase in translation rates [317] [318]. The phosphorylation of eIF4B by Rsk provides a transient response to mitogenic cues that contrasts with the more sustained and prolonged phosphorylation mediated by the mTor pathway [288]. In addition, Rsk also regulates translation by directly phosphorylating Rps6 on Ser-240 and 244 (also targeted by S6k1 and 2) as well as on Ser-235 and Ser-236 (preferentially targeted by Rsk). The phosphorylation of the latter two sites correlates with increased translation and provides an mTor-independent mitogen-induced control of protein synthesis.

1.5.3.2.3 Regulation of cell survival by Rsk

Rsk has been shown to promote cell survival by phosphorylating and inactivating the pro-apoptotic mitochondrial Bcl2 antagonist of cell death protein (Bad). Phosphorylation of Bad by Rsk enhances its ability to bind to the cytosolic 14-3-3

protein [273] [303] [319] and reduces its ability to antagonise the pro-survival factor Bcl-X_L. Similarly, phosphorylation of Bcl-2 Interacting Mediator of cell death (BimEL) blocked its capacity to interact with the F-box containing protein called β-Transducin repeat containing protein (β-TrCP) leading to proteosomal degradation of BimEL and cell survival [320]. Rsk can also phosphorylate the death associated protein kinase 1 (Dapk1) to inactivate its pro-apoptotic function [305]. Furthermore, Rsk phosphorylation of Creb was found to promote survival by increasing the transcription of pro-survival genes such as the B-cell lymphoma protein-2 (Bcl2) family members, Bcl2, Bcl-X_L, and Mcl1 [273] [274] [275]. Finally, by phosphorylating the NF-κB inhibitor IκBα, Rsk induces IκBα degradation thereby allowing NF-κB to promote cell survival and proliferation [281] [282].

1.5.3.2.4 Regulation of cell cycle by Rsk

Rsk activity has been shown to be involved in cell cycle progression. Indeed, Rsk1 and 2 promote G1 progression by phosphorylating the cyclin-dependent kinase (Cdk) inhibitor $p27^{Kip1}$. In the nucleus, $p27^{Kip1}$ inhibits G1 progression by sequestering and inactivating cyclin E–Cdk2 or cyclin A–Cdk2 complexes. Once phosphorylated by Rsk, cytosolic $p27^{Kip1}$ associates with 14-3-3 preventing its translocation to the nucleus [298]. Furthermore, Rsk2 has been shown to promote the G2-M phase of meiosis by phosphorylating and inhibiting Myt1 kinase [300]. On the other hand, studies performed in Xenopus laevis oocytes have shown that Rsk mediates metaphase arrest via the cytostatic factor (Csf) [321] [322]. By phosphorylating and activating the kinase Bub1, Rsk1 inhibits the anaphase promoting complex (Apc) causing an arrest in metaphase II. Rsk also phosphorylates and stabilises the Apc inhibitor endogenous meiotic inhibitor 2 (Emi2) thereby inhibiting Apc and inducing a metaphase arrest [301] [302].

1.5.3.2.5 Regulation of invasion and metastasis by Rsk

Initial reports suggested the involvement of Rsk in cell migration via the phosphorylation of proteins known to regulate the motility machinery. These include the membrane-associated and cytoskeletal protein, filamin A and the regulatory light chain of myosin II (Mrlc) [306, 315]. Recent publications have confirmed the importance of Rsk family members in modulating migration, invasion and metastasis [256, 323-324]. These studies propose Rsk1 and/or Rsk2 as determinant in mediating the pro-metastatic program driven by Erk. Over-expression of Rsk1 in two melanoma cell lines was shown to increase cell motility in a $p27^{Kip1}$/RhoA-dependent manner [324].

Moreover, inactivation of Rsk activity using pan-Rsk inhibitors (fmk, SL0101 and BI-D1870) inhibited Rsk-mediated migratory and invasive effects in multiple epithelial cell lines harbouring a hyperactive MAPK pathway [256, 323]. In contrast, isoform-specific down-regulation of Rsk family members using RNA interference in head and neck squamous cell carcinomas (HNSCC) did highlight the particular role of Rsk2 but not Rsk1 in this process [256]. However, Doehn et al. showed that combined silencing of Rsk1 and Rsk2 is necessary to significantly decrease invasiveness in the breast epithelial cell line, MCF10A. Thus, the involvement of each Rsk family member in cellular motility and invasiveness appears to be highly dependent on the cellular system studied. Two mechanisms have been proposed to mediate the effects of Rsk on cell motility and invasiveness. (1) The transcriptional activation of nuclear genes via the transcription factor Fra1 [323] and (2) the phosphorylation of cytoplasmic targets known to regulate cell motility and invasiveness [256, 324]. Hence, it is conceivable that the mode of action of Rsk family members will depend on the activation state and subcellular localisation (nucleus, cytoplasm or plasma membrane) of each Rsk isoform.

1.5.3.3 Expression of Rsk and mouse models

Expression of mRNA for Rsk family members is ubiquitous in human [251]. However, important differences in expression patterns exist between isoforms. Rsk1 is mainly expressed in the kidney and pancreas while Rsk2 and 3 are predominantly found in skeletal muscle, heart and pancreas. In adult mice, Rsk4 protein was found in the heart, skeletal muscles and kidney although at much lower level than the other Rsk isoforms. However no detectable Rsk4 protein was found in the lung, liver, pancreas and adipose tissue [325]. All four isoforms were detected in human and mouse brain tissue although in different sub-compartments. The highest levels of Rsk2 expression in adult mice were found in the regions of the brain harbouring high synaptic activity such as the neocortex, the hippocampus and the Purkinje cells [251]. This localisation correlates with the reported involvement of Rsk2 in neuronal function. Indeed inactivating mutations of Rsk2 are associated with the Coffin-Lowry syndrome, a disease characterised by severe psychomotor retardation, digital and facial dysmorphisms, and a progressive skeletal deformation [326]. The generation of a knock-out mouse model for Rsk2 has confirmed the human phenotype [327].

1.6 Lung Cancer

1.6.1 Lung cancer is the main cancer killer worldwide

Lung cancer kills 1.3 million individuals per year worldwide and is the commonest cause of cancer death in the developed world including the UK [328] (Figure 13 B and C). Smoking has been shown to be the major cause for this disease [329-330]. Epidemiology studies show an overall 5-year survival of 5-10% with a median survival that varies from 6 to 12 months in patient diagnosed with metastatic versus locally advanced disease, respectively [329]. This poor survival rate is explained by the high

metastasising potential of lung cancer and the development of resistance to therapy. Lung carcinomas are histologically classified into two subtypes; small cell lung carcinoma (SCLC) and the more prevalent non-SCLC (NSCLC) that accounts for 75-80% of cases. NSCLC can be divided into three sub-types: squamous cell lung carcinoma (SCC), adenocarcinoma, and large cell lung carcinoma. Whereas SCLC shows sensitivity to several chemotherapeutic agents, chemotherapeutic treatment of NSCLC offers only marginal improvement in survival [329]. Although the appearance of metastatic disease in NSCLCs mostly correlates with the progression of the primary tumour and the infiltration of proximal lymph nodes [329], metastatic sites can already be detected with stage I disease in approximately 1.4% of the cases [331].

A.

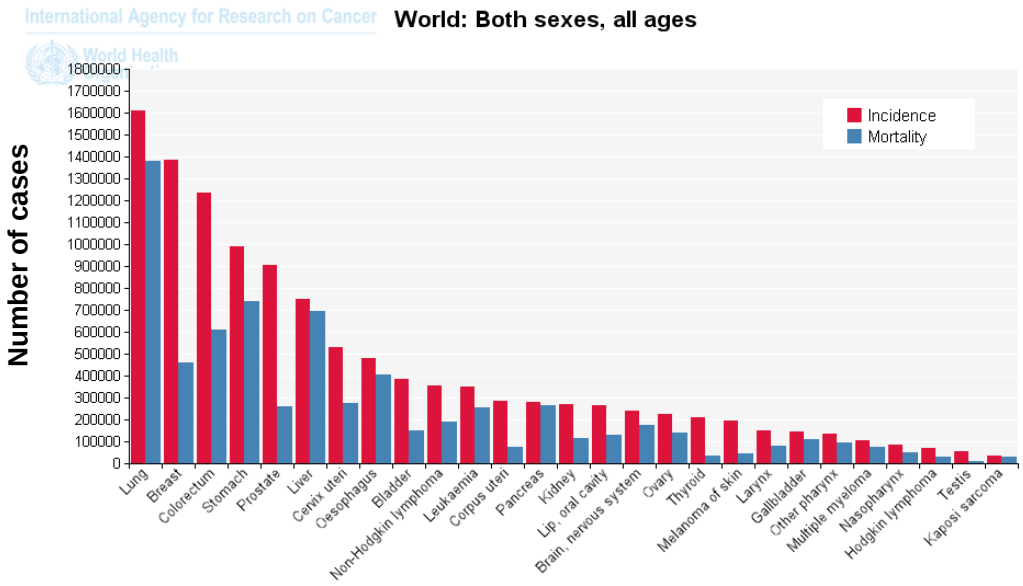

B.

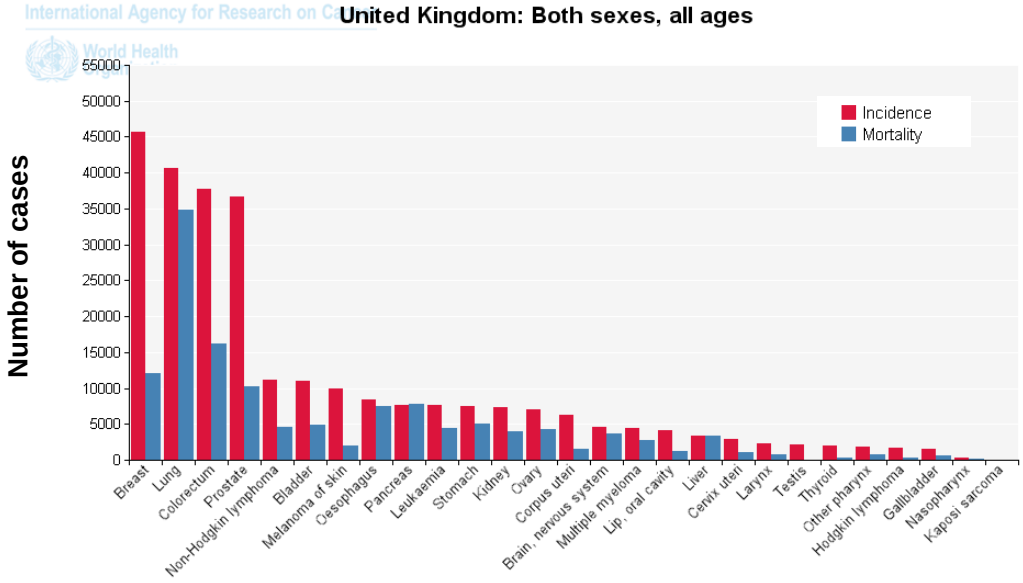

Figure 13: Lung cancer is the main cancer killer worldwide. (A) and (B) Comparison of the incidence and mortality of various cancers (A) worldwide and (B) in the UK (both sexes, all ages). Chart obtained from Globocan 2008 IARC [1].

1.6.2 Lung cancer biology

1.6.2.1 Pulmonary epithelium

The pulmonary epithelium is a ramified structure starting from the trachea that divides into main bronchi, bronchioles and finally the alveoli which make the most of the lung surface (Figure 14). Specialised cell types localise all along the pulmonary epithelium. Those include the goblet, basal and ciliated cells mainly found in the upper airway, the Clara cells that localise in the upper airway and bronchioles, the pulmonary neuroendocrines cells (PNEC) that cluster into neuroepithelial bodies in the mid-level bronchioles and finally the epithelial alveolar cells that form the extremely thin (approx. 0.5 micrometres) alveolar wall (Figure 14B and C). Two subtypes of epithelial alveolar cells are known, the alveolar type-I cells (type I pneumocytes or squamous alveolar cells) and the alveolar type-II cells (type II pneumocytes or great alveolar cells). Although the most numerous are the type II alveolar cells, the type I cells cover the largest surface area. Each alveolus is closely wrapped in a fine mesh of thin capillaries composed of monolayers of endothelial cells [332] (Figure 14B). While their structure provides maximal surface for gas exchange, they do not offer great resistance to metastasising malignant epithelial cells attempting to disseminate to distant sites through the blood circulation. This fact alone might explain the high metastasising potential of lung cancer (Figure 14B and C)[330].

A.

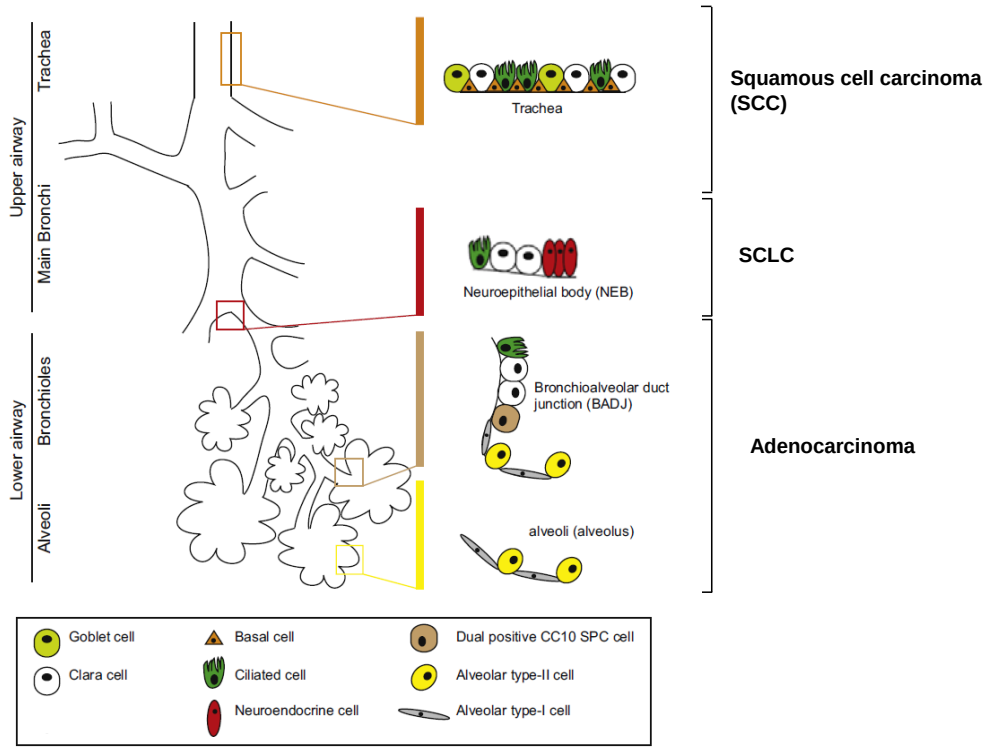

B.

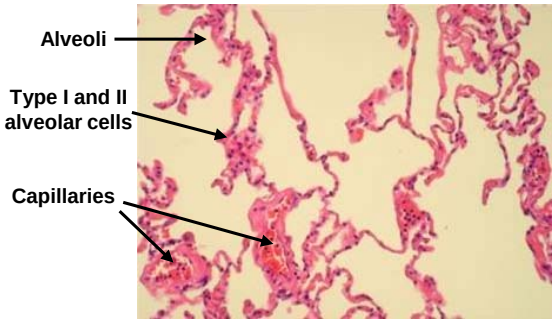

C.

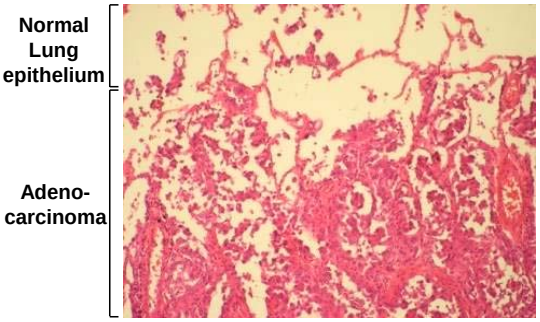

Figure 14: Pulmonary epithelium and lung cancer. (A) Schematic diagram of a lung highlighting the spatial structure, the different cell types and tumour sub-type associated with each region. Box describes the different colour coded cell types. Figure adapted from [333]. (B) Image of a normal lung tissue section stained with haematoxylin and eosin showing several alveoli. (C) Image of a tissue section from the border of a lung adenocarcinoma stained with haematoxylin and eosin. Haematoxylin reveals the nuclei in blue while the eosin stains the protein rich structures. Images were courtesy of Dr Francesco Mauri.

1.6.2.2 Origins of lung cancer

1.6.2.2.1 Cellular origins of lung cancer

Lung tumour subtypes generally follow a proximal-to-distal distribution with the squamous cell carcinoma (SCC) mainly localised in the upper airways, the SCLC commonly found in the midlevel bronchioles and the adenocarcinoma typically found in the lower airway (Figure 14). Hence, it has been hypothesised that different tumour subtypes arise from specific cell types localised within defined lung compartment (reviewed by [333] and [334]). Several lines of evidence support this hypothesis.

(1) The histopathology of SCC and the markers expressed by this tumour type, such as keratin 5 and 14, suggest that they may originate from tracheal basal cell progenitors located at the sub-mucosal gland duct junction [333-334].

(2) SCLC is characterised by the expression of neuroendocrine markers. This tumour type commonly arises in the midlevel bronchioles where the pulmonary PNEC cluster into neuroepithelial bodies. [335]. Hence PNEC cells have been proposed to be the progenitors of SCLC [336].

(3) Evidence for initiating NSCLC cells came from mouse models where oncogenic activation of K-Ras (see section 1.5.1.1.1) in the lung generated early lesions at the bronchioalveolar duct junction (BADJ) (Figure 14A) [337]. The BADJ contains a sub-population of cells expressing the Clara cell marker, CC10, and the type II alveolar cell marker, Surfactant Protein C (SPC). These cells were named bronchioalveolar stem cells (BASC) due to their self-renewal and multipotent capacity [337-338]. Tumour progression into lung adenocarcinoma in these mice correlated with increased number of BASC suggesting that Clara and type II alveolar cells might be at the origin of NSCLC (Figure 14A)[333]. However since patients can present with tumours composed

of both SCLC and NSCLC cellular subtypes, or have tumours that progress from one phenotype to another, there is also a hypothesis that there may be a common cell of origin for these tumours.

1.6.2.2.2 Molecular origins of lung cancer

Genome-wide sequencing and single nucleotide polymorphism (SNP) arrays have enabled the systematic identification of somatic mutations as well as copy-number alterations associated with lung adenocarcinoma [206, 214, 339]. These approaches have confirmed the association with NSCLC of many genes previously known to be mutated in lung adenocarcinoma including the tumour suppressor genes Tumour protein (Tp53), $p16^{INK4a}$, the serine threonine kinase 11 (Stk11), Nf1, adenomatous polyposis of the colon (Apc), Retinoblastoma (Rb) and Ataxia-telangiectasia mutated gene (Atm) as well as oncogenes such as K-Ras, N-Ras, Egfr, Erbb2 and 4 and the Vascular endothelial growth factor receptor 2 (Vegfr2). They also revealed chromosomic regions with high variability including amplification of the 14q13.3 region carrying genes such as the thyroid transcription factor 1 (Titf1) [339]. Variability in the 15q24–15q25.1 regions was also frequently identified. These regions contain two genes encoding subunits of the nicotinic acetylcholine receptor alpha (Chrna3 and Chrna5) known to be regulated by nicotine exposure [340]. We will here concentrate on the importance of few of these genes reported to have critical roles in NSCLC initiation and development.

Histological Type	Non–Small-Cell Lung Cancer		Small-Cell Lung Cancer
Histological Subtype	**Squamous-Cell Carcinoma (SCC)**	**Adenocarcinoma**	-
Genetic changes	-	-	-
K-Ras mutation	Very rare	10 to 30% [(1)]	Very rare
B-Raf mutation	3%	2%	Very rare
Egfr			
Kinase domain mutation	Very rare	10 to 40%	Very rare
Amplification [(2)]	30%	15%	Very rare
Variant III mutation	5%	Very rare	Very rare
Erbb2 (Her2)			
Kinase domain mutation	Very rare	4%	Very rare
Amplification	2%	6%	Not known
Eml4-Alk fusion [(3)]	Very rare	7%	Not known
cMet			
Mutation	12%	14%	13%
Amplification	21%	20%	Not known
Titf-1 amplification	15%	15%	Very rare
Tp53 inactivation	60 to 70%	50 to 70%	75%
Rb inactivation	15 to 30%		90%
$p16^{INK4a}$ (Cdkn2a) inactivation	30 to70%		0 to 10%
Stk11 (Lkb1) mutation	19%	34%	Very rare
Pik3CA			
Mutation	2%	2%	Very rare
Amplification	33%	6%	4%

Table 2: Genetic abnormalities in NSCLC and SCLC. NSCLC includes squamous-cell carcinoma (SCC) and adenocarcinoma. [(1)] Variations are based in part on smoking profiles. [(2)] Based on data acquired from resected cancers. [(3)] The fusion gene consisting of parts of Eml4 and Alk occurs in adenocarcinoma but not in other types of non–small-cell lung cancer or non lung cancers. (Table modified from [341] and [342])

1.6.2.2.2.1 Egfr and RTK involvement in lung cancer

Egfr is a plasma membrane bound tyrosine kinase receptor composed of an extracellular ligand-binding domain, a single trans-membrane domain linked to an intracellular tyrosine kinase domain and a non-catalytic carboxyl terminal tail [185]. Also known as Erbb-1, Egfr belongs to a family containing four members in mammals (Erbb-1 to 4) [343]. Both homo- and hetero-dimers of Erbb receptors have been described and are activated by eleven different ligands providing a range of activation options [344]. Three main regions have been identified to be frequently mutated within Egfr: the extracellular domain, the kinase domain and the C-terminal tail. These mutations lead to receptor activation by destabilising the inactive kinase conformation [345]. However, kinase mutated Egfr can still respond to ligand stimulation and get further activated [346] [347]. Yet, tyrosine phosphorylation in mutated Egfr is significantly lower than that of ligand-activated wild-type receptor. This difference has been shown to result in distinct gene expression signatures [348] in cells bearing mutant versus those with wild-type Egfr. Amongst the weakly phosphorylated tyrosine residues is the Tyr-1045 located within the receptor's tail. Phosphorylated Tyr-1045 promotes the recruitment of the ubiquitin-ligase Casitas B-lineage lymphoma proto-oncogene (Cbl) that targets the receptor for lysosomal degradation. Thus, aberrant Egfr activation induced by mutation in the kinase domain allows propagation of the signal downstream without triggering degradation of the receptor [178].

In lung cancer, several Egfr abnormalities are frequently detected including Egfr protein overexpression, gene amplification, and mutation [349] [350] [351]. These mutations frequently occur within the exons 18, 19, 20 and 21 coding for the kinase domain. In patients with adenocarcinoma, they are associated with female sex, Asian ethnic origin and no smoking history. Amongst these mutations, 46% involve in-frame deletions of

amino-acids 746 to 750 within exon 19 while 40% are mutations resulting in the substitution of the Lysine 858 to an Arginine (L858R) in exon 21. The remaining 14% of mutations are located within exons 18 and 20 [352] [353]. Initial experiments performed in vitro suggested that Egfr kinase domain mutations could transform fibroblasts and lung epithelial cells [354] [355] suggesting that these mutations were oncogenic. This was later confirmed using mouse models carrying inducible deletion of exon 19 or expression of a L858R mutant in type II alveolar cells. These mice developed atypical adenomatous hyperplasia, that progressed into lesions resembling bronchioalveolar carcinoma and finally invasive adenocarcinoma [356-357]. Thus, activating mutations in the Egfr kinase domain are sufficient to drive the development of lung adenocarcinoma. Moreover, de-induction of the expression of mutant Egfr in these mice led to regression of tumours, suggesting that persistent signalling from mutant Egfr is required for tumour maintenance in this model [356].

Other Egfr mutations have been described in NSCLC including the Egfr variant III mutation that correspond to an in-frame deletion of exons 2 to 7 that encode for part of the extracellular domain [358]. Mouse models engineered to express this mutation in the lung also developed tumours that were similarly dependant on the continuous expression of the mutant Egfr for their maintenance [359].

These observations were later confirmed by Tang et al. who showed that Egfr gene mutation and protein overexpression can be observed in the normal epithelium adjacent to tumours. Disease progression then correlates with an increase in Egfr gene copy number with metastatic sites harbouring Egfr gene mutation, protein overexpression and increased gene copy number [360].

Other RTKs have been reported to be mutated in lung cancer. These include Erbb2 and 4 (also named Her2 and 4) and the hepatocyte growth factor receptor c-Met.

Mutations and amplification in Erbb2 have also been identified in lung adenocarcinoma although with lower frequency than Egfr (mutated in 4% and amplified in 8% of patients) but similar association with female sex, Asian ethnic origin and no smoking history [351]. Similarly, Erbb4 kinase domain mutations have been found in 2 to 3% of Asian patients with lung adenocarcinoma [361]. c-Met was found to be frequently mutated (26%) and amplified (41%) in NSCLC. Moreover, both amplification and activation of cMet were observed in early K-Ras-induced lesions [362].

1.6.2.2.2.2 K-Ras activation

H-, K- and N-Ras are mutated in 19% of lung adenocarcinoma. The majority of these mutations (17%) are attributed to K-Ras [207] and frequently found in patients with smoking history [363]. Smoking-related K-Ras mutations affect the exon 12 in 90% of the patients and are substitutions of a purine for a pyrimidine leading to a transversions mutations from Guanine (G) to Thymine (T). They contrast with the transition mutations (Guanine (G) to Adenine (A)) associated with non-smoking related lung cancer [341, 364]. However, the functional relevance of this discrepancy is so far unclear.

Although, K-Ras mutations can be detected in early lung lesions similarly to Egfr [365], K-Ras and Egfr mutations are mutually exclusive [206]. These early lesions are predominantly associated with G to T transversion mutations and precede smoking-related lung adenocarcinoma. Mice models carrying oncogenic alleles of K-Ras activated by spontaneous recombination events throughout the animal are predisposed to a range of tumours with early lung lesions being predominant [337, 366]. Hence, similarly to Egfr, K-Ras mutations appear to be an early event in lung cancer development.

1.6.2.2.2.3 B-Raf activation

Activating B-Raf mutations are found in 5% of all NSCLC [367]. Mice carrying an inducible oncogenic B-Raf mutation (B-RafV600E) develop early lesions in the lung similarly to the K-Ras model [337, 367].

1.6.2.2.2.4 Pi3k/Pten/Pkb/mTor involvement in lung cancer

In their study, Ding et al. identified 17 genes taking part in the Pi3k/Pten/Pkb/mTor signalling pathway [206]. This set of genes were mutated in more than 30% of lung tumours (excluding the K-Ras mutated tumours) highlighting the importance of this pathway in lung cancer. Both mutations and amplification of Pi3kCA have been reported in lung cancer. While Pi3kCA mutations occur in only 4% of lung cancers, its amplification is more frequently reported and affect mainly SCC (33%), followed by adenocarcinoma (6%). Other proteins found mutated in the pathway include Akt1 (1.9%) and Pten (9%) [229]. Although the occurrence of Pi3kCA mutations appear independent of the Egfr or K-Ras mutation status [368], Pi3kCA was shown to be required for K-Ras-driven tumourigenesis *in vivo* [231, 369]. Indeed, mice harbouring a Pi3kCA mutant allele deficient in its ability to bind Ras displayed altered growth factor signalling and were protected from Kras‑driven tumourigenesis in the lung [231].

1.6.2.2.2.5 Tp53 inactivation

Tp53 is a homotetrameric transcription factor activated by many forms of cellular stress including irradiation, drug-induced genotoxic damage, hypoxia, and oncogenic signal [370]. Upon activation, Tp53 induces a transcriptional response leading either to cell cycle arrest or apoptosis. Hence Tp53 is classified as a tumour suppressor

gene and is found frequently inactivated in human cancer (reviewed by [370-371]). In Lung cancer, Tp53 mutations occur in both SCC (60 to 70%) and adenocarcinoma (50 to 60%) [341]. The mutations affecting Tp53 follow similar pattern to K-Ras mutations with transversion and transition mutations respectively associated with smoking and non-smoking related lung cancer [364]. Amongst the mutations affecting Tp53 is the substitution of the arginine 175 to a histidine (R175H) associated with the familial Li-Fraumeni cancer susceptibility syndrome [372] and found in a subset of NSCLC patients [373]. This mutation inhibits Tp53 activity by abrogating its transcriptional activity [374] and is conserved in mice (R172H) [375]. Mice model carrying Tp53 mutation R172H rarely developed lung adenocarcinomas (13% of mice). As previously described, mice carrying oncogenic K-Ras mutation spontaneously developed early lung adenocarcinoma but these rarely metastasised [366]. The generation of mice carrying both oncogenic K-Ras mutation [366] and inactivating Tp53 R172H mutation did not result in an increase in the number of lung adenocarcinoma lesions as compared to mice with K-Ras mutation only (62.5% and 70.8%, respectively). However, the additional presence of a Tp53 mutation promotes the development of advanced tumours with increased frequency of metastases (36.5% in K-Ras/p53 mutants versus 4.5% in K-Ras mutants) [366, 376]. These secondary lesions were observed at sites frequently colonised by NSCLC metastasis in humans including the mediastinal lymph nodes, heart, liver, adrenal glands, kidney and pancreas. Similarly, the early lesions observed in the B-RafV600E mouse model rarely progressed into adenomas and adenocarcinoma unless the mice also carried an inactivating mutation in Tp53 [367]. Hence, inactive Tp53 and oncogenic K-Ras or B-Raf mutations cooperate in animal models to reproduce more accurately the human disease.

1.6.2.2.2.6 Retinoblastoma (Rb) inactivation

Rb was identified as a protein mutated in both inherited and sporadic Retinoblastoma. It is part of a family of proteins containing two other members: p107 and p130 [370, 377]. Its functions include the regulation of cell cycle progression, apoptosis and differentiation [370]. In its hypophosphorylated state, Rb inhibits the activity of the family of transcription factors E2Fs that regulates the expression of genes required to initiate DNA synthesis. Thus, Rb is a critical regulator of the G1/S transition of the cell cycle [378]. Phosphorylation of Rb by cyclin dependent kinases (Cdk) in response to mitogenic signals, abrogates Rb-mediated repression of E2F and allows cell to proliferate. Hence inactivating mutations of Rb dissociate the cell cycle machinery from the extracellular mitogenic signals and promotes uncontrolled cell proliferation [371]. Rb inactivation can also be mediated by Tp53 via inhibition of p21 which in turn inhibits Cdk mediated Rb phosphorylation [370]. However, Tp53 has been reported to prevent tumour development by inducing apoptosis when Rb is inactive [379]. Indeed mouse models where both Tp53 and Rb are absent, frequently develop tumour due to defect in apoptosis [380] [381] suggesting that inactivation of Tp53 allows the development of Rb negatives tumours. In support of this notion, inactivation of both Tp53 and Rb are frequent in many cancers. In lung cancer, loss or mutation of Rb has been reported to be frequent, affecting more than 90% of SCLCs and 15 to 30% of NSCLCs [342]. Moreover, inactivation of Rb in NSCLC was found to be more frequent in advanced tumours [382].

1.6.2.2.2.7 $p16^{INK4a}$ inactivation

$p16^{INK4a}$ also named cyclin-dependent kinase inhibitor 2a (Cdkn2a) is a tumour suppressor gene frequently altered in human neoplasms. It functions as an inhibitor of

the Cdks leading to inactivation of Rb. $p16^{INK4a}$ inactivation has been reported in up to 70% of NSCLC but rarely occurs in SCLC. It can be mediated by mutations or deletion in the gene or through hypermethylation of $p16^{INK4a}$ promoter to prevent its expression. While mutations in $p16^{INK4a}$ are rarely found in NSCLC primary tumours, homozygous deletion of the gene occurs in 10 to 40% of cases [342]. Furthermore, both mutations and homozygous deletion of $p16^{INK4a}$ have been associated with tumours from patient with smoking history. In contrast, inactivation of $p16^{INK4a}$ in non-smokers correlates with promoter hypermethylation and occurs early in tumour development [383] [384]. Mice carrying oncogenic K-Ras mutations develop early adenomas that are positive for $p16^{INK4a}$ immunohistological staining. Progression of these lesions into advanced adenocarcinoma correlates with disappearance of $p16^{INK4a}$ staining suggesting that inactivation of this protein is necessary for progression of early lung tumour into advanced adenocarcinoma [385]. Indeed, mice carrying oncogenic K-Ras or B-Raf mutations together with deletion of $p16^{INK4a}$ develop advanced lung adenocarcinoma [367, 386]. Hence, similarly to Tp53 mutations, $p16^{INK4a}$ inactivation cooperates with oncogenic K-Ras or B-Raf in animal models to promote the development of advanced tumours that more closely mirror the human disease.

1.6.2.2.2.8 Eml4-Alk

Eml4-Alk is the result of an inversion within the chromosome 2p that generates a fusion gene made of the C-terminal part of echinoderm microtubule-associated protein-like 4 (Eml4) gene and the N-terminal part of the anaplastic lymphoma kinase (Alk) gene containing its kinase domain. Ectopic expression of the fusion protein in fibroblast induces cellular transformation [387]. In NSCLC, this gene fusion product was detected in 6.7% of patients and seems to be exclusive to Egfr, K-Ras or B-Raf mutations [387]. The translocation occurs in adenocarcinoma but not in other types of

NSCLC or other cancers [341]. Recent reports have described two new variants, Eml4-Alk variants 3a and 3b that both were able to transform fibroblast *in vitro* [388].

1.6.2.2.3 Lkb1

The serine/threonine kinase Stk11, also named Lkb1, was reported mutated or deleted in 19% of SCC and 34% of adenocarcinomas [341]. However, these alterations occur in less than 5% of adenocarcinoma from Asian patients [389-390]. While Lkb1 mutations were exclusive from Egfr mutations, they associated with K-Ras mutations and thus were frequent in patients with a smoking history [390]. Recent reports suggest that Lkb1 is involved in lung cancer progression from early tumorigenesis to the development of metastasis [391] [392]. Indeed, reduced Lkb1 protein levels were associated with high grades of lung dysplasia [393]. While Lkb1 mutation alone is not sufficient to initiate lung cancer in mice, inactivation of Lkb1 together with expression of oncogenic K-Ras in mice increased the incidence of lung tumours and promoted the development of metastasis. Furthermore, these lung tumours developed into all NSCLC histological subtypes including adenocarcinoma, SCC and large-cell carcinoma [391].

1.6.2.3 NSCLC treatment

The majority of patients diagnosed with lung cancer present with NSCLC (75 to 80%). Early symptoms of the disease are often non-specific for cancer and the final diagnosis often reveals tumours at an advanced stage [330]. Although surgery offers the best chance of cure, only a small proportion of patients are ever suitable for this procedure due to early dissemination of the disease. Instead, the majority of sufferers must rely on non-surgical therapies [329].

The identification of genomic alterations driving NSCLC has enabled major progress in the understanding of the molecular mechanisms driving this disease (see

section 1.6.2.2.2). This, in turn, led to the development of novel drugs. Amongst these are the Egfr reversible inhibitors gefitinib and erlotinib. These have been reported to provide considerable clinical benefit in patients diagnosed with tumours carrying Egfr kinase domain mutations such as non-smoker Asian females with lung adenocarcinoma [341]. However, treatment with these inhibitors of patients with tumours deprived of Egfr mutations can worsen their outcome. Furthermore, patients with lesions carrying K-Ras mutations do not respond to these drugs [352]. Hence, screening for Egfr mutations as well as K-Ras mutations in all patients with lung cancer is required to predict the clinical benefit of these inhibitors. However, even in patients that do initially respond to Egfr inhibitors, resistance to these drugs eventually occurs [352]. Several mechanisms have been reported to mediate this resistance including the appearance of additional mutations in Egfr such as the substitution of threonine 790 for a methionine (T790M) that alters the binding kinetic of the inhibitor to the receptor. Recently developed irreversible Egfr inhibitors have been shown to suppress T790M-mutant tumour cells *in vitro* and are promising candidates for future treatment of the disease [394] [395]. Another mechanism reported to mediate this resistance is the amplification of the oncogene c-Met which compensates for Egfr inhibition and drives cell proliferation [396]. Development of a c-Met inhibitor to treat patients with c-Met amplification following Egfr inhibitor treatment might provide clinical benefit. Several other inhibitors directed against proteins involved in NSCLC are currently under evaluation in clinical trials (Table 3).

Target	Inhibitor name (therapeutic)	Target	Company	Stage of development (tumour type)
p110α	PX-866 (in combination with gefitinib)	Pi3k	ProlX Pharmaceuticals	Preclinical (NSCLC)
mTOR	Sirolimus (in combination with Gefitinib)	mTor	Wyeth	Phase I/II (NSCLC, glioblastoma)
	Temsirolimus (CCI-779; in combination with erlotinib)	mTor	Wyeth	Phase I/II (glioblastoma)
	Everolimus (RAD001; in combination with gefitinib or erlotinib)	mTor	Novartis	Phase I/II (NSCLC, glioblastoma, breast)
	AP23573 (single agent)	mTor	Ariad	Phase I/II (endometrial)
MAPK pathway	Sorafenib (BAY49-9006; alone or in combination with erlotinib)	Raf	Bayer	Phase I/II (NSCLC, glioblastoma)
	PD-325901 (single agent)	Mek	Pfizer	Phase II (NSCLC)
Eml4-Alk	PF-02341066 (single agent)	Alk	Pfizer	Phase III (NSCLC)

Table 3: Therapeutic inhibitors under development. Examples of inhibitors that are under evaluation in phase I, II or III clinical trial. (Modified from [352])

Despite the recent therapeutic improvement, the overall survival of most patients diagnosed with advanced NSCLC remains modest. Thus, identification of the mechanisms promoting the dissemination of this disease is required if we aim at efficiently targeting advanced disease.

1.7 RNA interference and cell motility screen

1.7.1 RNA interference

RNA interference was initially described in plants (*petunia*) [397] and fungus (*Neurospora crassa*) [398] as a post-transcriptional gene expression inhibition mechanism mediated by mRNA degradation. Later work, led by Andrew Fire and Craig C. Mello, showed a potent gene silencing effect following injection of double stranded RNA (dsRNA) into *Caenorhabditis elegans* [399]. They showed that neither mRNA nor antisense RNA injections had an effect on gene expression, but that dsRNA

successfully silenced the targeted gene thus identifying for the first time the initiator of the silencing. Following its discovery, the RNA interference (RNAi) machinery was progressively found to be conserved in a variety of organisms. This included higher mammals allowing individual cells to control the expression of 'undesirable' mRNAs from endogenous (e.g. microRNA [400]) or exogenous (e.g. viral dsRNA [401]) origins. Indeed, its role has been extensively described in eukaryotes as an immune molecular defence preventing viral dsRNA from integrating into the host genome [402]. The RNAi pathway (Figure 15) is initiated in the cytoplasm by the ribonuclease DICER which recognises long double stranded RNAs (dsRNA) and cleaves them into short double-stranded RNA fragments of 21–25 base pairs called small interfering RNA (siRNA) duplexes [403]. Following DICER cleavage, one strand of the siRNA duplex (the guide strand) is recognised by the multiprotein RNA-induced silencing complex (RISC) catalytic component, the endoribonuclease Argonaute 2 [404]. Argonaute 2 slices the non-guide (passenger) strand while keeping the guide strand to further associate and slice complementary mRNA. Finally, the RISC complex is recycled for further round of slicing [405]. Thus, by degrading specific RNAs, the RNAi pathway can prevent their translation to regulate the expression of the corresponding proteins.

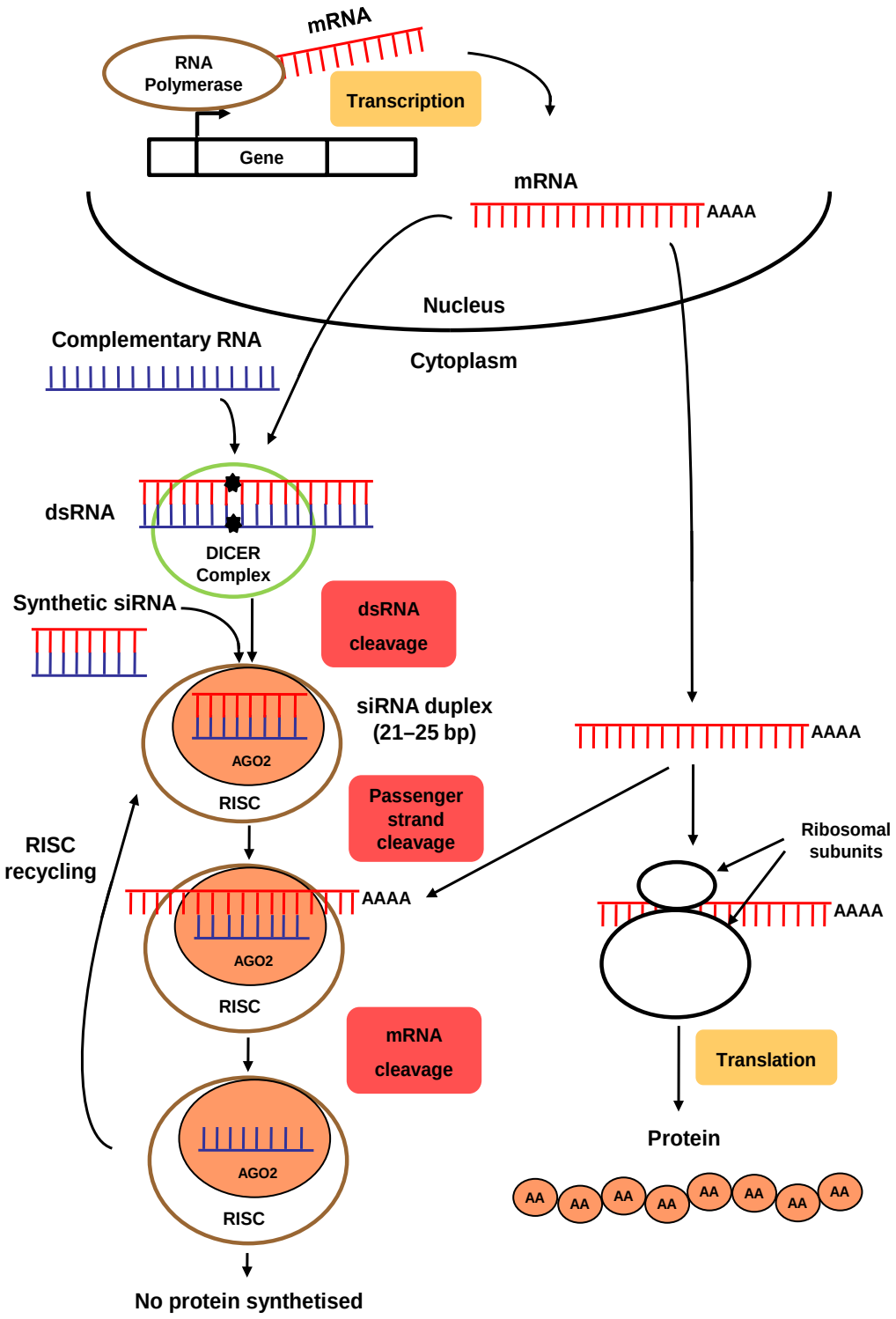

Figure 15: RNA interference pathway. Gene expression starts by the transcription of the genomic sequence into a messenger RNA (mRNA) by an RNA polymerase in the nucleus. Once exported into the cytoplasm the mRNA is translated by the ribosomal machinery into a protein (right panel). In the case of RNA interference (left panel), the presence of a complementary RNA sequence in the cytoplasm leads to the formation of a double stranded RNA (dsRNA) cleaved by the complex DICER into small interfering RNAs of 21 to 25 base pairs (bp). Alternatively synthetic siRNA duplex can be introduced into the cell using transfection. The RNA-induced silencing complex (RISC) and its catalytic subunit, Argonaute 2 (Ago2) load the siRNA duplex, slice the passenger strand and use the guide strand to further recognise and slice complementary mRNA before being recycled [405].

1.7.2 Screening signalling pathways involved in cell migration, invasion and metastasis

The use of RNA interference to silence the expression of specific genes has been expanded leading to the design of siRNA libraries targeting the entire genome. By performing an siRNA screen, one can specifically and systematically assess the effect of single-gene silencing on a cellular process of interest. This approach has been successfully used with small targeted [406] [407] as well as genome-wide libraries [408] [409]. Because cell motility involves large numbers of interacting players, all of which are not yet characterised, screens for signalling pathways involved in cell migration have been undertaken [406] [407]. However, no such screen has been performed in non-small cell lung cancer (NSCLC) where metastasis is a leading cause of death [329]. We propose that identifying kinases involved in NSCLC migration and invasion might reveal novel therapeutic targets to improve the treatment of patients suffering from this disease. Indeed, recent developments in the delivery of siRNA *in vivo* has enabled the efficient silencing of gene expression in animal models suggesting the possibility of RNA interference being used as a therapeutic strategy in the future [410].

1.8 The Thesis

The aims of this thesis are:

1. The identification of kinases regulating NSCLC cell migration and invasion using RNAi technology.
2. Elucidating the mechanisms of action of some promising candidates.
3. Highlighting the potential relevance of our *in vitro* findings *in vivo* using animal models and clinical samples.

The data collected here may provide valuable information that will help design novel therapeutic strategies to prevent NSCLC metastasis.

CHAPTER 2

Materials and methods

2.1 Materials

2.1.1 Reagents

A small interfering RNA (siRNA) library targeting the kinome as well as siRNA SMARTpools and deconvoluted single sequences were obtained from Dharmacon (Lafayette, CO, USA). FlexiTube siRNA sequences, RNAeasy RNA extraction and one-step RT-PCR kits were purchased from Qiagen (Qiagen, West Sussex, UK). Oligofectamine transfection reagent was obtained from Invitrogen (Oregon, USA). Cell Tracker Green CMFDA, the nuclear dye 4',6-diamidino-2-phenylindole (DAPI) and Alexa Fluor 488-conjugated Phalloidin were obtained from Molecular Probe, Invitrogen (Oregon, USA). Forskolin and Tetramethylrhodamine B isothiocyanate (TRITC) coupled phalloidin were purchased from Sigma-Aldrich (Steinhelm, Germany). Matrigel and type I rat tail Collagen were obtained from BD Bioscience (Erembodegem, Belgium). Foetal calf serum (FCS) was obtained from FirstLink (Birmingham, UK). L-glutamine and penicillin-streptomycin solutions were purchased from Biowhittaker (Verviers, Belgium). A 30% solution of acrylamide and bis-acrylamide (37.5:1 ratio) was purchased from National Diagnostics (Hull, UK). Phosphate Buffered Saline (PBS) was purchased from OXOID (Hampshire, UK). Glycine and paraformaldehyde were purchased from BDH Chemicals (Poole, UK). Milk was obtained from Fluka BioChemika (Buchs, Switzerland). Bromophenol blue and the Bio-Rad protein assay were obtained from Bio-Rad (Munich, Germany). Agarose was purchased from Fisher Scientific (Loughborough, UK). DNA 100 bp and 1kbp ladder were obtained from New England Biolabs (Hertfordshire, UK). Crystal violet was obtained from GURR (High Wycombe Bucks, UK). The enhanced chemiluminescence (ECL) kits were obtained from Amersham (Buckinghamshire,

UK). X-Ray films were purchased from Fujifilm (Minato-ku, Japan). Human recombinant Vasp was obtained from Origene (Rockville, MD, USA). Human recombinant active GST-Rsk1 was purchased from Cell Signaling (Danvers, USA). Recombinant GST-S6 peptide (A-K-R-R-R-L-S-S-L-R-A) was obtained from Professor Ivan Gout (University College London, Institute of Structural and Molecular Biology, London, UK).

2.1.2 Antibodies

Rsk1 (sc-231), Rsk2 (sc-9986), Csnk1a (sc-6477), Csnk1e (sc-6471) antibodies were purchased from Santa Cruz (California, USA). An antibody against Csnk1g2 (H00001455-M01) was obtained from Abnova (Taipei, Taiwan). The Vimentin antibody (AF2105) was purchased from R&D System (Minneapolis, USA). E-Cadherin (ab1416), N-Cadherin (ab12221) and Gapdh (ab9484) antibodies were obtained from Abcam (Cambridge, UK). Vasp (V40620) and Mena (610692) antibodies were purchased from BD Transduction Laboratories (Erembodegem, Belgium). Vasp phospho-Ser-157 (3111) and phospho-Ser-239 (3114) antibodies were obtained from Cell Signaling (Danvers, USA). The anti phospho-Thr-278 VASP antibody was a kind gift from Thomas Renne (Karolinska Institutet, Stockholm, Sweden). Secondary horseradish peroxidise (hrp) -coupled antibodies were purchased from Amersham.

2.2 Methods

2.2.1 Cell culture

A549, H23, HCC15 and H522 were obtained from (Cancer Research UK/London Research Institute cell services, London, UK). LNM35 cells were obtained

from Prof. Eric O. Aboagye (Imperial College London, School of Medicine). All five cell lines were adherent and cultured in Dulbecco's Modified Eagle's medium (DMEM) supplemented with 10% foetal bovine serum (FBS), 2 mM L-glutamine, 100 units/ml penicillin and 100µg/ml streptomycin. Cells were grown in a humidified atmosphere at 37°C and with 10% CO_2 and maintained at sub-confluent density by sub-culturing 1/10 twice a week following trypsinisation (0.5mg/ml solution of trypsin in 0.2 mg/ml ethylenediaminetetraacetic acid (EDTA) in Dulbecco's Phosphate Buffered Saline).

2.2.2 RNAi transfection

A549, H23 and LNM35 cells were plated and incubated overnight at 37^{o}C, 10% CO_2 prior to transfection with the relevant siRNA. Table 4 summarises the transfection condition for each assay.

Cell line	Cell density	Plate format	Assay	Volume of Oligofectamine per well
A549, H23 and LNM35	1 x 10^3 / well	96-well plate	Migration assay	0.7 µL
	3 x 10^3 / well	96-well plate	Invasion assay	0.7 µL
	2 x 10^3 / well	96-well plate	Viability assay	0.7 µL
	10 x 10^3 / well	24-well plate	RT-PCR	1.5 µL
	100 x 10^3 / well	6 well plate	SDS-PAGE western blotting	3 µL

Table 4: siRNA transfection conditions. RT-PCR; Reverse transcriptase – Polymerase chaine reaction, SDS-PAGE; Sodium dodecyl sulphate polyacrylamide gel electrophoresis.

Each protein was targeted using a mixture of 4 different sequences (SMARTpool) from Dharmacon (Lafayette, CO, USA). Deconvolution experiments were performed using each single sequence from the pool. Cells were transfected in the presence of 35 nM RNAi using Oligofectamine as a transfection reagent (Invitrogen, Oregon, USA) according to the manufacturer's instructions (Table 4). Cells were then incubated at 37°C/10% CO_2 for 48 h to allow for target down-regulation. Controls used

included untransfected cells and cells transfected with a non-targeting scramble sequences siRNA pool. Further validation of Rsk1 was performed using FlexiTube siRNA sequences from Qiagen (Qiagen, West Sussex, UK). A list of the sequence numbers used for the validation of the screen is provided in the Table 5.

Target Gene	Ref Seq ID	Dharmacon sequences numbers
Rsk1	NM_002953	06, 07, 08, 12
Rsk2	NM_004586	05, 06, 07, 08
Rsk4	NM_014496	01, 02, 03, 04
Csnk1g2	NM_001319	01, 02, 03, 04
Csnk1g3	NM_004384	02, 05, 06, 07
Csnk2b	NM_001320	01, 02, 03, 04
Csnk1a1	NM_001892	09, 10, 11, 12
Csnk1a1l	NM_145203	01, 02, 04, 05
Csnk1e	NM_001894	01, 02, 04, 05
Adck2	NM_052853	02, 03, 04, 05
Adck4	NM_024876	01, 02, 04, 05
Adck5	NM_174922	01, 02, 03, 04
Clk1	NM_004071	01, 02, 03, 04
Clk2	NM_001291	05, 06, 07, 08
Clk4	NM_020666	01, 02, 03, 04
Ckb	NM_001823	01, 02, 03, 05
Mark4	NM_001823	01, 02, 03, 05
		Qiagen sequences numbers
Rsk1	NM_002953	01, 09, 10, 14

Table 5: siRNA sequence numbers used for the validation of the migration screen. Ref Seq ID ; National Center for Biotechnology Information (NCBI) reference number for each transcript targeted.

2.2.3 Reverse transcriptase – Polymerase chain reaction (RT-PCR)

Following siRNA transfection, the efficiency of downregulation of the targeted mRNA was assessed by RT-PCR. Total cellular RNA was extracted using the Qiagen RNAeasy kit according to the manufacturer's instructions. Total RNA concentration was measured using a NanoDrop ND1000 spectrophotometer (Labtech international, East Sussex, UK). RT-PCRs were carried out using the Qiagen one-step RT-PCR kit (QIAGEN, West Sussex, UK). RT-PCR reactions of 25 µl (final volume) were prepared on ice. Each reaction contained 1X RT-PCR buffer, 400 µM of each dNTP (dATP, dTTP, dGTP dCTP), 600 nM of each primers (forward and reverse) (Table 6), 2 µl of RT-PCR enzyme mix [1mM dithiothreitrol (DTT), 0.1 mM EDTA, 0.5% (v/v) Nonidet P-40 (NP-40), 0.5% (v/v) Tween 20, 50% glycerol (v/v), pH 9.0] and 100 ng of RNA template. RT-PCR reactions were carried out using a DNA Engine Dyad thermal cycler

(BioRad, Munich, Germany) with a heated lid. The amplification programme followed 7 steps:

- Step 1: Reverse transcription: 30 min at 50 ºC
- Step 2: Hot start PCR activation: 15 min at 50 ºC
- Step 3: Denaturation of the template: 1 min at 94 ºC
- Step 4: Annealing of the primers: 30 sec at 55 ºC (Ta)
- Step 5: Extenssion: 1 min at 72 ºC
- Step 6: Repeation of the step 3 to 5 over 29 cycles.
- Step 7: Final extension: 10 min at 72 ºC

Forward and reverse primers were designed on separate exons for each target transcript to be amplified (Table 6). RT-PCR products were resuspended 1:5 in 6X DNA loading buffer [30% (v/v) glycerol, 0.25% (w/v) bromophenol blue, 0.25% (w/v) xylene cyanol] and loaded on a 1.2% agarose gel containing 0.7 µg/mL ethidium bromide (BET). A 100 bp DNA ladder was used to confirm the size of the amplified RT-PCR products. Amplification of a fragment of the glyceraldehyde 3-phosphate dehydrogenase (GAPDH) was used as a loading control. The absence of contaminant in the reagents was confirmed by performing an RT-PCR without template in parallel.

Target	Ref Seq ID	Forward sequence	Reverse sequence	Ta (˚C)	Product size (bp)
Rsk1	NM_002953	TCGTGAGATCAAGCCACCCTTCAA	AAACCAAAGTCACAGATGCGCAGG	55	687
Rsk2	NM_004586	AGGCTCTGATGCTAGGCAGCTTTA	AGACTCTGCGCTTCAGGACTCAAA	55	627
Rsk4	NM_014496	TGGCTGGCTACACTCCATTTGCTA	TGAAAGGTCTTGTGAGTCAGGGCA	55	313
Csnk1a1	NM_001892	TCTGAGGCAGCTATTCCGCATTCT	GCTTGCAGACAAGAAGCCAACCAT	55	709
Csnk1a1l	NM_145203	AGCCGACCAGATGATCAGCAGAAT	AGAATGCGGAATAGCTGCCTCAGA	55	504
Csnk1e	NM_001894	TGTTCCCGCAAATTCAGCCTCAAG	AGCCCAGGTTGAAGTACATGAGCA	55	343
Csnk1g2	NM_001319	AGCATGCCATCCACATCATCGACT	ACAGCAGCATTTGGTTTCATCGGC	55	662
Csnk1g3	NM_004384	AGTGTTGAACATGTGGTGCTGCTG	CCATTCACTGATGGGCAAAGCACT	55	317
Csnk2b	NM_001320	TTGGACCTGGAGCCTGATGAAGAA	ATGGCTTCACCTGGGATGTCTGAA	55	236
Gapdh	NM_002046	AAGGTCGGAGTCAACGGATTTGGT	AGTGATGGCATGGACTGTGGTCAT	55	534

Table 6: Forward and reverse sequences used for the RT-PCRs. Ref Seq ID ; National Center for Biotechnology Information (NCBI) reference number for each transcript amplified. Ta; annealing temperature. The RT-PCR products size is given in base pair (bp).

2.2.4 Protein extraction and Sodium dodecyl sulphate polyacrylamide gel electrophoresis (SDS-PAGE)

Cellular proteins were extracted using a lysis buffer [20 mM 4-(2-hydroxyethyl)-1-piperazineethanesulfonic acid HEPES-NaOH (pH 7.4), 150 mM NaCl, 2 mM EDTA, 0.5% (w/v) Triton X-100, 10% (w/v) glycerol]. This buffer was used for SDS-PAGE analysis of protein extracts, immunoprecipitation and co-immunoprecipitation. This lysis buffer was supplemented with a cocktail of protease inhibitors (Roche Diagnostics). Although the exact composition of this cocktail is not disclosed, it contains 4-(2-Aminoethyl)-benzenesulfonyl fluoride hydrochloride (AEBSF), aprotinin (a trypsin inhibitor), leupeptin (a lysosomal protein inhibitor) and pepstatin (an aspartyl proteases inhibitor). The buffer was further supplemented with inhibitor of phosphatases, 1 mM sodium orthovanadate (Na_3VO_4) (a tyrosine phosphatases inhibitor), 10 mM β-Glycerophosphate and 10 mM sodium fluoride (NaF) (serine/threonine phosphatases inhibitors). The lysates were clarified by centrifugation for 10 min at 14 000 rpm (G-force equivalent: 12500 g) and equalised for protein amount using the Bio-Rad protein assay based on the method of Bradford [411]. Equal protein amounts were analysed by SDS-PAGE. SDS-PAGE was performed according to the method of Laemmli [412]. Slab gels were prepared with a 5% acrylamide stacking gel [5% acrylamide, 0.125 M Tris, pH 6.8, 0.1% SDS, 0.075% ammonium persulphate (APS) and 0.083% Tetramethylethylenediamine (TEMED)] and a 8 or 10% acrylamide resolving gel [8-10% acrylamide, 0.375 M Tris, pH 8.8, 0.1% SDS, 0.06% APS, 0.07% TEMED] depending on the size of proteins being analysed. Samples diluted 1:1 in 2 x sample buffer [4% SDS, 20% glycerol, 10% β-mercaptoethanol, 0.125M Tris-HCl,

0.004% bromophenol blue, pH 6.8] were boiled at 95^{o}C for 5 min and pelleted by centrifugation for 1 min at 14 000 rpm (G-force equivalent: 12500 g) prior to either electrophoresis or storage at –20^{o}C. Stored samples were re-boiled at 95^{o}C for 5 min and pelleted by centrifugation for 1 min at 14 000 rpm (G-force equivalent: 12500 g) before SDS-PAGE separation. Electrophoresis was performed using a Tris-glycine running buffer [2.5 mM Tris, 0.2 M glycine and 0.1% SDS] at 20mA per gel using the SE 400 Sturdier Vertical Electrophoresis Unit (Hoefer, Holliston, MA, USA) for the large gels and the Mini-Protean BioRad gel electrophoresis for smaller gels (BioRad, Munich, Germany).

2.2.5 Western blotting

Following SDS-PAGE, the gels were electrophoretically transferred onto nitrocellulose membranes using a Hoefer wet-blotting apparatus for 2 h at 400 mA in 4^{o}C transfer buffer [20% methanol, 39mM glycine, 48mM Tris-HCl, pH 9.5]. Following the transfer, membranes were blocked for 1 h at room temperature (RT) in PBS containing 5% (w/v) fat-free milk before incubation with the relevant antibody diluted in PBS containing 3% (w/v) BSA overnight at 4^{o}C. Membranes were then washed four times 15 min in PBS, 0.05% (v/v) Tween 20 (PBS-T) prior to 1 h incubation at room temperature with the relevant secondary HRP-conjugated antibody diluted in PBS containing 1% (w/v) fat-free milk. The immunoblots were subsequently washed four times 15 min in PBS-T and subjected to enhanced chemo-luminescence (ECL) according to the manufacturer's instructions (Amersham, GE Healthcare). ECL signals were revealed using X-Ray films (Fujifilm, Minato-ku, Japan).

2.2.6 Immuno and co-Immunoprecipitation

100 x 10^3 A549 cells were plated in 6-well plates and incubated overnight at 37°C, 10% CO_2 prior to siRNA transfection or not. In the case of Vasp phosphorylation on Ser-157 and Ser-239, A549 cells were stimulated with Forskolin 10µM for 30 min. DMSO was used as a diluent-alone control. Fokskolin is a potent activator of Pka and Pkg previously reported to stimulate the phosphorylation of those two residues [149]. Cells were lysed at 4 ºC in 0.5 ml of LB (see above). Cell lysates were clarified by centrifugation for 10 min at 14 000 rpm (G-force equivalent: 12500 g), 4 °C, and equalised for protein amount using the Bio-Rad protein assay as previously explained. 0.5mg/mL of protein extract were immunoprecipitated for 2 h at 4 °C using 1 µg/ml of anti Vasp mouse monoclonal IgG1 antibody (BD, V40620), anti Rsk1 rabbit polyclonal IgG antibody (Santa Cruz, sc-231) or Rsk2 mouse monoclonal IgG1 antibody (Santa Cruz, sc-9986) together with Protein A- or G–Sepharose (Sigma-Aldrich, Steinhelm, Germany) (25 µl of a 50% slurry solution previously washed three time in PBS). Protein A-Sepharose was used with rabbit polyclonal IgG while the protein G–Sepharose was used with the mouse monoclonal IgG1 antibody. The immune complexes were then washed three times in 1mL of ice-cold LB (see above) (centrifugation step was performed at 5000 rpm (G-force equivalent: 2100 g) 30 sec at 4 °C). Immunoprecipitates were resuspended 1:1 in 2 x sample buffer and subjected to SDS-PAGE/ Western blotting as previously described.

2.2.7 *In vitro* kinase assay

1 µg human recombinant Vasp (Origene, Rockville, MD, USA) was incubated on ice in 5mM MOPS (pH 7.2), 2.5 mM β-glycerophosphate, 1mM EGTA, 0.4 mM EDTA, 5mM $MgCl_2$ and 0.05mM DTT in the presence or absence of 10ng of human

recombinant active GST-Rsk1 (Cell Signaling, Danvers, USA). The reaction was started by adding an ATP-mix resulting in a final concentration of 100 μM ATP with or without 10 nCi/μl [γ-^{32}P]ATP (Perkin Elmer, Waltham, MA, USA) and incubated for 30 min at 30ºC. As a positive control 1μg recombinant GST-S6 peptide (A-K-R-R-R-L-S-S-L-R-A) was used as a substrate for Rsk1. Reactions were terminated in SDS-sample buffer and analysed by SDS-PAGE and autoradiography.

2.2.8 Autoradiography

^{32}P-labelled samples were resolved by SDS-PAGE. Prior to drying, gels were fixed and stained with Coomassie Brilliant Blue R-250 (Sigma-Aldrich, Steinhelm, Germany) in 40% (v/v) methanol, 10% (v/v) acetic acid. Gels were then dried under vacuum for 2 h at 80^{o}C and exposed to X-Ray films.

2.2.9 Cell migration assay

Random migration speed was measured as previously reported [413]. 1 x 10^3 A549 cells were plated in a 96 well-plates and incubated overnight at 37^{o}C, 10% CO_2 prior to siRNA transfection with the relevant RNAi. 48h later, cells were fluorescently stained using either DioC6 (Molecular Probe, Invitrogen) or Cell tracker Green 5'chloromethylfluorescein diacetate (CMFDA) (Molecular Probe, Invitrogen) according to the manufacturer's instructions in phenol red-free DMEM supplemented with 10% foetal calf serum (FCS), 2 mM L-glutamine, 100 units/ml penicillin and 100μg/ml streptomycin. Cells were washed twice with fresh medium to remove the excess of dye and left 1h in the incubator to allow the pH to equilibrate before imaging. Cell tracker green CMFDA was used at a dilution of 1/20,000 in phenol red-free DMEM supplemented with 10% foetal calf serum (FCS), 2 mM L-glutamine, 100 units/ml penicillin and 100μg/ml streptomycin. Time-lapse imaging was performed

over 18 h (1 image every 10 min) using a motorised-staged environment-controlled Nikon microscope with the Metamorph imaging software (Molecular Devices). Each condition was performed in duplicate with two fields acquired for each replicate. Sixty cells per conditions were subsequently tracked using the Metamorph tracking module. Tracks were analysed using a previously published Mathematica notebook [413] (Wolfram Research). A one way ANOVA statistical test was used to assess the statistical significance of the results obtained with cells transfected with scrambled sequences used as reference.

2.2.10 Cell viability assay

2 x 10^3 A549 cells were plated at 50% confluence in 96 well-plates and incubated overnight at 37°C, 10% CO_2 prior to transfection. 48h following RNAi transfection, cells were subjected to a CellTiter-Glo® Luminescent Cell Viability Assay (Promega, Madison, WI) according to the manufacturer's instructions. Parallel experiments were performed using crystal violet staining. For the latter, 48h following RNAi transfection, cells were fixed and stained with 0.5% (w/v) crystal violet prepared in 25% (v/v) Methanol for 20 min. Fixed specimens were then washed in water three times, dried and resuspended for 30min in 10% (v/v) acetic acid. Crystal violet absorption was read on a spectrophotometer at 590nm. Mean and standard error of the mean (SEM) of independent experiments were calculated. Statistical analysis was performed using a two-tailed Student's t-test to determine the statistical significance of the differences observed. A p-value below 0.05 was considered significant.

2.2.11 Actin cytoskeleton staining and lamellipodia counting

Cells in 96 well-plates were fixed with 50µL of 4% (w/v) phosphate buffered paraformaldehyde (PFA) solution for 15 min, washed 3 times in PBS, permeabilised

using 50µL of 0.1% (v/v) Triton X-100 in PBS for 5 min, washed 3 times in PBS, and blocked using 50µL of 3% (w/v) Bovin Serum Albumin (BSA) in PBS for 1 hour. The staining of the actin cytoskeleton was achieved using Alexa Fluor 488-conjugated Phalloidin (Molecular Probe, Invitrogen) and the nuclear DNA revealed using 4',6-diamidino-2-phenylindole (DAPI) (Molecular Probe, Invitrogen). Image acquisition was performed for 36 fields per well using an ImageXpress high-throughput microscope (Molecular Devices) driven by the MetaXpress software (Molecular Devices). The average number of lamellipopdia per cell from 36 fields of view was determined by two independent observers. Cells partially outside the field of view were excluded. Mean and standard error of the mean (SEM) of independent experiments were calculated. Statistical analysis was performed using a two-tailed Student's t-test to determine the statistical significance of the differences between conditions.

2.2.12 Invasion assay

3 x10^3 A549 cells were plated in 96 well-plates and incubated overnight at 37^{o}C, 10% CO_2 prior to RNAi transfection. 24h following RNAi transfection, different extra cellular matrix were laid over the cells. These include Matrigel alone (final concentration ~10mg/mL), type I rat tail collagen (final concentration 3mg/mL) or a mixture of type I collagen diluted 1 in 10 in Matrigel (type I collagem final concentration: 1mg/mL). The collagen was prepared in 1x final concentration DMEM supplemented with 1% FCS. The plates were incubated for 4h at 37^{o}C, 10% CO_2 to allow for the matrix to polymerise. 25 µl of DMEM/1% FCS were added on the gel prior to incubation for 16h at 37^{o}C, 10% CO_2. 25 µl of DMEM/1% FCS supplemented or not with Egf (ranging from 10ng/mL to 2µg/mL) to stimulate invasion. A concentration of 1µg/mL Egf corresponding to a final concentration in the well of 166 ng/mL was used during the screen. Cells were then allowed to invade upward through

the matrix for 48h. The plates were then fixed in 150µL of 4% (w/v) PFA for 45 min, washed 3 times in PBS, permeabilised using 150µL of 0.1% (v/v) Triton X-100 in PBS for 30 min, washed 3 times in PBS and blocked using 150µL of 3% Bovin Serum Albumin (BSA) in PBS for 2 hour. The staining of the actin cytoskeleton was achieved using TRITC-conjugated phalloidin (Sigma-Aldrich, Steinhelm, Germany). Each condition was performed in triplicate. An autofocus, based on the reflection at the bottom of the plate of the 633nm wavelength laser, was performed for each field prior to acquisition of the stack. Nine fields of view were acquired at the centre of each well using a motorised Zeiss Invert confocal microscope using a 10x lens with a 0.45 numerical aperture (NA). Stacks of 150 µm were acquired for each field of view with a distance of 4µm between focal planes. The image stacks were analysed using a Mathematica notebook (Wolfram Research) programmed by Dr Alastair Nicol (Light Microscopy Department, CRUK, London, UK) to determine the extent of cell invasion (see Chapter 4 section 4.2.1.3). Results of nine stacks per well in triplicates were pooled before performing a one way ANOVA statistical analysis with scramble transfected cells as a reference. An siRNA pool targeting non-erythroid protein 4.1 brain types (4.1B) was used as a pro-invasive control (see section 4.2.1.5).

2.2.13 Zebrafish metastatic model.

Zebrafish embryos at 4 h post-fertilisation (hpf) were microinjected under stereomicroscopic observation with Histone 2B-GFP expressing A549 cells into the cell mass using a 12 µm guage borosilicate pipettes mounted on a Narishige microinjector. The embryos were then imaged under anaesthetic by widefield fluorescent microscopy at 48 hpf and the presence of A549 cells in 3 different compartments (head, middle and tail) recorded. H2B-GFP expression had no effect on baseline motility or invasiveness of A549 cells (data not shown). This work was performed in collaboration with the

laboratory of Prof. Maggy Dalman (Division of Cell and Molecular Biology, Department of Life Sciences, Faculty of Natural Sciences, Imperial College London, London, UK) and involved Dr. Olivier Pardo, Harriet Taylor, Alice Shia and Prof. Jonathan R Lamb. My participation to this work was marginal. Hence these results can be found in Annexe 1.

2.2.14 Bioinformatic analysis

A human protein-protein interaction (PPI) database was compiled from two previously published databases [414] [415] containing both predicted and demonstrated interactions. The query of the PPI database with our hit list of 70 kinases was performed using Python programming and Cytoscape (Cytoscape, www.cytoscape.org) tools. First-node level interactions amongst our hits as well as between our hits and other proteins in the interactome were determined. The positive interactions false-rate was assessed using 10 randomly generated lists of 70 proteins from the kinome library using Mersenne Twister random number generator under python programming.

2.2.15 Immuno-histopathology

A syngeneic primary tumour/metastasic tissue microarray (TMA) was compiled from 11268 post-mortem (PM) reports performed at the Hammersmith Hospital NHS Trust between 01.01.1970 and 31.12.2005 and reviewed (Ethic Reference: 06/Q0406/154). Lung cancer was identified in 499 cases with complete PM of which 213 did not receive any chemotherapy or radiotherapy treatment. All slides from these cases were reviewed to confirm histotype as well as metastatic distribution and evaluate tissue quality. Immunostaining for pan-cytokeratin MNF116 and Vimentin were performed to evaluate the suitability of the tissue for immunohistochemical studies. Subsequently, 100 cases were considered suitable to be included in the TMA.

The available data related to these cases including metastatic distribution were recorded. Three 1mm cores were obtained from the most representative and better preserved areas of the primary tumours and their metastases and re-embedded in microarray blocks. Antigen retrieval was carried out using a modification on a previously published method [416]. Briefly, the sections were rehydrated in graded alcohols, heated in a microwave oven at 900W for 20 min in Citrate buffer at pH6 and cooled at room temperature before immunostaining. Endogenous peroxidase activity was suppressed by incubation with a 3% solution of H_2O_2 for 5 min. The primary antibodies were used at the following concentrations Rsk1 (Santa Cruz, sc-231) 1/1200, Rsk2 (Sigma, HPA003221) 1/300, Rsk4 (Sigma, HPA002852) 1/100. The TMAs were incubated with the antibodies for 1 hour at room temperature and then processed using the Polymer-HRP Kit (BioGenex) with Diaminobenzidine development and Mayer's Haematoxylin counterstaining. External positive controls were used according to the antibodies' datasheets. Negative controls included omitting the primary antibody, competition with the peptide used to raise the primary antibody and staining of A549 cells treated with a non-targeting scramble sequences or a relevant (Rsk1, 2 or 4) siRNA. A semi quantitative immunohistochemical score (IHS) was used as previously described [417] including assessment of both the percentage of positive cells and the intensity of staining. For the intensity, a score of 0 to 3, corresponding to negative, weak, moderate and strong positivity, was recorded. The range of possible scores was thus 0 to 300. Each core was scored individually with three cores evaluated from each tumour/metastasis and the mean of the 3 readings calculated. If one core was uninformative the score applied was the mean of the remaining two cores. Two observers, blinded to all the clinical data, scored all cases and results were found to be consistent. TMAs for syngeneic primary non-small cell lung tumours and surrounding

normal tissue were purchased from US Biomax Inc. and treated as described above. This work was performed in collaboration with Dr. Francesco A. Mauri (Histopathology, Imperial College London, Hammersmith Campus, London, UK) and involved Dr. Robert J Shiner.

CHAPTER 3

A high-throughput screen identifies novel regulators of cell motility in lung cancer cells

3.1 Introduction

Lung cancer is the commonest cancer killer and most deaths are due to the presence of metastatic disease. Consequently, understanding the underlying mechanisms that govern metastasis in lung cancer could provide new therapeutic targets and are biomarkers predictive of outcome for this disease.

During the metastatic process, cells are required to change their morphology and develop a pro-motile phenotype. Hence, to increase our understanding of lung cancer cell metastasis, it was essential that we first identify molecules that regulate cell migration in this system.

RNA interference (RNAi) has become a powerful approach to characterise gene function. The use of small interfering RNA (siRNA) libraries has enabled investigators to systematically screen for the role of individual genes in various phenotypes [418]. Similarly, we have developed an automated kinome-based siRNA screen for cell migration. The optimisation, validation and results of this screen are presented in this chapter. We identified 48 novel regulators of A549 non-small cell lung cancer cell motility among which several kinase families were over represented. These were the Ribosomal protein S6 kinase (Rsk), Casein kinase, Adck (AarF domain containing kinase) and Clk (CDK-like kinase) families. We focussed our attention on the Rsk family and show that knockdown of these proteins leads to changes in cell morphology and modulation of the EMT markers E-Cadherin and Vimentin in agreement with the migration phenotype.

3.2 Results

3.2.1 Motility Screen set-up

3.2.1.1 Choice of the cell system

The screen was developed in a 96-well plate format to allow high-throughput processing of the library. BD Falcon™ Black 96-well Microtest™ Optilux™ Plate (BD Bioscience) were selected for their good optical property.

Prior to starting our siRNA screen, an appropriate cell system and adequate controls had to be identified. Four different non-small cell lung cancer cell lines (A549, HCC15, H23 and H522) were tested for their migratory ability. Among these, A549 and H23 cells migrated significantly faster than HCC15 and H522 cells (Figure 16A). It has been previously reported that A549 cells have invasive capabilities both *in vitro* and *in vivo* [419] [420] [421] [422] [423] [424] [425]. Hence we decided to perform our migration screen in this well characterised cell line.

3.2.1.2 Automated tracking

To enable us to perform automated cell tracking, fluorescent labelling of the cell was used to improve contrast between the image background and the migrating cells. Two different cell dyes were tested, DioC6, an ER and mitochondria stain [426] and Cell Tracker Green (Invitrogen (C2925)), a molecule that binds the cellular thiol moieties (Figure 16). We performed dose-range experiments to identify concentrations for both dyes that would provide an optimum signal to noise ratio without affecting the ability of the cells to migrate. While DiOC6 still inhibited cell migration at the lowest concentration tested, Cell Tracker Green used at 0,5nM gave a robust signal throughout the 18h of the assay with no detectable effect on cell migration (Figure 16B). The

signal was sufficient for migrating cells to be easily detected using Metamorph (Molecular Devices) and followed using the automated tracking plug-in available in this software (Figure 16C and D).

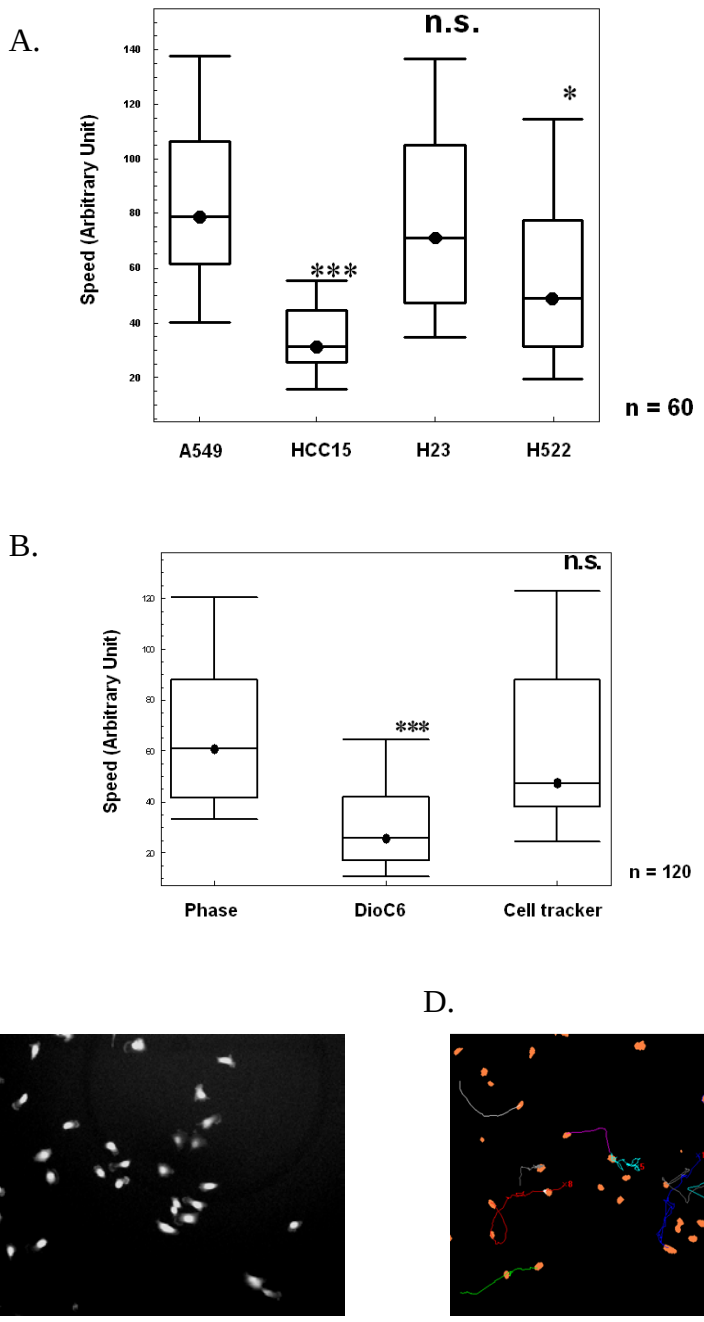

Figure 16: Optimisation of the migration assay. (A) Random migration assay results for the NSCLC cell lines A549, HCC15, H23 and H522. The average random migration speed distribution of 60 cells per condition is represented as a box and whisker plot. A549 cells were used as a reference for the statistical ANOVA analysis. A representative of 3 independent experiments performed in duplicate is shown. (B) Random migration assay results in A549 cells upon staining with the viable fluorescent cell dyes DioC6 and Cell tracker Green. The average random migration speed distribution of 120 cells per condition is represented as a box and whisker plot. Unlabelled cells imaged in phase were used as reference for the ANOVA statistical analysis. Random migration assays were performed by filming cells over 18h and tracked using Metamorph software. Tracks were then analysed using Mathematica to generate box and whisker plots of cell migration speed. Box represents 75% and side bar 12.5% of the cell population. Dot represents median speed. Statistical test were performed using ANOVA analysis. *; $p<0.05$, , ***; $p<0.001$, n.s.; not significant. A representative of 3 independent experiments performed in quadruplicate is shown. (C) Representative field of view showing A549 cells stained with Cell Tracker Green. (D) Corresponding cell tracking obtained using a Metamorph plug-in following binarisation and segmentation of the films.

3.2.1.3 Transfection control

To control for equivalent transfection efficiency between experimental plates throughout the screen, transfection of olinucleotides directed against Plk1 (Polo-like Kinase1), a kinase known to regulate the exit from mitosis, were used [427]. Plk1 siRNA transfection induced changes both in A549 migration and morphology (Figure 17). In the migration assay, cells silenced for Plk1 showed a reduction in their migration speed as compared to non-targeting scramble sequences (Sc) (Figure 17A). Morphological changes included increased cell spreading and the appearance of multiple nuclei accompanied by a decrease in total cell number (Figure 17B).

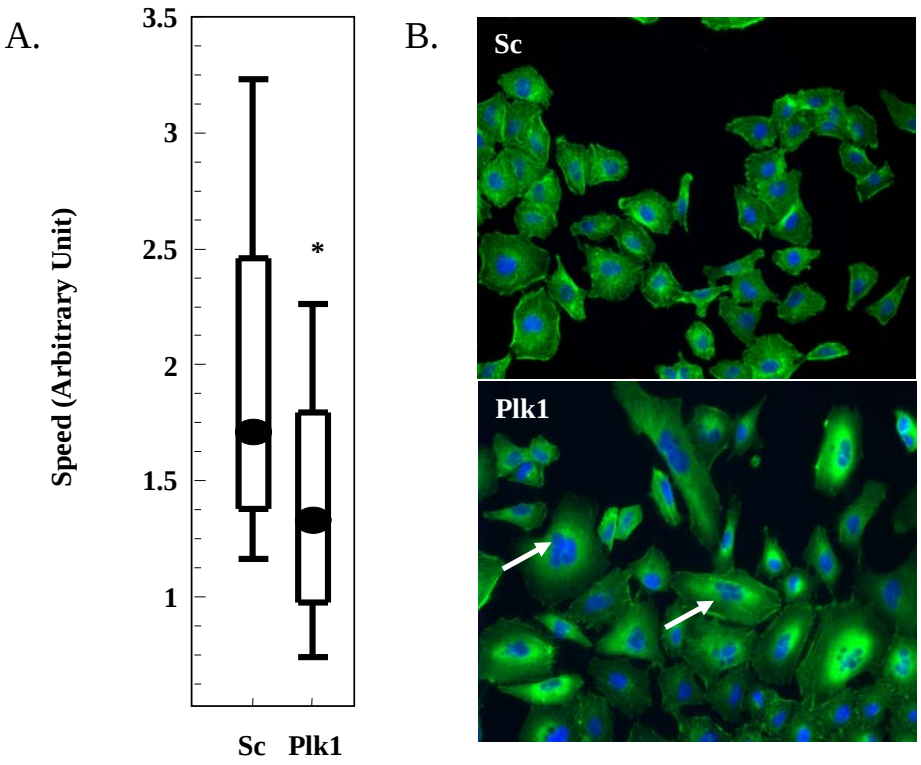

Figure 17: Plk1 as a transfection control in A549 cells. (A) Representative random migration results from the migration screen showing decreased A549 migration speed upon Plk1 knock-down compared to treatment with a non-targeting Scramble sequences (Sc). The speed of cell migration is represented as a box and whisker plot. ANOVA analysis was performed using Scramble transfected cells as reference. Box represents 75% and side bar 12.5% of the cell population. Dot represents median speed. Statistical tests were performed using ANOVA analysis. * corresponds to $p<0.05$. (B) Actin cytoskeleton staining of A549 cells using Alexa Fluor 488 phalloidin (green) together with the nuclear dye 4',6-diamidino-2-phenylindole (DAPI) (blue). An increased cell spreading and the appearance of multiple nuclei (white arrow) can be observed upon Plk1 knock-down. Representative experiment taken from the migration screen.

3.2.2 Migration screen results

At the end of the screening process, mean speed values for each condition were calculated and normalised to the scramble control for each plate. Amongst the 779 proteins targeted by the library, 160 conditions showed a significant modification of migration speed as compared to transfection with non-targeting scramble sequences (Figure 18B). Plotting of the mean speed distribution revealed a reduction of cell motility speed following silencing of two third of the proteins targeted by our library. In contrast, only one third of the targets enhanced cell migration speed upon downregulation (Figure 18A). This difference could be correct or might be explained by the high baseline motility level of A549 cells (Figure 16A) that may limit our ability to further increase A549 migration speed upon siRNA treatment. Alternatively, siRNA-mediated down regulation of some targets might be toxic to the cells, leading to an artifactual reduction in cell migration. In order to assess this possibility, our list of hits was compared against results from a parallel screen for cell toxicity performed in A549 cells using the same library [428]. Any hit showing toxicity greater than 10% was sidelined, reducing the hit list to 70 proteins (Table 7). Among those 70 hits, 56 showed a reduction, whereas 14 enhanced migration speed. Finally, 22 of these proteins had already been reported in the literature as being involved in cell migration. Those 22 hits included Akt2 [429], Map4k4 [406] and Ephb6 [430] and provided a measure of the validity of our screen (Figure 18). Hence, our screen revealed 48 previously unreported regulators of cell migration.

A.

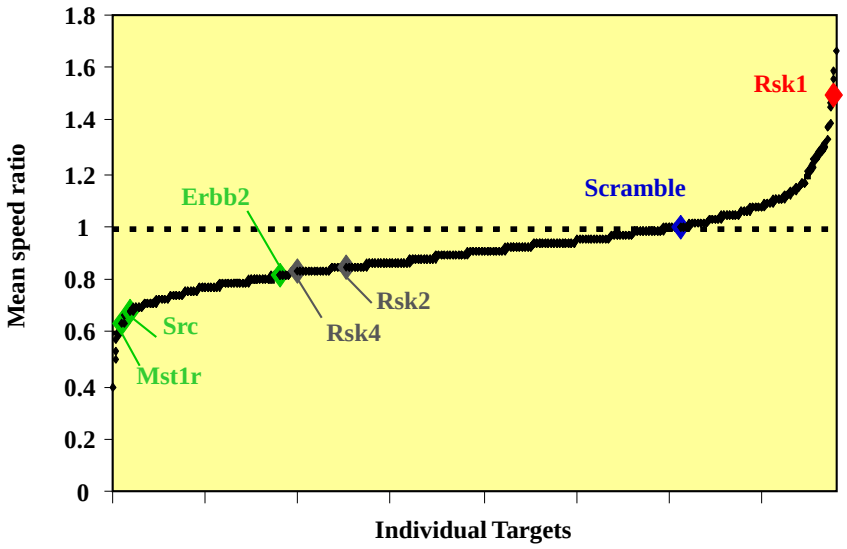

B.

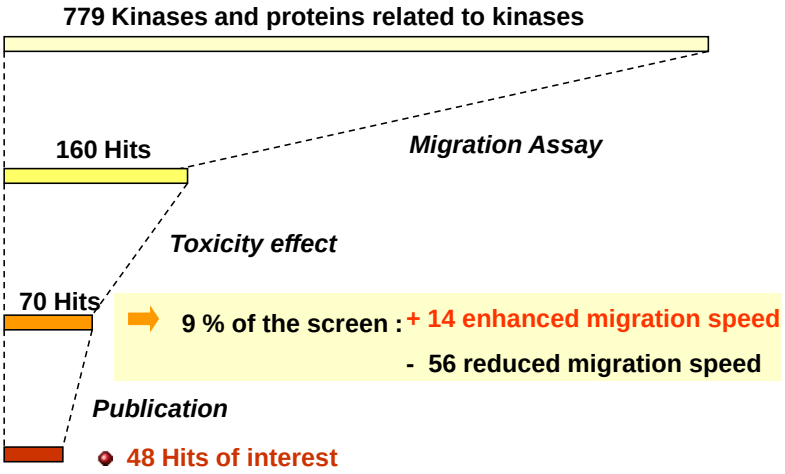

Figure 18: Cell motility screen result (A) Distribution of the mean migration speed ratio obtained following the downregulation of the 779 targets of the Dharmacon kinome library. Mean migration speed for each RNAi condition was normalised to the scramble mean migration speed of the corresponding plate and plotted in an ascending order. Green spots indicate three targets (Erythroblastic Leukemia Viral Oncogene Homolog 2 (Erbb2), Sarcoma viral oncogene (Src) and Macrophage Stimulating 1 Receptor (Mst1r)) previously reported to regulate NSCLC cell motility. The p90 Ribosomal S6 Kinase 2 and 4 (Rsk2 and 4) (gray spots) that decrease and p90 Ribosomal S6 Kinase 1 (Rsk1) that increase cell migration speed upon knockdown are highlighted. (B) Overview of the migration screen showing the successive steps in the selection of hits based on the migration speed results, the control for cell toxicity of the siRNAs and previously published reports.

Amongst our 70 hits, four families were represented by several members modulating A549 mobility. These were the Ribosomal protein S6 kinase, Casein kinase, Adck (AarF domain-containing kinase) and Clk (CDK-like kinase) families (Table 8). Each family contained both members that increased and decreased A549 migration speed suggesting the possible existence of a balance between the different isoforms. RNAi screens have inherent rates of false positives and false negatives and various validation steps are required to address this issue [431]. For further validation work, we decided to focus on these 4 families as well as the best hits decreasing (Map/microtubule affinity-regulating kinase 4; Mark4) and increasing (creatine kinase brain type; Ckb) cell migration speed upon knockdown.

Gene Symbol	Protein Name	Ref Seq ID	Ratio to Sc	ANOVA
ACK1	Activated p21cdc42 kinase	NM_005781	0.86	*
ADCK2	AarF domain containing kinase 2	NM_052853	0.72	*
ADCK4	AarF domain containing kinase 4	NM_024876	0.72	*
ADCK5	AarF domain containing kinase 5	NM_174922	1.67	**
AKT1	V-akt murine thymoma viral oncogene homolog 1	NM_005163	**0.61**	*
AKT2	V-akt murine thymoma viral oncogene homolog 2	NM_001626	**0.83**	*
ALS2CR2	Amyotrophic lateral sclerosis 2 juvenile chromosome region gene2	NM_018571	**0.81**	**
ANGPT4	Angiopoietin 4	NM_015985	**0.71**	**
AURKC	Aurora kinase C	NM_003160	**0.49**	***
CDC42BPB	Cell division cycle 42 binding protein kinase β	NM_006035	**0.79**	*
CDKL3	Cyclin-dependent kinase-like 3	NM_016508	**0.76**	*
CDKL5	Cyclin-dependent kinase-like 5	NM_003159	**0.75**	*
CDKN2B	Cyclin-dependent kinase inhibitor 2B	NM_004936	**0.76**	*
CDKN2D	Cyclin-dependent kinase inhibitor 2D	NM_001800	**0.74**	*
CHEK2	Checkpoint kinase 2	NM_007194	**1.37**	*
CHKB	Choline kinase β	NM_005198	**0.79**	*
CKB	Creatine kinase, brain type	NM_001823	**1.59**	*
CLK1	Cdc-like kinase 1	NM_004071	**1.40**	*
CLK2	Cdc-like kinase 2	NM_001291	**0.71**	*
CLK4	Cdc-like kinase 4	NM_020666	**0.79**	*
CSNK1A1L	Casein kinase 1 α-1 like	NM_145203	**0.73**	**
CSNK1G2	Casein kinase 1 γ-2	NM_001319	**1.29**	**
CSNK1G3	Casein kinase 1 γ-3	NM_004384	**1.28**	**
CSNK2B	Casein kinase 2β	NM_001320	**1.26**	*
DDR2	Discoidin domain receptor family, member 2	NM_006182	**1.46**	*
EDN2	Endothelin 2	NM_001956	**1.49**	*
EPHB6	Ephrin receptor ephb6	NM_004445	**1.30**	*
GALK1	Galactokinase 1	NM_000154	**0.86**	*
GMFG	Glia maturation factor, γ	NM_004877	**0.85**	*
MAP4K4	Mitogen-activated protein kinase kinase kinase kinase 4	NM_004834	**0.82**	*
MAPK11	Mitogen-activated protein kinase 11	NM_002751	**0.76**	**
MAPK13	Mitogen-activated protein kinase 13	NM_002754	**0.82**	*
MAPK3	Mitogen-activated protein kinase 3	NM_002746	**0.84**	*
MARK4	Map/microtubule affinity-regulating kinase 4	NM_002747	**0.53**	***
MELK	Maternal embryonic leucine zipper kinase	NM_014791	**0.75**	*
MGC45428	Doublecortin-like kinase 2	NM_152619	**0.69**	*
MGC8407	Cam kinase-like vesicle-associated	NM_024046	**0.73**	**
MPP3	Membrane protein, palmitoylated 3	NM_001932	**1.23**	*
MVD	Mevalonate pyrophosphate decarboxylase	NM_002461	**0.77**	*
MYO3A	Myosin 3a	NM_017433	**1.38**	*
NAGK	N-acetylglucosamine kinase	NM_017567	**0.75**	*
NEK6	Never in mitosis gene a-related kinase 6	NM_014397	**0.78**	*
NPR1	Natriuretic peptide receptor a/guanylate cyclase a	NM_000906	**0.68**	***
PANK4	Pantothenate kinase 4	NM_018216	**0.83**	*
PCK2	Phosphoenolpyruvate carboxykinase 2	NM_004563	**0.80**	*
PDK3	Pyruvate dehydrogenase kinase, isoenzyme 3	NM_005391	**0.79**	*
PFKFB1	6-phosphofructo-2-kinase/fructose-2,6-biphosphatase 1	NM_002625	**0.73**	*
PFKFB4	6-phosphofructo-2-kinase/fructose-2,6-biphosphatase 4	NM_004567	**0.79**	*
PIK3C2G	Phosphatidylinositol 3-kinase, class 2 γ	NM_004570	**0.64**	*
PIP5KL1	Phosphatidylinositol-4-phosphate-5-kinase-like 1	NM_173492	**0.68**	**
PKIB	Protein kinase cAMP-dependent catalytic inhibitor β	NM_032471	**0.74**	*
PKN3	Protein kinase N3	NM_013355	**0.82**	*
PPP2CA	Protein phosphatase 2a catalytic subunit α isoform	NM_002715	**0.81**	**
PPP4C	Protein phosphatase 4 catalytic subunit	NM_002720	**0.84**	*
PRKACB	Protein kinase camp-dependent catalytic β	NM_002731	**0.79**	**
PRKAG1	Protein kinase, amp-activated, noncatalytic γ-1	NM_002733	**0.87**	*
PRKCL2	Protein kinase C-like 2	NM_006256	**0.68**	*
PRKCM	Protein kinase C μ	NM_002742	**0.77**	*
PRKCSH	Protein kinase C substrate, 80-kd, heavy chain	NM_002743	**0.76**	*
PRKWNK1	Protein kinase lysine-deficient 1	NM_018979	**0.77**	*
PTPRG	Protein-tyrosine phosphatase receptor-type γ	NM_002841	**0.78**	*
RFK	Riboflavin kinase	NM_018339	**0.87**	*
RSK1	Ribosomal S6 kinase 1	NM_002953	**1.46**	*
RSK2	Ribosomal S6 kinase 2	NM_004586	**0.86**	*
RSK4	Ribosomal S6 kinase 6	NM_014496	**0.83**	**
RPS6KC1	Ribosomal protein S6 kinase, 52kDa, polypeptide 1	NM_012424	**0.71**	**
STK23	Serine/threonine-protein kinase 23	NM_014370	**0.76**	**
STK29	Serine/threonine-protein kinase 29	NM_003957	**0.75**	**
STK6	Serine/threonine-protein kinase 6	NM_003600	**0.73**	**
TRIB3	Tribbles, drosophila, homolog 3	NM_021158	**0.67**	*

Table 7: List of 70 Hits modulating A549 cell migration speed. List of hits identified in the migration screen to increase (red) or decrease (black) migration speed upon RNAi downregulation. siRNA library

Gene symbol, corresponding protein name, alternative symbol and NCBI GenBank Reference Sequence ID (Ref Seq ID) are shown. Ratio of migration speed to Scramble (Sc) is given with the result of the ANOVA statistical analysis performed with the scramble condition used as reference.*; p<0.05, **; p<0.005, ***; p<0.001.

Family	Proteins	
	Toxicity ≤ 10%	Toxicity > 10%
RPS6 kinase	Rsk1(RPS6KA1), Rsk2 (RPS6KA3), Rsk4 (RPS6KA6), Rps6kc1	Msk1 (RPS6KA5) (30%)
Caseine kinase	Csnk2b, Csnk1g2, Csnk1g3, Csnk1a1l	Csnk1a1 (25%), Csnk1d (25%), Csnk1e (12%)
Adck	Adck2, Adck4, Adck5	
Clk	Clk1, Clk2, Clk4	

Table 8: Families of proteins over-represented in our migration screen hit list. The identified isoforms are shown including those having more than 10% toxicity (right panel). Red text denotes targets that enhance whilst black text indicates targets that suppress migration upon RNAi downregulation.

3.2.3 Migration screen validation

First, a second toxicity assay was performed using the cell viability assay CellTiter-Glo® (Promega) following the initial toxicity screen procedure [428]. By doing so, we were able to confirm that the changes in cell viability did not account for the observed motility effects (Figure 19A). Then, we repeated the cell migration speed acquisition on A549 cells treated with the pool of four sequences used for the initial screen as well as the deconvoluted four individual sequences. Amongst the 17 targets selected, 14 validated with at least 2 of the 4 deconvoluted individual sequences (Figure 19A). Figure 19B and C shows representative validation experiments for Rsk1, Rsk2 and Rsk4. These effects correlated with target downregulation at the protein and/or mRNA levels (Figure 19C and Figure 20). A large number of somatic mutations identified in lung adenocarcinomas are located within the MAP Kinase pathway leading to phosphorylation and activation of Erk [206, 214]. Erk activation has been associated with cell migration and invasion in epithelial cells [200, 432]. Rsk family members being a

direct downstream target of Erk [197], we decided to focus our subsequent work on these.

Validation work in two additional NSCLC cell lines (LNM35 and H23) confirmed the effects on cell migration seen in A549 cells in response to Rsk1 downregulation (Figure 19, Figure 21A and B). However, in these cells, knockdown of Rsk2 and 4 did not significantly decrease cell motility despite efficient target downregulation (Figure 21A and B). A possible reason for this discrepancy may be that the functions of Rsk2 and 4 are more cell-line specific than that of Rsk1. To further confirm that Rsk1 effect in those three cell lines was on target we tested the effect of sequences from a different provider (Qiagen) (Figure 21C). Transfection of both pool and deconvoluted individual oligonucleotides showed an increased migration speed upon Rsk1 knockdown thus confirming the role of this kinase in modulating cell migration in NSCLC.

A.

Family	Hits	Speed	Tox.	Pool	Deconv.
-	Scramble		100	n/a	n/a
Rps6k	Rsk1 (Rps6ka1)	+	92.4	Yes	Yes
	Rsk2 (Rps6ka3)	-	94.7	Yes	Yes
	Rsk4 (Rps6ka6)	-	115.0	Yes	Yes
Csnk	Csnk1g2	+	97.4	Yes	Yes
	Csnk1g3	+	109.9	No	n/a
	Csnk2b	+	116.4	Yes	No
	Csnk1a1l	-	102.1	Yes	Yes
	Csnk1a1	-	92.8	Yes	Yes
	Csnk1e	-	88.4	Yes	Yes
Adck	Adck2	-	85.1	Yes	Yes
	Adck4	-	88.0	Yes	Yes
	Adck5	+	95.3	Yes	Yes
Clk	Clk1	+	95.2	Yes	Yes
	Clk2	-	106.3	Yes	Yes
	Clk4	-	96.7	No	n/a
Others	Ckb	+	94.2	Yes	Yes
	Mark4	-	88.1	Yes	Yes
	Rate		-	15 / 17	14/ 17

B.

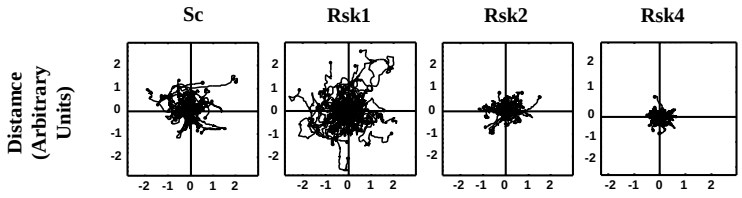

C.

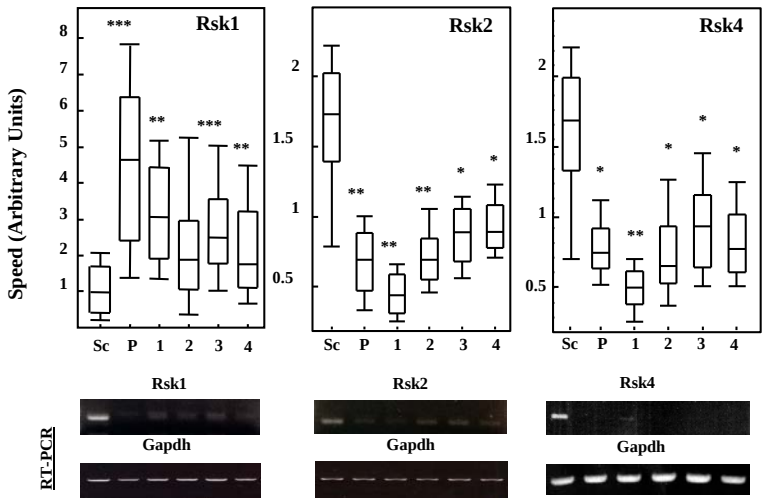

Figure 19: Validation of a selected subset of our hits. (A) Validation rate for targets from four families of proteins over-represented in our hit list. Effects of siRNA down regulation on cell migration speed (+, increase; -, decrease), Toxicity (Tox.) as % of scramble and validation of the migration phenotypes using the pooled or deconvoluted (Deconv.) oligonucleotides. A representative of 2 independent experiments performed in duplicate is shown. (B) Representative cell trajectory plots in an acquired field of view (n=15). A549 cell were transfected with either Rsk1, 2, 4 or scramble (Sc) siRNA pools made of 4 oligonucleotide sequences. (C) Representative validation experiment following transfection with Rsk1, 2 and 4 sequences. P; pool, 1-4; deconvoluted single oligonucleotides. The average random migration speed distribution of 60 cells per condition is represented as a box and whisker plot. Box; 75% and side

bar; 12.5% of the cell population. Dot represents median speed. ANOVA analysis performed with Scramble (Sc) as reference: *; $p<0.05$, **; $p<0.005$, ***; $p<0.001$. Representative RT-PCRs (RT) performed following siRNA down regulation of Rsk1, 2 and 4 using primers directed against the mRNA for each isoform. Primers directed against Gapdh mRNA were used as loading control.

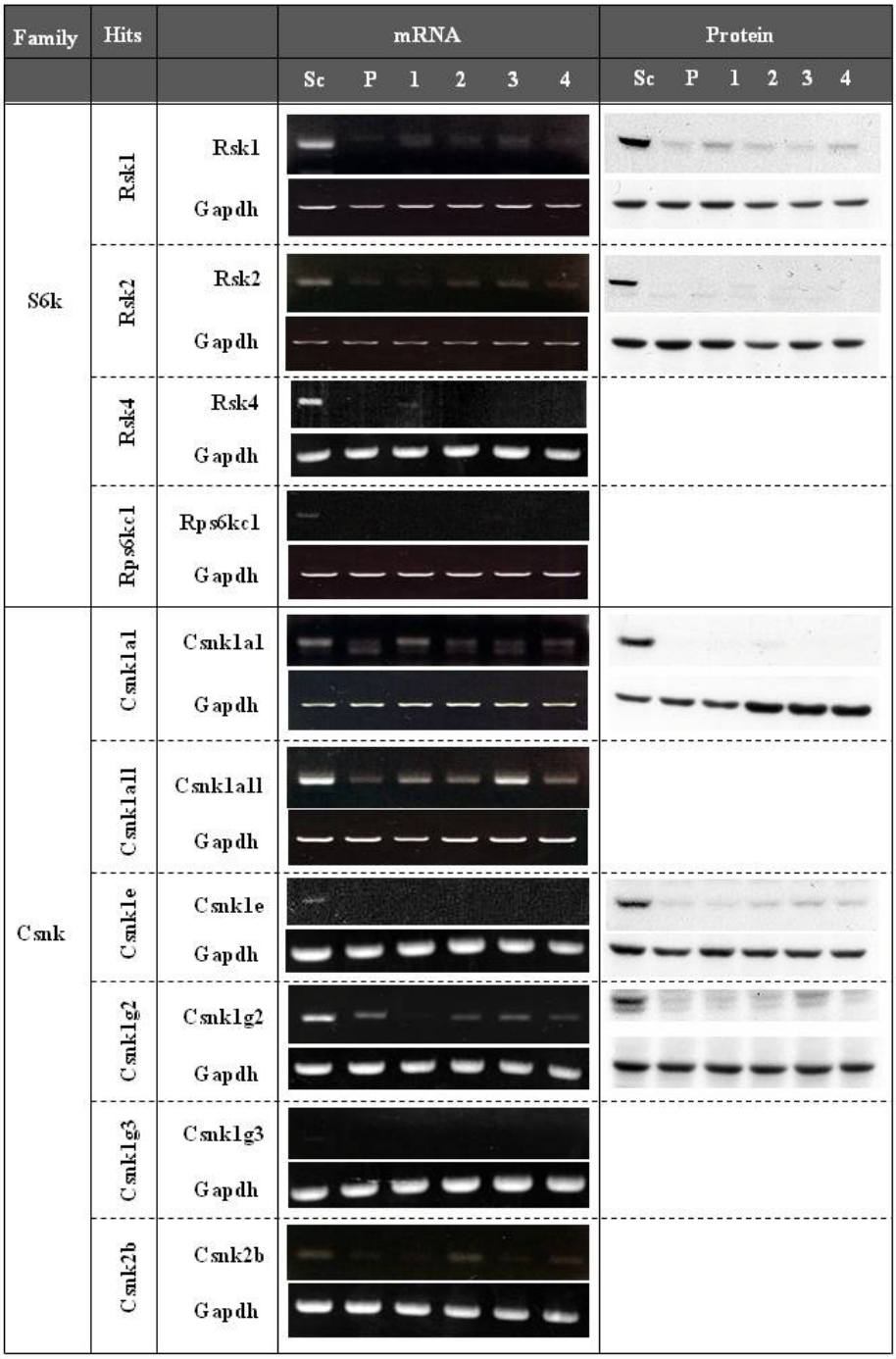

Figure 20: Validation of target down regulation for the Rsk and Csnk family members. Validation was performed using both Smartpools (P) and deconvoluted single oligonucleotides (1-4). Target knock-down was assessed at the mRNA level (RT-PCR) using specific primers for each target and protein level (Western blotting) when a working antibody was identified. Gapdh mRNA and protein levels were used as loading control. A representative of 3 independent experiments is shown.

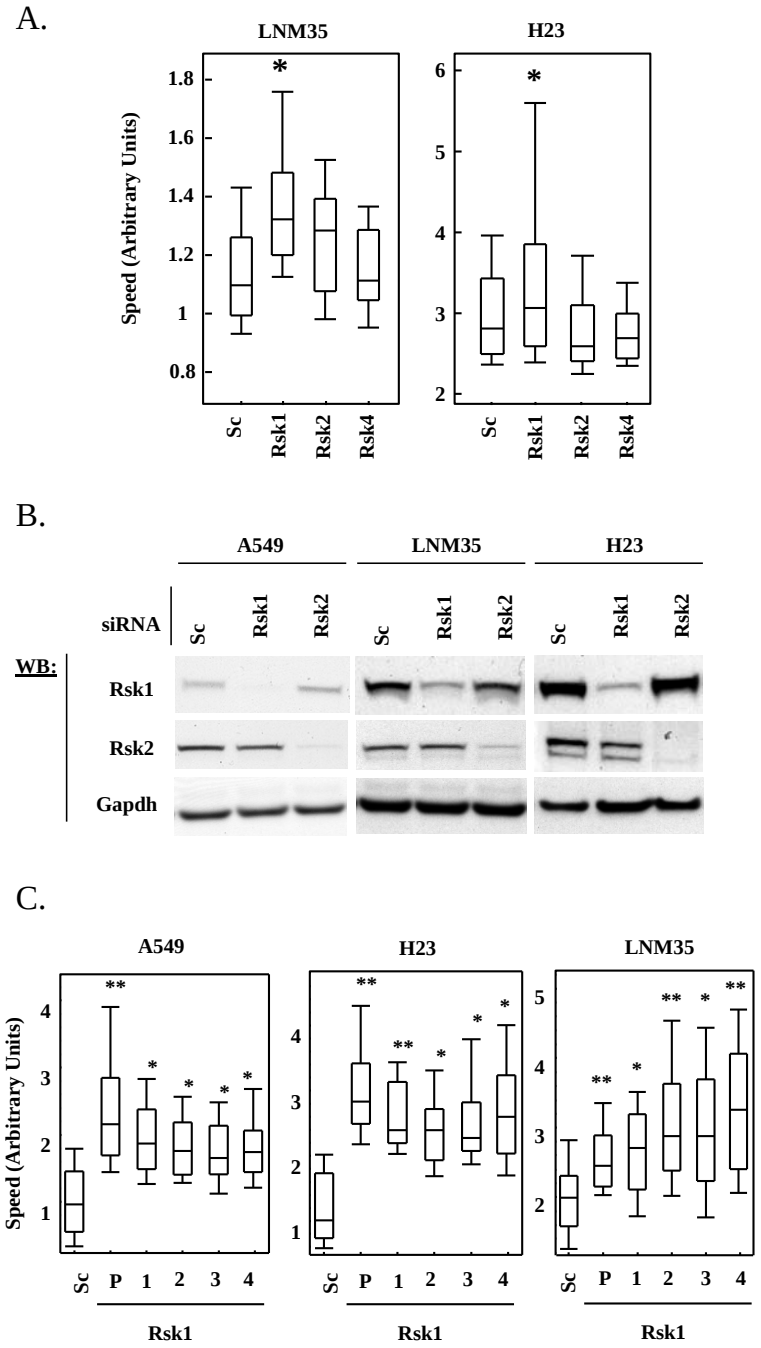

Figure 21: Validation of the results obtained in A549 cells upon downregulation of Rsk isoforms in additional NSCLC cell lines. (A) Cell migration experiments following transfection with pool of 4 sequences directed against Rsk1, 2 and 4 in H23 and LNM35. A representative of 3 independent experiments performed in duplicate is shown. (B) Comparison of the efficiency of Rsk1 and 2 silencing following transfection with oligonucleotides directed against these two isoforms in A549, H23 and LNM35 cells. Cell lysates were subjected to western blotting (WB) using Rsk1 and 2 antibodies. Detection of Gapdh was used as a loading control. A representative of 3 independent experiments is shown. (C) Cell migration validation experiments for Rsk1 in A549, H23 and LNM35 cell lines using oligonucleotides from a different provider (Qiagen). P; pool, 1-4; deconvoluted single oligonucleotides. The average random migration speed distribution of 60 cells per condition is represented as a box and whisker plot. Box; 75% and side bar; 12.5% of the cell population. Dot represents median speed. ANOVA analysis performed with Scramble (Sc) as reference: *; $p<0.05$, **; $p<0.005$. A representative of 3 independent experiments performed in duplicate is shown.

3.2.4 Balance between the activity of Rsk isoforms may regulate cell motility

An alternative explanation for the lack of validation of Rsk2 and Rsk4 in LNM35 and H23 could be that Rsk1 acts as a dominant Rsk isoform regulating NSCLC cell motility. If so, changes observed upon knock-down of other Rsks could be mediated via Rsk1. To test this hypothesis, we silenced Rsk 1, 2 and 4 and looked for changes in protein expression of Rsk1 and 2 (no suitable Rsk4 antibody could be identified). Downregulation of Rsk4 led to a concomitant increase in Rsk1 protein levels but not Rsk2 (Figure 22A). This might explain why Rsk4 and Rsk1 knock-down have opposing effects in A549 cells migration and suggest that the effects of Rsk4 on cell motility might be mediated through Rsk1. To confirm this hypothesis, we looked at the effect on cell migration of the concomitant knockdown of several Rsk isoforms. Figure 22B shows that Rsk1 downregulation appeared dominant over the migratory effects of Rsk4 silencing in A549 cells. Indeed, concomitant suppression of Rsk4 and Rsk1 did not significantly differ from the effects of Rsk1 targeting alone (Figure 22B). In contrast, Rsk2 downregulation could repress the pro-migratory effects of Rsk1 silencing (Figure 22B), suggesting that a balance may exist between the activity of these two isoforms on cell motility. Consistent with our finding that Rsk4 downregulation leads to Rsk1 upregulation, the effects of Rsk4 silencing on cell migration were additive to those of Rsk2 targeting (Figure 22B). Taken together, our data suggest the possible existence of a balance between the biological activities of Rsk1 and Rsk2 on cell migration, while the effects of Rsk4 might be mediated through modulating Rsk1 protein levels.

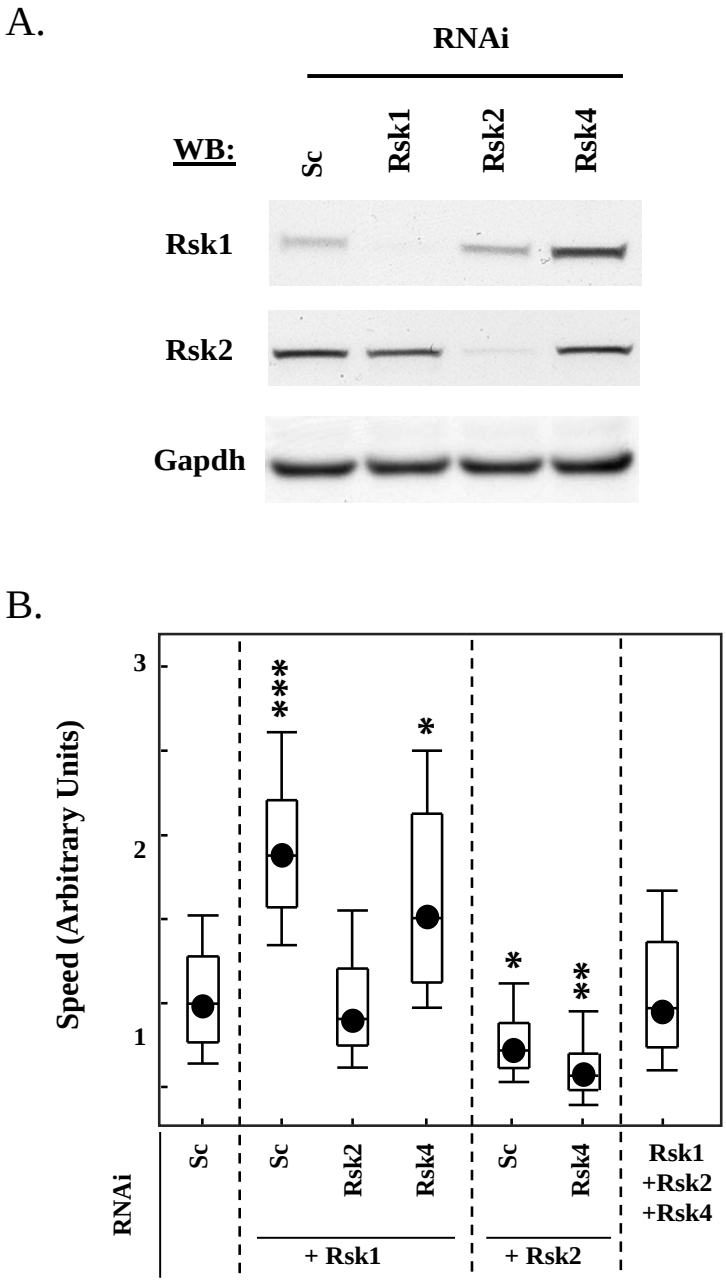

Figure 22: Balance between the activity of Rsk isoforms. (A) Modulation of Rsk1 and 2 protein levels upon knock-down of Rsk family members. Following downregulation using scramble (Sc), Rsk1, 2 and 4 siRNAs, cell lysates were extracted analysed by SDS-PAGE/Western blotting (WB) using antibodies against Rsk1 and 2. Detection of Gapdh was used as a loading control. A representative of 3 independent experiments is shown. (B) Effect of multiple Rsk knock-down combinations on random cell migration speed. Sc; Scramble. The average random migration speed distribution of 60 cells per condition is represented as a box and whisker plot. Box; 75% and side bar; 12.5% of the cell population. Dot represents median speed. ANOVA analysis performed with Sc (Scramble) as reference: *; $p<0.05$, **; $p<0.005$, ***; $p<0.001$. A representative of 3 independent experiments performed in duplicate is shown.

3.2.5 Rsk family members modulate cell morphology

The staining of the actin cytoskeleton following the downregulation of Rsk isoforms in A549 cells reveals changes in cell morphology that correlate with the observed effects on cell motility. Figure 23A shows that increased cell migration speed in response to Rsk1 downregulation (Figure 19B and C) was matched by a rise in the numbers of actin-based lamellipodia (Figure 23A white arrows) and a pronounced cell scattering as compared to that observed in cells transfected with non-targeting sequences (Sc). In contrast, inhibition of cell migration speed following Rsk2 silencing (Figure 19B and C) correlated with increased cellular clustering (Figure 23A). The morphological changes observed as a consequence of Rsk1 targeting suggested an increase in cell polarisation, such as that observed during epithelial to mesenchymal transition (EMT). Typical markers for this phenomenon include a decrease in the levels of epithelial marker E-cadherin, as well as an increase in the mesenchymal marker vimentin [16]. We therefore compared the expression of these two markers in A549 cells transfected with Rsk1, Rsk2 or non-targeting scramble sequences (Sc) siRNA pools. Rsk1 downregulated cells demonstrated decreased E-cadherin and increased Vimentin protein levels (Figure 23B). However, N-cadherin levels were unaffected by Rsk1 downregulation suggesting that the pro-motile phenotype induced by Rsk1 downregulation might not reflect a true EMT programme such as described in the literature [16] but rather a change in cell-cell contacts. In contrast, no changes in E-cadherin, Vimentin or N-cadherin occurred upon silencing of Rsk2 downregulation in A549. Hence, the clustering phenotype observed upon Rsk2 silencing (Figure 23A) cannot be attributed to a changes in E-Cadherin protein levels but may reflect a change in E-Cadherin subcellular localisation.

A.

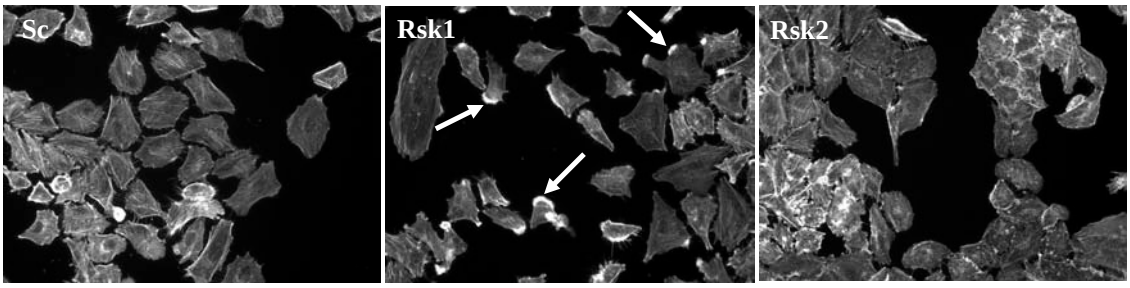

B.

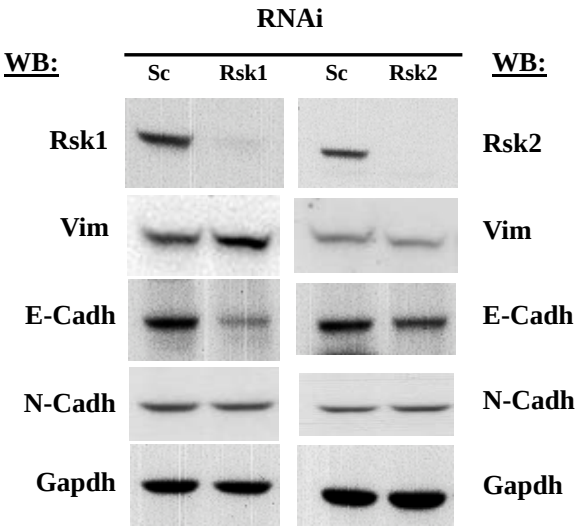

Figure 23: Rsks regulate cell morphology and the expression of EMT markers. (A) Actin cytoskeleton staining of A549 cells using Alexa Fluor 488 phalloidin upon Rsk1 and 2 downregulation. White arrows show the lamellipodia induced upon Rsk1 knock-down. Sc; Scramble. A representative of 3 independent experiments performed in duplicate is shown. (B) Representative Western blotting showing the expression of EMT markers following Rsk1 and 2 knock-down or transfection with scramble siRNAin A549 cells. Cell lysates were analysed by SDS-PAGE/Western blotting (WB) using antibodies against Rsk1, Rsk2, Vimentin (Vim), E-Cadherin (E-Cadh) and N-Cadherin (N-Cadh). Detection of Gapdh was used as a loading control. A representative of 3 independent experiments is shown.

3.3 Discussion

Lung cancers, like other common neoplasms, are fatal for several reasons including the dissemination of tumour cells to distant sites. Therefore, a better understanding of the molecular mechanisms responsible for this phenomenon should yield novel therapeutic approaches to prevent, and biomarkers to predict, this process. Although much has been learnt about key events in the metastatic process, only a few kinases have been shown to play a role. This is somewhat surprising given that there are more than 500 kinases in the human kinome. Here we describe an RNA interference screen to identify genes influencing cell migration in A549 cells. Based on a previously reported assay measuring random cell migration [413], an automated version of this assay was set-up in a 96-well plate format using fluorescent labelling and autotracking of A549 NSCLC cells. This enabled us to identify 48 kinases, previously unknown to regulate cell migration, as modulators of A549 cell motility. Amongst these, four families of kinases were overrepresented. These are the Ribosomal protein S6 kinase (Rsk), Casein kinase, Adck (AarF domain containing kinase) and Clk (CDK-like kinase) families (Table 8). Those families include proteins that have been heavily investigated for their role in other biological phenomenons such as Rsk1 (RPS6KA1) and Rsk2 (RPS6KA3) [251]. However, they also contain less-well characterised proteins such as Rps6kc1 and Adck proteins. Interestingly, we noticed that hits from the same family could induce opposite effects on cell migration speed suggesting the existence of an equilibrium between protein isoforms. Indeed downregulation of Rsk1 dramatically increases cell migration whilst silencing of Rsk2 and 4 impairs this process in A549 cells. The changes seen in cell migration upon knockdown of our targets were reproduced across multiple siRNA targeting sequences suggesting that the effects seen were target-related. Further validation in two more NSCLC cell lines (H23 and

LNM35) confirmed the role of Rsk1 in NSCLC cell motility. However, similar experiments performed for Rsk2 or 4 did not reproduce in additional cell lines the effects seen for these isoforms in A549 cells. One reason for this discrepancy may be that the functions of Rsk2 and 4 are more cell-line specific than that of Rsk1. Alternatively, Rsk1 might act as a dominant Rsk isoform regulating NSCLC cell motility. Here we show some preliminary evidence that Rsk4 effects on cell motility might indeed be mediated by an increase in Rsk1 protein levels (Figure 22A). Our data further suggest the existence of a balance between the biological activities of Rsk1 and Rsk2. Indeed, concomitant silencing of Rsk1 and 2 in A549 cells cancels out the cell motility effects of downregulating each isoform separately (Figure 22B).

The effects on cell motility seen upon Rsk1 and Rsk2 knockdown correlated with changes in the actin cytoskeleton as Rsk1 knockdown led to an increase in the number of lamellipodia, promoting cell scattering, while Rsk2 silencing increased cell-cell contact. The effects of Rsk1 silencing on lamellipodia formation suggest an involvement of Rsk1 with the actin machinery. However, Rsk1 does not harbour domains reported to be involved in regulating actin dynamics [251] and it is therefore unlikely that these effects are directly mediated by this protein. Alternatively, Rsk1 might regulate the activity of proteins implicated in regulating the actin cytoskeleton. We will show in Chapter 5 that this is the case as Rsk1 phosphorylates Vasodilator-Stimulated Phosphoprotein (Vasp), a protein known to be involved in actin polymerisation [107]. Moreover, the effects of Rsk1 on the epithelial marker E-Cadherin and mesenchymal marker Vimentin suggest that Rsk1 might regulate the entire metastatic process by participating to the Epithelial to mesenchymal transition (EMT) [15].

CHAPTER 4

Secondary invasion screen

4.1 Introduction

Cell motility has previously been heavily studied using two-dimensional experimental systems providing important insights into the molecular machinery driving cell migration [82]. However, the mechanical properties of the rigid surfaces used in 2D migration assays are not comparable to those found in the *in vivo* setting. Indeed, epithelial cells *in vivo* are supported by both a basal membrane and the extracellular matrix (ECM) (Chapter1 Figure 2). These structures play a dual role during the invasion process by providing both a mechanical barrier preventing the invasion of the deeper tissue and a substratum allowing malignant cells to adhere and migrate (Chapter1 section 1.1.2 and 1.2.1.1.1). Tumour cells leaving the primary tumour must become deformable and acquire the ability to invade the surrounding matrix in order to reach the vasculature. We previously identified 70 proteins capable of modulating A549 cell migration (Chapter 3). To assess the ability of our motility hits to regulate cell invasion, we developed a secondary 3-dimensional invasion screen based on a 96-well plate format where cells invade upward from the bottom of the well through a collagen matrix in response to a chemo-attractant. This chapter describes the development and results of this invasion screen using the NSCLC cell line, A549.

4.2 Results

4.2.1 Invasion Screen set-up

The invasion assay was developed in a 96-well plate format to enable high-throughput screening of our 70 motility hits. A workflow of the assay is represented in Figure 24A and B. The cellular system (A549) and siRNA transfection protocol were the same as those used for the migration screen to enable direct comparison of the results obtained in the two assays. 24 hours following siRNA transfection, a matrix was overlaid on top of the transfected cells. A day later, medium containing a chemoattractant was added over the gel to provide the cells with a directional stimulus. Cells were allowed to invade upward through the matrix for 48 hours before being fixed. The gels were then stained using Tetramethylrhodamine B isothiocyanate (TRITC) coupled phalloidin to reveal the cellular actin cytoskeleton. Finally, three-dimensional stacks were acquired across the 96 well-plate using a motorised inverted confocal microscope.

A.

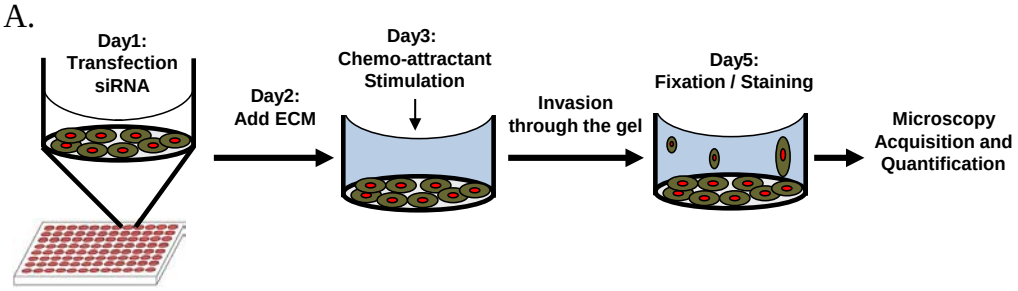

B.

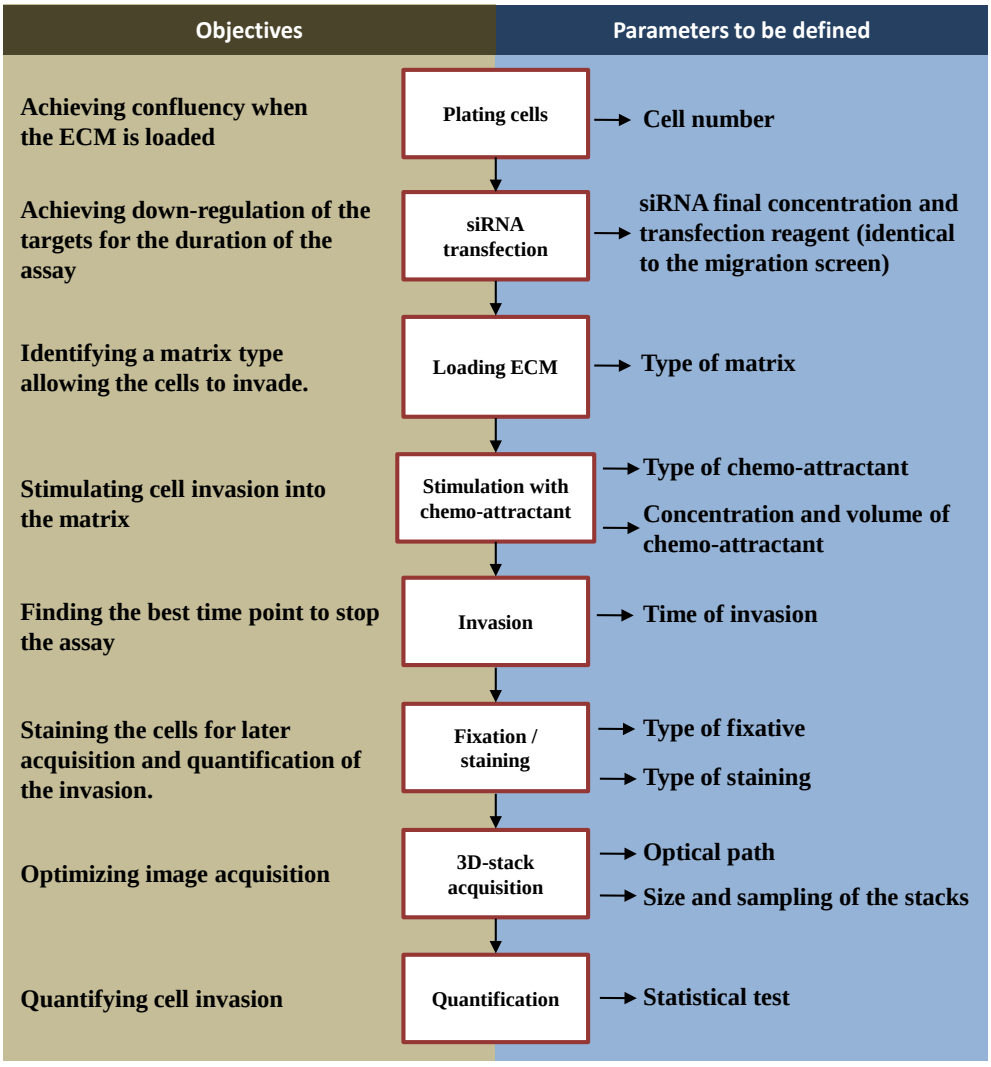

Figure 24: Overview of the invasion screen setup. (A) Overview of the invasion assay. (B) Workflow of the invasion assay describing the parameters to be optimised at each step of the assay.

In order to reduce the number of variables influencing the invasion readout, a set of parameters were fixed.

1. A plating cell number of 3000 per well was found to provide a confluent monolayer at the time when the chemo-attractant is added on the gel 48 h later. This cell number was chosen to limit the lateral migration and proliferation of the cells at the bottom of the well while cell invasion is being assessed.
2. A final concentration of 1% Foetal Calf Serum (FCS) was used to prepare the matrix. This concentration reduces cellular stress without compromising further stimulation by the chemo-attractant (Figure 25 and Figure 27).
3. Epidermal growth factor was selected as a chemo-attractant due to its capacity to stimulate lung cancer invasion *in vitro* [420, 433] and *in vivo* [434].

Based on this initial protocol, the matrix and concentration of chemo-attractant were optimised in order to increase to sensitivity of the assay.

4.2.1.1 ECM and chemo-attractant

Previous reports have shown the capacity of A549 cells to invade within Matrigel and type I collagen matrices using Egf as a chemoattractant [420, 433, 435]. Matrigel is a commercial name for a preparation of the ECM secreted by Engelbreth-Holm-Swarm (EHS) mouse sarcoma cells. Using the highly invasive fibrosarcoma HT1080 and breast cancer MDA-MB-231 cell line, Wolf et al. have previously shown that low concentrations of type I collagen (3mg/mL) allowed cell invasion without the requirement for proteolytic activity [45]. This contrasts with what can be observed in the presence of higher collagen concentrations (10 to 12 mg/mL) when proteolytic activity

is required for cells to infiltrate the dense matrix [45]. In order not to limit the hits to those that would regulate protease activity, we decided to use a low concentration of collagen (3mg/mL) for our assay. Hence, we tested in our invasion assay the capacity of A549 cells to invade in Matrigel (~10mg/mL), type I collagen (3mg/mL) or a mixture of type I collagen diluted 1 in 10 in Matrigel (type I collagen final concentration: 1mg/mL). Each type of matrix was overlaid on the cells and left to polymerise over-night. Various concentrations of Egf were then added on top of the gels. Cells were allowed to invade upward for two days before fixation, staining and microscopy acquisition. Figure 25A and B shows that in the presence of Matrigel or Matrigel mixed with Collagen, A549 cells were unable to invade in response to Egf. However, the same stimulus enabled A549 cells to invade through a collagen-alone matrix (Figure 25C). Hence, a 3mg/mL type I collagen matrix was selected to perform the screen.

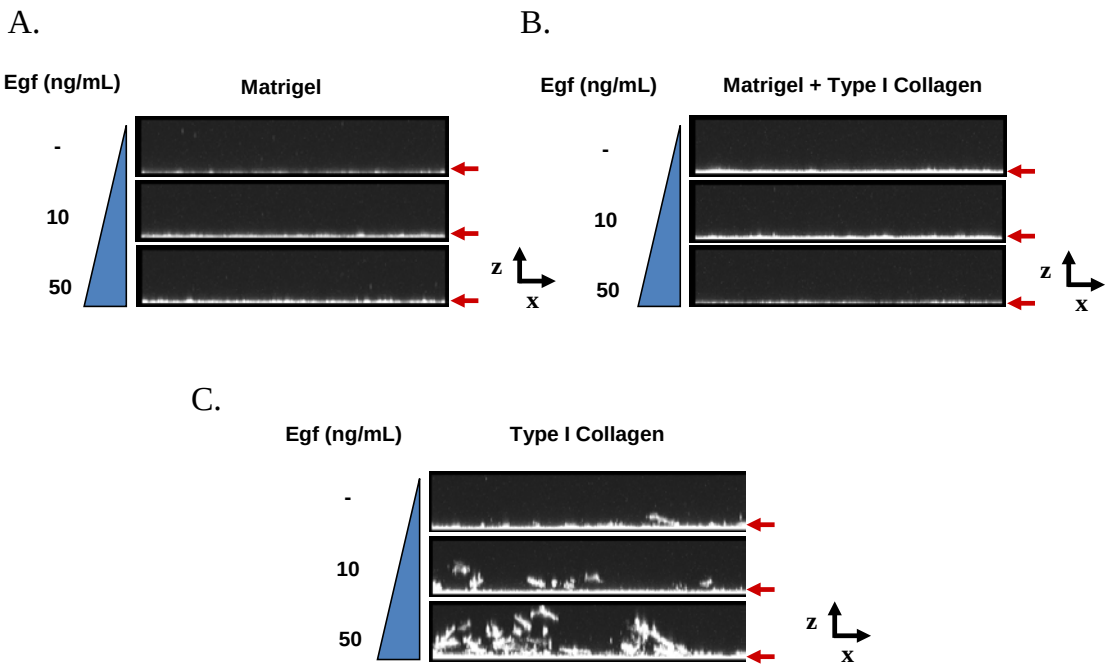

Figure 25: Test of A549 invasion through different extra cellular matrix (ECM). Side views of representative confocal stacks showing TRITC-conjugated phalloidin stained A549 cells (white) overlaid with (A) Matrigel (B) a mixture of Matrigel with type I collagen diluted 1 in 10 (1mg/mL final concentration) or (C) a type I collagen matrix (3mg/mL) and stimulated with different concentrations of Egf. Stacks are acquired from the bottom of the well (red arrows) over 150µm upward. Orientations of the stacks are given by the x- and z-coordinates. A representative of 3 independent experiments performed in triplicate is shown.

4.2.1.2 Microscopy acquisition

Microscopy acquisition was performed using a motorised inverted confocal microscope. Stacks of 150µm were acquired upward from the bottom of the plate with a distance of 4µm between focal planes. The acquisition of each stack was preceded by an autofocus based on the reflection at the bottom of the plate of the 633nm wavelength laser. To increase the acquisition coverage, a tile of nine stacks was acquired per well using a 10x lens with a 0.45 numerical aperture (NA). These settings allowed the acquisition of a surface of 1.3 mm^2 representing 40.6% of the total well surface. Increased invasion was observed at the border of each well independently of the treatment applied. One reason explaining this experimental artefact could be an increased surface tension at the border of the well affecting the collagen matrix polymerisation and/or cellular behaviour [436]. To avoid this impacting on our readout, tiles were only acquired at the center of each well.

4.2.1.3 Quantification

Two parameters were considered to evaluate the extent of invasion in our assay; the number of cells invading and the distance of invasion from the bottom of the well. By plotting the total intensity of the Phalloidin-TRITC staining for each plan of the stack (Σ[intensity (x, y)]) as a function of the distance of invasion (z axis), we were able to reliably represent the proportion of cells present at each level of the stack (Figure 26B). Results obtained by staining the cell nuclei, instead of the actin cytoskeleton, and counting the number of cells per plane using a specially-written Mathematica notebook provided similar results (data not shown). However, the first method was more amenable to high-content analysis as the determination of cell numbers required 3D image analysis and consequently a far lengthier computation. The acquisition of each

stack was preceded by an autofocus based on the reflection at the bottom of the plate of a 633nm wave-length laser. The inherent lack of accuracy of the autofocus was responsible for a shift in the stack acquisition as represented in the Figure 26B. To overcome this pitfall, acquisition of the stacks were started 30μm further down from the bottom of the well. By doing so, we were able to reproducibly collect in our acquisition all the cells present at the bottom of the well and include their fluorescent intensity to our invasion plot (see arrow on Figure 26B and C). The curves for various experimental conditions were then aligned to overlay the picks corresponding to the cells at the bottom of each well, thereby correcting the autofocus inaccuracy (Figure 26C). Following alignment of the curves, a cut-off was applied in the z stack to highlight the level beyond which cells could be considered asinvading the matrix (Figure 26C). This cut-off was determined to give the maximum difference between Egf stimulated and un-stimulated scramble transfected conditions. To estimate the proportion of cells invading in a given condition, the area under the curve representing the invading cells was then compared to the total area under the curve including all cells. Finally, the results of nine stacks per well in triplicates were pooled before performing an ANOVA statistical test. This quantification process was programmed into a Mathematica notebook by Dr Alastair Nicol (Light Microscopy Department, CRUK, London, UK) to automate data processing.

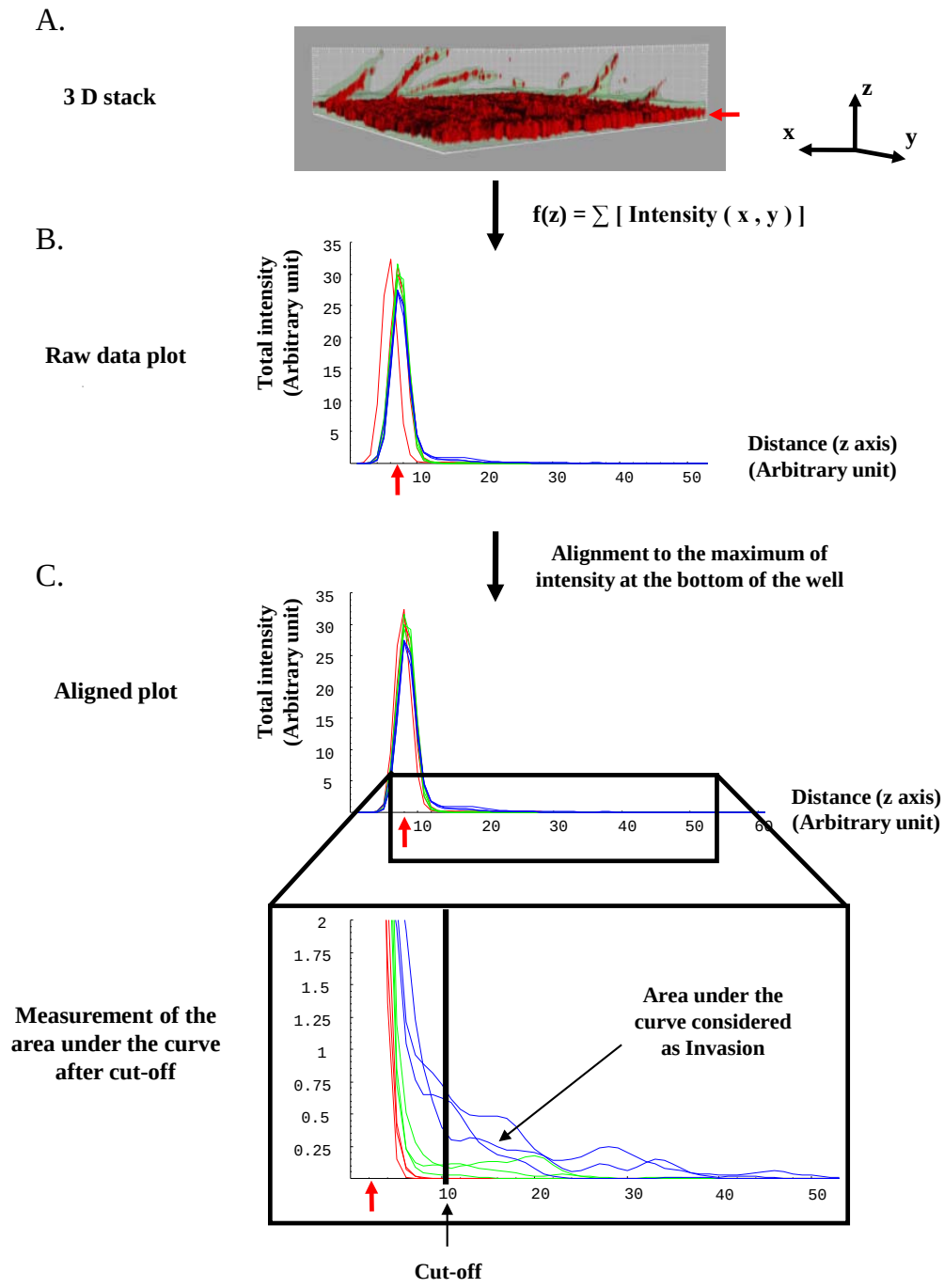

Figure 26: Quantification of the invasion in each stack acquired. (A) 3D rendering of a representative stack using IMARIS® 7.0. Red; Phalloidin-TRITC staining. Orientations of the stack are given by the x-, y- and z-coordinates. (B) Representative raw data plot showing the total intensity of the staining as a function of the distance from the bottom of the well for 9 stacks. (C) Alignment of the raw data plots and determination of the cut-off. Red arrows indicate the cells at the bottom of the well.

4.2.1.4 Chemo-attractant concentration

We previously showed that A549 cells were able to invade in a type I collagen matrix in response to Egf (Figure 25C). To determine the concentration of Egf saturating the assay we extended the dose range of Egf and quantified the invasion using our Mathematica notebook. Figure 27A shows that neither 10 nor 100 ng/mL (final concentration 1.66 and 16.6 ng/mL) of Egf were sufficient to significantly increase A549 cell invasion. However, A549 cells stimulated with Egf 1000 ng/mL (final concentration 166 ng/mL) or 2000 ng/mL (final concentration 333 ng/mL) were reliably invading into the collagen matrix. We therefore chose a concentration of 1000 ng/mL Egf to perform the screen.

4.2.1.5 Positive control

To control for invasion efficiency between experimental plates and confirm that A549 invasiveness could be further enhanced, transfection of oligonucleotides directed against non-erythroid protein 4.1 brain types (4.1B) was tested. 4.1B is a tumour suppressor gene [437] the downregulation of which has been shown to increase cell migration and correlate with metastasis in rat sarcoma cells [438]. In our assay, RNAi directed against 4.1B increased A549 cell invasion as compared to scramble transfected cells (Figure 27B). Furthermore, scramble tranfection did not significantly affect cell invasion as compared to untransfected cells stimulated with Egf (Figure 27B). Hence, scramble and 4.1B transfection were respectively used as reference and positive control throughout our invasion screen.

A.

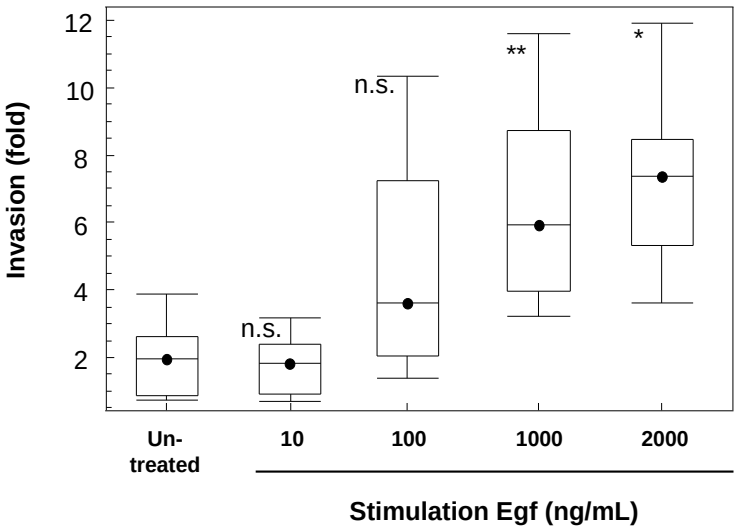

B.

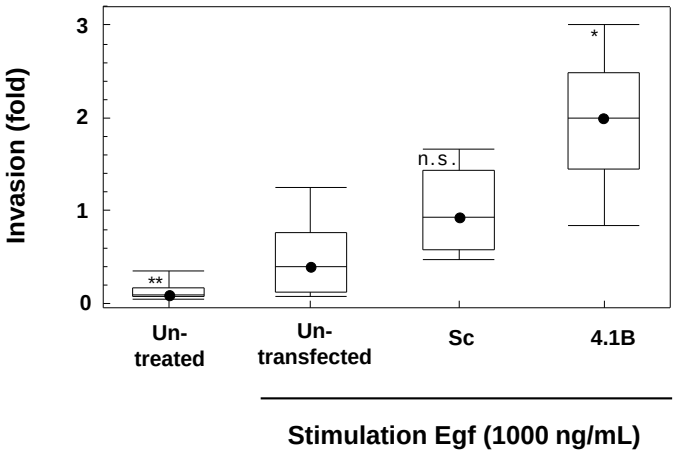

Figure 27: Determination of the Egf concentration and siRNA control to be used for the invasion screen. (A) Egf titration experiment. A representative of 3 independent experiments performed in triplicate is shown. (B) Effect of 4.1B downregulation on A549 invasion under Egf stimulation. (A and B) Sc; Scramble. Confocal stacks were analysed using Mathematica to generate box and whisker plots of A549 cell invasion. Box represents 75% and side bar 12.5% of the data population. Dots represent median intensities. Statistical significance was determined using ANOVA analysis. *; $p<0.05$, **; $p<0.005$. A representative of 3 independent experiments performed in triplicate is shown.

4.2.2 Invasion screen results

Amongst the 70 targets tested, 60% decreased, 19% increased and 21% had no effect on A549 cell invasiveness when compared to scramble transfected cells (Figure 28A and B). Figure 28A shows a comparative analysis of our motility and invasion screen results. 54% (thirty eight) of the hits tested similarly modulated cell migration (primary screen) and cell invasion (secondary screen) (Figure 28C). In addition, 20% of the targets tested did not alter invasion despite changing cell motility while 26% of our hits showed opposite effects in the two screens (Figure 28C). This demonstrated that changes in cell migration cannot be directly extrapolated to cell invasiveness. However, hits that decreased cell migration had a better correlation rate with invasion than those that increased motility (Figure 28D). This suggested that while impairment of cell migration will often thwart cellular invasiveness, increased motility is not sufficient to produce an invasive phenotype.

Within the Rsk family, silencing of Rsk1 increased invasiveness of A549 cells further than our positive control 4.1B (Figure 29A and B). In contrast to Rsk1, Rsk4 targeting decreased cell invasiveness (Figure 29A and B). These effects mirrored those seen in the migration assays (Chapter3 Figure 19B and C). However, Rsk2 downregulation did not impair invasion despite its effects on cell motility (Figure 29A and B). Hence, silencing of Rsk1 and Rsk4 similarly alter invasion and migration.

A.

Cross-correlation			
Hit	Migration	Invasion	ANOVA
ADCK2	-	-	***
ADCK4	-	-	*
AKT1	-	-	*
AKT2	-	-	
ALS2CR2	-	-	***
ANGPT4	-	-	***
AURKC	-	-	***
CDC42BPB	-	-	***
CDKL3	-	-	***
CDKL5	-	-	*
CDKN2B	-	-	***
CDKN2D	-	-	
CHEK2	+	+	*
CLK1	+	+	
CLK4	-	-	**
EPHB6	+	+	***
GMFG	-	-	**
MAPK13	-	-	**
MARK4	-	-	
MELK	-	-	***
MYO3A	+	+	
PCK2	-	-	*
PDK3	-	-	*
PFKFB1	-	-	
PFKFB4	-	-	
PIK3C2G	-	-	
PIP5KL1	-	-	**
PPP2CA	-	-	
PRKAG1	-	-	**
PNK2	-	-	***
PRKCM	-	-	
PRKCSH	-	-	*
PTPRG	-	-	***
RFK	-	-	***
RSK1	+	+	*
RSK4	-	-	*
RPS6KC1	-	-	
WINK1	-	-	**

No cross-correlation			
Hit	Migration	Invasion	ANOVA
ACVRL1	+	-	***
ADCK5	+	-	*
AURKA	-	0	
BRSK2	-	0	
CAMKV	-	0	
CHKB	-	0	
CKB	+	-	*
CLK2	-	0	
CSNK1A1L	-	+	
CSNK1G2	+	-	
CSNK1G3	+	-	
CSNK2B	+	-	
DCLK2	-	0	
DDR2	+	-	**
EDN2	+	-	**
GALK1	-	+	**
MAP4K4	-	+	**
MAPK11	-	0	
MPP3	+	-	**
MVD	-	+	*
NAGK	-	0	
NEK6	-	0	
NPR1	-	0	
PANK4	-	0	
PKIB	-	0	
PKN3	-	+	
PPP4C	-	0	
PRKACB	-	0	
RSK2	-	0	
SRPK3	-	+	*
TNK2	-	+	**
TRIB3	-	0	

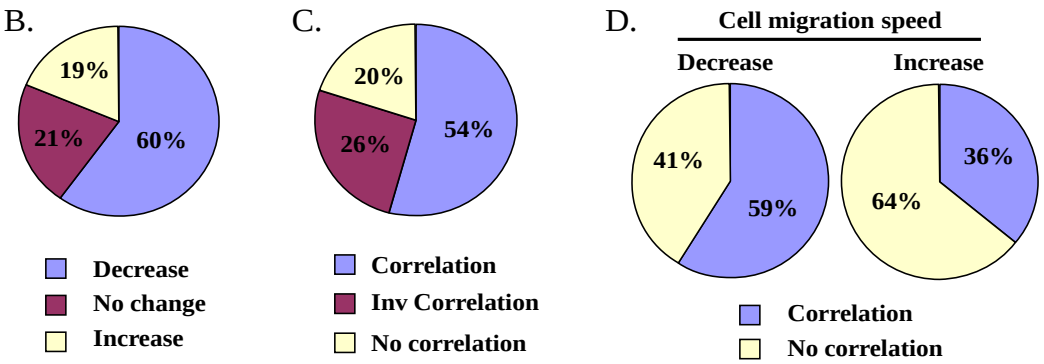

Figure 28: Cross-correlation between the effects of silencing the 70 migration screen hits on cell motility and invasion. Comparative tables showing the effects on A549 cell migration and invasion of silencing the migration hits. The left table shows hits for which effects on migration correlated with those on invasion. The right table shows hits that do not cross-correlate in the two assays. (-); decrease, (+); increase, (0); no effect. ANOVA for the invasion alone with Sc as reference: *; $p<0.05$, **; $p<0.005$, ***; $p<0.001$. (B) Percentage of hits decreasing, increasing or having no effect on cell invasion. (C) Percentage of hits showing cross-correlation, inverse (Inv) correlation or no correlation between the migration and the invasion phenotypes. (D) Percentage of cross-correlation between invasion and migration depending on whether the hits decreased or increased cell migration speed.

A.

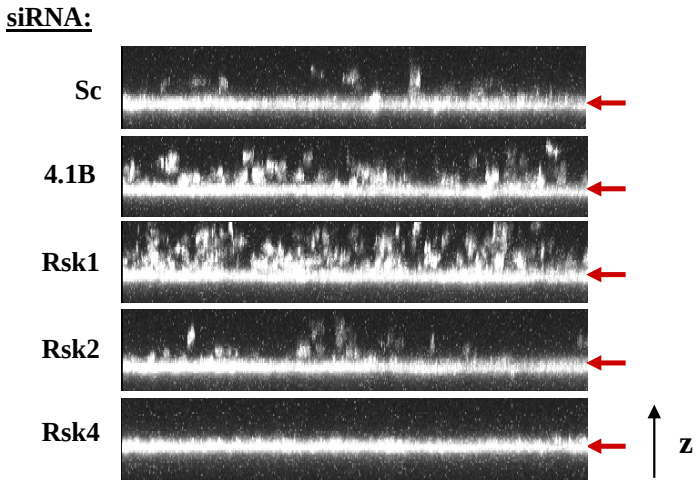

B.

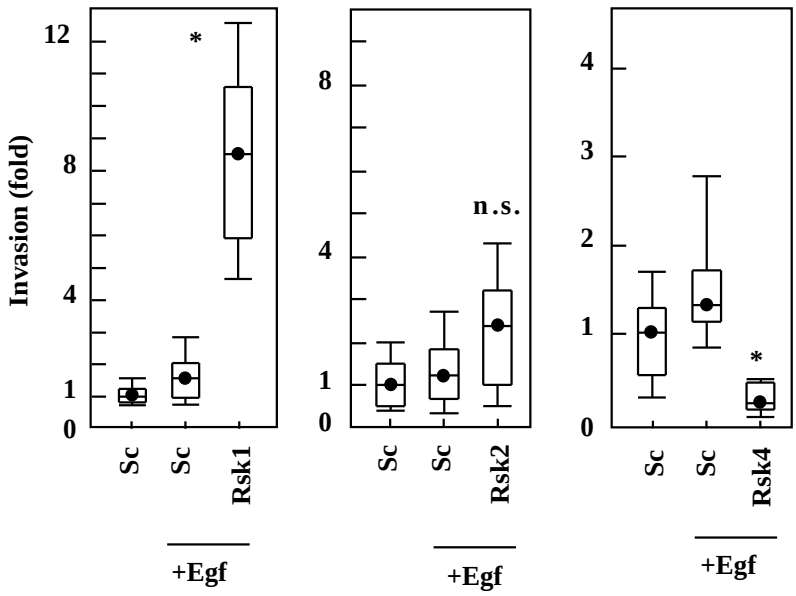

Figure 29: Effect of Rsks silencing on cell invasion. (A) Side views of representative confocal stacks of A549 cells invading upward into a collagen matrix upon silencing of Rsk family members. Sc; Scramble. Red arrows represent the bottom of the wells for each condition. Stack size 150 μm. (B) Box and whisker plots of A549 cell invasion following Rsk1, 2 and 4 silencing. 27 fields of view similar to those pictured in (A) were acquired for each condition. Box represents 75% and side bar 12.5% of the data population. Dot represents median speed. Statistical test was performed using ANOVA analysis with Sc as reference. * correspond to $p<0.05$, n.s.; non-significant. A representative of 3 independent experiments performed in triplicate is shown.

4.3 Discussion

We previously performed a kinome-wide RNA interference screen for cell motility in a 2D environment using the NSCLC cell line, A549. Our screen identified 70 hits modulating the migration of these cells. To further assess how our motility hits could be involved in the metastatic process we performed a secondary invasion screen for the same cell line using a 3D collagen matrix.

We show that A549 cells were able to invade in a Type I collagen matrix in response to Egf. However, contrary to previous reports [420, 433], A549 cells were unable to invade in Matrigel in our assay. Matrigel is a preparation of ECM components secreted by Engelbreth-Holm-Swarm (EHS) mouse sarcoma cells. EHS cells produce a large amount of basement membrane (BM) components including Laminin and Collagen type IV [439] as well as various growth factors such as transforming growth factor-β (Tgf-β), fibroblast growth factor (Fgf), and tissue plasminogen activator. The exact composition of Matrigel is unknown and subject to variability in composition and concentration that might explain this discrepancy. Furthermore, the Matrigel we used was not reduced for its content in growth factors. Thus, it is possible that the effects of the Egf stimulation in our assay were masked by the growth factors already present in the matrix. Indeed Hauck et al. used growth factor depleted matrigel in their study [433].

Several points need to be taken into account in the interpretation of the results of our screen:

(1) Type I collagen is the most abundant structural protein in the interstitial tissue. However, Collagen matrices lack other ECM components such as fibronectin and laminin that play an important role during invasion [48]. Thus, our invasion screen might select for invasion dependent on the type I collagen receptor (integrin α2β1) as well as on proteases known to have type I

collagenolytic activity such as the matrix metalloproteinases Mmp-1, Mmp-2, Mmp-8, Mmp-9, Mmp-13 and the membrane-type-1 matrix metalloproteinase MT1-Mmp (also known as Mmp-14) [47]. Indeed, MT1-Mmp has been reported to be required for tumour cells to invade through type I collagen matrices [440].

(2) It has previously been shown that different concentrations of collagen were associated with different type of invasion. Low collagen concentrations (3mg/mL) promote non-proteolytic amoeboid-type invasion while high concentrations (10 to 12 mg/mL) promote proteolytic-dependent mesenchymal-type invasion [45, 441] (Chapter 1 section 1.2.1.1.1.1). Here we decided to use a low collagen concentration of 3mg/mL in order to lower the stringency of the assay. However, by doing so, we might have biased our assay towards the identification of siRNA treatments affecting amoeboid type invasion.

(3) In contrast to invasion assays performed using Boyden chambers [420, 433], our screen allowed cells to adhere to the well before overlaying the collagen matrix. Hence, cells needed to detach first in order to invade upward. Although this made the assay more stringent, it might mimic more closely the *in vivo* setting where tumour cells need to detach from the primary tumour before invading.

Our screen showed 54% of correlation between the motility and invasion phenotypes, suggesting that changes in cell migration cannot be directly extrapolated to cell invasiveness using our experimental approach. One reason explaining this discrepancy could be the nature of our experimental approach that limits our readout to

invasion through a type I collagen matrix and in response to Egf. Further development of our protocol using different ECM compositions as well as chemo-attractants might reveal a higher degree of correlation between changes in motility and invasiveness. Alternatively, tumour cells do not require to be invasive *per se* to metastasise *in vivo* as mesenchymal cells have been shown to create tracts that cancer cells can passively follow [51]. In this setting, changes on cell migration will dictate the ability of the tumour cells to disseminate. Finally, Rsk1 and Rsk4 but not Rsk2 showed correlation between motility and invasiveness in A549 cells. Considering that neither Rsk2 nor Rsk4 motility phenotype validated across multiple cell lines, Rsk1 appears to be dominant Rsk isoform in the regulation of cell migration and invasion.

CHAPTER 5

Rsk family members interact with proteins involved in the regulation of the actin cytoskeleton

5.1 Introduction

Cell motility is a complex biological process that has been shown to involve several cellular signalling pathways [82] (Chaper 1 section 1.3). While these pathways have frequently been described as linear cascades it is now generally accepted that they are part of evolutionary conserved signalling networks [442]. Indeed, analysis performed in *Saccharomyces cerevisiae* has shown that the phenotypic consequence of a single gene deletion is affected to a large extent by the topological localisation of the protein product within these networks [443]. Similarly, cancer progression is associated with multiple genomic alterations that are likely to affect the structure and dynamic of these protein networks [442]. We previously identified 70 hits on the basis of their ability to modulate A549 cell motility. We now wished to investigate the possibility that these proteins might be part of one such network. To assess the likelihood of this possibility, we queried a human protein-protein interactome (PPI) database with our 70 motility hits and found that 21 of our hits were linked in a highly interactive hub containing members from the Rsk and Casein kinase families. By extending our network analysis to first-node interactions between our hits and the rest of the proteome, we revealed the possibility of Rsks interacting with the actin regulator Vasp. We confirmed this biochemically and identified specific phosphosites on Vasp that are modulated by Rsk1. Rsks also interacted with the actin regulator Mena, possibly via its ability to heterotetramerise with Vasp. Finally we show that Vasp and Mena downregulation prevented the migratory effects of Rsk1 silencing suggesting that both proteins mediate the effects of Rsk1 on cellular motility.

5.2 Results

5.2.1 Protein–Protein Interactome analysis

To gain insight into whether the Rsks and our other identified targets interact with each other we performed an interactome analysis. A human protein-protein interaction (PPI) database was assembled that integrated two previously published collections containing both experimentally verified and *in-silico* predicted interactions [414] [415] (Figure 30A). This database was queried for first-node level interactions between our 70 hits (Figure 30B). Although most hits did not show interaction with other members of the list, a subgroup of highly interactive 21 proteins was identified (Figure 30B). This subgroup contained several proteins from the S6 kinase and Casein kinase families. To ensure that this high frequency of association was not due to chance, we also analysed 10 randomly generated lists of 70 targets from our siRNA library. None of these lists produced groupings of >13 proteins (Figure 30C), suggesting that our hit-list genuinely is enriched for interacting partners. To shed light on why our hits might regulate cell motility, the PPI database was next queried for interactions between these hits and proteins outside the kinome. This analysis predicted that several well-known modulators of cell migration, including Vasp [107], Vinculin (VCL) [444] and Vimentin (VIM) [445], might interact (average of 3 first-node interactions) with our network of 21 hits (Figure 30B and D), including the Rsk family members (Figure 30D). The changes in the actin cytoskeleton mediated by the downregulation of Rsk isoforms (Chapter 3 Figure 23), suggested a link with modulators of actin dynamics.

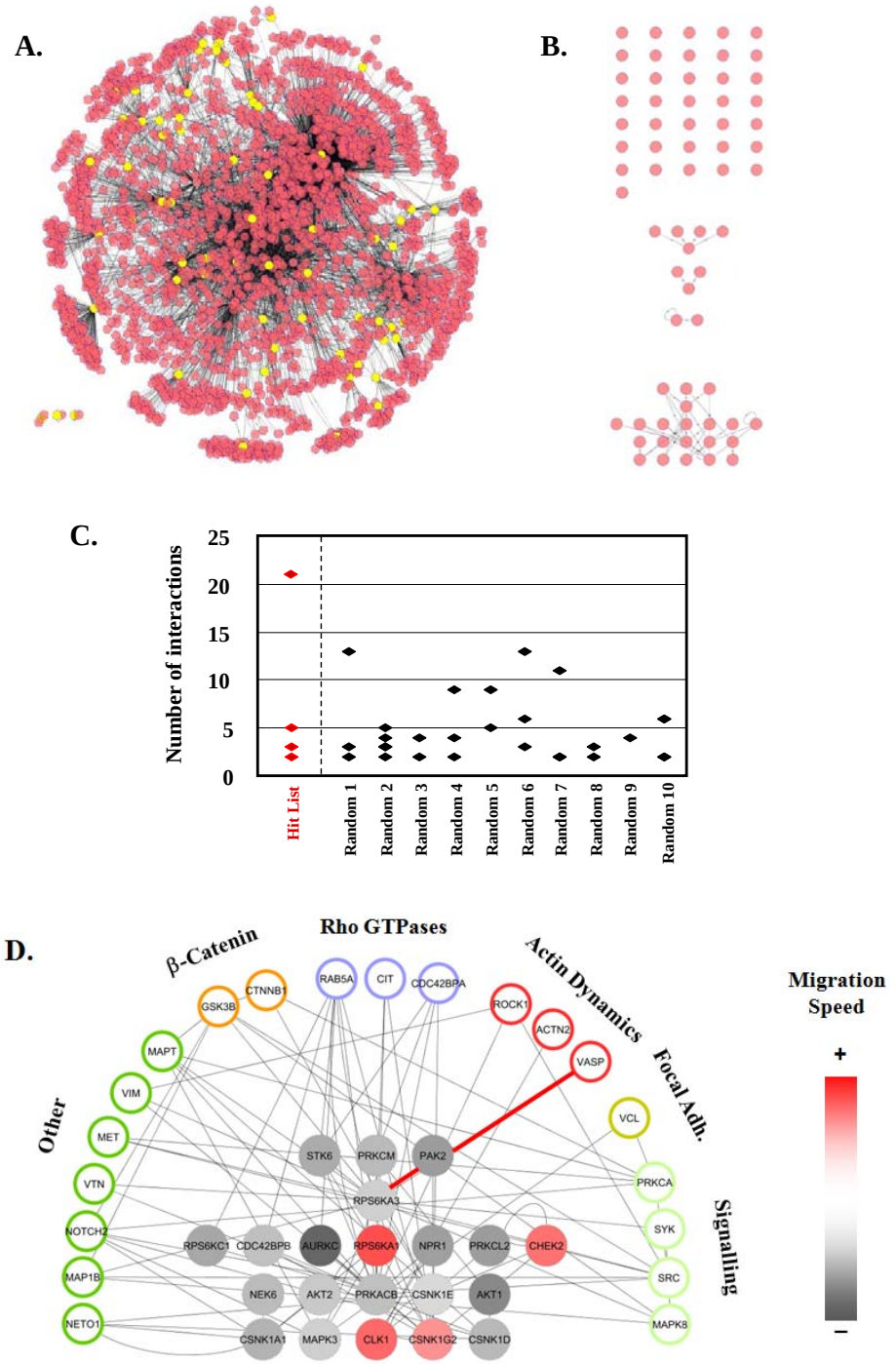

Figure 30: Bioinformatics analysis. (A) Human protein-protein interaction (PPI) database. Nodes represent individual proteins. Links symbolise protein-protein interactions. Proteins from the cell migration hit list (70) are represented in yellow. The rest of the proteome is in red. (B) A query for the first-node level interaction between our hits reveals a subgroup of 21 highly interactive hits (lower panel) and 3 smaller groupings of interactors (middle panel), while most do not cross-interact (upper panel) . (C) The "false-rate" of interaction was assessed using 10 randomly generated lists of 70 kinases to query the PPI for first-node interaction. The graph displays the size of interaction groupings obtained with the experimental hit list as compared to those generated with the 10 random lists. Each individual grouping is represented as a dot. (D) Representative first-node interactions between our grouping of 21 hits and the rest of the proteome. Only proposed interactors with a documented effect on cell migration are shown. The link between Rsk2 (RPS6KA3) and Vasp is highlighted in red. Proteins within the group of 21 hits are colour-coded from grey (decreased migration speed (-)) to red (increased migration speed (+)) according to the effect of their downregulation on cell migration speed. RPS6KA1 and RPS6KA3 stand for Rsk1 and 2 respectively.

5.2.2 Rsk1 and Rsk2 interact with Vasp and Mena

Vasp is a known mediator of actin dynamics [143-144]. Hence, we tested whether the predicted interaction between Vasp and Rsks could be validated. Figure 31A (upper panel) shows that immunoprecipitation of Rsk2 pulled down endogenous Vasp in A549 cells grown in serum-containing medium. Similarly, immunoprecipitates for Vasp demonstrated immunoreactivity for Rsk2. While the interaction of Rsk2 with Vasp was predicted by our PPI database, an interaction with Rsk1 was not. This was surprising given the high degree of homology for Rsk family members. We found that Rsk1 co-immunoprecipitated with Vasp whether the immunoprecipitating antibody was directed towards Rsk1 or Vasp (Figure 31A lower panel). Since Vasp is known to heterotetramerise with its close homologue Mena [446], another protein regulating actin dynamics [447], we next tested the potential for Mena to associate with Rsks. Co-immunoprecipitation experiments confirmed that both Rsk1 and Rsk2 associate with endogenous Mena in A549 cells (Figure 31B). Reverse co-immunoprecipitation could not be performed as our Mena antibody was not immunoprecipitating. Our PPI database also predicted that Rsk1 and 2 should interact and we confirmed this by co-immunoprecipitation of the 2 proteins in A549 cells (Figure 31C). Although the preceding results do not demonstrate whether these interactions are direct or indirect, our observation that Rsk1 and 2 associate with two well-known actin regulators could explain the migratory phenotypes observed upon Rsk downregulation.

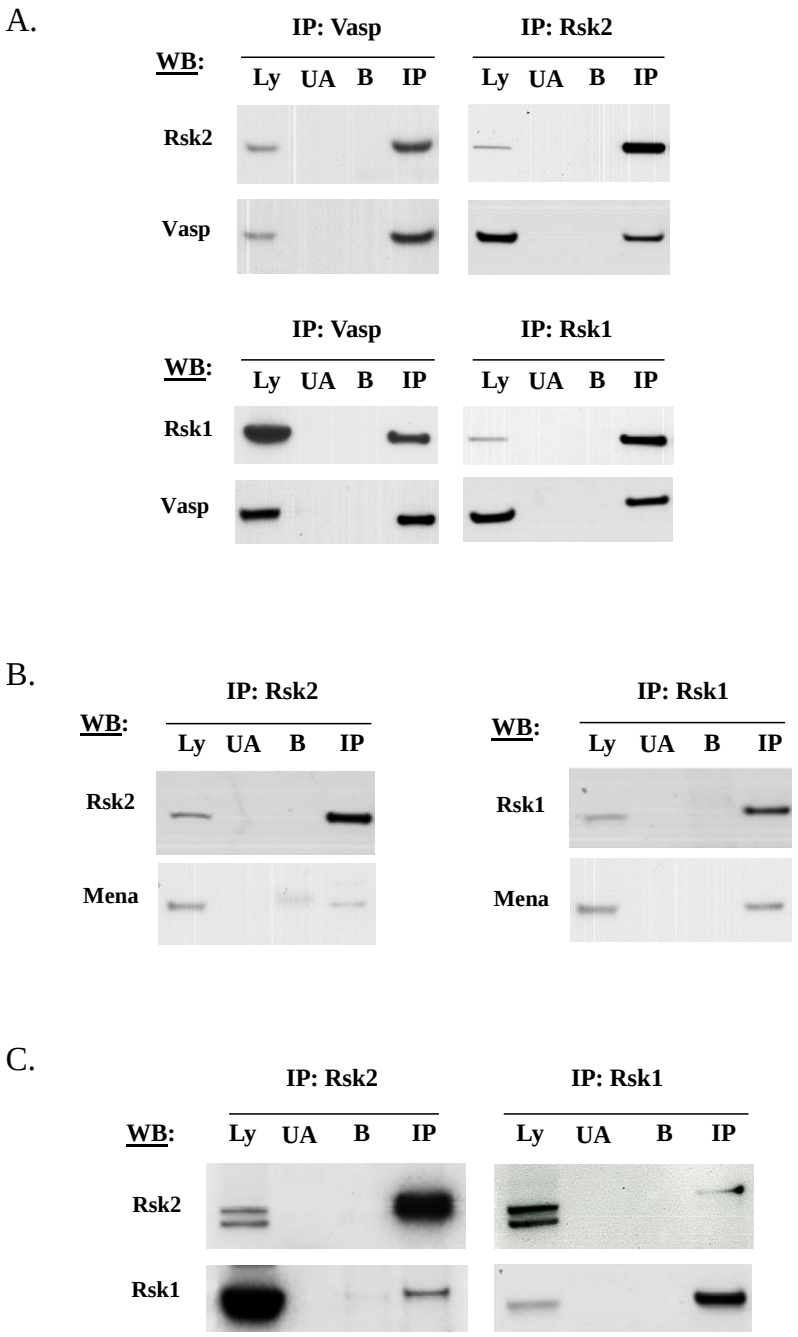

Figure 31: Vasp and Mena interact with Rsk1 and 2. (A, B and C) Co-immunoprecipitation experiments validating interactions between Rsk2 (upper panel), Rsk1 (lower panel) and Vasp (A), between Rsk1, Rsk2 and Mena (B) and between Rsk1 and Rsk2 (C). Cell lysates were immunoprecipitated (IP) for Rsk1, Rsk2 or Vasp. Unspecific antibody (UA) and Beads without antibody (B) were used as control. (Ly) stands for total cell lysate. Blots shown are representative of at least 3 independent experiments. A representative of 3 independent experiments is shown.

To investigate the functional relevance of the Rsk1/2-Vasp interaction and determine whether these proteins directly interact, we performed *in vitro* kinase assays using purified proteins. Figure 32A shows that both human recombinant (hr) activated Rsk1 and 2 could directly phosphorylate hrVasp *in vitro* more efficiently than Rsk's classical substrate, S6 protein. To determine the nature of the phosphorylation sites targeted, the phosphorylated Vasp was analysed by mass spectrometry following trypsin or thermolysin digestion (Figure 32B). This work was performed by our collaborators Dr. Rita Derua and Pr. Etienne Waelkens (Labo Proteïne Fosforylatie en Proteomics, Katholieke Universiteit Leuven). Figure 32B and C shows that Thr-278, a site known to be involved in actin polymerisation [149], was the only site specifically phosphorylated by Rsk1. Indeed, neither recombinant Rsk2 nor Rsk4 induced phosphorylation of this site. On the other hand, Rsk2 targeted specifically the Ser-2 and/or Thr-4, Ser-8 and/or Ser-9 as well as the Ser-322 and/or Ser-323, Ser-324, Ser-325. The mass spectrometry resolution could not distinguish if one or more of these sites were preferentially phosphorylated (Figure 32B and C). While the Ser-2, Thr-4, Ser-8 and Ser-9 have never been described before, the Ser-322, Ser-323 and Ser-234 have previously been identified in high throughput proteomic analysis and reported in the online PhosphositePlus repository (http://www.phosphosite.org). Although Rsk4 was capable of phosphorylating Vasp, no phosphorylation site was specific for this enzyme (Figure 32B). Finally, all three RSK isoforms were able to phosphorylate the Thr-12, the Ser-255 and/or Ser-258, as well as the Thr-315 and/or Thr-316 (Figure 32B and C).

A.

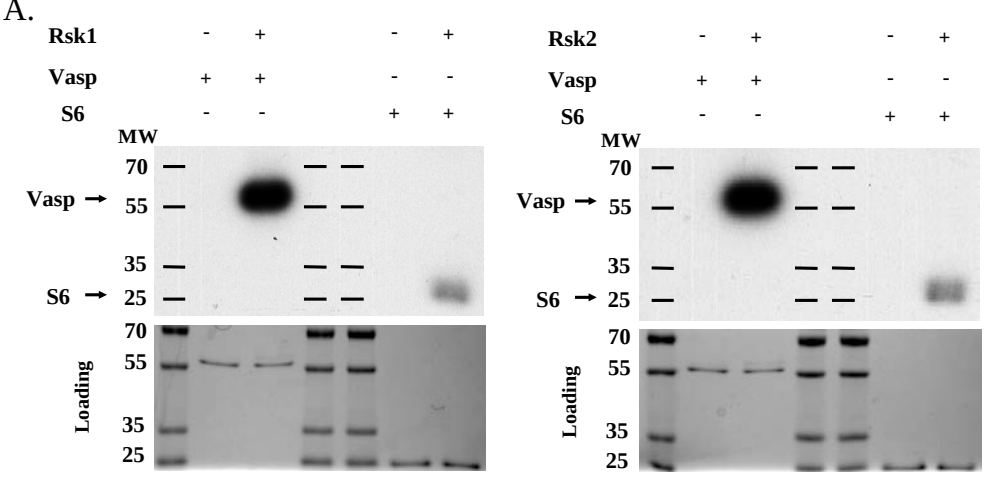

B.

	Mr peptide	Identity of the peptide	no Rsk	Rsk1	Rsk2	Rsk4	Corresponding phosphosites
Trypsin digestion	1158.6	NSTTLPRMK		*	*	*	T315-p or T316-p
	1284.8	KATQVGEKTPK		*			T278-p or T284-p
	940.5	KATQVGEK		*			T278-p
	2335.2	AESGRSGGGGLMEEMNAMLAR		*	*	*	S255-p or S258-p
	2459.4	AESGRSGGGGLMEEMNAMLARR		*	*	*	S255-p or S258-p
	2621.4	VMSETVICSSRATVMLYDDGNK		*	*	*	S2-p or T4-p or S8-p or S9-p or T12-p
Thermolysin digestion	648.4	MSET			*		S2-p or T4-p
	1325.6	MLARRRKATQ	*	*			T278-p
	1329.6	VQELRKRGSP	*	*		*	S379-p
	1361.4	MSETVICSSR	*	*	*	*	S2-p or T4-p or S8-p or S9-p
	724.4	ICSSR			*		S8-p or S9-p
	736.4	MKSSSS			*		S322-p or S323-p or S324-p or S325-p

C.

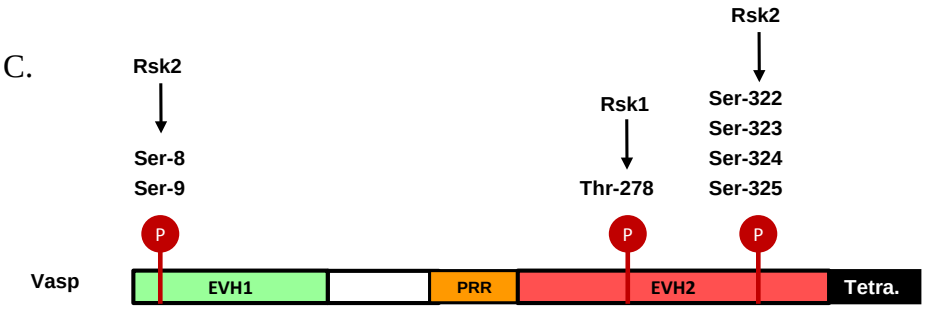

Figure 32: Vasp is phosphorylated by Rsk1, 2 and 4 *in vitro*. (A) Representative experiments in which Human recombinant Vasp was subjected to *in vitro* kinase assays using human recombinant Rsk1 or Rsk2 in the presence of ^{32}P-γATP. Ribosomal S6 peptide was used as a positive control. Upper panel: autoradiogram; black bars indicate Molecular Weight markers (MW). Lower panel: The gel was Coomassie stained as a loading control. (B) Mass-spectrometric analysis of Vasp phosphorylation sites targeted by Rsks isoforms *in vitro*. Recombinant Vasp was incubated *in vitro* in the presence or absence of the relevant human recombinant Rsk isoform and ^{32}P-γATP. "*" represents the detection of phosphorylation in the identified peptides by mass spectrometry following trypsin or thermolysin digestion. The sequence of the corresponding peptide and the putative phosphorylation site(s) within that sequence are presented. (Mr) Relative molecular mass. (C) Schematic representation of Vasp functional domain showing Rsk1 and 2 specific phosphorylation sites identified by mass spectrometry. Ena/Vasp homology domain 1 and 2 (EVH1 and 2), Proline-rich region (PRR)

Previous reports have described three principal phosphorylation sites on Vasp, against which phospho-specific antibodies have been raised [149] [448] [449] [450] [451] [452]. These include the Ser-157, Ser-239 and the newly identified Rsk1 target, Thr-278. We therefore tested whether Rsk1 might modulate the phosphorylation of Thr-278 in intact cells. Figure 33A, demonstrates that Rsk1 silencing prevented phosphorylation of Vasp on Thr-278 in A549 cells growing in 10% serum while Rsk2 and 4 silencing had no effect on this site. Knockdown of Vasp confirmed that the Thr-278 phosphosignal detected was specific for Vasp. We further confirmed the role of Rsk1 in the phosphorylation of Thr-278 on Vasp in H23 NSCLC cell line (Figure 33B). We also examined the phosphorylation of Ser-157 and Ser-239, two other sites involved in the binding of Vasp to actin. Unlike Thr-278, basal phosphorylation of these sites was low and was unaffected by Rsk1 downregulation. However, treatment with forskolin, a potent stimulator of Protein kinase cAMP-dependent (Pka) and Protein kinase cGMP-dependent (Pkg) activity, could induce both Ser-157 and Ser-239 phosphorylation as previously reported [155] (Figure 33C and D). Thus, using phosphospecific antibodies, we were able to validate the mass-spectrometric data and confirm that Rsk1 specifically modulates phosphorylation of Vasp on the Thr-278.

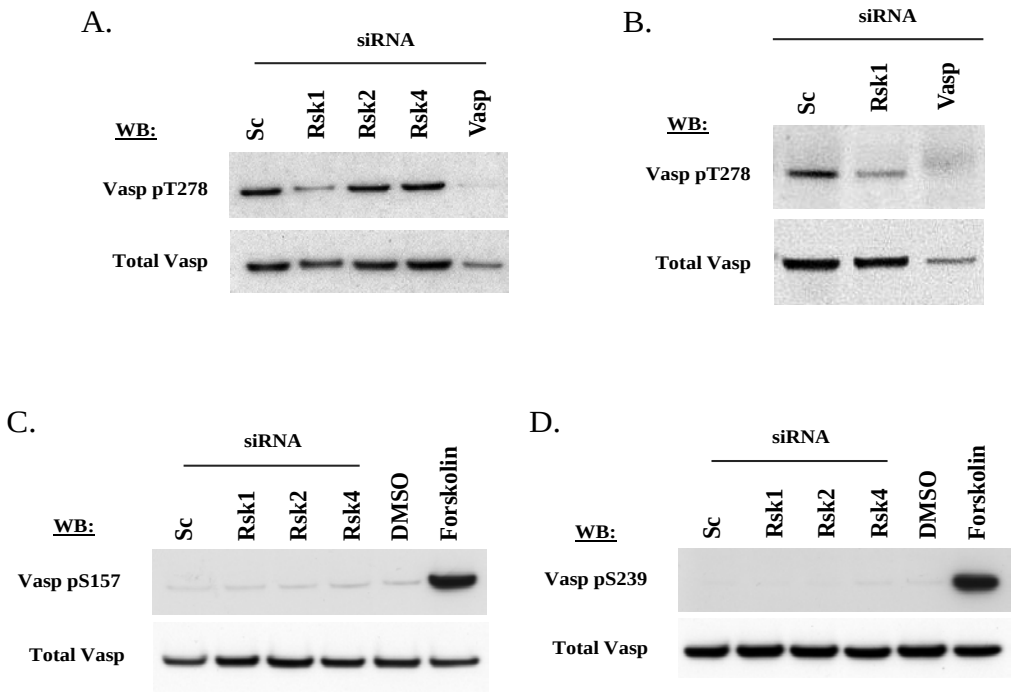

Figure 33: Vasp Thr-278 phosphorylation is dependent on Rsk1 expression. (A, C and D) A549 or (B) H23 cells grown in serum were washed then transfected in serum free medium with siRNAs targeting Rsk1, 2, 4, Vasp or a scrambled control (Sc) as indicated. (C and D) Untransfected A549 cells were stimulated with Forskolin 10µM for 30 min as a positive control for Ser-157 and Ser-239 Vasp phosphorylation. DMSO was used as a diluent-alone control. (A-D) Cell lysates were subjected to Vasp immuno-precipitation before being analysed by SDS-PAGE/Western blotting (WB) using antibodies against the indicated targets. A representative of 3 independent experiments is shown.

5.2.3 Vasp and Mena mediate the effects of Rsk1 on cell motility and morphology

In addition, because Vasp heterotetramerises with Mena and the latter protein was found to associate with Rsk1 in A549 cells, Mena might participate in controlling Rsk1 effects on cell migration. Figure 34A, B and C shows that knockdown of either Vasp or Mena decreased A549 cell migration to a similar extent to that observed upon Rsk2 downregulation (Chapter 3 Figure 19C and Figure 34B). Moreover, reminiscent of data shown in Chapter 3 Figure 22, combined silencing of Vasp and Rsk1 or Mena and Rsk1 produced similar effects on migration as concomitant Rsk1 and 2 knockdown (Figure 34A). Also, combined knockdown of Vasp and Mena completely reversed the effects of Rsk1 silencing (Figure 34A). In addition to these effects on cell migration, Vasp or Mena silencing alone reproduced the changes in the actin cytoskeleton (Figure 35A) previously seen following Rsk2 downregulation (Chapter 3 Figure 23A). Furthermore, while Rsk1 silencing induced a 10-fold increase in the number of lamellipodia per cell, combined Vasp and Mena knockdown dramatically reduced this effect (Figure 35B). In contrast to their modulation of the outcome of Rsk1 silencing, Vasp downregulation did not and Mena's only slightly potentiated the inhibition of cell migration triggered by Rsk2 and/or Rsk4 knockdown (Figure 34B and C). Taken together, these data suggest that Vasp and/or Mena mediate the opposing effects of Rsk1 and Rsk2 on A549 cell migration.

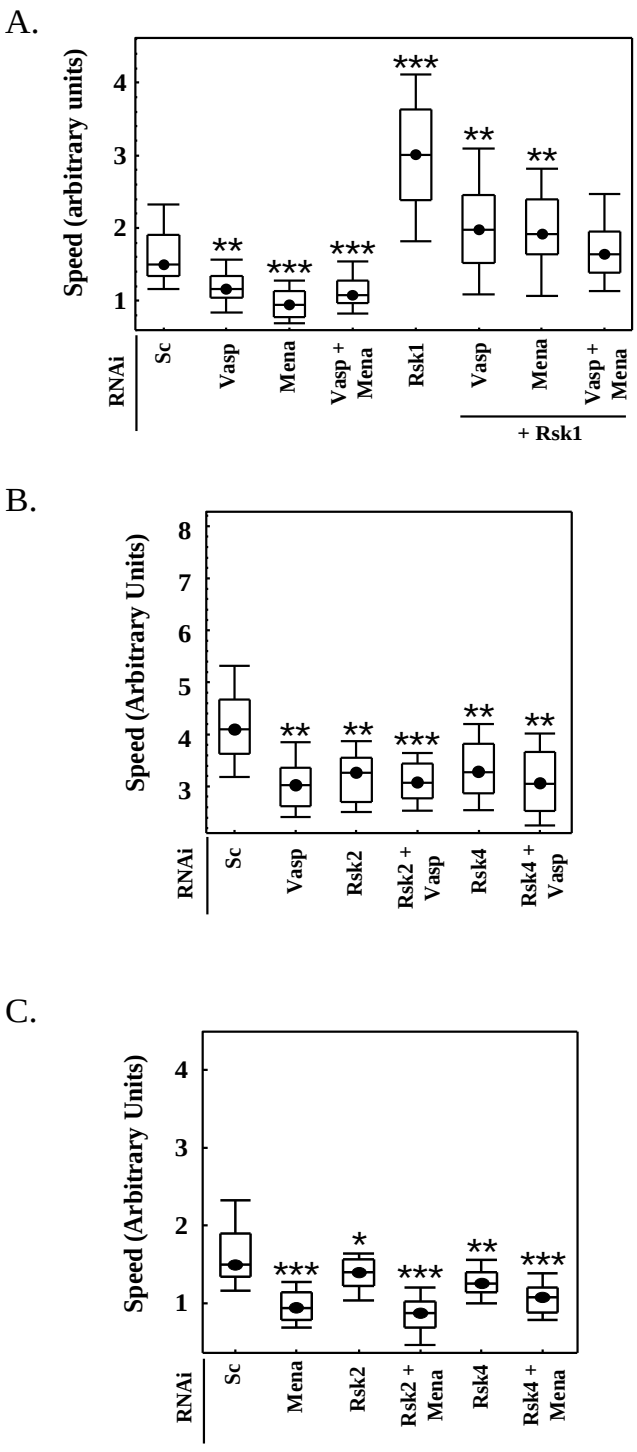

Figure 34: Effects of Vasp and Mena silencing on the motility phenotypes induced by Rsks downregulation. (A) Both Vasp and Mena knockdown are required to counterbalance the effects of Rsk1 silencing. (B and C) Effect of co-silencing of Vasp (B) or Mena (C) on the motility changes induced by downregulation of Rsk2 and 4. The average random migration speed distribution of 60 cells per condition is represented as a box and whisker plot. The box contains 75% and each side bar 12.5% of the cell population. The spot represents the median speed. ANOVA with Sc as reference: *; $p<0.05$, **; $p<0.005$, ***; $p<0.001$. A representative of 3 independent experiments performed in duplicate is shown.

A.

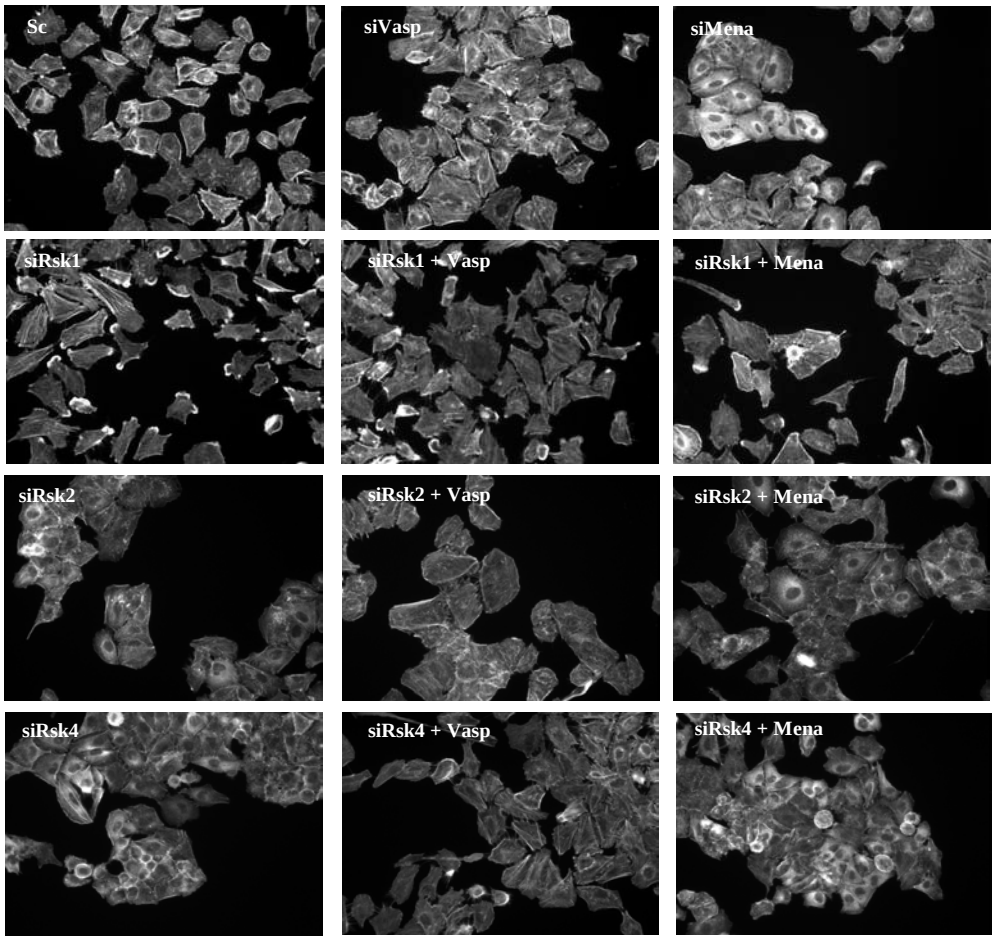

B.

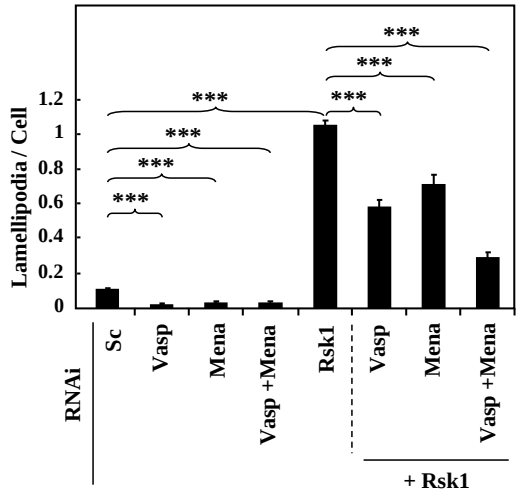

Figure 35: Effects of Vasp and Mena silencing on the cytoskeletal phenotypes induced by Rsks downregulation. (A) Representative images from the actin cytoskeleton staining of A549 cells upon Rsk1, 2 and 4 downregulation with or without co-silencing of Vasp and Mena. Staining was performed using Alexa Fluor 488 phalloidin (white). 36 Images per condition were acquired using the high-throughput microscope ImageXpress Micro (IMX). (B) Effect of VASP and Mena co-silencing with RSK1 on the number of lamellipodia per cell. The average numbers of lamellipopdia per cell from 36 fields of view as in (A) were determined by two independent observers. Cells partially outside the field of view were excluded. Error bars represent SEM. Statistical analysis was performed using a Student's t-test. ***; $p<0.001$. A representative of 3 independent experiments performed in duplicate is shown.

5.3 Discussion

Bioinformatic analysis using the hit list from our cellular motility screen highlighted a sub-group of 21 proteins including several members from the S6 kinase and Casein kinase families (Figure 30). This *in silico* analysis further revealed that Rsk1 and 2 interact with Vasp, a well known regulator of actin dynamics (Figure 30)[107]. Using co-immunoprecipitation, we confirmed this interaction in A549 and H23 NSCLC cell lines (Figure 31, Figure 32 and Figure 33). As in other published reports [140, 453], we showed that silencing of Vasp and Mena decreases cell migration speed (Figure 34). Moreover, co-silencing of these proteins with Rsk1 abolished the promigratory and cytoskeletal effects of selective Rsk1 downregulation (Figure 34 and Figure 35). Using *in vitro* kinase assays on purified proteins, we show that Rsk1, Rsk2 and Rsk4 can phosphorylate Vasp (Figure 32). Helpfully, three principal phosphorylation sites (Ser-157, Ser-239 and Thr-278) have been described on Vasp that regulate its activity and for which antibodies are available [448] [449] [450] [451] [452]. Our results suggest that Thr-278 might be of particular importance here as Rsk1, but not Rsk2 or Rsk4, silencing reduces phosphorylation on this site (Figure 33) in intact cells. In keeping with this hypothesis, the phosphorylation of Thr-278 was previously predicted to suppress migration [149] [155]. Furthermore, our data show that Vasp knockdown partially reversed the effects of Rsk1 silencing (Figure 34). However, Vasp and/or Mena knockdown mimics the effects of Rsk2 and Rsk4 silencing on cell migration and actin organisation (Figure 35). This suggests that Vasp and Mena might still mediate the effects of Rsk2 and 4 but through a mechanism distinct from Thr-278 phosphorylation. Indeed, mass-spectrometric analysis of our *in vitro* kinase assay products suggests that Rsk2 and 4 are capable of phosphorylating Vasp *in vitro* on residues distinct from Thr-278. Although this analysis did not highlight residues

selectively targeted by Rsk4, the specific effects of this isoform could result from its ability to phosphorylate Vasp in distinct sub-cellular localisations. Alternatively, we showed that Rsk4 downregulation leads to an increase in Rsk1 protein levels (Chapter 3 Figure 22), an effect that might in itself explain the modulation of cell migration by Rsk4. However, additional experimental work is warranted to test these or other potential hypotheses.

CHAPTER 6

Rsks mediate metastasis *in vivo*

6.1 Introduction

Activating Mutations within the MAP Kinase pathway have been reported in greater than 30% of human cancers [205]. These mutations are typically gain of function mutations leading to Erk activation [190] [206] and have been reported to drive cell motility, invasiveness and metastasis [200] [454] [455]. Using two successive screening approaches, we previously identified Rsk1, 2 and 4 as regulators of lung cancer migration and invasion. Previous reports have demonstrated Rsk over expression in cancer including breast cancer [252] and head and neck squamous cell carcinomas [256]. However, to our knowledge, Rsk expression in lung tumour and associated metastatic sites remains unknown. To address the clinical relevance of our findings, we first examine the expression of Rsk family members in tissue microarrays (TMA) containing matched primary non-small cell lung cancers (adenocarcinomas) and adjacent normal lung. We then compiled a TMA containing isogenically-matched primary and metastatic tumour samples from 100 untreated patients with lung cancer to compare Rsk1, 2 and 4 expressions between these two sites. This work was performed in collaboration with Dr. Francesco A. Mauri (Histopathology, Imperial College London, Hammersmith Campus, London, UK) and involved Dr. Robert J Shiner. We show that lung cancers, like other neoplasms, over express Rsk family members. Furthermore, in keeping with our *in vitro* findings, we reveal that Rsk1 was downregulated, while Rsk2 and 4 were overexpressed in metastatic lung cancer samples compared to isogenically matched primary tumours. To further demonstrate the relevance of our findings *in vivo*, we developed a zebrafish model based on previous reports [59] [456] [457]. This work was performed in collaboration with the laboratory of Prof. Maggie Dallman (Division of Cell and Molecular Biology, Department of Life Sciences, Faculty of Natural Sciences, Imperial College London, London, UK) and involved Dr. Olivier Pardo, Harriet Taylor,

Alice Shia and Prof. Jonathan R Lamb. My involvement in this work was confined to some analysis only so these results can be found in Annexe 1. Using this model we showed that Rsk1 silencing enhanced the metastatic potential of A549 cells in vivo. In short, our data propose that Rsk family members are important determinants of lung cancer metastatic potential.

6.2 Results

6.2.1 Rsk family members expression in lung tumour

Prior to performing immunohistochemical staining of the TMA, we verified the specificity of the Rsk antibodies using formalin fixed paraffin-embedded pellets of A549 cells treated with scramble or Rsk1, 2 or 4 siRNAs. Figure 36A (left panel) shows that Rsk1, 2 or 4 antibodies reveal a clear staining in scramble treated A549 cells. Silencing of Rsk1, 2 or 4, abrogated the staining for the corresponding antibody compared to scramble transfected cells (Figure 36A right panel) and thus confirmed the specificity of each antibody. Figure 36B shows representative tissue staining of normal lung as well as adenocarcinoma using Rsk1, 2 or 4 antibodies. Positive staining in adenocarcinoma revealed both nuclear and cytoplasmic localisation of the signal for all three Rsk isoforms (Figure 36B). Our *in vitro* results suggested the existence of an equilibrium between the expression levels of Rsk1 and Rsk4 as Rsk4 downregulation led to an increase in Rsk1 protein levels (Chapter 3 Figure 22). Thus, we wondered whether these findings would extend to expression of these two Rsk isoforms *in vivo*. To address this possibility, we used tissue microarrays (TMA) containing matched primary non-small cell lung cancers (adenocarcinomas) and adjacent normal lung.

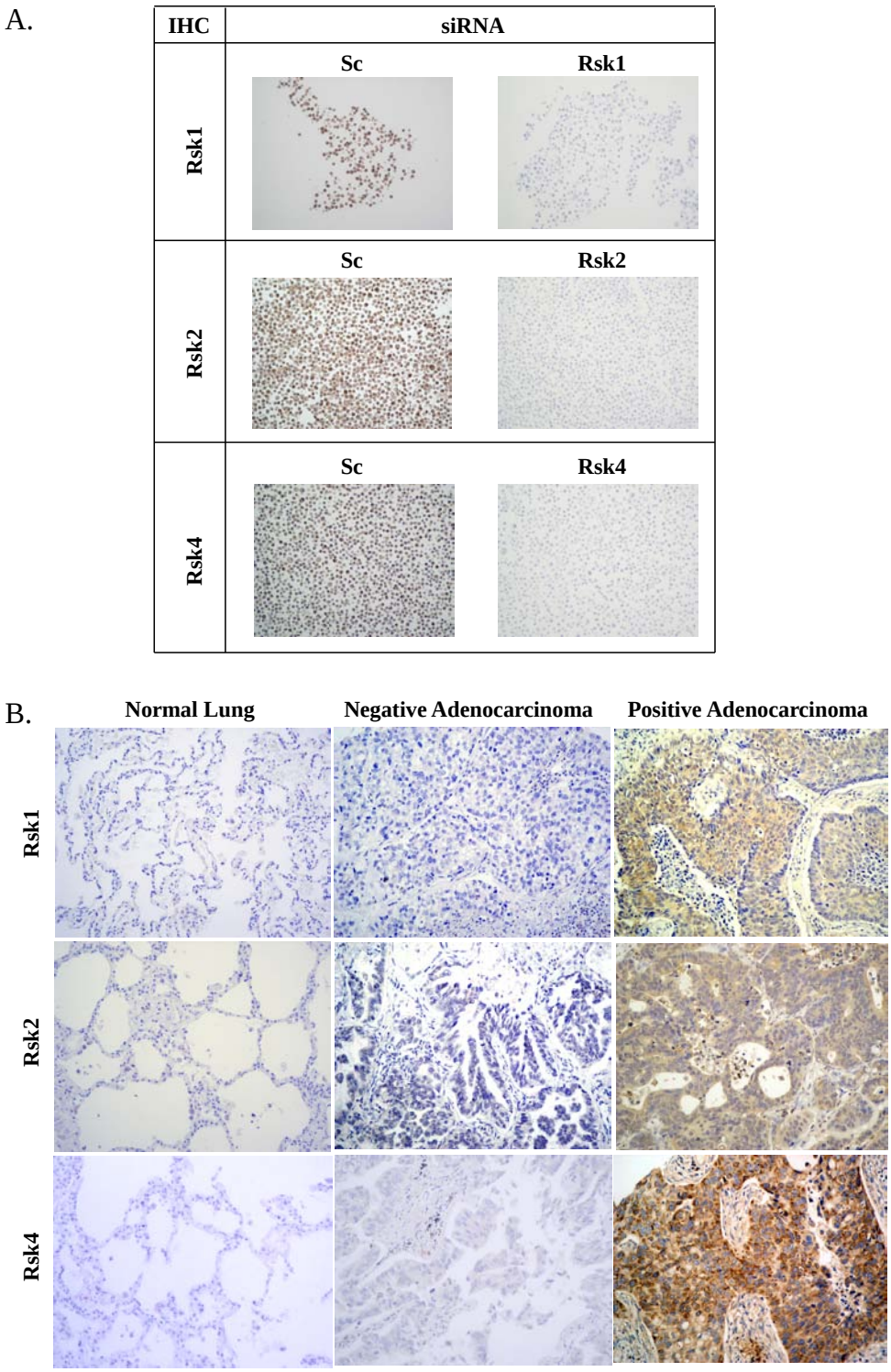

Figure 36: Representative immunohistochemistry (IHC) staining for Rsk1, 2 and 4. (A) Controls for Rsk1, 2 and 4 antibody specificity. A549 cells treated with scramble (Sc), Rsk1, 2 or 4 siRNAs were fixed and paraffin-embedded prior to IHC with the relevant antibody. (B) Representative IHC of tissue samples using Rsk1, 2 and 4 antibodies. Staining of a normal lung specimen together with adenocarcinoma samples positive and negative for expression of the indicated proteins are shown. (A) and (B) Immunoreactivity was revealed using HRP together with Diamino-benzidine (DAB) secondary staining. Blue; haematoxylin counter-stain, Brown; HRP/DAB.

In agreement with previous reports (Zeniou et al., 2002), Rsk1 and Rsk4 protein expression was not detected in normal lung tissue (Figure 36B). However, 49% and 57% of lung tumours were positive for Rsk1 and 4, respectively (Figure 37A), suggesting a possible role for these kinases in tumourigenesis. In keeping with our *in vitro* data, absence of Rsk4 associated with the presence of Rsk1 expression and vice versa in 71% of cases (Figure 37B). These results lend weight to the hypothesis of an equilibrium between Rsk1 and 4 expression in lung cancer.

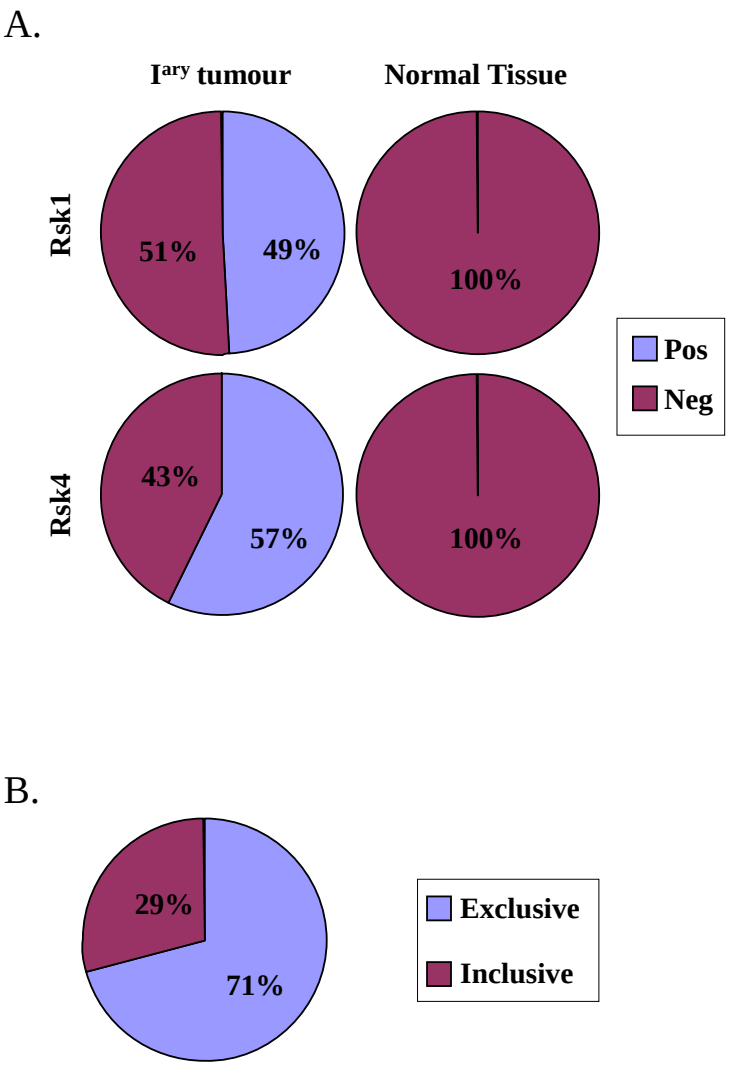

Figure 37: Rsk1 and 4 expression pattern in matched normal lung and primary lung adenocarcinoma samples. (A) and (B) Histoimmunopathological analysis of a human lung tissue micro-array (TMA) containing primary tumours and surrounding normal tissue. (A) Percentage of cases with Rsk1 and Rsk4 variation of positive staining in primary tumours and surrounding normal tissue. (B) Percentage of primary lung tumours samples where Rsk1 or Rsk4 staining was exclusive.

6.2.2 Loss of Rsk1 correlates with increased metastatic frequency

Our previous results demonstrating enhanced migration and invasion upon knockdown of Rsk1 raised the possibility that this kinase might be lost during the metastatic process. To test this hypothesis, we compiled a TMA containing isogenically matched primary and secondary tumour samples from 100 untreated patients with lung cancer. Figure 38A and B demonstrates that in patients where primary tumours stained positively for Rsk1, most showed reduced expression of this protein in the metastatic as compared to the matched primary lesions (I > II). In addition, the 37% of patients with primary tumours negative for Rsk1 staining (I & II neg) demonstrated increased numbers of metastatic lesions when compared to patients with Rsk1-positive tumours (Figure 38C). Moreover, in cases with Rsk1-positive primary tumours, most of the patients within the “0-3 metastatic sites” group had a single secondary lesion. Taken together, these results correlate with our *in vitro* findings and suggest that Rsk1 negativity in primary tumours may be a clinical biomarker for metastasis and poor prognosis.

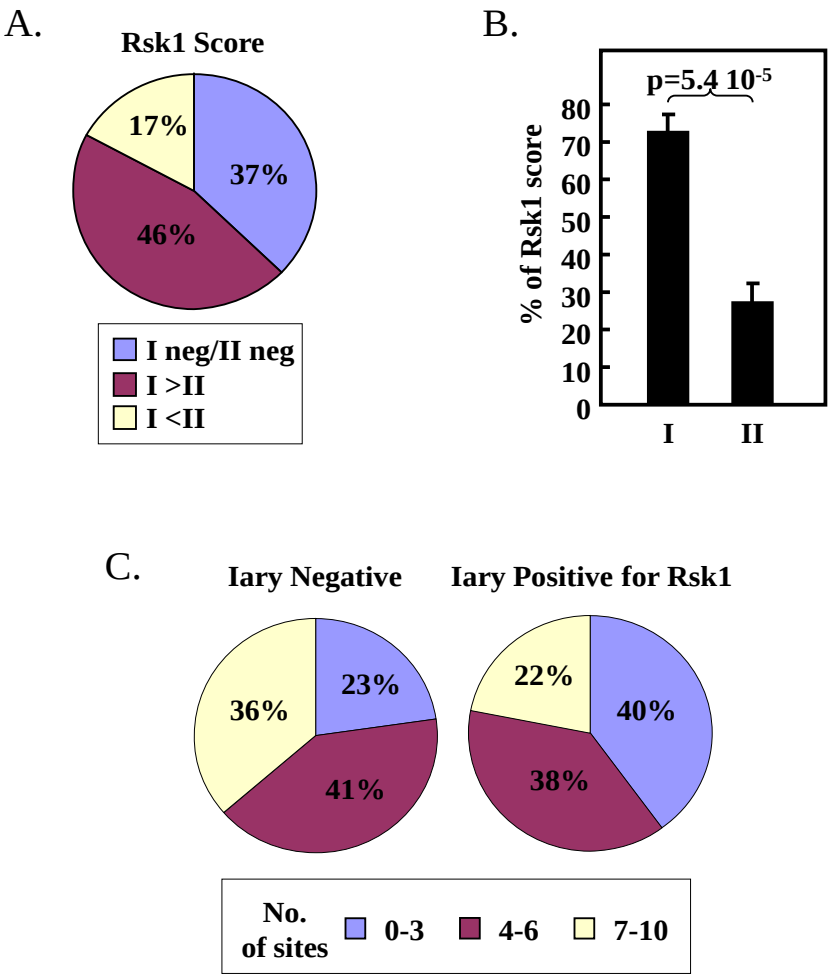

Figure 38: Changes in Rsk1 expression levels correlate with the occurrence of distant metastasis. (A) to (C) A TMA containing matched primary and secondary tumour samples from 100 untreated patients were stained for Rsk1. (A) Comparison of Rsk1 staining score between primary and secondary sites. "I & II neg"; both primary and secondary lesions are negative for Rsk1. "I > II" ; staining higher in primary than secondary sites. "I < II" ; staining lower in primary than secondary sites. (B) Percentage of Rsk1 scores in the primary ("I") and the secondary ("II") tumours of cases with positive Rsk1 staining. Error bars are SEM. Statistical analysis was performed using a Student's test. (C) Number of secondary lesions per patients depending on Rsk1 positive or negative staining in the primary tumour. Numbers represent percent of cases.

6.2.3 Rsk2 and/or 4 expression increases in metastasis versus primary lesions

Because of the effects of both Rsk2 and 4 knockdown on A549 cell migration and those of Rsk4 siRNA on A549 cell invasion in vitro, we next examined immunohistochemical staining for Rsk2 and 4 in the same TMAs. Figure 39 A – D show that neither protein alone could predict for metastases. A possible explanation for this is that for a given tumour these two isoforms act inter-changeably. This hypothesis predicts that where altered Rsk2 levels do not correlate with metastasis, changes in Rsk4 expression would substitute and vice versa. In agreement with this notion, 59% of patients showed increased Rsk2 or 4 staining in the secondary compared to their primary lesions (Figure 39E). Also, a greater number of metastatic lesions were observed in cases where Rsk2 or 4 were increased in the secondary sites compared to the primary tumour (Figure 39F). Interestingly, increase in Rsk2/4 expression could account for the metastatic status of half the cases where Rsk1 staining had failed to do so (Figure 39G). Thus, 75% of all cases could have their metastatic status explained based on staining for these 3 Rsk isoforms (Figure 39G). A much larger cohort of patients is now required to examine the predictive power of these proteins for metastasis in the clinic.

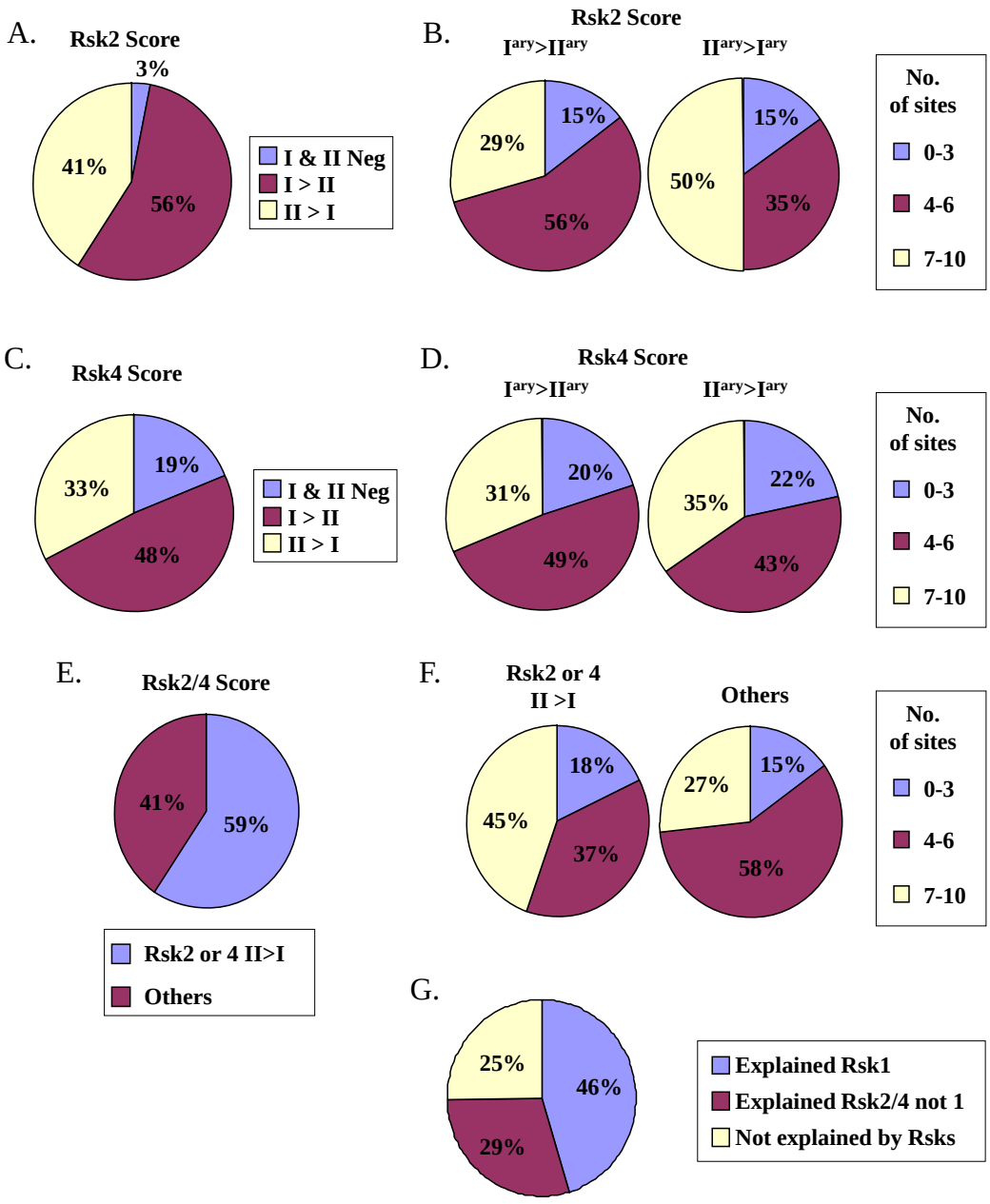

Figure 39: Rsk2 and 4 immunohistochemistry (IHC) scores in primary vs metastatic lesions. (A-F) A TMA containing matched primary and secondary tumour samples from 100 untreated patients were stained for Rsk2 or 4. (A) and (C) Comparison of Rsk2 (A) or Rsk4 (C) staining between primary and secondary sites. (B) and (D) Number of secondary lesions per patients depending on Rsk2 (B) or Rsk4 (D) staining in the primary vs the secondary tumours. Numbers represent percent of cases in each category. (A-D) "I & II neg"; both primary and secondary lesions are negative for Rsk2 or 4. "I > II" ; staining higher in primary than secondary sites. "II > I"; staining higher in secondary than primary sites. "No. of sites"; number of metastatic sites reported per clinical case. (E) Comparison of Rsk2 or 4 staining intensity between primary and secondary sites. "Rsk2 or 4 II>I"; Rsk2 and/or 4 staining higher in the secondary than the primary lesion. (F) Number of secondary lesions per patients depending on Rsk2 or 4 expression status in the secondary vs the primary tumour. Numbers represent percent of cases. (G) Proportion of cases where the metastatic status can be explained by Rsk1, 2 or 4 comparative staining between primary and secondary tumours. "Explained Rsk1"; cases that can be explained based on Rsk1 staining alone. "Explained Rsk2/4 not 1"; cases explained by by Rsk2 or 4 but not Rsk1 staining. "Not explained by Rsks"; cases where Rsk1, 2 or 4 staining cannot account for the patients metastatic status.

6.2.4 Rsk1 modulates invasion in vivo

Our preceding results indicated that Rsk1 downregulation enhanced cell motility and invasion in A549 cells *in vitro*. We further correlated these *in vitro* findings in human clinical samples and showed that Rsk1 was downregulated in metastatic lung cancer samples compared to isogenically matched primary tumours. To demonstrate that Rsk1 downregulation can induce dissemination of tumour cells *in vivo* we established a cancer metastasis zebrafish model. In this model, A549 cells stably expressing a histone 2B-GFP fusion protein were established to allow for convenient visualisation of the cells by fluorescence microscopy. Cells expressing high levels of GFP were selected using flow cytometric cell sorting to obtain a more homogenous cell population. 30 cells were injected into the cell mass of 4 h post-fertilisation zebrafish embryos. Annexe 1A shows that the injected tumour cells could easily be visualised using widefield fluorescent microscopy. Whole fish imaging after 48 h demonstrated that the injected cells formed a tight tumour mass in the head of all injected fish with only very limited dissemination into the fish body (Annexe 1B). Using this model, we hypothesised that down-regulation of Rsk1 might enhance dissemination of A549 cells away from this mass. Indeed, injection of A549 cells silenced for Rsk1 resulted in a more diffuse tumour mass in the fish head accompanied by single cell invasion throughout the fish body including the tail (Annexe 1B). In contrast, fish injected with A549 cells transfected with a scrambled siRNA displayed tight tumours in the head with control levels of invasion and total absence of dissemination to the fish tail (Annexe 1B). This difference in phenotype could be quantified by scoring for the presence or absence of tumour cells within 3 defined regions of the fish body; Head, Middle and Tail (Annexe 1C, n=120 fish per condition). We further imaged the dissemination of the Rsk1 silenced cells to the tail at different time-points (Annexe

1D). Importantly, the cells which had migrated to the tail, retained the ability to proliferate, a condition required for the formation of metastatic tumours (Annexe 1D). Thus, Rsk1 knockdown enhances the ability of A549 cells to invade and disseminate *in vivo*.

6.3 Discussion

We previously revealed Rsk1, 2 and 4 as modulators of NSCLC motility. We further established that Rsk1 and 4 knockdowns could modulate A549 cell invasiveness *in vitro* suggesting that these isoforms might be important in regulating metastasis in human lung cancer. To show the clinical relevance of our findings, we compared the expression of Rsks family members in a TMA containing matched primary non-small cell lung cancers (adenocarcinomas) and adjacent normal lung. While expression of Rsk1 and Rsk4 was not detected in normal lung tissue, primary adenocarcinoma showed a positive staining for Rsk1 and Rsk4 in more than 50% of the cases (Figure 37A). Previous reports also revealed increased expression of Rsk2 in breast [252] and prostate cancer [253] hence suggesting a possible involvement of these kinases in tumourigenesis. In addition, in 71% of cases, absence of Rsk4 associated with the presence of Rsk1 expression and vice versa (Figure 37B). This result supports our previous *in vitro* findings (Chapter 3 Figure 22) suggesting an equilibrium between Rsk1 and 4 expression in lung cancer. Furthermore, we assembled a second TMA comprising primary human lung cancers isogenically matched with their metastases from 100 post-mortem cases. In this TMA, while Rsk1 was often highly expressed in the primary tumours, its expression was downregulated in secondary lesions (Figure 38A and B). Moreover, loss of Rsk1 in the primary tumour correlated with an increased incidence of metastasis (Figure 38C) in accordance with our *in vitro* data. Although Rsk2 did not alter invasion *in vitro*, its control of cell migration alone could still

contribute to the metastatic process *in vivo*. Indeed, Rsk2 and 4 were upregulated in 59% of the metastatic lesions compared to the primary tumours. Thus, our results show that the Rsk family targets identified in the *in vitro* screens can translate into clinically relevant findings in patient samples. To further demonstrate our findings *in vivo*, we established a zebrafish model for lung cancer metastasis. In this system A549 cells stably expressing a histone 2B-GFP fusion protein were injected into the cell mass of 4 h post-fertilisation zebrafish embryos. After 48 h, these cells formed a tight mass of cells in the head of the developing zebrafish and only slowly invade and disseminate down the body of the fish towards the tail. We show that Rsk1 silencing markedly increased the dissemination of cells in the fish body as compared to scramble treated cells (Annexe 1) thus confirming our previous *in vitro* results. Since Rsk1 and 2 effects might be mediated by Mena and/or Vasp *in vitro*, one might expect that the expression of the latter proteins in cancers could also correlate with metastatic potential *in vivo*. In agreement with this notion, several reports have recently shown that upregulation of Vasp, Evl or Mena correlates with increased metastasis and disease progression in xenograft models or clinical biopsies [458] [172] [171] [173]. The preceding results suggest that Rsks might be useful biomarkers for lung cancer metastasis. Indeed, 75% of our 100 post-mortem cases could have their metastatic status explained by a decrease in Rsk1 and/or an increase in Rsk2 or 4 expressions. However, since all patients in our TMA had metastases and the number of cases was limited, further work is required to determine the true predictive value for these potential biomarkers.

CHAPTER 7

General discussion

In the course of this thesis, we performed an siRNA kinome library screen to identify modulators of cell migration in A549 human lung adenocarcinoma cells. In a secondary 3D invasion screen, we revealed a set of hits that modulated A549 cell invasion *in vitro*. Our data highlighted the importance of the Rsk family members in modulating NSCLC metastasis. We show that Rsk isoforms mediate opposite effects on NSCLC metastasis and identify Vasp, a regulator of cell migration, as a novel substrate of Rsks. This knowledge provides us with new insights into the biology of NSCLC metastasis and we believe will help us design new treatments for this disease.

7.1.1 Results from the high-throughput screens for cellular motility and invasion show limited overlap

Our migration and invasion screen show 54% of correlation suggesting that changes in cell migration cannot be directly extrapolated to cell invasiveness. Several screens looking for changes in cancer cell motility, invasiveness and metastasis have recently been reported (Table 9). The overlap between these and our own screen is very limited. Indeed, we identified four hits (Csnk1g2, Prkce, Als2cr2 and Akt1) in common with a published screen performed in the non-tumorigenic breast epithelial cell line MCF10A [407] and one (Map4k4) that similarly decreased the migration of the ovarian SKOV-3 cells [406]. However, when comparing seven other migration screens, two invasion screens and an *in vivo* metastasis screen, the results generated by these screens show limited if any overlap between them (Table 9). This is somewhat surprising. Indeed, if a gene signature was to drive cancer metastasis, one expects that it would be highlighted by such a comparison.

One reason explaining this discrepancy could be that the experimental approaches (e.g. cellular system, library, assay) used were different. Moreover, each of

these screens measured a single parameter (e.g. migration speed, migration distance, number of cells invading) to identify proteins regulating a complex multistep mechanism (metastasis) (Chapter 1 section 1.2.1). The comparison of our migration and invasion screens using the same cellular system suggests that the measurement of a single parameter taking part in the metastatic cascade cannot be extrapolated to metastasis itself. The emergence of multiparametric screens [459] [460] [461] [462] that use a set of parameters to characterise gene-specific effects regulating a phenotype successfully identified gene signatures controlling complex biological processes such as mitosis [462] and endocytosis [459]. The implementation of similar approaches to investigate metastasis might reveal a gene signature common to a wide range of tumour cell types.

Alternatively, the discrepancy observed amongst the screens performed so far may suggest that the network of kinases regulating cell migration, invasiveness and metastasis is adaptive and variable between cancer types. In that case, screening approaches centred on the downregulation or overexpression of one gene at a time will remain informative for the cellular system or the cancer type studied but will have limited wider relevance.

Phenotype	Migration										Invasion		Metastasis
Screen	NSCLC	Collins	Simpson	Seo	Naffar-Abu-Amara	Brugge lab 1	Brugge lab 2	Brugge lab 3	Brugge lab 4	Brugge lab 5	Gobeil	Finlayson	Gumireddy
Reference	-	Collins et al. 2006	Simpson et al. 2008	Seo et al. 2010	Naffar-Abu-Amara et al. 2008	CMC	CMC	CMC	CMC	CMC	Gobeil et al. 2008	Finlayson et al. 2009	Gumireddy et al. 2007
Target cells	A549 (NSCLC)	SKOV-3 (ovarian)	MCF10A (breast)	NIH3T3 (mouse fibroblast)	MCF-7 (breast)	MCF10A (breast)	MCF10A (breast)	MCF10A - Erbb2 (breast)	MCF10A - Csf1r (breast)	MCF10A - Csf1r stimulated Csf (breast)	B16-F10 (mouse melanoma)	immortalized mouse mammary epithelial cell line EpH4	Mouse 168FARN (breast)
Library	siRNA - Kinome	siRNA - Genome	siRNA - Kinases, phosphatases, migration hits	Mouse brain cDNA library	cDNA – BC1000	cDNA – BC1000	cDNA - Mcf7 library	cDNA - Mcf7 library	cDNA - Mcf7 library	cDNA - Mcf7 library	pool shRNA - Genome	cDNA - Genome	cDNA library from day 13.5 embryonic mice
Assay	Random walk	Wound healing	Wound healing	Transwell	Phagokinetic track	Transwell	Transwell	Transwell	Transwell	Transwell	3D invasion assay	Transwell coated with Matrigel	In vivo metastasis
Number of hits	70	4	66	12	4	39	6	3	4	4	22	3	2
NSCLC	70/70	1/4	4/66	0/12	0/4	0/39	0/6	0/3	0/4	0/4	0/22	0/3	0/2
Collins		4/4	0/66	0/12	0/4	0/39	0/6	0/3	0/4	0/4	0/22	0/3	0/2
Simpson			66/66	0/12	0/4	0/39	0/6	0/3	0/4	0/4	0/22	0/3	1/2
Seo				12/12	0/4	0/39	0/6	0/3	0/4	0/4	0/22	0/3	0/2
Naffar-Abu-Amara					4/4	1/39	0/6	0/3	0/4	0/4	0/22	0/3	0/2
Brugge lab 1						39/39	0/6	0/3	0/4	0/4	0/22	0/3	0/2
Brugge lab 2							6/6	1/3	1/4	1/4	0/22	0/3	0/2
Brugge lab 3								3/3	1/4	1/4	0/22	0/3	0/2
Brugge lab 4									4/4	3/4	0/22	0/3	0/2
Brugge lab 5										4/4	0/22	0/3	0/2
Gobeil											22/22	0/3	0/2
Finlayson												3/3	0/2
Gumireddy													2/2

Table 9: Comparison of migration, invasion and metastasis screens currently reported. 9 migration, two invasion and one *in vivo* metastasis screens are described. The upper part of the table (green) describes the targeted cells used and the organ of origin. The library used (cDNA or siRNA used the assay chosen and the number of hits identified are reported. The lower part of the table shows the result of comparing the hit lists between screens. Results are highlighted in red when overlaps are identified. Brugge Lab 1, 2, 3, 4 and 5 refer to screens from Joan Brugge's lab referenced in the **Cell Migration Consortium (CMC)** http://www.cellmigration.org**.** BC1000: cDNA library integrating a collection of 1000 genes associated with breast cancer Breast Cancer. cDNA - MCF7 library: cDNA library obtained from MCF7 cells.

7.1.2 The involvement of Rsk in cellular motility

Our motility screen revealed several Rsk family members as regulators of NSCLC migration. In particular, Rsk1 increased while Rsk2 and 4 decreased A549 migration speed upon downregulation. The effects of Rsk1 silencing could be reversed by Rsk2 suggesting that a balance between the activities of these two Rsk isoforms may exist. On the other hand, silencing of Rsk4 increased the expression levels of Rsk1. Unfortunately, the reverse experiment could not be performed due to the absence of a Rsk4 antibody suitable for Western blotting. Nevertheless, these results suggest that Rsk1 and Rsk4 may regulate each others activity through cross-modulation of their expression levels. Taken together, our data potentially indicate a complex and intricate relationship between Rsk isoforms.

We also show that Rsk1 downregulation strongly increased cell invasiveness *in vitro* and metastasis in an *in vivo* zebrafish model. In contrast, Rsk4 silencing inhibited invasion *in vitro.* However, the effects of Rsk2 on A549 cell migration did not extend to cell invasiveness in our assay. Recent reports have highlighted the importance of Rsk family members in modulating migration, invasion and metastasis [256, 323-324]. These studies propose Rsk1 and/or Rsk2 as being determinant factors in mediating the pro-metastatic programme driven by Erk. Over-expression of kinase active Rsk1 in two melanoma cell lines was shown to increase cell motility in a $p27^{Kip1}$/RhoA-dependent manner [324]. However, contradictory reports suggest that loss of $p27^{Kip1}$ leads to increased cellular motility and invasiveness [463] [464]. While treating cells with pan-Rsk inhibitors (fmk, SL0101 and BI-D1870) inhibited Rsk-mediated migratory and invasive effects [256, 323], isoform-specific down-regulation of Rsk family members using RNA interference in head and neck squamous cell carcinomas (HNSCC) did highlight the particular role of Rsk2 in this process. Indeed, silencing of Rsk1 alone in HNSCC does

not reproduce the effects observed in melanoma cells [256, 324]. On the other hand, Doehn et al. showed that the silencing of either Rsk1 or Rsk2 alone is unable to significantly decrease invasiveness in the normal breast epithelial MCF10A cells but that downregulation of both isoforms is required to achieve this effect. Thus, it would appear that the contribution of each Rsk isoform to cellular motility and invasiveness is cell type-dependent.

Our data show that Rsk1 silencing in NSCLC leads to an increase in cell motility, invasiveness and metastasis. Interestingly, in their cell migration screen, Simpson et al. showed that Rsk1 silencing was impairing migration of MCF10A cells. However, in a secondary screen using the same cell line overexpressing the receptor tyrosine kinase Erbb2, Rsk1 silencing increased cell migration in a similar fashion as that observed in our screen [407]. This suggests that the involvement of Rsk1 in cell migration might be dictated by the signalling context of the cell system considered.

In *Drosophila melanogaster*, Rsk is represented by a single gene [465]. Development of Rsk-null mutant flies revealed an increased dependency on Erk for cellular differentiation. In contrast, over expression of Rsk in flies suppressed Erk-dependent differentiation by preventing Erk translocation to the nucleus, thereby inhibiting the Erk transcriptional programme [466]. Recently, Erk2 has been shown to activate the expression of pro-motile and pro-invasive genes via the transcription factor Fra1 [200]. Hence, it is tempting to speculate that Rsk isoforms might regulate cell motility by differentially affecting Erk localisation (e.g. membranous, cytoplasmic or nuclear).

7.1.3 The role of Rsk isoforms in the regulation of the actin cytoskeleton

We have shown that the effect of Rsk1 and 2 downregulation on cell motility correlated with changes in cell shape and actin cytoskeleton. In Particular, Rsk1 downregulation led to an increase in number of lamellipodia suggesting an involvement of Rsk1 in actin dynamics. Indeed, using a combination of bioinformatic analysis and co-immunoprecipitation experiments, we have demonstrated that Rsk 1 and 2 interact with Vasp and Mena, two proteins involved in the regulation of actin polymerisation. Moreover, we showed that silencing of Vasp and Mena decreases cell migration speed and that co-silencing of Vasp and Mena with Rsk1 abolished the promigratory and cytoskeletal effects of selective Rsk1 downregulation. Using mass spectrometry analysis, we identified Vasp residues phosphorylated by Rsk1, 2 and 4. In particular, we show that the Thr-278 is specifically targeted by Rsk1.

7.1.3.1 Rsk1 phosphorylates Vasp on the Thr-278

Vasp and Mena act as anti-capping, anti-branching, actin bundling proteins via their EVH2 domain and promote profilin-actin recruitment to the actin filament barbed end via their central proline rich region (reviewed by [144]). While recruitment of profilin-actin is not a requirement for Vasp activity, the anti-capping, anti-branching, actin bundling activities are essential for it to promote F-actin polymerisation [144]. These functions are mediated via separated motifs within the EVH2 domain that interact with G-actin, F-actin and promote Vasp tetramerisation. Previous reports have highlighted the importance of the phosphorylation of the Ser-239 located next to the G-actin binding motif (GAB: residues 234 to 237) and the Thr-278 adjacent to the F-actin binding motifs (FAB: residues 260 to 277) in the regulation of Vasp activity. Indeed,

actin filaments and profilin-actin are negatively charged and show high affinity for Vasp-located F- and G-actin binding domains respectively. Hence, the addition of negative charges by phosphorylation of these sites (or phospho-mimetic mutation) reduces the affinity of Vasp for actin and impairs Vasp-mediated actin filament assembly [149] [155]. The Ser-239 is a known substrate of the cyclic-nucleotide-dependent kinases Pka and Pkg [149]. Interestingly, double phospho-mimetic mutation of the Ser-239 and Thr-278 has an additive and maximising effect on Vasp function [149]. This suggests the possibility that Rsk1 and Pka/Pkg collaborate in the regulation of Vasp activity. Indeed, recent reports have shown that Rsk1 (but not Rsk2) and Pka regulate each other's activities and localisation [467].

7.1.3.2 Rsk family members differentially phosphorylate Vasp

Our mass spectrometry analysis of Vasp phosphorylation by Rsk1, 2 and 4 revealed that Rsk1 and 2 could target distinct residues on Vasp while Rsk4 did not. This analysis identified Ser-2 and/or Thr-4, Ser-8 and/or Ser-9 as well as Ser-322 and/or Ser-323, Ser-324, Ser-325 as potential Rsk2 specific substrates. Furthermore, all three Rsk isoforms were able to phosphorylate Thr-12, Ser-255 and/or Ser-258, as well as Thr-315 and/or Thr-316. Interestingly, recent proteomic high-throughput screens support our *in vitro* findings. Indeed, the phosphorylation of Ser-321, Ser-322, Ser-323, Ser-324, Thr-315 and Thr-316 located in the EVH2 domain were also highlighted in HeLa cells [468]. However, the effect of these phosphorylation sites on Vasp function remains to be demonstrated. The EVH1-located Ser-2, Thr-4, Ser-8 and Ser-9 targeted by RSk2 could potentially affect the function of Vasp by modulating the binding of the EVH1 domain to proline-rich sequences (PRS) containing proteins such as Vinculin and Zyxin [469]. Indeed, Vasp interaction with these proteins is particularly important for

Vasp localisation to the tips of the filopodia, the lamellipodia and the focal adhesion complexes [107].

7.1.3.3 Implications for the design of new therapies for Lung Cancer metastasis

Three pan-inhibitors have been described that inhibit Rsk kinase activity specifically. These are SL0101 and BI-D1870 that target the NTKD [179, 252, 470] and the pyrolopyrimidine fmk that target the CTKD of Rsk [471]. Our data, showing that downregulation of Rsk2 and/or Rsk4 suppresses migration, suggest that a Rsk2/4 inhibitor might prevent metastasis in human lung cancer cells. Unfortunately, all Rsk inhibitors currently available target the kinase domains (NTKD or CTKD) which are well conserved amongst all Rsk isoforms [251, 471] [252, 470, 472]. This could be of concern as inhibition of Rsk1 may not be desirable. Indeed, siRNA-mediated silencing of this protein enhances cell migration/invasion and knockdown of all 3 Rsk isoforms (Rsk1/2 and 4) cancels out the effects of each one individually in NSCLC (Chapter 3 Figure 22). Consequently, at best, a pan-inhibitor may simply exert no effect on metastatic potential of NSCLC while in the worst case scenario it might actually promote tumour cell dissemination. However, this hypothesis needs to be validated experimentally.

7.1.4 Future directions

In the light of the results presented in this thesis, several questions remain to be addressed.

- **How do the 70 migration hits affect the invasiveness of additional cell types and how does ECM composition modulate this effect?**

The comparison of our two screens revealed a limited correlation (54%) between cell migration and invasion. One reason explaining this discrepancy could lie in the type of ECM used to perform our 3D invasion screen. Indeed, by using a type I collagen matrix, we might have selected migration hits that require this component to modulate invasiveness. *In vivo*, metastasising tumour cells are exposed to a more complex extracellular environment (Chapter 1 section 1.1.2 and 1.2.1.1.1.1). Hence, the use of additional ECM components as well as different chemo-attractants might reveal a higher degree of correlation between cell motility and invasiveness modulators. Furthermore, re-screening the 70 motility hits for cellular motility and invasiveness in a panel of cell lines from various origins should provide a better appreciation of the correlation between the two processes.

- **Can we extend our observation on the role of Rsk isoforms in NSCLC to additional cancer types?**

Several reports suggest that our observations on the role of Rsk1 in NSCLC cell migration cannot be extended to other cancer types [256, 323-324]. However, a systematic assessment of cell migration following silencing of each Rsk isoforms in a panel of cell lines of various origins should provide a more complete understanding of the roles of Rsks in this process.

- **What are the molecular mechanisms responsible for the different phenotypes observed following Rsk1, 2 and 4 targeting in NSCLC?**

Our data suggest that Rsk1 might act as a dominant Rsk isoform regulating NSCLC metastasis. Indeed, we showed that Rsk4 silencing leads to an increase in Rsk1 protein levels suggesting that Rsk4 effects on cell motility might be mediated by Rsk1.

However, we have not uncovered the mechanism underlying this balance. Several hypotheses could be proposed. First, Rsk4 downregulation could enhance expression of Rsk1 by transcriptional or translational mechanisms. Alternatively, Rsk4 silencing could lead to a stabilisation of Rsk1 protein. Furthermore, our data show that Rsk1 and 2 co-immunoprecipitate in A549 cells and that concomitant silencing of Rsk1 and 2 cancel their respective effects on cell migration. This suggests the existence of a balance between the biological activities of Rsk1 and Rsk2. Different molecular mechanisms could account for this effect. First, Rsk1 and 2 could inhibit each other through interaction. Second, Rsk1 and 2 could induce a mislocalisation of the other isorform thereby preventing it from interacting with its substrates. Finally, Rsk1 and 2 might be competing for their downstream binding partners or upstream activators such as Erk.

- **What is the importance of Vasp phosphorylation by Rsk1 during invasion and metastasis?**

Using both mass spectrometry and phospho-specific antibodies, we have shown that Rsk1, but not Rsk2 or Rsk4, phosphorylates Vasp on the Thr-278. Phosphorylation of Thr-278 was previously predicted to suppress cell migration [149] [155] suggesting that Thr-278 might be of particular importance in mediating Rsk1 effect on cell motility. Indeed, Vasp knockdown partially reversed the effects of Rsk1 silencing. To address this hypothesis, it would be necessary to assess how Rsk1 silencing affects the migration of cells over-expressing phospho-mimetic (Thr-278 to Glutamic acid) or non-phosphosphorylable (Thr-278 to Alanine) mutants of Vasp. However, the endogenous expression levels for Vasp are high and likely to mask the effects of the overexpressed cDNAs if their effects are not dominant. Alternatively, mouse embryonic fibroblasts

(MEF) obtained from Vasp knockout mice could be used. However, previous reports have shown that re-expression of Vasp in these cells decreases migration speed in contradiction to what is observed in epithelial tumour cells [140]. Finally, the relevance of the phosphorylation of Vasp by Rsk1 during invasion and metastasis needs to be assessed.

7.1.5 Final comments

This work has enabled us to identify novel modulators of lung cancer cell motility, invasiveness and metastasis. In particular, we have highlighted the importance of Rsk isoforms in these processes. Our data suggest that the phosphorylation of the actin binding protein Vasp by Rsk1 might be relevant to the effects of this kinase on cell motility. However, further work is needed to fully demonstrate this hypothesis and assess the importance of this interaction to invasion and metastasis. Our *in vitro* data correlated with findings in human tissue arrays of primary and metastastatic lung cancer suggesting that expression levels for Rsks may be useful biomarkers to follow the progression of this disease in patients. Moreover, it is conceivable that the development of isoform-specific Rsk inhibitors might provide novel therapeutic agents to prevent metastasis in lung cancer patients.

ANNEXES

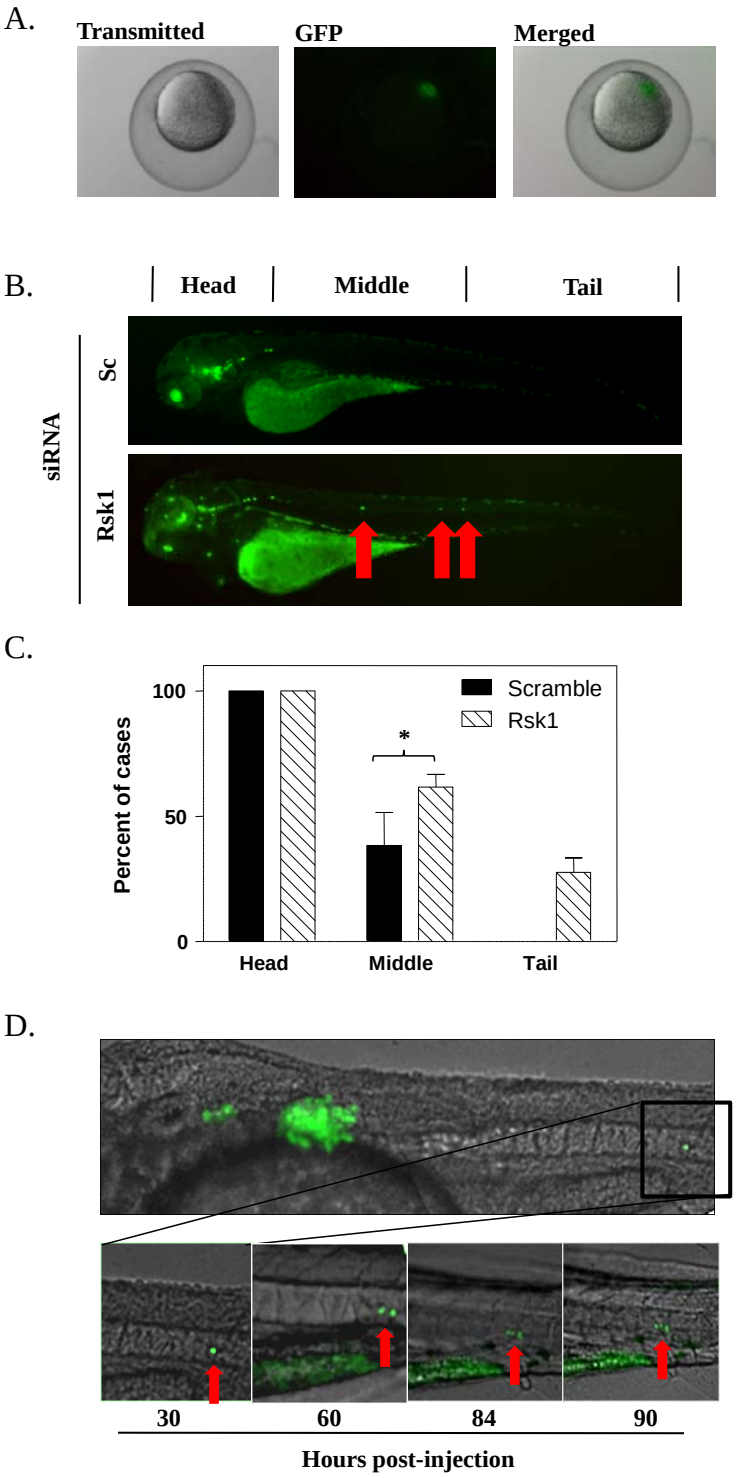

Annexe 1: Rsk1 silencing promotes metastasis in zebrafish. H2B-GFP expressing A549 cells were injected into zebrafish embryos 4 h post-fertilisation (hpf). (A) Representative picture showing injected cells in the cell mass of 4 hpf embryos. (B) Cells treated with Rsk1 or Scramble (Sc) RNAi were injected at 4 hpf. Representative fish (from n=120 per condition) are shown at 48 hpf. Red arrows point to single invading cells. (C) Quantification of invasion from fish injected as in (B). Percent of cases refers to presence or absence of tumour cell in the "Head", "Middle" or "Tail" compartment as indicated in (B). n=120 per condition. *; $p<0.05$ (t-test). (C) Representative fish injected with H2B-GFP A549 cells imaged at the indicated time points. Lower panels show detail of single invading cell dividing.

REFERENCES

1. Ferlay J SH, Bray F, Forman D, Mathers C and Parkin DM. (2010) GLOBOCAN 2008, Cancer Incidence and Mortality Worldwide: IARC CancerBase No. 10.

2. Truong T, *et al.* (2010) Replication of lung cancer susceptibility loci at chromosomes 15q25, 5p15, and 6p21: a pooled analysis from the International Lung Cancer Consortium. *J Natl Cancer Inst* 102(13):959-971.

3. Sambamoorthi U & McAlpine DD (2003) Racial, ethnic, socioeconomic, and access disparities in the use of preventive services among women. *Prev Med* 37(5):475-484.

4. Valsecchi MG & Steliarova-Foucher E (2008) Cancer registration in developing countries: luxury or necessity? *Lancet Oncol* 9(2):159-167.

5. Infobase WG (2010) The Impact of Cancer In United Kingdom

6. Mathers CD & Loncar D (2006) Projections of global mortality and burden of disease from 2002 to 2030. *PLoS Med* 3(11):e442.

7. Knowles MA & Selby P (2005) *Introduction to the cellular and molecular biology of cancer* (Oxford University Press, New York) pp xvii, 532 p.

8. Yurchenco PD & O'Rear JJ (1994) Basal lamina assembly. *Curr Opin Cell Biol* 6(5):674-681.

9. Hay ED (1991) *Cell biology of extracellular matrix* (Plenum Press, New York) 2nd Ed pp xvii, 468 p.

10. Mu\ller J & West CMD (1840) *On the Nature and Structural Characteristics of Cancer, and of those morbid growths which may be confounded with it ... Translated from the German, with notes, by C. West. Illustrated with numerous steel plates and wood-engravings* (Pt. 1. London) p 8º.

11. Hanahan D & Weinberg RA (2000) The hallmarks of cancer. *Cell* 100(1):57-70.

12. Husemann Y, *et al.* (2008) Systemic spread is an early step in breast cancer. *Cancer cell* 13(1):58-68.

13. Briasoulis E & Pavlidis N (1997) Cancer of Unknown Primary Origin. *Oncologist* 2(3):142-152.

14. Friedl P & Gilmour D (2009) Collective cell migration in morphogenesis, regeneration and cancer. *Nature reviews* 10(7):445-457.

15. Thiery JP, Acloque H, Huang RY, & Nieto MA (2009) Epithelial-mesenchymal transitions in development and disease. *Cell* 139(5):871-890.

16. Mani SA, *et al.* (2008) The epithelial-mesenchymal transition generates cells with properties of stem cells. *Cell* 133(4):704-715.

17. Batlle E, *et al.* (2000) The transcription factor snail is a repressor of E-cadherin gene expression in epithelial tumour cells. *Nature cell biology* 2(2):84-89.

18. Briegel KJ (2006) Embryonic transcription factors in human breast cancer. *IUBMB Life* 58(3):123-132.

19. Peinado H, Olmeda D, & Cano A (2007) Snail, Zeb and bHLH factors in tumour progression: an alliance against the epithelial phenotype? *Nat Rev Cancer* 7(6):415-428.

20. Shih JY, *et al.* (2005) Transcription repressor slug promotes carcinoma invasion and predicts outcome of patients with lung adenocarcinoma. *Clin Cancer Res* 11(22):8070-8078.

21. Al-Hajj M, Wicha MS, Benito-Hernandez A, Morrison SJ, & Clarke MF (2003) Prospective identification of tumorigenic breast cancer cells. *Proceedings of the National Academy of Sciences of the United States of America* 100(7):3983-3988.

22. Lim SC (2005) CD24 and human carcinoma: tumor biological aspects. *Biomed Pharmacother* 59 Suppl 2:S351-354.

23. Kristiansen G, *et al.* (2003) CD24 is an independent prognostic marker of survival in nonsmall cell lung cancer patients. *Br J Cancer* 88(2):231-236.

24. Kristiansen G, *et al.* (2003) CD24 expression is a new prognostic marker in breast cancer. *Clin Cancer Res* 9(13):4906-4913.

25. Kristiansen G, *et al.* (2004) CD24 expression is a significant predictor of PSA relapse and poor prognosis in low grade or organ confined prostate cancer. *Prostate* 58(2):183-192.

26. Jacob J, *et al.* (2004) Expression of CD24 in adenocarcinomas of the pancreas correlates with higher tumor grades. *Pancreatology* 4(5):454-460.

27. Weichert W, *et al.* (2005) Cytoplasmic CD24 expression in colorectal cancer independently correlates with shortened patient survival. *Clin Cancer Res* 11(18):6574-6581.

28. Ponta H, Sherman L, & Herrlich PA (2003) CD44: from adhesion molecules to signalling regulators. *Nature reviews* 4(1):33-45.

29. Gunthert U, *et al.* (1991) A new variant of glycoprotein CD44 confers metastatic potential to rat carcinoma cells. *Cell* 65(1):13-24.

30. Kim H, Yang XL, Rosada C, Hamilton SR, & August JT (1994) CD44 expression in colorectal adenomas is an early event occurring prior to K-ras and p53 gene mutation. *Arch Biochem Biophys* 310(2):504-507.

31. Wielenga VJ, *et al.* (1993) Expression of CD44 variant proteins in human colorectal cancer is related to tumor progression. *Cancer research* 53(20):4754-4756.

32. Wielenga VJ, *et al.* (1999) Expression of CD44 in Apc and Tcf mutant mice implies regulation by the WNT pathway. *Am J Pathol* 154(2):515-523.

33. Shtivelman E & Bishop JM (1991) Expression of CD44 is repressed in neuroblastoma cells. *Molecular and cellular biology* 11(11):5446-5453.

34. De Marzo AM, Bradshaw C, Sauvageot J, Epstein JI, & Miller GJ (1998) CD44 and CD44v6 downregulation in clinical prostatic carcinoma: relation to Gleason grade and cytoarchitecture. *Prostate* 34(3):162-168.

35. Gao AC, Lou W, Dong JT, & Isaacs JT (1997) CD44 is a metastasis suppressor gene for prostatic cancer located on human chromosome 11p13. *Cancer research* 57(5):846-849.

36. Ilina O & Friedl P (2009) Mechanisms of collective cell migration at a glance. *Journal of cell science* 122(Pt 18):3203-3208.

37. Hart IR (2009) New evidence for tumour embolism as a mode of metastasis. *J Pathol* 219(3):275-276.

38. Kats-Ugurlu G, *et al.* (2009) Circulating tumour tissue fragments in patients with pulmonary metastasis of clear cell renal cell carcinoma. *J Pathol* 219(3):287-293.

39. Prall F (2007) Tumour budding in colorectal carcinoma. *Histopathology* 50(1):151-162.

40. Wicki A, *et al.* (2006) Tumor invasion in the absence of epithelial-mesenchymal transition: podoplanin-mediated remodeling of the actin cytoskeleton. *Cancer cell* 9(4):261-272.

41. Kato Y, *et al.* (2005) Enhanced expression of Aggrus (T1alpha/podoplanin), a platelet-aggregation-inducing factor in lung squamous cell carcinoma. *Tumour Biol* 26(4):195-200.

42. Chuang WY, *et al.* (2009) Tumor cell expression of podoplanin correlates with nodal metastasis in esophageal squamous cell carcinoma. *Histol Histopathol* 24(8):1021-1027.

43. Makinen T, Norrmen C, & Petrova TV (2007) Molecular mechanisms of lymphatic vascular development. *Cell Mol Life Sci* 64(15):1915-1929.

44. Friedl P & Wolf K (2010) Plasticity of cell migration: a multiscale tuning model. *The Journal of cell biology* 188(1):11-19.

45. Wolf K, *et al.* (2007) Multi-step pericellular proteolysis controls the transition from individual to collective cancer cell invasion. *Nature cell biology* 9(8):893-904.

46. Rowe RG & Weiss SJ (2008) Breaching the basement membrane: who, when and how? *Trends in cell biology* 18(11):560-574.

47. Rowe RG & Weiss SJ (2009) Navigating ECM barriers at the invasive front: the cancer cell-stroma interface. *Annual review of cell and developmental biology* 25:567-595.

48. Wolf K, *et al.* (2009) Collagen-based cell migration models in vitro and in vivo. *Semin Cell Dev Biol* 20(8):931-941.

49. Harley BA, *et al.* (2008) Microarchitecture of three-dimensional scaffolds influences cell migration behavior via junction interactions. *Biophys J* 95(8):4013-4024.

50. Condeelis J & Pollard JW (2006) Macrophages: obligate partners for tumor cell migration, invasion, and metastasis. *Cell* 124(2):263-266.

51. Gaggioli C, *et al.* (2007) Fibroblast-led collective invasion of carcinoma cells with differing roles for RhoGTPases in leading and following cells. *Nature cell biology* 9(12):1392-1400.

52. Wyckoff JB, *et al.* (2007) Direct visualization of macrophage-assisted tumor cell intravasation in mammary tumors. *Cancer research* 67(6):2649-2656.

53. Bacac M & Stamenkovic I (2008) Metastatic cancer cell. *Annu Rev Pathol* 3:221-247.

54. Davidson B (2004) Malignant effusions: from diagnosis to biology. *Diagn Cytopathol* 31(4):246-254.

55. Gazdar AF, Gao B, & Minna JD (2010) Lung cancer cell lines: Useless artifacts or invaluable tools for medical science? *Lung cancer (Amsterdam, Netherlands)* 68(3):309-318.

56. Weidner N, Carroll PR, Flax J, Blumenfeld W, & Folkman J (1993) Tumor angiogenesis correlates with metastasis in invasive prostate carcinoma. *Am J Pathol* 143(2):401-409.

57. Sundar SS & Ganesan TS (2007) Role of lymphangiogenesis in cancer. *J Clin Oncol* 25(27):4298-4307.

58. Cady B (2007) Regional lymph node metastases; a singular manifestation of the process of clinical metastases in cancer: contemporary animal research and clinical reports suggest unifying concepts. *Ann Surg Oncol* 14(6):1790-1800.

59. Stoletov K, Montel V, Lester RD, Gonias SL, & Klemke R (2007) High-resolution imaging of the dynamic tumor cell vascular interface in transparent zebrafish. *Proceedings of the National Academy of Sciences of the United States of America* 104(44):17406-17411.

60. Kufe DW, Holland JF, Frei E, & American Cancer Society. (2003) *Cancer medicine 6* (BC Decker, Hamilton, Ont. ; Lewiston, NY) 6th Ed pp 2 v. (xxiv, 2699, 2640 p.).

61. Liu MC, *et al.* (2009) Circulating tumor cells: a useful predictor of treatment efficacy in metastatic breast cancer. *J Clin Oncol* 27(31):5153-5159.

62. Cristofanilli M, *et al.* (2005) Circulating tumor cells: a novel prognostic factor for newly diagnosed metastatic breast cancer. *J Clin Oncol* 23(7):1420-1430.

63. Frisch SM & Francis H (1994) Disruption of epithelial cell-matrix interactions induces apoptosis. *The Journal of cell biology* 124(4):619-626.

64. Meredith JE, Jr., Fazeli B, & Schwartz MA (1993) The extracellular matrix as a cell survival factor. *Molecular biology of the cell* 4(9):953-961.

65. Frisch SM & Ruoslahti E (1997) Integrins and anoikis. *Curr Opin Cell Biol* 9(5):701-706.

66. Kroemer G, Dallaporta B, & Resche-Rigon M (1998) The mitochondrial death/life regulator in apoptosis and necrosis. *Annu Rev Physiol* 60:619-642.

67. Taylor RC, Cullen SP, & Martin SJ (2008) Apoptosis: controlled demolition at the cellular level. *Nature reviews* 9(3):231-241.

68. Gilmore AP (2005) Anoikis. *Cell Death Differ* 12 Suppl 2:1473-1477.

69. Douma S, *et al.* (2004) Suppression of anoikis and induction of metastasis by the neurotrophic receptor TrkB. *Nature* 430(7003):1034-1039.

70. Geiger TR & Peeper DS (2007) Critical role for TrkB kinase function in anoikis suppression, tumorigenesis, and metastasis. *Cancer research* 67(13):6221-6229.

71. Geiger TR & Peeper DS (2005) The neurotrophic receptor TrkB in anoikis resistance and metastasis: a perspective. *Cancer research* 65(16):7033-7036.

72. Ewing J (1928) *Neoplastic diseases; a treatise on tumors* (W.B. Saunders, Philadelphia, London,) 3d ed rev. and enl., with 546 illustrations. Ed p 1127 p.

73. Paget S (1989) The distribution of secondary growths in cancer of the breast. 1889. *Cancer Metastasis Rev* 8(2):98-101.

74. Hart IR & Fidler IJ (1980) Role of organ selectivity in the determination of metastatic patterns of B16 melanoma. *Cancer research* 40(7):2281-2287.

75. Borsig L, Wong R, Hynes RO, Varki NM, & Varki A (2002) Synergistic effects of L- and P-selectin in facilitating tumor metastasis can involve non-mucin ligands and implicate leukocytes as enhancers of metastasis. *Proceedings of the National Academy of Sciences of the United States of America* 99(4):2193-2198.

76. Erpenbeck L & Schon MP (2010) Deadly allies: the fatal interplay between platelets and metastasizing cancer cells. *Blood* 115(17):3427-3436.

77. Al-Mehdi AB, *et al.* (2000) Intravascular origin of metastasis from the proliferation of endothelium-attached tumor cells: a new model for metastasis. *Nat Med* 6(1):100-102.

78. Fokas E, Engenhart-Cabillic R, Daniilidis K, Rose F, & An HX (2007) Metastasis: the seed and soil theory gains identity. *Cancer Metastasis Rev* 26(3-4):705-715.

79. Sun YX, *et al.* (2005) Skeletal localization and neutralization of the SDF-1(CXCL12)/CXCR4 axis blocks prostate cancer metastasis and growth in osseous sites in vivo. *J Bone Miner Res* 20(2):318-329.

80. Hwang RF, *et al.* (2003) Inhibition of platelet-derived growth factor receptor phosphorylation by STI571 (Gleevec) reduces growth and metastasis of human

pancreatic carcinoma in an orthotopic nude mouse model. *Clin Cancer Res* 9(17):6534-6544.

81. Zhang T, *et al.* (2005) Overexpression of platelet-derived growth factor receptor alpha in endothelial cells of hepatocellular carcinoma associated with high metastatic potential. *Clin Cancer Res* 11(24 Pt 1):8557-8563.

82. Ridley AJ, *et al.* (2003) Cell migration: integrating signals from front to back. *Science (New York, N.Y* 302(5651):1704-1709.

83. Fraley SI, *et al.* (2010) A distinctive role for focal adhesion proteins in three-dimensional cell motility. *Nature cell biology* 12(6):598-604.

84. Lammermann T & Sixt M (2009) Mechanical modes of 'amoeboid' cell migration. *Curr Opin Cell Biol* 21(5):636-644.

85. Sanz-Moreno V, *et al.* (2008) Rac activation and inactivation control plasticity of tumor cell movement. *Cell* 135(3):510-523.

86. Yoshida K & Soldati T (2006) Dissection of amoeboid movement into two mechanically distinct modes. *Journal of cell science* 119(Pt 18):3833-3844.

87. Condeelis J & Segall JE (2003) Intravital imaging of cell movement in tumours. *Nat Rev Cancer* 3(12):921-930.

88. Maghazachi AA (2000) Intracellular signaling events at the leading edge of migrating cells. *Int J Biochem Cell Biol* 32(9):931-943.

89. Gupton SL & Waterman-Storer CM (2006) Spatiotemporal feedback between actomyosin and focal-adhesion systems optimizes rapid cell migration. *Cell* 125(7):1361-1374.

90. Wang W, *et al.* (2004) Identification and testing of a gene expression signature of invasive carcinoma cells within primary mammary tumors. *Cancer research* 64(23):8585-8594.

91. Pollard TD & Borisy GG (2003) Cellular motility driven by assembly and disassembly of actin filaments. *Cell* 112(4):453-465.

92. Insall RH & Machesky LM (2009) Actin dynamics at the leading edge: from simple machinery to complex networks. *Developmental cell* 17(3):310-322.

93. Urban E, Jacob S, Nemethova M, Resch GP, & Small JV (2010) Electron tomography reveals unbranched networks of actin filaments in lamellipodia. *Nature cell biology* 12(5):429-435.

94. Welch MD (1999) The world according to Arp: regulation of actin nucleation by the Arp2/3 complex. *Trends in cell biology* 9(11):423-427.

95. Ochs HD & Thrasher AJ (2006) The Wiskott-Aldrich syndrome. *J Allergy Clin Immunol* 117(4):725-738; quiz 739.

96. Weaver AM, Young ME, Lee WL, & Cooper JA (2003) Integration of signals to the Arp2/3 complex. *Curr Opin Cell Biol* 15(1):23-30.

97. Kovar DR (2006) Molecular details of formin-mediated actin assembly. *Curr Opin Cell Biol* 18(1):11-17.

98. Kovar DR & Pollard TD (2004) Insertional assembly of actin filament barbed ends in association with formins produces piconewton forces. *Proceedings of the National Academy of Sciences of the United States of America* 101(41):14725-14730.

99. Romero S, *et al.* (2004) Formin is a processive motor that requires profilin to accelerate actin assembly and associated ATP hydrolysis. *Cell* 119(3):419-429.

100. Kwiatkowski DJ & Bruns GA (1988) Human profilin. Molecular cloning, sequence comparison, and chromosomal analysis. *The Journal of biological chemistry* 263(12):5910-5915.

101. Honore B, Madsen P, Andersen AH, & Leffers H (1993) Cloning and expression of a novel human profilin variant, profilin II. *FEBS Lett* 330(2):151-155.

102. Witke W, *et al.* (1998) In mouse brain profilin I and profilin II associate with regulators of the endocytic pathway and actin assembly. *The EMBO journal* 17(4):967-976.

103. Braun A, *et al.* (2002) Genomic organization of profilin-III and evidence for a transcript expressed exclusively in testis. *Gene* 283(1-2):219-225.

104. Behnen M, *et al.* (2009) Testis-expressed profilins 3 and 4 show distinct functional characteristics and localize in the acroplaxome-manchette complex in spermatids. *BMC Cell Biol* 10:34.

105. Kursula P, *et al.* (2008) High-resolution structural analysis of mammalian profilin 2a complex formation with two physiological ligands: the formin homology 1 domain of mDia1 and the proline-rich domain of VASP. *J Mol Biol* 375(1):270-290.

106. Yang C, *et al.* (2000) Profilin enhances Cdc42-induced nucleation of actin polymerization. *The Journal of cell biology* 150(5):1001-1012.

107. Krause M, Dent EW, Bear JE, Loureiro JJ, & Gertler FB (2003) Ena/VASP proteins: regulators of the actin cytoskeleton and cell migration. *Annual review of cell and developmental biology* 19:541-564.

108. dos Remedios CG, *et al.* (2003) Actin binding proteins: regulation of cytoskeletal microfilaments. *Physiol Rev* 83(2):433-473.

109. Oser M & Condeelis J (2009) The cofilin activity cycle in lamellipodia and invadopodia. *J Cell Biochem* 108(6):1252-1262.

110. Carlier MF, *et al.* (1997) Actin depolymerizing factor (ADF/cofilin) enhances the rate of filament turnover: implication in actin-based motility. *The Journal of cell biology* 136(6):1307-1322.

111. Kiuchi T, Ohashi K, Kurita S, & Mizuno K (2007) Cofilin promotes stimulus-induced lamellipodium formation by generating an abundant supply of actin monomers. *The Journal of cell biology* 177(3):465-476.

112. Ichetovkin I, Grant W, & Condeelis J (2002) Cofilin produces newly polymerized actin filaments that are preferred for dendritic nucleation by the Arp2/3 complex. *Curr Biol* 12(1):79-84.

113. DesMarais V, Ghosh M, Eddy R, & Condeelis J (2005) Cofilin takes the lead. *Journal of cell science* 118(Pt 1):19-26.

114. Mouneimne G, *et al.* (2004) Phospholipase C and cofilin are required for carcinoma cell directionality in response to EGF stimulation. *The Journal of cell biology* 166(5):697-708.

115. Mouneimne G, *et al.* (2006) Spatial and temporal control of cofilin activity is required for directional sensing during chemotaxis. *Curr Biol* 16(22):2193-2205.

116. Gorbatyuk VY, *et al.* (2006) Mapping the phosphoinositide-binding site on chick cofilin explains how PIP2 regulates the cofilin-actin interaction. *Molecular cell* 24(4):511-522.

117. Arber S, *et al.* (1998) Regulation of actin dynamics through phosphorylation of cofilin by LIM-kinase. *Nature* 393(6687):805-809.

118. Wang W, Eddy R, & Condeelis J (2007) The cofilin pathway in breast cancer invasion and metastasis. *Nat Rev Cancer* 7(6):429-440.

119. Beningo KA, Dembo M, Kaverina I, Small JV, & Wang YL (2001) Nascent focal adhesions are responsible for the generation of strong propulsive forces in migrating fibroblasts. *The Journal of cell biology* 153(4):881-888.

120. Rodriguez OC, *et al.* (2003) Conserved microtubule-actin interactions in cell movement and morphogenesis. *Nature cell biology* 5(7):599-609.

121. Small JV, Geiger B, Kaverina I, & Bershadsky A (2002) How do microtubules guide migrating cells? *Nature reviews* 3(12):957-964.

122. Etienne-Manneville S & Hall A (2003) Cell polarity: Par6, aPKC and cytoskeletal crosstalk. *Curr Opin Cell Biol* 15(1):67-72.

123. Howard J & Hyman AA (2009) Growth, fluctuation and switching at microtubule plus ends. *Nature reviews* 10(8):569-574.

124. Akhmanova A & Steinmetz MO (2008) Tracking the ends: a dynamic protein network controls the fate of microtubule tips. *Nature reviews* 9(4):309-322.

125. Ezratty EJ, Partridge MA, & Gundersen GG (2005) Microtubule-induced focal adhesion disassembly is mediated by dynamin and focal adhesion kinase. *Nature cell biology* 7(6):581-590.

126. Kaverina I, *et al.* (2000) Enforced polarisation and locomotion of fibroblasts lacking microtubules. *Curr Biol* 10(12):739-742.

127. Enomoto T (1996) Microtubule disruption induces the formation of actin stress fibers and focal adhesions in cultured cells: possible involvement of the rho signal cascade. *Cell Struct Funct* 21(5):317-326.

128. Arnaout MA, Goodman SL, & Xiong JP (2007) Structure and mechanics of integrin-based cell adhesion. *Curr Opin Cell Biol* 19(5):495-507.

129. Webb DJ, *et al.* (2004) FAK-Src signalling through paxillin, ERK and MLCK regulates adhesion disassembly. *Nature cell biology* 6(2):154-161.

130. Zaidel-Bar R, Itzkovitz S, Ma'ayan A, Iyengar R, & Geiger B (2007) Functional atlas of the integrin adhesome. *Nature cell biology* 9(8):858-867.

131. Zaidel-Bar R, Ballestrem C, Kam Z, & Geiger B (2003) Early molecular events in the assembly of matrix adhesions at the leading edge of migrating cells. *Journal of cell science* 116(Pt 22):4605-4613.

132. Zaidel-Bar R, Milo R, Kam Z, & Geiger B (2007) A paxillin tyrosine phosphorylation switch regulates the assembly and form of cell-matrix adhesions. *Journal of cell science* 120(Pt 1):137-148.

133. Franco SJ, *et al.* (2004) Calpain-mediated proteolysis of talin regulates adhesion dynamics. *Nature cell biology* 6(10):977-983.

134. Mitra SK, Hanson DA, & Schlaepfer DD (2005) Focal adhesion kinase: in command and control of cell motility. *Nature reviews* 6(1):56-68.

135. Etienne-Manneville S & Hall A (2002) Rho GTPases in cell biology. *Nature* 420(6916):629-635.

136. Fukata M, Nakagawa M, & Kaibuchi K (2003) Roles of Rho-family GTPases in cell polarisation and directional migration. *Curr Opin Cell Biol* 15(5):590-597.

137. Jaffe AB & Hall A (2005) Rho GTPases: biochemistry and biology. *Annual review of cell and developmental biology* 21:247-269.

138. Gomes ER, Jani S, & Gundersen GG (2005) Nuclear movement regulated by Cdc42, MRCK, myosin, and actin flow establishes MTOC polarization in migrating cells. *Cell* 121(3):451-463.

139. Higashi M, *et al.* (2009) Human Mena associates with Rac1 small GTPase in glioblastoma cell lines. *PLoS One* 4(3):e4765.

140. Philippar U, *et al.* (2008) A Mena invasion isoform potentiates EGF-induced carcinoma cell invasion and metastasis. *Developmental cell* 15(6):813-828.

141. Scott JA, *et al.* (2006) Ena/VASP proteins can regulate distinct modes of actin organization at cadherin-adhesive contacts. *Molecular biology of the cell* 17(3):1085-1095.

142. Drees F & Gertler FB (2008) Ena/VASP: proteins at the tip of the nervous system. *Current opinion in neurobiology* 18(1):53-59.

143. Trichet L, Sykes C, & Plastino J (2008) Relaxing the actin cytoskeleton for adhesion and movement with Ena/VASP. *The Journal of cell biology* 181(1):19-25.

144. Bear JE & Gertler FB (2009) Ena/VASP: towards resolving a pointed controversy at the barbed end. *Journal of cell science* 122(Pt 12):1947-1953.

145. Bachmann C, Fischer L, Walter U, & Reinhard M (1999) The EVH2 domain of the vasodilator-stimulated phosphoprotein mediates tetramerization, F-actin binding, and actin bundle formation. *The Journal of biological chemistry* 274(33):23549-23557.

146. Zimmermann J, *et al.* (2002) Relaxation, equilibrium oligomerization, and molecular symmetry of the VASP (336-380) EVH2 tetramer. *Biochemistry* 41(37):11143-11151.

147. Ahern-Djamali SM, *et al.* (1998) Mutations in Drosophila enabled and rescue by human vasodilator-stimulated phosphoprotein (VASP) indicate important functional roles for Ena/VASP homology domain 1 (EVH1) and EVH2 domains. *Molecular biology of the cell* 9(8):2157-2171.

148. Carl UD, *et al.* (1999) Aromatic and basic residues within the EVH1 domain of VASP specify its interaction with proline-rich ligands. *Curr Biol* 9(13):715-718.

149. Benz PM, *et al.* (2009) Differential VASP phosphorylation controls remodeling of the actin cytoskeleton. *Journal of cell science* 122(Pt 21):3954-3965.

150. Ball LJ, *et al.* (2000) Dual epitope recognition by the VASP EVH1 domain modulates polyproline ligand specificity and binding affinity. *The EMBO journal* 19(18):4903-4914.

151. Huttelmaier S, *et al.* (1998) The interaction of the cell-contact proteins VASP and vinculin is regulated by phosphatidylinositol-4,5-bisphosphate. *Curr Biol* 8(9):479-488.

152. Huttelmaier S, *et al.* (1999) Characterization of the actin binding properties of the vasodilator-stimulated phosphoprotein VASP. *FEBS Lett* 451(1):68-74.

153. Reinhard M, *et al.* (1995) The proline-rich focal adhesion and microfilament protein VASP is a ligand for profilins. *The EMBO journal* 14(8):1583-1589.

154. Harbeck B, Huttelmaier S, Schluter K, Jockusch BM, & Illenberger S (2000) Phosphorylation of the vasodilator-stimulated phosphoprotein regulates its interaction with actin. *The Journal of biological chemistry* 275(40):30817-30825.

155. Blume C, *et al.* (2007) AMP-activated protein kinase impairs endothelial actin cytoskeleton assembly by phosphorylating vasodilator-stimulated phosphoprotein. *The Journal of biological chemistry* 282(7):4601-4612.

156. Barzik M, *et al.* (2005) Ena/VASP proteins enhance actin polymerization in the presence of barbed end capping proteins. *The Journal of biological chemistry* 280(31):28653-28662.

157. Pasic L, Kotova T, & Schafer DA (2008) Ena/VASP proteins capture actin filament barbed ends. *The Journal of biological chemistry* 283(15):9814-9819.

158. Bear JE, *et al.* (2002) Antagonism between Ena/VASP proteins and actin filament capping regulates fibroblast motility. *Cell* 109(4):509-521.

159. Skoble J, Auerbuch V, Goley ED, Welch MD, & Portnoy DA (2001) Pivotal role of VASP in Arp2/3 complex-mediated actin nucleation, actin branch-

formation, and Listeria monocytogenes motility. *The Journal of cell biology* 155(1):89-100.

160. Applewhite DA, *et al.* (2007) Ena/VASP proteins have an anti-capping independent function in filopodia formation. *Molecular biology of the cell* 18(7):2579-2591.

161. Kuhnel K, *et al.* (2004) The VASP tetramerization domain is a right-handed coiled coil based on a 15-residue repeat. *Proceedings of the National Academy of Sciences of the United States of America* 101(49):17027-17032.

162. Ferron F, Rebowski G, Lee SH, & Dominguez R (2007) Structural basis for the recruitment of profilin-actin complexes during filament elongation by Ena/VASP. *The EMBO journal* 26(21):4597-4606.

163. Vasioukhin V, Bauer C, Yin M, & Fuchs E (2000) Directed actin polymerization is the driving force for epithelial cell-cell adhesion. *Cell* 100(2):209-219.

164. Worth DC, *et al.* (2010) Alpha v beta3 integrin spatially regulates VASP and RIAM to control adhesion dynamics and migration. *The Journal of cell biology* 189(2):369-383.

165. Kwiatkowski AV, *et al.* (2007) Ena/VASP Is Required for neuritogenesis in the developing cortex. *Neuron* 56(3):441-455.

166. Furman C, *et al.* (2007) Ena/VASP is required for endothelial barrier function in vivo. *The Journal of cell biology* 179(4):761-775.

167. Aszodi A, *et al.* (1999) The vasodilator-stimulated phosphoprotein (VASP) is involved in cGMP- and cAMP-mediated inhibition of agonist-induced platelet aggregation, but is dispensable for smooth muscle function. *The EMBO journal* 18(1):37-48.

168. Hauser W, *et al.* (1999) Megakaryocyte hyperplasia and enhanced agonist-induced platelet activation in vasodilator-stimulated phosphoprotein knockout mice. *Proceedings of the National Academy of Sciences of the United States of America* 96(14):8120-8125.

169. Lanier LM, *et al.* (1999) Mena is required for neurulation and commissure formation. *Neuron* 22(2):313-325.

170. Han G, *et al.* (2008) Positive regulation of migration and invasion by vasodilator-stimulated phosphoprotein via Rac1 pathway in human breast cancer cells. *Oncology reports* 20(4):929-939.

171. Toyoda A, *et al.* (2009) Aberrant expression of human ortholog of mammalian enabled (hMena) in human colorectal carcinomas: implications for its role in tumor progression. *International journal of oncology* 34(1):53-60.

172. Hu LD, Zou HF, Zhan SX, & Cao KM (2008) EVL (Ena/VASP-like) expression is up-regulated in human breast cancer and its relative expression level is correlated with clinical stages. *Oncology reports* 19(4):1015-1020.

173. Dertsiz L, *et al.* (2005) Differential expression of VASP in normal lung tissue and lung adenocarcinomas. *Thorax* 60(7):576-581.

174. Manning G, Whyte DB, Martinez R, Hunter T, & Sudarsanam S (2002) The protein kinase complement of the human genome. *Science (New York, N.Y* 298(5600):1912-1934.

175. Olsen JV, *et al.* (2006) Global, in vivo, and site-specific phosphorylation dynamics in signaling networks. *Cell* 127(3):635-648.

176. Ubersax JA & Ferrell JE, Jr. (2007) Mechanisms of specificity in protein phosphorylation. *Nature reviews* 8(7):530-541.

177. Rowley JD (1973) Letter: A new consistent chromosomal abnormality in chronic myelogenous leukaemia identified by quinacrine fluorescence and Giemsa staining. *Nature* 243(5405):290-293.

178. Pines G, Kostler WJ, & Yarden Y (2010) Oncogenic mutant forms of EGFR: lessons in signal transduction and targets for cancer therapy. *FEBS Lett* 584(12):2699-2706.

179. Bain J, *et al.* (2007) The selectivity of protein kinase inhibitors: a further update. *Biochem J* 408(3):297-315.

180. Marshall CJ (1995) Specificity of receptor tyrosine kinase signaling: transient versus sustained extracellular signal-regulated kinase activation. *Cell* 80(2):179-185.

181. Ballif BA & Blenis J (2001) Molecular mechanisms mediating mammalian mitogen-activated protein kinase (MAPK) kinase (MEK)-MAPK cell survival signals. *Cell Growth Differ* 12(8):397-408.

182. Kolch W (2005) Coordinating ERK/MAPK signalling through scaffolds and inhibitors. *Nature reviews* 6(11):827-837.

183. Downward J, Parker P, & Waterfield MD (1984) Autophosphorylation sites on the epidermal growth factor receptor. *Nature* 311(5985):483-485.

184. Schlessinger J (2000) Cell signaling by receptor tyrosine kinases. *Cell* 103(2):211-225.

185. Schlessinger J (2002) Ligand-induced, receptor-mediated dimerization and activation of EGF receptor. *Cell* 110(6):669-672.

186. Schlessinger J (1994) SH2/SH3 signaling proteins. *Curr Opin Genet Dev* 4(1):25-30.

187. Pawson T, Gish GD, & Nash P (2001) SH2 domains, interaction modules and cellular wiring. *Trends in cell biology* 11(12):504-511.

188. Rozakis-Adcock M, Fernley R, Wade J, Pawson T, & Bowtell D (1993) The SH2 and SH3 domains of mammalian Grb2 couple the EGF receptor to the Ras activator mSos1. *Nature* 363(6424):83-85.

189. Donovan S, Shannon KM, & Bollag G (2002) GTPase activating proteins: critical regulators of intracellular signaling. *Biochim Biophys Acta* 1602(1):23-45.

190. Downward J (2003) Targeting RAS signalling pathways in cancer therapy. *Nat Rev Cancer* 3(1):11-22.

191. Marais R, Light Y, Paterson HF, Mason CS, & Marshall CJ (1997) Differential regulation of Raf-1, A-Raf, and B-Raf by oncogenic ras and tyrosine kinases. *The Journal of biological chemistry* 272(7):4378-4383.

192. Weber CK, *et al.* (2000) Mitogenic signaling of Ras is regulated by differential interaction with Raf isozymes. *Oncogene* 19(2):169-176.

193. Wellbrock C, Karasarides M, & Marais R (2004) The RAF proteins take centre stage. *Nature reviews* 5(11):875-885.

194. Kolch W (2000) Meaningful relationships: the regulation of the Ras/Raf/MEK/ERK pathway by protein interactions. *Biochem J* 351 Pt 2:289-305.

195. Alessi DR, *et al.* (1994) Identification of the sites in MAP kinase kinase-1 phosphorylated by p74raf-1. *The EMBO journal* 13(7):1610-1619.

196. Jacobs D, Glossip D, Xing H, Muslin AJ, & Kornfeld K (1999) Multiple docking sites on substrate proteins form a modular system that mediates recognition by ERK MAP kinase. *Genes Dev* 13(2):163-175.

197. Roux PP & Blenis J (2004) ERK and p38 MAPK-activated protein kinases: a family of protein kinases with diverse biological functions. *Microbiol Mol Biol Rev* 68(2):320-344.

198. Tanoue T & Nishida E (2003) Molecular recognitions in the MAP kinase cascades. *Cellular signalling* 15(5):455-462.

199. Fantl WJ, Johnson DE, & Williams LT (1993) Signalling by receptor tyrosine kinases. *Annu Rev Biochem* 62:453-481.

200. Shin S, Dimitri CA, Yoon SO, Dowdle W, & Blenis J (2010) ERK2 but not ERK1 induces epithelial-to-mesenchymal transformation via DEF motif-dependent signaling events. *Molecular cell* 38(1):114-127.

201. Santos SD, Verveer PJ, & Bastiaens PI (2007) Growth factor-induced MAPK network topology shapes Erk response determining PC-12 cell fate. *Nature cell biology* 9(3):324-330.

202. Markevich NI, Hoek JB, & Kholodenko BN (2004) Signaling switches and bistability arising from multisite phosphorylation in protein kinase cascades. *The Journal of cell biology* 164(3):353-359.

203. Owens DM & Keyse SM (2007) Differential regulation of MAP kinase signalling by dual-specificity protein phosphatases. *Oncogene* 26(22):3203-3213.

204. Pratilas CA, *et al.* (2009) (V600E)BRAF is associated with disabled feedback inhibition of RAF-MEK signaling and elevated transcriptional output of the pathway. *Proceedings of the National Academy of Sciences of the United States of America* 106(11):4519-4524.

205. Hoshino R, *et al.* (1999) Constitutive activation of the 41-/43-kDa mitogen-activated protein kinase signaling pathway in human tumors. *Oncogene* 18(3):813-822.

206. Ding L, *et al.* (2008) Somatic mutations affect key pathways in lung adenocarcinoma. *Nature* 455(7216):1069-1075.

207. Karnoub AE & Weinberg RA (2008) Ras oncogenes: split personalities. *Nature reviews* 9(7):517-531.

208. Rodriguez-Viciana P, *et al.* (1994) Phosphatidylinositol-3-OH kinase as a direct target of Ras. *Nature* 370(6490):527-532.

209. Warne PH, Viciana PR, & Downward J (1993) Direct interaction of Ras and the amino-terminal region of Raf-1 in vitro. *Nature* 364(6435):352-355.

210. Kelley GG, Reks SE, Ondrako JM, & Smrcka AV (2001) Phospholipase C(epsilon): a novel Ras effector. *The EMBO journal* 20(4):743-754.

211. Lambert JM, *et al.* (2002) Tiam1 mediates Ras activation of Rac by a PI(3)K-independent mechanism. *Nature cell biology* 4(8):621-625.

212. Shields JM, Pruitt K, McFall A, Shaub A, & Der CJ (2000) Understanding Ras: 'it ain't over 'til it's over'. *Trends in cell biology* 10(4):147-154.

213. Weiss B, Bollag G, & Shannon K (1999) Hyperactive Ras as a therapeutic target in neurofibromatosis type 1. *Am J Med Genet* 89(1):14-22.

214. Lee W, *et al.* (2010) The mutation spectrum revealed by paired genome sequences from a lung cancer patient. *Nature* 465(7297):473-477.

215. Lowe DG, *et al.* (1987) Structure of the human and murine R-ras genes, novel genes closely related to ras proto-oncogenes. *Cell* 48(1):137-146.

216. Reuther GW & Der CJ (2000) The Ras branch of small GTPases: Ras family members don't fall far from the tree. *Curr Opin Cell Biol* 12(2):157-165.

217. Marte BM, Rodriguez-Viciana P, Wennstrom S, Warne PH, & Downward J (1997) R-Ras can activate the phosphoinositide 3-kinase but not the MAP kinase arm of the Ras effector pathways. *Curr Biol* 7(1):63-70.

218. Self AJ, Caron E, Paterson HF, & Hall A (2001) Analysis of R-Ras signalling pathways. *Journal of cell science* 114(Pt 7):1357-1366.

219. Gotoh T, *et al.* (1997) Activation of R-Ras by Ras-guanine nucleotide-releasing factor. *The Journal of biological chemistry* 272(30):18602-18607.

220. Zhang Z, Vuori K, Wang H, Reed JC, & Ruoslahti E (1996) Integrin activation by R-ras. *Cell* 85(1):61-69.

221. Sethi T, Ginsberg MH, Downward J, & Hughes PE (1999) The small GTP-binding protein R-Ras can influence integrin activation by antagonizing a Ras/Raf-initiated integrin suppression pathway. *Molecular biology of the cell* 10(6):1799-1809.

222. Holly SP, Larson MK, & Parise LV (2005) The unique N-terminus of R-ras is required for Rac activation and precise regulation of cell migration. *Molecular biology of the cell* 16(5):2458-2469.

223. Mora N, Rosales R, & Rosales C (2007) R-Ras promotes metastasis of cervical cancer epithelial cells. *Cancer Immunol Immunother* 56(4):535-544.

224. Fehrenbacher N, Bar-Sagi D, & Philips M (2009) Ras/MAPK signaling from endomembranes. *Mol Oncol* 3(4):297-307.

225. Bivona TG, *et al.* (2006) PKC regulates a farnesyl-electrostatic switch on K-Ras that promotes its association with Bcl-XL on mitochondria and induces apoptosis. *Molecular cell* 21(4):481-493.

226. Fivaz M & Meyer T (2005) Reversible intracellular translocation of KRas but not HRas in hippocampal neurons regulated by Ca2+/calmodulin. *The Journal of cell biology* 170(3):429-441.

227. Chiu VK, *et al.* (2002) Ras signalling on the endoplasmic reticulum and the Golgi. *Nature cell biology* 4(5):343-350.

228. Oertli B, *et al.* (2000) The effector loop and prenylation site of R-Ras are involved in the regulation of integrin function. *Oncogene* 19(43):4961-4969.

229. Liu P, Cheng H, Roberts TM, & Zhao JJ (2009) Targeting the phosphoinositide 3-kinase pathway in cancer. *Nat Rev Drug Discov* 8(8):627-644.

230. Cantley LC (2002) The phosphoinositide 3-kinase pathway. *Science (New York, N.Y* 296(5573):1655-1657.

231. Gupta S, *et al.* (2007) Binding of ras to phosphoinositide 3-kinase p110alpha is required for ras-driven tumorigenesis in mice. *Cell* 129(5):957-968.

232. Hawkins PT, Jackson TR, & Stephens LR (1992) Platelet-derived growth factor stimulates synthesis of PtdIns(3,4,5)P3 by activating a PtdIns(4,5)P2 3-OH kinase. *Nature* 358(6382):157-159.

233. Maehama T & Dixon JE (1998) The tumor suppressor, PTEN/MMAC1, dephosphorylates the lipid second messenger, phosphatidylinositol 3,4,5-trisphosphate. *The Journal of biological chemistry* 273(22):13375-13378.

234. Pearce LR, Komander D, & Alessi DR (2010) The nuts and bolts of AGC protein kinases. *Nature reviews* 11(1):9-22.

235. Salmena L, Carracedo A, & Pandolfi PP (2008) Tenets of PTEN tumor suppression. *Cell* 133(3):403-414.

236. Cully M, You H, Levine AJ, & Mak TW (2006) Beyond PTEN mutations: the PI3K pathway as an integrator of multiple inputs during tumorigenesis. *Nat Rev Cancer* 6(3):184-192.

237. Alessi DR, *et al.* (1997) Characterization of a 3-phosphoinositide-dependent protein kinase which phosphorylates and activates protein kinase Balpha. *Curr Biol* 7(4):261-269.

238. Dufner A & Thomas G (1999) Ribosomal S6 kinase signaling and the control of translation. *Experimental cell research* 253(1):100-109.

239. Jensen CJ, *et al.* (1999) 90-kDa ribosomal S6 kinase is phosphorylated and activated by 3-phosphoinositide-dependent protein kinase-1. *The Journal of biological chemistry* 274(38):27168-27176.

240. Guertin DA & Sabatini DM (2007) Defining the role of mTOR in cancer. *Cancer cell* 12(1):9-22.

241. Laplante M & Sabatini DM (2009) mTOR signaling at a glance. *Journal of cell science* 122(Pt 20):3589-3594.

242. Vander Haar E, Lee SI, Bandhakavi S, Griffin TJ, & Kim DH (2007) Insulin signalling to mTOR mediated by the Akt/PKB substrate PRAS40. *Nature cell biology* 9(3):316-323.

243. Wang L, Harris TE, Roth RA, & Lawrence JC, Jr. (2007) PRAS40 regulates mTORC1 kinase activity by functioning as a direct inhibitor of substrate binding. *The Journal of biological chemistry* 282(27):20036-20044.

244. Inoki K, Li Y, Zhu T, Wu J, & Guan KL (2002) TSC2 is phosphorylated and inhibited by Akt and suppresses mTOR signalling. *Nature cell biology* 4(9):648-657.

245. Isotani S, *et al.* (1999) Immunopurified mammalian target of rapamycin phosphorylates and activates p70 S6 kinase alpha in vitro. *The Journal of biological chemistry* 274(48):34493-34498.

246. Duvel K, *et al.* (2010) Activation of a metabolic gene regulatory network downstream of mTOR complex 1. *Molecular cell* 39(2):171-183.

247. Sarbassov DD, Guertin DA, Ali SM, & Sabatini DM (2005) Phosphorylation and regulation of Akt/PKB by the rictor-mTOR complex. *Science (New York, N.Y* 307(5712):1098-1101.

248. Garcia-Martinez JM & Alessi DR (2008) mTOR complex 2 (mTORC2) controls hydrophobic motif phosphorylation and activation of serum- and glucocorticoid-induced protein kinase 1 (SGK1). *Biochem J* 416(3):375-385.

249. Enomoto A, *et al.* (2005) Akt/PKB regulates actin organization and cell motility via Girdin/APE. *Developmental cell* 9(3):389-402.

250. Li J, *et al.* (2005) Phosphorylation of ACAP1 by Akt regulates the stimulation-dependent recycling of integrin beta1 to control cell migration. *Developmental cell* 9(5):663-673.

251. Anjum R & Blenis J (2008) The RSK family of kinases: emerging roles in cellular signalling. *Nature reviews* 9(10):747-758.

252. Smith JA, *et al.* (2005) Identification of the first specific inhibitor of p90 ribosomal S6 kinase (RSK) reveals an unexpected role for RSK in cancer cell proliferation. *Cancer research* 65(3):1027-1034.

253. Clark DE, *et al.* (2005) The serine/threonine protein kinase, p90 ribosomal S6 kinase, is an important regulator of prostate cancer cell proliferation. *Cancer research* 65(8):3108-3116.

254. Cho YY, *et al.* (2007) Ribosomal S6 kinase 2 is a key regulator in tumor promoter induced cell transformation. *Cancer research* 67(17):8104-8112.

255. Kang S, *et al.* (2007) FGFR3 activates RSK2 to mediate hematopoietic transformation through tyrosine phosphorylation of RSK2 and activation of the MEK/ERK pathway. *Cancer cell* 12(3):201-214.

256. Kang S, *et al.* (2010) p90 ribosomal S6 kinase 2 promotes invasion and metastasis of human head and neck squamous cell carcinoma cells. *J Clin Invest* 120(4):1165-1177.

257. Blenis J & Erikson RL (1984) Phosphorylation of the ribosomal protein S6 is elevated in cells transformed by a variety of tumor viruses. *J Virol* 50(3):966-969.

258. Nielsen PJ, Thomas G, & Maller JL (1982) Increased phosphorylation of ribosomal protein S6 during meiotic maturation of Xenopus oocytes. *Proceedings of the National Academy of Sciences of the United States of America* 79(9):2937-2941.

259. Jones SW, Erikson E, Blenis J, Maller JL, & Erikson RL (1988) A Xenopus ribosomal protein S6 kinase has two apparent kinase domains that are each similar to distinct protein kinases. *Proceedings of the National Academy of Sciences of the United States of America* 85(10):3377-3381.

260. Roux PP, Richards SA, & Blenis J (2003) Phosphorylation of p90 ribosomal S6 kinase (RSK) regulates extracellular signal-regulated kinase docking and RSK activity. *Molecular and cellular biology* 23(14):4796-4804.

261. Dimitri CA, Dowdle W, MacKeigan JP, Blenis J, & Murphy LO (2005) Spatially separate docking sites on ERK2 regulate distinct signaling events in vivo. *Curr Biol* 15(14):1319-1324.

262. Larkin MA, *et al.* (2007) Clustal W and Clustal X version 2.0. *Bioinformatics (Oxford, England)* 23(21):2947-2948.

263. Richards SA, Dreisbach VC, Murphy LO, & Blenis J (2001) Characterization of regulatory events associated with membrane targeting of p90 ribosomal S6 kinase 1. *Molecular and cellular biology* 21(21):7470-7480.

264. Kang S, *et al.* (2008) Epidermal growth factor stimulates RSK2 activation through activation of the MEK/ERK pathway and src-dependent tyrosine phosphorylation of RSK2 at Tyr-529. *The Journal of biological chemistry* 283(8):4652-4657.

265. Hu Y, *et al.* (2004) 90-kDa ribosomal S6 kinase is a direct target for the nuclear fibroblast growth factor receptor 1 (FGFR1): role in FGFR1 signaling. *The Journal of biological chemistry* 279(28):29325-29335.

266. Pan ZZ, Devaux Y, & Ray P (2004) Ribosomal S6 kinase as a mediator of keratinocyte growth factor-induced activation of Akt in epithelial cells. *Molecular biology of the cell* 15(7):3106-3113.

267. Kang S, *et al.* (2009) Fibroblast growth factor receptor 3 associates with and tyrosine phosphorylates p90 RSK2, leading to RSK2 activation that mediates hematopoietic transformation. *Molecular and cellular biology* 29(8):2105-2117.

268. Chen RH, Sarnecki C, & Blenis J (1992) Nuclear localization and regulation of erk- and rsk-encoded protein kinases. *Molecular and cellular biology* 12(3):915-927.

269. Chen RH, Abate C, & Blenis J (1993) Phosphorylation of the c-Fos transrepression domain by mitogen-activated protein kinase and 90-kDa ribosomal S6 kinase. *Proceedings of the National Academy of Sciences of the United States of America* 90(23):10952-10956.

270. Wingate AD, Campbell DG, Peggie M, & Arthur JS (2006) Nur77 is phosphorylated in cells by RSK in response to mitogenic stimulation. *Biochem J* 393(Pt 3):715-724.

271. Dalby KN, Morrice N, Caudwell FB, Avruch J, & Cohen P (1998) Identification of regulatory phosphorylation sites in mitogen-activated protein kinase (MAPK)-activated protein kinase-1a/p90rsk that are inducible by MAPK. *The Journal of biological chemistry* 273(3):1496-1505.

272. Gavin AC, Ni Ainle A, Chierici E, Jones M, & Nebreda AR (1999) A p90(rsk) mutant constitutively interacting with MAP kinase uncouples MAP kinase from p34(cdc2)/cyclin B activation in Xenopus oocytes. *Molecular biology of the cell* 10(9):2971-2986.

273. Bonni A, *et al.* (1999) Cell survival promoted by the Ras-MAPK signaling pathway by transcription-dependent and -independent mechanisms. *Science (New York, N.Y* 286(5443):1358-1362.

274. Ginty DD, Bonni A, & Greenberg ME (1994) Nerve growth factor activates a Ras-dependent protein kinase that stimulates c-fos transcription via phosphorylation of CREB. *Cell* 77(5):713-725.

275. Xing J, Ginty DD, & Greenberg ME (1996) Coupling of the RAS-MAPK pathway to gene activation by RSK2, a growth factor-regulated CREB kinase. *Science (New York, N.Y* 273(5277):959-963.

276. Yang TT, Xiong Q, Graef IA, Crabtree GR, & Chow CW (2005) Recruitment of the extracellular signal-regulated kinase/ribosomal S6 kinase signaling pathway to the NFATc4 transcription activation complex. *Molecular and cellular biology* 25(3):907-920.

277. Cho YY, *et al.* (2007) RSK2 mediates muscle cell differentiation through regulation of NFAT3. *The Journal of biological chemistry* 282(11):8380-8392.

278. Yang X, *et al.* (2004) ATF4 is a substrate of RSK2 and an essential regulator of osteoblast biology; implication for Coffin-Lowry Syndrome. *Cell* 117(3):387-398.

279. Zhao J, Yuan X, Frodin M, & Grummt I (2003) ERK-dependent phosphorylation of the transcription initiation factor TIF-IA is required for RNA polymerase I transcription and cell growth. *Molecular cell* 11(2):405-413.

280. Wu J & Janknecht R (2002) Regulation of the ETS transcription factor ER81 by the 90-kDa ribosomal S6 kinase 1 and protein kinase A. *The Journal of biological chemistry* 277(45):42669-42679.

281. Ghoda L, Lin X, & Greene WC (1997) The 90-kDa ribosomal S6 kinase (pp90rsk) phosphorylates the N-terminal regulatory domain of IkappaBalpha and stimulates its degradation in vitro. *The Journal of biological chemistry* 272(34):21281-21288.

282. Schouten GJ, *et al.* (1997) IkappaB alpha is a target for the mitogen-activated 90 kDa ribosomal S6 kinase. *The EMBO journal* 16(11):3133-3144.

283. Erikson E & Maller JL (1985) A protein kinase from Xenopus eggs specific for ribosomal protein S6. *Proceedings of the National Academy of Sciences of the United States of America* 82(3):742-746.

284. Zhang L, Ma Y, Zhang J, Cheng J, & Du J (2005) A new cellular signaling mechanism for angiotensin II activation of NF-kappaB: An IkappaB-

independent, RSK-mediated phosphorylation of p65. *Arterioscler Thromb Vasc Biol* 25(6):1148-1153.

285. Xu S, Bayat H, Hou X, & Jiang B (2006) Ribosomal S6 kinase-1 modulates interleukin-1beta-induced persistent activation of NF-kappaB through phosphorylation of IkappaBbeta. *Am J Physiol Cell Physiol* 291(6):C1336-1345.

286. Rivera VM, *et al.* (1993) A growth factor-induced kinase phosphorylates the serum response factor at a site that regulates its DNA-binding activity. *Molecular and cellular biology* 13(10):6260-6273.

287. Roux PP, Ballif BA, Anjum R, Gygi SP, & Blenis J (2004) Tumor-promoting phorbol esters and activated Ras inactivate the tuberous sclerosis tumor suppressor complex via p90 ribosomal S6 kinase. *Proceedings of the National Academy of Sciences of the United States of America* 101(37):13489-13494.

288. Shahbazian D, *et al.* (2006) The mTOR/PI3K and MAPK pathways converge on eIF4B to control its phosphorylation and activity. *The EMBO journal* 25(12):2781-2791.

289. Wang X, *et al.* (2001) Regulation of elongation factor 2 kinase by p90(RSK1) and p70 S6 kinase. *The EMBO journal* 20(16):4370-4379.

290. Roux PP, *et al.* (2007) RAS/ERK signaling promotes site-specific ribosomal protein S6 phosphorylation via RSK and stimulates cap-dependent translation. *The Journal of biological chemistry* 282(19):14056-14064.

291. Joel PB, *et al.* (1998) pp90rsk1 regulates estrogen receptor-mediated transcription through phosphorylation of Ser-167. *Molecular and cellular biology* 18(4):1978-1984.

292. Sutherland C, Leighton IA, & Cohen P (1993) Inactivation of glycogen synthase kinase-3 beta by phosphorylation: new kinase connections in insulin and growth-factor signalling. *Biochem J* 296 (Pt 1):15-19.

293. Takahashi E, *et al.* (1999) p90(RSK) is a serum-stimulated Na+/H+ exchanger isoform-1 kinase. Regulatory phosphorylation of serine 703 of Na+/H+ exchanger isoform-1. *The Journal of biological chemistry* 274(29):20206-20214.

294. Wu M, *et al.* (2000) c-Kit triggers dual phosphorylations, which couple activation and degradation of the essential melanocyte factor Mi. *Genes Dev* 14(3):301-312.

295. Sapkota GP, *et al.* (2001) Phosphorylation of the protein kinase mutated in Peutz-Jeghers cancer syndrome, LKB1/STK11, at Ser431 by p90(RSK) and

cAMP-dependent protein kinase, but not its farnesylation at Cys(433), is essential for LKB1 to suppress cell vrowth. *The Journal of biological chemistry* 276(22):19469-19482.

296. Douville E & Downward J (1997) EGF induced SOS phosphorylation in PC12 cells involves P90 RSK-2. *Oncogene* 15(4):373-383.

297. Chen RH, Juo PC, Curran T, & Blenis J (1996) Phosphorylation of c-Fos at the C-terminus enhances its transforming activity. *Oncogene* 12(7):1493-1502.

298. Fujita N, Sato S, & Tsuruo T (2003) Phosphorylation of p27Kip1 at threonine 198 by p90 ribosomal protein S6 kinases promotes its binding to 14-3-3 and cytoplasmic localization. *The Journal of biological chemistry* 278(49):49254-49260.

299. Schwab MS, *et al.* (2001) Bub1 is activated by the protein kinase p90(Rsk) during Xenopus oocyte maturation. *Curr Biol* 11(3):141-150.

300. Palmer A, Gavin AC, & Nebreda AR (1998) A link between MAP kinase and p34(cdc2)/cyclin B during oocyte maturation: p90(rsk) phosphorylates and inactivates the p34(cdc2) inhibitory kinase Myt1. *The EMBO journal* 17(17):5037-5047.

301. Inoue D, Ohe M, Kanemori Y, Nobui T, & Sagata N (2007) A direct link of the Mos-MAPK pathway to Erp1/Emi2 in meiotic arrest of Xenopus laevis eggs. *Nature* 446(7139):1100-1104.

302. Nishiyama T, Ohsumi K, & Kishimoto T (2007) Phosphorylation of Erp1 by p90rsk is required for cytostatic factor arrest in Xenopus laevis eggs. *Nature* 446(7139):1096-1099.

303. Shimamura A, Ballif BA, Richards SA, & Blenis J (2000) Rsk1 mediates a MEK-MAP kinase cell survival signal. *Curr Biol* 10(3):127-135.

304. Buck M, Poli V, Hunter T, & Chojkier M (2001) C/EBPbeta phosphorylation by RSK creates a functional XEXD caspase inhibitory box critical for cell survival. *Molecular cell* 8(4):807-816.

305. Anjum R, Roux PP, Ballif BA, Gygi SP, & Blenis J (2005) The tumor suppressor DAP kinase is a target of RSK-mediated survival signaling. *Curr Biol* 15(19):1762-1767.

306. Woo MS, Ohta Y, Rabinovitz I, Stossel TP, & Blenis J (2004) Ribosomal S6 kinase (RSK) regulates phosphorylation of filamin A on an important regulatory site. *Molecular and cellular biology* 24(7):3025-3035.

307. Wong EV, Schaefer AW, Landreth G, & Lemmon V (1996) Involvement of p90rsk in neurite outgrowth mediated by the cell adhesion molecule L1. *The Journal of biological chemistry* 271(30):18217-18223.

308. Yoon SO, *et al.* (2008) Ran-binding protein 3 phosphorylation links the Ras and PI3-kinase pathways to nucleocytoplasmic transport. *Molecular cell* 29(3):362-375.

309. Song T, *et al.* (2007) p90 RSK-1 associates with and inhibits neuronal nitric oxide synthase. *Biochem J* 401(2):391-398.

310. Zhu J, Blenis J, & Yuan J (2008) Activation of PI3K/Akt and MAPK pathways regulates Myc-mediated transcription by phosphorylating and promoting the degradation of Mad1. *Proceedings of the National Academy of Sciences of the United States of America* 105(18):6584-6589.

311. Geraghty KM, *et al.* (2007) Regulation of multisite phosphorylation and 14-3-3 binding of AS160 in response to IGF-1, EGF, PMA and AICAR. *Biochem J* 407(2):231-241.

312. Carriere A, *et al.* (2008) Oncogenic MAPK signaling stimulates mTORC1 activity by promoting RSK-mediated raptor phosphorylation. *Curr Biol* 18(17):1269-1277.

313. Stratford AL, *et al.* (2008) Y-box binding protein-1 serine 102 is a downstream target of p90 ribosomal S6 kinase in basal-like breast cancer cells. *Breast Cancer Res* 10(6):R99.

314. Abe Y, *et al.* (2009) p90 ribosomal S6 kinase and p70 ribosomal S6 kinase link phosphorylation of the eukaryotic chaperonin containing TCP-1 to growth factor, insulin, and nutrient signaling. *The Journal of biological chemistry* 284(22):14939-14948.

315. Suizu F, Ueda K, Iwasaki T, Murata-Hori M, & Hosoya H (2000) Activation of actin-activated MgATPase activity of myosin II by phosphorylation with MAPK-activated protein kinase-1b (RSK-2). *J Biochem* 128(3):435-440.

316. Ma XM & Blenis J (2009) Molecular mechanisms of mTOR-mediated translational control. *Nature reviews* 10(5):307-318.

317. Holz MK, Ballif BA, Gygi SP, & Blenis J (2005) mTOR and S6K1 mediate assembly of the translation preinitiation complex through dynamic protein interchange and ordered phosphorylation events. *Cell* 123(4):569-580.

318. Etchison D, Milburn SC, Edery I, Sonenberg N, & Hershey JW (1982) Inhibition of HeLa cell protein synthesis following poliovirus infection correlates with the proteolysis of a 220,000-dalton polypeptide associated with

eucaryotic initiation factor 3 and a cap binding protein complex. *The Journal of biological chemistry* 257(24):14806-14810.

319. Tan Y, Ruan H, Demeter MR, & Comb MJ (1999) p90(RSK) blocks bad-mediated cell death via a protein kinase C-dependent pathway. *The Journal of biological chemistry* 274(49):34859-34867.

320. Dehan E, *et al.* (2009) betaTrCP- and Rsk1/2-mediated degradation of BimEL inhibits apoptosis. *Molecular cell* 33(1):109-116.

321. Bhatt RR & Ferrell JE, Jr. (1999) The protein kinase p90 rsk as an essential mediator of cytostatic factor activity. *Science (New York, N.Y* 286(5443):1362-1365.

322. Gross SD, Schwab MS, Lewellyn AL, & Maller JL (1999) Induction of metaphase arrest in cleaving Xenopus embryos by the protein kinase p90Rsk. *Science (New York, N.Y* 286(5443):1365-1367.

323. Doehn U, *et al.* (2009) RSK is a principal effector of the RAS-ERK pathway for eliciting a coordinate promotile/invasive gene program and phenotype in epithelial cells. *Molecular cell* 35(4):511-522.

324. Larrea MD, *et al.* (2009) RSK1 drives p27Kip1 phosphorylation at T198 to promote RhoA inhibition and increase cell motility. *Proceedings of the National Academy of Sciences of the United States of America* 106(23):9268-9273.

325. Dummler BA, *et al.* (2005) Functional characterization of human RSK4, a new 90-kDa ribosomal S6 kinase, reveals constitutive activation in most cell types. *The Journal of biological chemistry* 280(14):13304-13314.

326. Trivier E, *et al.* (1996) Mutations in the kinase Rsk-2 associated with Coffin-Lowry syndrome. *Nature* 384(6609):567-570.

327. Poirier R, *et al.* (2007) Deletion of the Coffin-Lowry syndrome gene Rsk2 in mice is associated with impaired spatial learning and reduced control of exploratory behavior. *Behav Genet* 37(1):31-50.

328. WHO (2009) WHO Fact sheet Cancer N 297.

329. Spiro SG & Porter JC (2002) Lung cancer--where are we today? Current advances in staging and nonsurgical treatment. *American journal of respiratory and critical care medicine* 166(9):1166-1196.

330. Spiro SG & Silvestri GA (2005) One hundred years of lung cancer. *American journal of respiratory and critical care medicine* 172(5):523-529.

331. Tanaka K, Kubota K, Kodama T, Nagai K, & Nishiwaki Y (1999) Extrathoracic staging is not necessary for non-small-cell lung cancer with clinical stage T1-2 N0. *Ann Thorac Surg* 68(3):1039-1042.

332. Tortora GJ & Grabowski SR (2003) *Principles of anatomy and physiology* (Wiley, New York) 10th Ed pp xxxii, 1104, 1197 p.

333. Sutherland KD & Berns A (2010) Cell of origin of lung cancer. *Mol Oncol.*

334. Giangreco A, Groot KR, & Janes SM (2007) Lung cancer and lung stem cells: strange bedfellows? *American journal of respiratory and critical care medicine* 175(6):547-553.

335. Onganer PU, Seckl MJ, & Djamgoz MB (2005) Neuronal characteristics of small-cell lung cancer. *Br J Cancer* 93(11):1197-1201.

336. Sutherland C, Campbell DG, & Cohen P (1993) Identification of insulin-stimulated protein kinase-1 as the rabbit equivalent of rskmo-2. Identification of two threonines phosphorylated during activation by mitogen-activated protein kinase. *Eur J Biochem* 212(2):581-588.

337. Jackson EL, *et al.* (2001) Analysis of lung tumor initiation and progression using conditional expression of oncogenic K-ras. *Genes Dev* 15(24):3243-3248.

338. Kim CF, *et al.* (2005) Identification of bronchioalveolar stem cells in normal lung and lung cancer. *Cell* 121(6):823-835.

339. Weir BA, *et al.* (2007) Characterizing the cancer genome in lung adenocarcinoma. *Nature* 450(7171):893-898.

340. Amos CI, *et al.* (2008) Genome-wide association scan of tag SNPs identifies a susceptibility locus for lung cancer at 15q25.1. *Nat Genet* 40(5):616-622.

341. Herbst RS, Heymach JV, & Lippman SM (2008) Lung cancer. *N Engl J Med* 359(13):1367-1380.

342. Mitsuuchi Y & Testa JR (2002) Cytogenetics and molecular genetics of lung cancer. *Am J Med Genet* 115(3):183-188.

343. Citri A & Yarden Y (2006) EGF-ERBB signalling: towards the systems level. *Nature reviews* 7(7):505-516.

344. Lenferink AE, *et al.* (1998) Differential endocytic routing of homo- and hetero-dimeric ErbB tyrosine kinases confers signaling superiority to receptor heterodimers. *The EMBO journal* 17(12):3385-3397.

345. Landau M & Ben-Tal N (2008) Dynamic equilibrium between multiple active and inactive conformations explains regulation and oncogenic mutations in ErbB receptors. *Biochim Biophys Acta* 1785(1):12-31.

346. Chen YR, *et al.* (2006) Distinctive activation patterns in constitutively active and gefitinib-sensitive EGFR mutants. *Oncogene* 25(8):1205-1215.

347. Lynch TJ, *et al.* (2004) Activating mutations in the epidermal growth factor receptor underlying responsiveness of non-small-cell lung cancer to gefitinib. *N Engl J Med* 350(21):2129-2139.

348. Pedersen MW, *et al.* (2005) Analysis of the epidermal growth factor receptor specific transcriptome: effect of receptor expression level and an activating mutation. *J Cell Biochem* 96(2):412-427.

349. Hirsch FR, *et al.* (2003) Epidermal growth factor receptor in non-small-cell lung carcinomas: correlation between gene copy number and protein expression and impact on prognosis. *J Clin Oncol* 21(20):3798-3807.

350. Scagliotti GV, Selvaggi G, Novello S, & Hirsch FR (2004) The biology of epidermal growth factor receptor in lung cancer. *Clin Cancer Res* 10(12 Pt 2):4227s-4232s.

351. Shigematsu H, *et al.* (2005) Clinical and biological features associated with epidermal growth factor receptor gene mutations in lung cancers. *J Natl Cancer Inst* 97(5):339-346.

352. Sharma SV, Bell DW, Settleman J, & Haber DA (2007) Epidermal growth factor receptor mutations in lung cancer. *Nat Rev Cancer* 7(3):169-181.

353. Sequist LV, Bell DW, Lynch TJ, & Haber DA (2007) Molecular predictors of response to epidermal growth factor receptor antagonists in non-small-cell lung cancer. *J Clin Oncol* 25(5):587-595.

354. Greulich H, *et al.* (2005) Oncogenic transformation by inhibitor-sensitive and -resistant EGFR mutants. *PLoS Med* 2(11):e313.

355. Godin-Heymann N, *et al.* (2007) Oncogenic activity of epidermal growth factor receptor kinase mutant alleles is enhanced by the T790M drug resistance mutation. *Cancer research* 67(15):7319-7326.

356. Ji H, *et al.* (2006) The impact of human EGFR kinase domain mutations on lung tumorigenesis and in vivo sensitivity to EGFR-targeted therapies. *Cancer cell* 9(6):485-495.

357. Politi K, *et al.* (2006) Lung adenocarcinomas induced in mice by mutant EGF receptors found in human lung cancers respond to a tyrosine kinase inhibitor or to down-regulation of the receptors. *Genes Dev* 20(11):1496-1510.

358. Okamoto I, *et al.* (2003) Expression of constitutively activated EGFRvIII in non-small cell lung cancer. *Cancer Sci* 94(1):50-56.

359. Ji H, *et al.* (2006) Epidermal growth factor receptor variant III mutations in lung tumorigenesis and sensitivity to tyrosine kinase inhibitors. *Proceedings of the National Academy of Sciences of the United States of America* 103(20):7817-7822.

360. Tang X, *et al.* (2008) Epidermal growth factor receptor abnormalities in the pathogenesis and progression of lung adenocarcinomas. *Cancer Prev Res (Phila Pa)* 1(3):192-200.

361. Soung YH, *et al.* (2006) Somatic mutations of the ERBB4 kinase domain in human cancers. *Int J Cancer* 118(6):1426-1429.

362. Yang Y, *et al.* (2008) A selective small molecule inhibitor of c-Met, PHA-665752, reverses lung premalignancy induced by mutant K-ras. *Molecular cancer therapeutics* 7(4):952-960.

363. Le Calvez F, *et al.* (2005) TP53 and KRAS mutation load and types in lung cancers in relation to tobacco smoke: distinct patterns in never, former, and current smokers. *Cancer research* 65(12):5076-5083.

364. Sun S, Schiller JH, & Gazdar AF (2007) Lung cancer in never smokers--a different disease. *Nat Rev Cancer* 7(10):778-790.

365. Westra WH (2000) Early glandular neoplasia of the lung. *Respir Res* 1(3):163-169.

366. Johnson L, *et al.* (2001) Somatic activation of the K-ras oncogene causes early onset lung cancer in mice. *Nature* 410(6832):1111-1116.

367. Dankort D, *et al.* (2007) A new mouse model to explore the initiation, progression, and therapy of BRAFV600E-induced lung tumors. *Genes Dev* 21(4):379-384.

368. Yamamoto H, *et al.* (2008) PIK3CA mutations and copy number gains in human lung cancers. *Cancer research* 68(17):6913-6921.

369. Yang Y, *et al.* (2008) Phosphatidylinositol 3-kinase mediates bronchioalveolar stem cell expansion in mouse models of oncogenic K-ras-induced lung cancer. *PLoS One* 3(5):e2220.

370. Sherr CJ (2004) Principles of tumor suppression. *Cell* 116(2):235-246.

371. Sherr CJ & McCormick F (2002) The RB and p53 pathways in cancer. *Cancer cell* 2(2):103-112.

372. Malkin D, *et al.* (1990) Germ line p53 mutations in a familial syndrome of breast cancer, sarcomas, and other neoplasms. *Science (New York, N.Y* 250(4985):1233-1238.

373. Gibbons DL, *et al.* (2009) Expression signatures of metastatic capacity in a genetic mouse model of lung adenocarcinoma. *PLoS One* 4(4):e5401.

374. Olivier M, Hollstein M, & Hainaut P (2010) TP53 mutations in human cancers: origins, consequences, and clinical use. *Cold Spring Harb Perspect Biol* 2(1):a001008.

375. Lang GA, *et al.* (2004) Gain of function of a p53 hot spot mutation in a mouse model of Li-Fraumeni syndrome. *Cell* 119(6):861-872.

376. Zheng S, El-Naggar AK, Kim ES, Kurie JM, & Lozano G (2007) A genetic mouse model for metastatic lung cancer with gender differences in survival. *Oncogene* 26(48):6896-6904.

377. Cavenee WK, *et al.* (1983) Expression of recessive alleles by chromosomal mechanisms in retinoblastoma. *Nature* 305(5937):779-784.

378. Harbour JW & Dean DC (2000) Rb function in cell-cycle regulation and apoptosis. *Nature cell biology* 2(4):E65-67.

379. Morgenbesser SD, Williams BO, Jacks T, & DePinho RA (1994) p53-dependent apoptosis produced by Rb-deficiency in the developing mouse lens. *Nature* 371(6492):72-74.

380. Williams BO, Morgenbesser SD, DePinho RA, & Jacks T (1994) Tumorigenic and developmental effects of combined germ-line mutations in Rb and p53. *Cold Spring Harb Symp Quant Biol* 59:449-457.

381. Williams BO, *et al.* (1994) Cooperative tumorigenic effects of germline mutations in Rb and p53. *Nat Genet* 7(4):480-484.

382. Xu HJ, Hu SX, Cagle PT, Moore GE, & Benedict WF (1991) Absence of retinoblastoma protein expression in primary non-small cell lung carcinomas. *Cancer research* 51(10):2735-2739.

383. Belinsky SA, *et al.* (1998) Aberrant methylation of p16(INK4a) is an early event in lung cancer and a potential biomarker for early diagnosis. *Proceedings*

of the National Academy of Sciences of the United States of America 95(20):11891-11896.

384. Panani AD & Roussos C (2006) Cytogenetic and molecular aspects of lung cancer. *Cancer Lett* 239(1):1-9.

385. Collado M, *et al.* (2005) Tumour biology: senescence in premalignant tumours. *Nature* 436(7051):642.

386. Bennecke M, *et al.* (2010) Ink4a/Arf and oncogene-induced senescence prevent tumor progression during alternative colorectal tumorigenesis. *Cancer cell* 18(2):135-146.

387. Soda M, *et al.* (2007) Identification of the transforming EML4-ALK fusion gene in non-small-cell lung cancer. *Nature* 448(7153):561-566.

388. Choi YL, *et al.* (2008) Identification of novel isoforms of the EML4-ALK transforming gene in non-small cell lung cancer. *Cancer research* 68(13):4971-4976.

389. Matsumoto S, *et al.* (2007) Prevalence and specificity of LKB1 genetic alterations in lung cancers. *Oncogene* 26(40):5911-5918.

390. Koivunen JP, *et al.* (2008) Mutations in the LKB1 tumour suppressor are frequently detected in tumours from Caucasian but not Asian lung cancer patients. *Br J Cancer* 99(2):245-252.

391. Ji H, *et al.* (2007) LKB1 modulates lung cancer differentiation and metastasis. *Nature* 448(7155):807-810.

392. Shackelford DB & Shaw RJ (2009) The LKB1-AMPK pathway: metabolism and growth control in tumour suppression. *Nat Rev Cancer* 9(8):563-575.

393. Ghaffar H, *et al.* (2003) LKB1 protein expression in the evolution of glandular neoplasia of the lung. *Clin Cancer Res* 9(8):2998-3003.

394. Kwak EL, *et al.* (2005) Irreversible inhibitors of the EGF receptor may circumvent acquired resistance to gefitinib. *Proceedings of the National Academy of Sciences of the United States of America* 102(21):7665-7670.

395. Zhou W, *et al.* (2009) Novel mutant-selective EGFR kinase inhibitors against EGFR T790M. *Nature* 462(7276):1070-1074.

396. Bean J, *et al.* (2007) MET amplification occurs with or without T790M mutations in EGFR mutant lung tumors with acquired resistance to gefitinib or

erlotinib. *Proceedings of the National Academy of Sciences of the United States of America* 104(52):20932-20937.

397. Ecker JR & Davis RW (1986) Inhibition of gene expression in plant cells by expression of antisense RNA. *Proceedings of the National Academy of Sciences of the United States of America* 83(15):5372-5376.

398. Romano N & Macino G (1992) Quelling: transient inactivation of gene expression in Neurospora crassa by transformation with homologous sequences. *Mol Microbiol* 6(22):3343-3353.

399. Fire A, *et al.* (1998) Potent and specific genetic interference by double-stranded RNA in Caenorhabditis elegans. *Nature* 391(6669):806-811.

400. Ryan BM, Robles AI, & Harris CC (2010) Genetic variation in microRNA networks: the implications for cancer research. *Nat Rev Cancer* 10(6):389-402.

401. Voinnet O (2005) Induction and suppression of RNA silencing: insights from viral infections. *Nat Rev Genet* 6(3):206-220.

402. Bagasra O & Prilliman KR (2004) RNA interference: the molecular immune system. *J Mol Histol* 35(6):545-553.

403. Macrae IJ, *et al.* (2006) Structural basis for double-stranded RNA processing by Dicer. *Science (New York, N.Y* 311(5758):195-198.

404. Rand TA, Ginalski K, Grishin NV, & Wang X (2004) Biochemical identification of Argonaute 2 as the sole protein required for RNA-induced silencing complex activity. *Proceedings of the National Academy of Sciences of the United States of America* 101(40):14385-14389.

405. Jinek M & Doudna JA (2009) A three-dimensional view of the molecular machinery of RNA interference. *Nature* 457(7228):405-412.

406. Collins CS, *et al.* (2006) A small interfering RNA screen for modulators of tumor cell motility identifies MAP4K4 as a promigratory kinase. *Proceedings of the National Academy of Sciences of the United States of America* 103(10):3775-3780.

407. Simpson KJ, *et al.* (2008) Identification of genes that regulate epithelial cell migration using an siRNA screening approach. *Nature cell biology* 10(9):1027-1038.

408. Sepp KJ, *et al.* (2008) Identification of neural outgrowth genes using genome-wide RNAi. *PLoS Genet* 4(7):e1000111.

409. Tsui M, *et al.* (2009) An intermittent live cell imaging screen for siRNA enhancers and suppressors of a kinesin-5 inhibitor. *PLoS One* 4(10):e7339.

410. Davis ME, *et al.* (2010) Evidence of RNAi in humans from systemically administered siRNA via targeted nanoparticles. *Nature* 464(7291):1067-1070.

411. Bradford MM (1976) A rapid and sensitive method for the quantitation of microgram quantities of protein utilizing the principle of protein-dye binding. *Anal Biochem* 72:248-254.

412. Laemmli UK (1970) Cleavage of structural proteins during the assembly of the head of bacteriophage T4. *Nature* 227(5259):680-685.

413. Katso RM, *et al.* (2006) Phosphoinositide 3-Kinase C2beta regulates cytoskeletal organization and cell migration via Rac-dependent mechanisms. *Molecular biology of the cell* 17(9):3729-3744.

414. Jonsson PF & Bates PA (2006) Global topological features of cancer proteins in the human interactome. *Bioinformatics (Oxford, England)* 22(18):2291-2297.

415. Linding R, *et al.* (2007) Systematic discovery of in vivo phosphorylation networks. *Cell* 129(7):1415-1426.

416. Shi SR, Key ME, & Kalra KL (1991) Antigen retrieval in formalin-fixed, paraffin-embedded tissues: an enhancement method for immunohistochemical staining based on microwave oven heating of tissue sections. *J Histochem Cytochem* 39(6):741-748.

417. Herberger B, *et al.* (2007) Activated mammalian target of rapamycin is an adverse prognostic factor in patients with biliary tract adenocarcinoma. *Clin Cancer Res* 13(16):4795-4799.

418. Friedman A & Perrimon N (2007) Genetic screening for signal transduction in the era of network biology. *Cell* 128(2):225-231.

419. Uekita T, *et al.* (2007) CUB domain-containing protein 1 is a novel regulator of anoikis resistance in lung adenocarcinoma. *Molecular and cellular biology* 27(21):7649-7660.

420. Nikolova DA, *et al.* (2009) Cetuximab attenuates metastasis and u-PAR expression in non-small cell lung cancer: u-PAR and E-cadherin are novel biomarkers of cetuximab sensitivity. *Cancer research* 69(6):2461-2470.

421. Mase K, *et al.* (2002) Intrabronchial orthotopic propagation of human lung adenocarcinoma--characterizations of tumorigenicity, invasion and metastasis. *Lung cancer (Amsterdam, Netherlands)* 36(3):271-276.

422. Qian J, *et al.* (2007) Suppression of type 1 Insulin-like growth factor receptor expression by small interfering RNA inhibits A549 human lung cancer cell invasion in vitro and metastasis in xenograft nude mice. *Acta biochimica et biophysica Sinica* 39(2):137-147.

423. Rao JS, *et al.* (2005) Inhibition of invasion, angiogenesis, tumor growth, and metastasis by adenovirus-mediated transfer of antisense uPAR and MMP-9 in non-small cell lung cancer cells. *Molecular cancer therapeutics* 4(9):1399-1408.

424. Meng XN, *et al.* (2009) Characterisation of fibronectin-mediated FAK signalling pathways in lung cancer cell migration and invasion. *Br J Cancer* 101(2):327-334.

425. Roato I, *et al.* (2010) Bone invading NSCLC cells produce IL-7: mice model and human histologic data. *BMC Cancer* 10:12.

426. Koning AJ, Lum PY, Williams JM, & Wright R (1993) DiOC6 staining reveals organelle structure and dynamics in living yeast cells. *Cell motility and the cytoskeleton* 25(2):111-128.

427. Eckerdt F & Strebhardt K (2006) Polo-like kinase 1: target and regulator of anaphase-promoting complex/cyclosome-dependent proteolysis. *Cancer research* 66(14):6895-6898.

428. Swanton C, *et al.* (2007) Regulators of mitotic arrest and ceramide metabolism are determinants of sensitivity to paclitaxel and other chemotherapeutic drugs. *Cancer cell* 11(6):498-512.

429. Irie HY, *et al.* (2005) Distinct roles of Akt1 and Akt2 in regulating cell migration and epithelial-mesenchymal transition. *The Journal of cell biology* 171(6):1023-1034.

430. Matsuoka H, Obama H, Kelly ML, Matsui T, & Nakamoto M (2005) Biphasic functions of the kinase-defective Ephb6 receptor in cell adhesion and migration. *The Journal of biological chemistry* 280(32):29355-29363.

431. Echeverri CJ, *et al.* (2006) Minimizing the risk of reporting false positives in large-scale RNAi screens. *Nature methods* 3(10):777-779.

432. Reddy KB, Nabha SM, & Atanaskova N (2003) Role of MAP kinase in tumor progression and invasion. *Cancer Metastasis Rev* 22(4):395-403.

433. Hauck CR, *et al.* (2001) Inhibition of focal adhesion kinase expression or activity disrupts epidermal growth factor-stimulated signaling promoting the migration of invasive human carcinoma cells. *Cancer research* 61(19):7079-7090.

434. Gazdar AF (2010) Epidermal growth factor receptor inhibition in lung cancer: the evolving role of individualized therapy. *Cancer Metastasis Rev* 29(1):37-48.

435. Adiseshaiah P, Lindner DJ, Kalvakolanu DV, & Reddy SP (2007) FRA-1 proto-oncogene induces lung epithelial cell invasion and anchorage-independent growth in vitro, but is insufficient to promote tumor growth in vivo. *Cancer research* 67(13):6204-6211.

436. Cottingham MG, Bain CD, & Vaux DJ (2004) Rapid method for measurement of surface tension in multiwell plates. *Lab Invest* 84(4):523-529.

437. Haase D, *et al.* (2007) FRMD3, a novel putative tumour suppressor in NSCLC. *Oncogene* 26(30):4464-4468.

438. Cavanna T, Pokorna E, Vesely P, Gray C, & Zicha D (2007) Evidence for protein 4.1B acting as a metastasis suppressor. *Journal of cell science* 120(Pt 4):606-616.

439. Futaki S, *et al.* (2003) Molecular basis of constitutive production of basement membrane components. Gene expression profiles of Engelbreth-Holm-Swarm tumor and F9 embryonal carcinoma cells. *The Journal of biological chemistry* 278(50):50691-50701.

440. Devy L, *et al.* (2009) Selective inhibition of matrix metalloproteinase-14 blocks tumor growth, invasion, and angiogenesis. *Cancer research* 69(4):1517-1526; Sabeh F, *et al.* (2004) Tumor cell traffic through the extracellular matrix is controlled by the membrane-anchored collagenase MT1-MMP. *The Journal of cell biology* 167(4):769-781.

441. Friedl P (2004) Prespecification and plasticity: shifting mechanisms of cell migration. *Curr Opin Cell Biol* 16(1):14-23.

442. Jorgensen C & Linding R (2010) Simplistic pathways or complex networks? *Curr Opin Genet Dev* 20(1):15-22.

443. Jeong H, Mason SP, Barabasi AL, & Oltvai ZN (2001) Lethality and centrality in protein networks. *Nature* 411(6833):41-42.

444. Ziegler WH, Liddington RC, & Critchley DR (2006) The structure and regulation of vinculin. *Trends in cell biology* 16(9):453-460.

445. Ivaska J, Pallari HM, Nevo J, & Eriksson JE (2007) Novel functions of vimentin in cell adhesion, migration, and signaling. *Experimental cell research* 313(10):2050-2062.

446. Gertler FB, Niebuhr K, Reinhard M, Wehland J, & Soriano P (1996) Mena, a relative of VASP and Drosophila Enabled, is implicated in the control of microfilament dynamics. *Cell* 87(2):227-239.

447. Kwiatkowski AV, Gertler FB, & Loureiro JJ (2003) Function and regulation of Ena/VASP proteins. *Trends in cell biology* 13(7):386-392.

448. Eckert RE & Jones SL (2007) Regulation of VASP serine 157 phosphorylation in human neutrophils after stimulation by a chemoattractant. *Journal of leukocyte biology* 82(5):1311-1321.

449. Geese M, *et al.* (2002) Contribution of Ena/VASP proteins to intracellular motility of listeria requires phosphorylation and proline-rich core but not F-actin binding or multimerization. *Molecular biology of the cell* 13(7):2383-2396.

450. Gomez TM & Robles E (2004) The great escape; phosphorylation of Ena/VASP by PKA promotes filopodial formation. *Neuron* 42(1):1-3.

451. Lindsay SL, Ramsey S, Aitchison M, Renne T, & Evans TJ (2007) Modulation of lamellipodial structure and dynamics by NO-dependent phosphorylation of VASP Ser239. *Journal of cell science* 120(Pt 17):3011-3021.

452. Loureiro JJ, *et al.* (2002) Critical roles of phosphorylation and actin binding motifs, but not the central proline-rich region, for Ena/vasodilator-stimulated phosphoprotein (VASP) function during cell migration. *Molecular biology of the cell* 13(7):2533-2546.

453. Boeda B, *et al.* (2007) Tes, a specific Mena interacting partner, breaks the rules for EVH1 binding. *Molecular cell* 28(6):1071-1082.

454. Gioeli D, Mandell JW, Petroni GR, Frierson HF, Jr., & Weber MJ (1999) Activation of mitogen-activated protein kinase associated with prostate cancer progression. *Cancer research* 59(2):279-284.

455. Vicent S, *et al.* (2004) ERK1/2 is activated in non-small-cell lung cancer and associated with advanced tumours. *Br J Cancer* 90(5):1047-1052.

456. Stoletov K, *et al.* (2010) Visualizing extravasation dynamics of metastatic tumor cells. *Journal of cell science* 123(Pt 13):2332-2341.

457. Stoletov K & Klemke R (2008) Catch of the day: zebrafish as a human cancer model. *Oncogene* 27(33):4509-4520.

458. Gurzu S, *et al.* (2008) The expression of cytoskeleton regulatory protein Mena in colorectal lesions. *Romanian journal of morphology and embryology = Revue roumaine de morphologie et embryologie* 49(3):345-349.

459. Collinet C, *et al.* (2010) Systems survey of endocytosis by multiparametric image analysis. *Nature* 464(7286):243-249.

460. Winograd-Katz SE, Itzkovitz S, Kam Z, & Geiger B (2009) Multiparametric analysis of focal adhesion formation by RNAi-mediated gene knockdown. *The Journal of cell biology* 186(3):423-436.

461. Bakal C, Aach J, Church G, & Perrimon N (2007) Quantitative morphological signatures define local signaling networks regulating cell morphology. *Science (New York, N.Y* 316(5832):1753-1756.

462. Neumann B, *et al.* (2010) Phenotypic profiling of the human genome by time-lapse microscopy reveals cell division genes. *Nature* 464(7289):721-727.

463. Berton S, *et al.* (2009) The tumor suppressor functions of p27(kip1) include control of the mesenchymal/amoeboid transition. *Molecular and cellular biology* 29(18):5031-5045.

464. Gao Y, *et al.* (2006) Up-regulation of GPR48 induced by down-regulation of p27Kip1 enhances carcinoma cell invasiveness and metastasis. *Cancer research* 66(24):11623-11631.

465. Wassarman DA, Solomon NM, & Rubin GM (1994) The Drosophila melanogaster ribosomal S6 kinase II-encoding sequence. *Gene* 144(2):309-310.

466. Kim M, *et al.* (2006) Inhibition of ERK-MAP kinase signaling by RSK during Drosophila development. *The EMBO journal* 25(13):3056-3067.

467. Chaturvedi D, Poppleton HM, Stringfield T, Barbier A, & Patel TB (2006) Subcellular localization and biological actions of activated RSK1 are determined by its interactions with subunits of cyclic AMP-dependent protein kinase. *Molecular and cellular biology* 26(12):4586-4600.

468. Dephoure N, *et al.* (2008) A quantitative atlas of mitotic phosphorylation. *Proceedings of the National Academy of Sciences of the United States of America* 105(31):10762-10767.

469. Ball LJ, Jarchau T, Oschkinat H, & Walter U (2002) EVH1 domains: structure, function and interactions. *FEBS Lett* 513(1):45-52.

470. Sapkota GP, *et al.* (2007) BI-D1870 is a specific inhibitor of the p90 RSK (ribosomal S6 kinase) isoforms in vitro and in vivo. *Biochem J* 401(1):29-38.

471. Cohen MS, Zhang C, Shokat KM, & Taunton J (2005) Structural bioinformatics-based design of selective, irreversible kinase inhibitors. *Science (New York, N.Y* 308(5726):1318-1321.

472. Nguyen TL (2008) Targeting RSK: an overview of small molecule inhibitors. *Anti-cancer agents in medicinal chemistry* 8(7):710-716.